



Universidade do Minho
Escola de Engenharia

Filipe André Oliveira Barroso
Combining neuromuscular and biomechanical features to
assess sensorimotor impairments after spinal cord injury or stroke

Filipe André Oliveira Barroso

Combining neuromuscular and biomechanical
features to assess sensorimotor impairments
after spinal cord injury or stroke



Universidade do Minho
Escola de Engenharia

Filipe André Oliveira Barroso

Combining neuromuscular and biomechanical
features to assess sensorimotor impairments
after spinal cord injury or stroke

Doctoral Thesis
Doctoral Program in Biomedical Engineering

Supervisors:
Cristina Manuela Peixoto dos Santos, Ph.D
Juan Camilo Moreno, Ph.D
Diego Torricelli, Ph.D

STATEMENT OF INTEGRITY

I hereby declare having conducted my thesis with integrity. I confirm that I have not used plagiarism or any form of falsification of results in the process of the thesis elaboration.

I further declare that I have fully acknowledged the Code of Ethical Conduct of the University of Minho.

University of Minho, _____

Full name: Filipe André Oliveira Barroso

Signature: _____

*Dedicated to my parents José Carlos and Delfina, for their
unfathomable love!*

“Learn from yesterday, live for today, hope for tomorrow. The important thing is to not stop questioning.”

Albert Einstein

Acknowledgements

After more than four years totally dedicated to this Ph.D. Project, I can finally say that it was rewarding. Despite the hard work it implied, this was not a solo journey. Many people and institutions have offered their valuable support along the way. I will be forever grateful to them.

I want to start by expressing all my gratefulness to my advisor Professor Cristina Santos, for her continuous and opportune supervising, always paying attention to the detail and always incentivizing me when I thought things could go wrong. I must say that the sense of responsibility and perseverance of my three advisors are a golden standard for my professional career.

I am very thankful to my co-advisor Doctor Juan C. Moreno, who have been working with me since 2010. His knowledge and experience in the area were fundamental for this work. He guided me along this period and it was an honor to work with him.

A special word goes to my other co-advisor and friend Doctor Diego Torricelli. He showed me the real beauty of science, always questioning the results and looking for answers to unexpected results. I am very lucky to have been in this struggle together with him, preparing novel studies to explore the potential of muscle synergies and preparing workshops together along these years.

I also want to show gratitude to Professor José Luis Pons, Principal Investigator of Neural Rehabilitation Group (CSIC, Madrid), for the opportunity he gave me to perform the Ph.D. research in the framework of the HYPER and BETTER projects.

I also acknowledge with thanks FEDER funds and Portuguese funds from *Fundação para a Ciência e Tecnologia* (FCT) in the scope of my Ph.D. scholarship (reference SFRH/BD/81105/2011).

I would also like to thank the participating patients and volunteers for their valuable time and effort. It was a pleasure to meet each one of them.

During the Ph.D. period, I had the great opportunity to work with two world references in the field of muscle synergies. That is the case of Andrea d'Avella and Yuri P. Ivanenko (from Foundation Santa Lucia, Rome). Their brilliant ideas about muscle synergies were fundamental to me.

The results here presented would not be possible without the help of the clinical personnel from LAMBECOM (Faculty of Health Sciences - Rey Juan Carlos University,

Madrid, Spain). They performed most of the clinical experiments with poststroke patients. For that, I want to individually thank Paco, Roberto, Isabel, Juan, Esther, Alicia, María, Fran and Javi.

It would also be impossible to perform the experiments with iSCI patients without the help and collaboration of the clinical personnel from the National Paraplegia Hospital (Toledo, Spain). They are part of the great human potential of such an important institution. Thus, I want to individually thank Elisabeth, Soraya, Julian and Julio.

I would especially like to express my appreciation to my colleagues from the Neural Rehabilitation Group for their continuous enthusiasm and to create such a pleasant work environment. A special word goes to Stefano Piazza, who was the main responsible to setup the bicycle. He was a great partner.

To all my friends from all over the world, I will be forever grateful for their never-ending encouragement, friendship, belief in my value, those unforgettable travels and delightful talks. All of that gave me the peace and strength I needed to finish this journey.

Finally, I am thankful to my parents, grandparents, cousins and uncles. I feel fortunate to belong to such a wonderful family. They taught me priceless values that I will take with me during my life and my career. They are the best examples of strength, hardwork and perseverance I could ever had. To all of them, Thank You!

Abstract

Stroke and spinal cord injury (SCI) are the most common causes of paresis and paralysis. Disabilities that follow stroke (hemiparesis, hemiplegia) or SCI (paraplegia, tetraplegia) are the result of an inappropriate muscle coordination and activation, leading to impaired motor functions (*e.g.*, walking, cycling) and, thereby, preventing affected people from healthy-like participation in daily activities.

The assessment of sensorimotor impairments has been mainly performed with qualitative methods (classical clinical scales) or subjective assessment from clinical personnel (based on visual observation). These techniques may lead to low inter-rater reliability and, as a consequence, to inadequate interventions. Gait training must have the ability to adapt to individual progression of each patient. Therefore, it is necessary to quantitatively assess locomotor responses after neurological diseases.

The main goal of this Ph.D. Thesis is to generate meaningful quantitative metrics to assess sensorimotor impairments of patients that suffered a stroke or an incomplete spinal cord injury (iSCI). To achieve this main goal, it is necessary to advance neurophysiological and biomechanical conceptual foundations underlying gait function. Further design of appropriate protocols and the generation of these metrics may improve future rehabilitation treatments tailored to each of the aforementioned patients.

Recent researches on pathological conditions strongly recommend gait analysis to adequately assess and follow-up patients and to support clinical decision on the best treatment. Measures derived from gait analysis provide detailed and quantitative description of motor impairments. On the other hand, a technique called analysis of muscle synergies (groups of co-activated muscles responsible for the control of motor tasks), which is based on statistical analysis of electromyographic (EMG) features, has emerged as a promising tool that can offer the clinician a better view of the neural structure underlying motor behaviors and how they change during the rehabilitation process. Thus, a combination of metrics informing about biomechanical and neuromuscular performance in realistic conditions should lead to a better assessment of motor impairments. To achieve the main goal of this Ph.D. Thesis, four distinct and complementary studies were performed.

The first study investigated similar features of walking and cycling under the muscle synergies hypothesis. This study was motivated by the need for novel tools to measure and predict motor performance of neural injured patients. This need has emerged because some patients who suffered neural injuries do not have sufficient muscle force to walk

during the early stage of rehabilitation and, as a consequence, cannot be assessed properly during walking tasks. Due to similarities in kinematics and muscle control, cycling might be explored as a possible framework. Results of this study provided evidences for common neuromuscular mechanisms of the two motor tasks.

The results of study 1 supported the hypothesis of using cycling to assess gait-related motor performance. Thus, the second study of this research aimed to test this hypothesis on subjects affected by iSCI. First of all, results showed that iSCI patients preserved a synergistic control of muscles during cycling and the similarity of synergies with respect to healthy controls correlated with the degree of impairment. Second, muscle synergies outcomes extracted during cycling correlated with clinical measurements of gait performance and/or spasticity caused by abnormal spatiotemporal muscle co-activation.

After iSCI, both body sides may be affected differently, resulting in asymmetric motor control and functional behavior. The third study of this Thesis used some biomechanical features, as well as the analysis of muscle synergies to differentiate most and less affected sides. Results showed that biomechanical analysis was more effective than the analysis of muscle synergies to detect differences between the most and the less affected sides of iSCI patients.

Based on the findings of studies 2 and 3, which showed the usefulness of muscle synergies and biomechanical features to assess iSCI patients, the fourth and last study of this Thesis tested whether the combination of a small set of gait features and the analysis of muscle synergies could better predict walking function poststroke than the gold-standard scale (Fugl-Meyer Assessment, FMA). It was possible to find some variables (from both the most and the less affected side) that correlated better with walking function than FMA.

In conclusion, this Thesis presented novel methodologies and metrics that allow for a quantitative assessment of sensorimotor impairments in patients that suffered an iSCI or a stroke. In particular, the use of metrics based on EMG and biomechanical features gave a new insight into the motor recovery mechanisms as well as the performance after neural damage. These metrics may be explored in the future as a complement to the current clinical assessment procedures.

Resumo

Os acidentes vasculares cerebrais (AVCs) e as lesões medulares são a causa mais comum de paresia e paralisia. As incapacidades resultantes de um AVC (hemiparesia, hemiplegia) ou de uma lesão medular (paraplegia, tetraplegia) são o resultado de uma coordenação e ativação muscular inadequadas, conduzindo a funções motoras (marcha, ciclismo, por exemplo) inadequadas e, desse modo, impedindo as pessoas afetadas de terem uma participação saudável em atividades diárias.

A avaliação das deficiências sensoriais e motoras tem sido efetuada sobretudo com base em métodos qualitativos (escalas clínicas clássicas) ou avaliações subjetivas de pessoal clínico (com base na observação visual). Estas técnicas podem resultar numa baixa confiabilidade entre avaliadores e, como consequência, a intervenções inadequadas. O treino da marcha deve ter a capacidade de se adaptar à progressão individual de cada paciente. Portanto, é necessário avaliar quantitativamente as respostas locomotoras após doenças neurológicas.

O principal objetivo desta Tese de Doutorado é gerar métricas quantitativas para avaliar deficiências sensoriais e motoras de pacientes que sofreram um AVC ou uma lesão medular incompleta. Para atingir este objetivo principal, é necessário desenvolver os princípios neurofisiológicos e biomecânicos subjacentes à marcha. A conceção adicional de protocolos adequados e a geração destas métricas pode melhorar os futuros tratamentos de reabilitação.

As investigações mais recentes sobre condições patológicas aconselham vivamente a análise da marcha para poder avaliar e acompanhar adequadamente os pacientes e também para apoiar decisões clínicas sobre o melhor tratamento a executar. As medidas auferidas através da análise da marcha fornecem uma descrição detalhada e quantitativa de deficiências motoras. Por outro lado, uma técnica chamada análise de sinergias musculares (grupos de músculos co-ativados responsáveis pelo controlo de tarefas motoras), que se baseia na análise estatística das características eletromiográficas (EMG), tem emergido como um instrumento promissor que pode oferecer ao pessoal clínico uma melhor visão das estruturas neuronais subjacentes às tarefas motoras e como estas mudam durante o processo de reabilitação. Sendo assim, uma combinação de métricas que forneçam informação sobre o desempenho biomecânico e neuromuscular em condições reais poderá levar a uma melhor avaliação de deficiências motoras. Para atingir o objetivo principal desta Tese de Doutorado, foram realizados quatro estudos distintos e complementares.

O primeiro estudo investigou características semelhantes da marcha e do ciclismo sob a hipótese das sinergias musculares. Este estudo foi motivado pela necessidade de novos instrumentos de medida e predição do desempenho motor de pacientes que sofreram lesões neuronais. Esta necessidade surgiu visto que alguns pacientes que sofreram lesões neuronais não têm a força muscular suficiente para caminhar durante a fase inicial de reabilitação e, por conseguinte, não pode ser avaliados adequadamente durante tarefas de marcha. Devido às semelhanças cinemáticas e de controlo muscular, o ciclismo pode ser explorado como uma possível solução. Os resultados deste estudo forneceram evidências de que estas duas tarefas motoras apresentam mecanismos neuromusculares comuns.

Os resultados do estudo 1 sustentaram a hipótese de utilizar o ciclismo para avaliar o desempenho motor relacionado com a marcha. Assim, o segundo estudo desta investigação teve como objetivo testar essa hipótese em pacientes afetados por uma lesão medular incompleta. Em primeiro lugar, os resultados mostraram que estes pacientes preservam um controlo sinérgico dos músculos durante o ciclismo e também que a similaridade destas mesmas sinergias com as sinergias apresentadas por sujeitos controlo saudáveis se correlaciona com o grau de debilidade apresentado pelo paciente. Em segundo lugar, alguns valores da análise de sinergias correlacionaram-se com medidas clínicas de desempenho da marcha e/ou espasticidade causada pela ativação espaciotemporal anormal.

Após uma lesão medular incompleta, ambos os lados do corpo podem ser afetados de forma distinta, o que resulta num controlo motor e comportamento funcional distinto. O terceiro estudo desta Tese utilizou algumas variáveis biomecânicas, bem como a análise das sinergias musculares para diferenciar os lados mais e menos afetados. Os resultados mostraram que a análise biomecânica foi mais eficaz que a análise das sinergias musculares para detetar diferenças os lados mais e menos afetados destes pacientes.

Baseado nas descobertas apresentadas nos estudos 2 e 3, o quarto e último estudo desta Tese testou se a combinação de um pequeno conjunto de variáveis da marcha e da análise das sinergias musculares poderia prever melhor a função de marcha após um AVC do que utilizando a escala clínica padrão (Avaliação de Fugl-Meyer). Foi possível encontrar algumas variáveis (tanto do lado mais afetado como do lado menos afetado) que se correlacionaram melhor com a função de marcha do que os resultados de predição apresentados pela Avaliação de Fugl-Meyer.

Em conclusão, esta Tese apresenta novas metodologias e métricas que permitem uma avaliação quantitativa de danos sensoriais e motores em pacientes que sofreram uma lesão medular ou um AVC. A utilização de métricas baseadas em EMG e variáveis biomecânicas possibilitaram a avaliação dos mecanismos de recuperação motora, bem como o desempenho após danos neuronais. Estas métricas podem ser exploradas no futuro como um complemento para os procedimentos atuais de avaliação clínica.

Contents

Declaration of Authorship	ii
Acknowledgements	vii
Abstract	ix
Resumo	xi
Contents	xiii
List of Figures	xix
List of Tables	xxi
Abbreviations	xxiii
1 Introduction	1
1.1 Motivations and problem statement	1
1.2 Hypotheses and Research Questions	4
1.3 Thesis Organization	5
2 Insight into sensorimotor control	9
2.1 The Nervous System	9
2.1.1 Neurons	10
2.1.2 Spinal cord and central pattern generators	11
2.1.3 Brain	12
2.2 Muscle activation	12
2.2.1 Human Locomotor System	12
2.2.2 Motor unit action potential	13
2.3 Muscle synergies hypothesis	14
2.3.1 General concepts	14
2.3.2 The case for and against synergies	16
2.3.3 EMG factorization into muscle synergies	18

2.3.3.1	Recording EMG	18
2.3.3.2	Processing the EMG	18
2.3.3.3	Algorithms to extract muscle synergies	20
2.3.3.4	Reconstruction goodness scores	23
2.3.4	Implications for the clinical setting	23
3	Assessment of spinal cord injury and stroke	25
3.1	Biomechanics of normal gait	25
3.1.1	Spatio-temporal parameters	28
3.1.2	Kinematics	28
3.1.3	Kinetics	30
3.2	Instrumented gait analysis systems	33
3.2.1	Spatio-temporal parameters	34
3.2.2	Kinematics	34
3.2.3	Kinetics	35
3.3	General Concepts of Stroke	35
3.3.1	Abnormal gait after stroke	37
3.3.2	Assessment of sensorimotor impairments poststroke	38
3.3.2.1	Clinical scales	39
3.3.2.2	Emerging measures of sensorimotor impairments post-stroke	40
3.4	General Concepts of Spinal Cord Injury	41
3.4.1	Abnormal gait after spinal cord injury	42
3.4.2	Assessment of sensorimotor impairments after spinal cord injury	42
3.4.2.1	Clinical scales	43
3.4.2.2	Emerging measures of sensorimotor impairments after spinal cord injury	45
4	Study 1 - Shared synergies in human walking and cycling	47
4.1	Introduction	48
4.2	Goals	49
4.3	Materials and Methods	49
4.3.1	Subjects	49
4.3.2	Experimental protocol	49
4.3.3	EMG analysis	52
4.3.4	Muscle synergies analysis	53
4.3.5	Statistical analysis	55
4.4	Results	55
4.4.1	Independent analysis of walking	55
4.4.1.1	EMG envelopes	55
4.4.1.2	Muscle synergies	57
4.4.2	Independent analysis of cycling	60
4.4.2.1	EMG envelopes	60
4.4.2.2	Muscle synergies	60
4.4.3	Comparison between walking and cycling	62
4.4.3.1	Cadence	62
4.4.3.2	Direct comparison of muscle synergy vectors	63

4.4.3.3	Cross-reconstruction of EMG envelopes	64
4.4.3.4	Merging of muscle synergy vectors	65
4.5	Discussion	69
4.5.1	Novelty of the work	69
4.5.2	Cadence	70
4.5.3	Electromyographic patterns in walking and cycling	70
4.5.4	Dimensionality of synergistic control	71
4.5.5	Reconstruction quality	72
4.5.6	Functional interpretation of muscle synergies	72
4.5.7	Comparison between walking and cycling	74
4.5.8	Methodological considerations	76
5	Study 2 - Muscle synergies during cycling as a measure of sensorimotor function in SCI	77
5.1	Introduction	78
5.2	Goals	79
5.3	Materials and Methods	80
5.3.1	Subjects	80
5.3.2	Experimental protocol	80
5.3.3	EMG analysis	84
5.3.4	Muscle synergies analysis	84
5.3.5	Statistical analysis	85
5.4	Results	86
5.4.1	Cadence	86
5.4.2	Individual EMG profiles	87
5.4.3	Muscle synergies	87
5.4.3.1	Reconstruction goodness	87
5.4.3.2	Synergy vectors and activation coefficients	91
5.4.4	Stepwise regressions to predict gait performance	94
5.4.5	Stepwise regressions to predict spasticity	95
5.5	Discussion	97
5.5.1	Electromyographic patterns in iSCI patients during cycling	97
5.5.2	Reconstruction goodness scores	98
5.5.3	Similarity of synergy vectors and activation coefficients	98
5.5.4	Predictions of gait performance	100
5.5.5	Predictions of spasticity	100
6	Study 3 - Combining biomechanical and neuromuscular analysis to assess walking symmetry post iSCI	103
6.1	Introduction	104
6.2	Goals	105
6.3	Materials and Methods	105
6.3.1	Subjects	105
6.3.2	Experimental protocol and data collection	106
6.3.3	Data analysis	108
6.3.3.1	Analysis of muscle synergies	109
6.3.3.2	Kinematics	110

6.3.3.3	Spatio-temporal parameters	110
6.3.3.4	Kinetics	111
6.3.4	Statistical analysis	111
6.4	Results	111
6.4.1	Biomechanical differences between sides	111
6.4.2	Synergistic control of gait	112
6.5	Discussion	118
6.5.1	Biomechanical differences between sides	119
6.5.2	Synergistic control of gait	120
6.5.3	Limitations of the study	121
7	Study 4 - Combining biomechanical and neuromuscular analysis to assess walking poststroke	123
7.1	Introduction	124
7.2	Goals	125
7.3	Materials and Methods	125
7.3.1	Subjects	125
7.3.2	Experimental protocol and data collection	126
7.3.3	Data analysis	128
7.3.3.1	Analysis of muscle synergies	128
7.3.3.2	Kinematics	129
7.3.3.3	Spatio-temporal parameters	129
7.3.3.4	Kinetics	129
7.3.4	Statistical analysis	130
7.4	Results	131
7.4.1	Synergistic control of gait	131
7.4.2	Biomechanical differences between sides	131
7.4.3	Correlation between FMA-LE and walking performance indicators	132
7.4.4	Stepwise regressions to predict speed	132
7.4.5	Stepwise regressions to predict % stance of the paretic side	135
7.4.6	Stepwise regressions to predict paretic propulsion	136
7.4.7	Stepwise regressions to predict paretic step ratio	136
7.5	Discussion	136
8	Concluding Remarks	139
8.1	General Conclusions	140
8.1.1	Study 1	140
8.1.2	Study 2	141
8.1.3	Study 3	141
8.1.4	Study 4	142
8.2	Future Work	142
8.3	Technical Contributions	143
8.4	Publications	144
	Bibliography	147

A Muscular system	167
B ASIA Scale	169
C SynergiesLAB	171
D MATLAB code to implement NNMF	173
E Informed Consents from the Ethical Committees	177
E.1 Study 2	177
E.2 Study 3	177
E.3 Study 4	177

List of Figures

2.1	Role of brain and the spinal cord in human walking.	13
2.2	Conceptual model of motor coordination, in which motor neurons represent the motor output of the nervous system and activate muscles.	15
2.3	Example of sEMG signal processing.	19
2.4	Representation of matrices EMG_0 , W and H	21
2.5	Process of estimating the activation coefficients (matrix H) and synergy vectors (matrix W) from eight experimental EMG signals.	22
3.1	Main divisions of the human gait cycle.	26
3.2	Representation of step length and step width.	28
3.3	References for human kinematics.	29
3.4	Comparison of time-normalized kinematics between the right and left side of a healthy subject.	31
3.5	3D representation of ground reaction forces (GRF).	32
3.6	GRF acting on a healthy subject during walking.	33
4.1	MOTOMed viva2, Reck, Betzenweiler, Germany.	50
4.2	EMG recordings during a walking trial and a pedaling trial.	51
4.3	Representation of the merging process using linear combinations of synergy vectors from walking to reconstruct synergy vectors from cycling.	55
4.4	Group averaged EMG envelopes of the eight recorded muscles, for each of the four studied conditions in walking.	56
4.5	Variability accounted for (VAF_{total}) values according to the number of muscle synergies used to reconstruct EMG envelopes, for each speed condition in walking and cycling.	57
4.6	Variability accounted for (VAF_{muscle}) values for each muscle.	58
4.7	Reconstruction of concatenated EMGs from the 8 subjects with the NNMF algorithm.	59
4.8	Group averaged EMG envelopes of the eight recorded muscles, for each of the four studied conditions in cycling.	61
4.9	Individual example of the cross-reconstruction of the cycling EMG envelopes at MWS condition.	66
4.10	Quality of cross-reconstruction of EMG envelopes.	67
4.11	Cycling synergy vectors reconstructed as a merging (linear combination) of walking synergy vectors for MWS condition.	69

5.1	EMG recordings during cycling trials of a iSCI patient who performed the cycling trials on her own wheelchair.	82
5.2	Schematic representation of the steps included in the stepwise multiple regressions to predict motor performance or spasticity scales scores.	86
5.3	Group average EMG envelopes of the 13 recorded muscles for each of the 4 speeds during cycling.	88
5.4	Comparison of mean EMG envelopes from iSCI patients and the mean EMG envelopes from the healthy group for the 13 recorded muscles for each of the 4 speed conditions.	89
5.5	Variability accounted for (VAF_{total}) and coefficient of determination (r^2), according to the number of synergies, for each of the 4 speeds.	90
5.6	Reconstruction of EMG envelopes in four speeds using concatenated data from the 10 healthy subjects, as well as individual data from a patient with spasticity and a patient without spasticity.	92
5.7	Stepwise multiple linear regressions using reconstruction goodness indexes as predictors of gait performance.	95
5.8	Multiple linear regressions using similarity scores as input to predict the score of some spasticity scales.	96
6.1	Incomplete SCI patient walking during one trial.	108
6.2	Biomechanical indicators that showed significant differences between most and less affected side in iSCI patients.	114
6.3	Reconstruction of EMG envelopes using concatenated data from the 8 healthy subjects and 4 muscle synergies.	117
6.4	Muscle synergies components for the iSCI patients.	119
7.1	Poststroke patient walking during one trial.	127
7.2	Schematic representation of the steps included in the stepwise multiple regressions to predict walking performance indicators.	130
7.3	VAF_{total} and r^2 , according to the number of synergies, for both paretic and non-paretic sides.	131
7.4	Kinematic variables that showed significant differences between paretic and non-paretic side.	134
7.5	Spatio-temporal and kinetic variables that showed significant differences between paretic and non-paretic side.	135
A.1	Muscular system.	167
B.1	Neurological classification of spinal cord injury proposed by the American Spinal Injury Association (ASIA).	169

List of Tables

3.1	American Spinal Injury Association (ASIA) Impairment Scale (AIS). . . .	43
4.1	Normalized scalar product between matching synergy vectors from walking and cycling.	63
4.2	Normalized scalar product between the three synergy vectors from cycling and the three most similar synergy vectors from walking.	64
4.3	Representation of the merging coefficients.	68
4.4	Similarity between reconstructed synergy vectors resulting from the merging process and corresponding synergy vectors of cycling.	68
5.1	Individual iSCI patients' description.	81
5.2	Amount of physical assistance needed, gait performance and spasticity syndrome scores of iSCI patients.	82
5.3	Normalized scalar product between matching muscle synergy vectors from matrices W and the matrix W_0 , considering the set of 13 muscles.	93
5.4	Normalized scalar product between matching muscle synergy vectors from matrices W and the matrix W_0 , considering the set of 8 muscles.	93
6.1	Individual iSCI patients' information.	106
6.2	Comparison of kinematic indicators between most and less affected sides of iSCI patients.	113
6.3	Comparison of spatio-temporal and kinetic indicators between most and less affected sides of iSCI patients.	115
6.4	Number of muscle synergies and VAF_{total} values obtained for the three groups.	116
6.5	Similarity of synergy vectors ($W \cdot W_0$) and activation coefficients ($H \cdot H_0$) with the control group (CG) reference, using four synergies to reconstruct the EMG envelopes of the less affected side (iSCI) and the most affected side (iSCIa) of iSCI patients.	118
7.1	Individual description of nine hemiparetic stroke subjects.	126
7.2	Comparison of quality of reconstruction indicators between paretic and non-paretic side.	132
7.3	Comparison of biomechanical indicators that showed significant differences between paretic and non-paretic side.	133
7.4	Spearman's correlations between Fugl-Meyer assessment for lower extremity (FMA-LE) and walking performance indicators.	134

Abbreviations

6MWT	6-Minute Walk Test
10MWT	10-Meter Walk Test
ADLs	Activities of daily living
AIS	ASIA Impairment Scale
AL	Adductor Longus
AP	Anteroposterior
ASIA	American Spinal Injury Association
BF	Biceps Femoris
BWS	Body weight support
CG	Control group
CNS	Central nervous system
CPGs	Central pattern generators
CVA	Cerebrovascular accident
EMG	Electromyography
FAC	Functional Ambulatory Classification
FES	Functional electrical stimulation
FMA	Fugl-Meyer Assessment
FMA-LE	Fugl-Meyer assessment for lower extremity
GaL	Gastrocnemius Lateralis
GaM	Gastrocnemius Medialis
GMa	Gluteus Maximus
GMe	Gluteus Medius
GRF	Ground Reaction Force

IMUs	Inertial Measurement Units
iSCI	Incomplete spinal cord injury
MAS	Modified Ashworth Scale
MUAP	Motor unit action potential
NNMF	Non-negative matrix factorization
PNS	Peripheral nervous system
PP	Paretic propulsion
PSR	Paretic step ratio
RF	Rectus Femoris
Sar	Sartorius
SCATS	Spinal Cord Assessment Tool for Spastic Reflexes
SCI	Spinal Cord Injury
SCIM	Spinal Cord Independence Measure
Sem	Semitendinosus
sEMG	Surface electromyography
Sol	Soleus
TA	Tibialis Anterior
TFL	Tensor Fascia Latae
TUG	Timed Up and Go
VL	Vastus Lateralis
VM	Vastus Medialis
WISCI II	Walking Index for Spinal Cord Injury

Introduction

This thesis presents the work developed during the past four years and three months in the scope of the Doctoral Program in Biomedical Engineering at University of Minho, Portugal. This work addresses the field of neurorehabilitation and its ultimate goal is to generate meaningful quantitative metrics to assess gait disorders in the clinical setting, with particular interest in stroke and spinal cord injury (SCI) patients. To achieve that goal, it is first necessary to advance neurophysiological and biomechanical conceptual foundations to understand motor control of human walking. The successful design of appropriate protocols and the generation of novel quantitative metrics for the assessment of sensorimotor impairments may improve future rehabilitation treatments tailored to individual unique needs of the aforementioned patients.

The Ph.D. project was mostly conducted in the framework of the HYPER and BETTER projects, both coordinated by CSIC's (*Consejo Superior de Investigaciones Científicas*, Madrid, Spain) Neural Rehabilitation Group. Trials with patients were performed at National Paraplegia Hospital (Toledo, Spain) and Faculty of Health Sciences - Rey Juan Carlos University (Madrid, Spain), which worked as partners in these projects.

1.1 Motivations and problem statement

Nowadays there is a high percentage of elderly people ([Barroso, 2011](#)) and the world population is aging at a at fast rate ([Nations, 2013](#)). Since 1950 the average age of population has increased from 28 to 32 years old and is expected to be 42 years old by 2100 ([Nations, 2013](#)). This rise of population aging rate has profound implications on healthcare, namely the inherent risks associated with the aging, like the occurrence of a stroke ([Russo et al., 2011](#)) or SCI (associated with falls) ([Jain et al., 2015](#)). Stroke and

SCI are the most common causes of paralysis and paresis, with an estimated prevalence of 12,000 per million and 800 per million, respectively (De Mauro et al., 2011). Neurological disabilities after stroke or SCI events may result in impaired walking, preventing patients from having healthy-like participation in daily activities.

Walking is a very complex function, as it involves the coordination of several muscles and its correct activation (Rosa et al., 2014). Walking functioning is usually affected in people with impairments of central nervous system (CNS) (Rosa et al., 2014). Consequently, one of the prime goals of people recovering from stroke or SCI is to recover the ability to walk again (Nadeau et al., 2011). Motor neurorehabilitation is an iterative, continuous and active process, which can be divided into four main steps: assessment, goals setting, intervention and evaluation of the results. The assessment step of neurorehabilitation has traditionally been done based on qualitative methods (classic clinical scales) or subjective assessment from physiotherapists (based on visual observation) (Safavynia et al., 2011). Despite being less time-consuming and cheaper than techniques requiring instrumentation (*e.g.*, 3D gait analysis), these assessment techniques may lead to low inter-rater reliability and, as a consequence, to inadequate interventions. In addition, clinical tests focused on behavioral outcomes provide little information about the underlying differences between healthy and impaired nervous system (Safavynia et al., 2011). The correct understanding of the specific patient's impairments is crucial to prescribe effective customized treatments. To improve diagnostic procedures and treatment options, motor neurorehabilitation should be driven by more reliable metrics that allow a quantitative assessment of patients' performance and recovery.

Recent researches on pathological conditions strongly recommend gait analysis to adequately assess and follow up patients and to support clinical decision on the best treatment (Nadeau et al., 2011). Clinical gait analysis involves a variety of techniques including kinematic or joint motion measurements, kinetic or joint torque assessment, electromyographic (EMG) measurements and video analysis (DeLisa and States, 1998). Measures derived from gait analysis provide detailed and quantitative description. This might further be used to extract important information to select a task-oriented approach that might enhance therapeutic response, which cannot be provided by clinical evaluation alone (Nadeau et al., 2011).

Some researchers may argue that behavioral outcomes like function or quality of life are sufficient outcomes. Others may argue that improvements in gait are more important clinical outcomes (Wright and Theologis, 2015). The main assumption behind this Ph.D. research is that improvements in gait should be a main goal in patients' rehabilitation. In that sense, measures derived from gait analysis will be explored as potential metrics to objectively assess gait impairments.

In the past ten years, the idea that EMG features provide useful information concerning brain motor control strategies has emerged (Barroso et al., 2013). Specifically, muscle synergies extracted with computational techniques have been proposed as a potential technique to measure motor recovery following therapeutic interventions (Routson et al., 2013). Muscle synergies, also known as motor modules, are groups of co-activated muscles responsible for the control of a task in different conditions by adapting a small number of neural parameters (d’Avella and Lacquaniti, 2013) (Steele et al., 2013). In the past decade, experimental results in animals and humans (Cheung et al., 2012) (d’Avella and Bizzi, 2005) (De Marchis et al., 2013) (Dominici et al., 2011) (Gizzi et al., 2012) (Hug et al., 2011) (Ivanenko et al., 2005) (Moreno et al., 2013) (Ting and Macpherson, 2005), as well as simulations (Allen and Neptune, 2012) (Neptune et al., 2009) supported the hypothesis that biomechanical tasks reflect synergistic control of muscles.

According to Safavynia et al. (2011), muscle synergies may offer new insight into the underlying motor strategies responsible for impaired locomotion. This can be done after identifying a set of muscle synergies responsible for the control of walking in healthy people (Clark et al., 2010). If muscle synergies are the responsible for specific biomechanical functions, it is critical to understand if patients with impaired walking have access to the same muscle synergies of healthy subjects or if these muscle synergies are also impaired (Ting and McKay, 2007). Thus, muscle synergies will be also explored in this work as potential metrics to objectively assess sensorimotor impairments in SCI and stroke patients.

Frequently, patients lack the required muscle strength to walk during the early stage of rehabilitation, even with an amount of body weight support. Modern electronically braked cycle ergometers provide the necessary assistance and allow for unlimited repetitions, which enables the training to be executed at home. Thus, cycling can be a potential tool to deliver therapies from the acute rehabilitation phase. Rehabilitation treatments based on cycling exercise alone and combined with feedback have shown promising results (Barbosa et al., 2015). Due to similarities in kinematics and muscle control with walking (both are cyclical tasks, with flexion and extension movements of hip, knee and ankle joints, requiring activation of agonists and antagonists muscles), cycling may be explored as a novel framework for the assessment of motor performance. In fact, Zehr et al. (2007) proposed a “common core hypothesis” suggesting that different forms of rhythmic movements such as cycling, stepping and walking may share common neuromuscular patterns.

Given the aforementioned limitations and drawbacks of traditional techniques used to assess sensorimotor impairments, the general motivation for this work is to develop novel tools and metrics to continuously assess patients' rehabilitation. In particular, cycling will be explored as a novel framework and a combination of neurophysiological and biomechanical measurements will also be explored toward the design of quantitative metrics. The main goal can be split into two sub-goals: 1) advancing neurophysiological and biomechanical understanding of motor control principles of locomotor functions; 2) generating meaningful metrics to quantitatively assess gait disorders in the clinical setting. Due to their major prevalence among the causes of paralysis and paresis, two main groups of patients were detected as potential participants to be evaluated with this approach:

1. Poststroke patients (either ischemic or hemorrhagic), with a motor disability, typically hemiparesis affecting lower (and upper) limbs.
2. Incomplete spinal cord injury (iSCI) patients, presenting walking disabilities but maintaining acceptable upper limb control.

1.2 Hypotheses and Research Questions

The Ph.D. Thesis is guided by the conceptual hypothesis that the use of quantitative metrics based on electromyography and biomechanical features will give a new insight into the motor recovery mechanisms and performance outcomes after neural damage. To tackle the conceptual hypothesis, four distinct but complementary studies were performed, being each one associated to a specific hypothesis:

Hypothesis I. In healthy participants, walking and pedaling tasks share common neural mechanisms. The confirmation of this hypothesis will justify the use of pedaling exercise as a novel tool to assess walking in people with impaired neuromotor control. In this study, muscle synergies were used as the main indicators of neuromotor activity. The scientific questions associated to this hypothesis are:

- How does the nervous system control human walking and cycling?
- Do pedaling and walking share similar synergies?

Hypothesis II. Novel metrics based on the analysis of muscle synergies during pedaling can provide detailed quantitative assessment of sensorimotor impairments after iSCI. In particular, muscle synergies components can predict the scores of traditional

clinical scales. As in the case of Study 1, the confirmation of this hypothesis will also contribute to justify the use of cycling as a novel and convenient tool to assess walking in iSCI patients, specially at the first stages of recovery. The scientific questions associated to this hypothesis are:

- Do iSCI patients preserve a synergistic control of pedaling?
- Do healthy controls and iSCI patients share some common synergies during pedaling?
- Can synergies give new insight on the sensorimotor impairments of iSCI patients?

Hypothesis III. Muscle synergies and biomechanics are distinct in iSCI patients if compared with healthy controls, and are also different between sides. The confirmation of this hypothesis will support the importance of studying bilateral control of lower limb functions in iSCI patients, as well as the use of muscle synergies as a complementary tool to clinical scales. The scientific questions associated to this hypothesis are:

- Do healthy controls and iSCI patients have similar synergies during walking?
- Do iSCI patients present similar muscle synergies and biomechanical features between the two lower limbs during walking?

Hypothesis IV. The combination of gait features with the analysis of muscle synergies will improve the assessment of stroke-related disorders. Specifically, these set of measures will correlate better with walking performance indicators than the gold standard clinical scales like Fugl-Meyer Assessment (FMA), which is one of the most used measures of motor impairment. The scientific questions associated to this hypothesis are:

- Do biomechanical and synergistic variables differentiate between the affected and unaffected side?
- Which of these variables predict the score of walking performance indicators?
- Is this prediction better than the prediction made by FMA?

1.3 Thesis Organization

This PhD Thesis is composed by eight chapters and is organized as follows:

- Chapter One introduces the reader to the main limitations and drawbacks of traditional techniques used in the clinical setting to assess sensorimotor impairments in patients who suffered a stroke or iSCI. This Chapter continues with the overview of the research work, as well as the hypotheses and research questions presented by each of the four distinct studies performed.
- Chapter Two presents the main neurophysiological mechanisms underlying human walking, which is fundamental to understand the effects of neural injury for the impaired walking. This Chapter includes the description of the hypothesis of muscle synergies, which will be the basis of the four studies presented in this Thesis.
- Chapter Three gives an overview on the biomechanics of normal gait, as well as the most used instrumented gait analysis systems. This Chapter also presents the clinical scales used for the assessment of sensorimotor mechanisms underlying impaired walking in patients that suffered a stroke or a iSCI.
- Chapter Four presents the first study of this Thesis, in which similar features of walking and cycling were investigated under the muscle synergies hypothesis. Results provide evidences for common neuromuscular mechanisms of the two motor tasks. Due to similarities in kinematics and muscle control, cycling was explored as a novel framework.
- Chapter Five presents the second study of this Thesis, in which cycling was explored as a novel tool to assess sensorimotor impairments in iSCI patients, based on the findings presented in the previous Chapter. Results show that the analysis of muscle synergies during pedaling can provide detailed quantitative assessment of sensorimotor impairments after iSCI. This analysis can complement current assessment procedures.
- Chapter Six presents the research performed on Study 3, in which the analysis of muscle synergies was combined with the study of biomechanics of each side of iSCI patients, in order to detect differences between the most and less affected side. The results may be used to improve customized therapy delivered to iSCI patients.
- Chapter Seven presents the research performed on Study 4, which tested whether the combination of a small set of gait features and the analysis of muscle synergies could better predict walking function poststroke than the gold-standard scale (Fugl-Meyer Assessment, FMA). By using some predictors from each side (most and less affected side), it was possible to better predict walking function than by using FMA.

-
- Finally, Chapter Eight summarizes the main conclusions of the present work. This Chapter also provides some suggestions for future research. The final part of the Chapter presents the main scientific and technical contributions resulting from this Ph.D. Thesis.

Insight into sensorimotor control

The accurate execution of activities of daily living (ADLs), including walking, strongly relies on the proper functioning of the nervous and the musculoskeletal system. In order to understand gait control after a neurological injury, it is of primary importance to study and understand how the nervous system controls normal gait, and in particular how it copes with the redundancy of the musculoskeletal system.

When we perform a movement, as simple as it may seem, there is always a co-ordinated activation of a large set of muscles. The apparent simplicity of movement execution may hide the complexity of its control. The activation of each muscle produces a torque in one or more joints. Given that there are more muscles than joints, a variety of combinations of muscle activation patterns can produce the same functional movement. That is, the system is redundant. A long-standing idea is that the central nervous system (CNS) controls muscle activation by using a synergistic organization constituted by basic control elements, called synergies. The main neurophysiological mechanisms underlying human walking, as well as the hypothesis of muscle synergies are described in this chapter.

2.1 The Nervous System

The nervous system is the part of human body responsible for the coordination of voluntary and involuntary actions, as well as the maintenance and regulation of body functions, through the transmission of signals between different parts of the body ([Seeley et al., 2008](#)). Nervous system can be divided into central nervous system (CNS) and peripheral nervous system (PNS).

The CNS consist of the brain and the spinal cord, in continuity one with the other by the occipital bone (Tortora and Bryan, 2006). The CNS plays a major role on the proper functioning of mammal locomotion.

The PNS is the part of nervous system outside the CNS. It comprises sensory receptors¹, nerves² and ganglia³, and its main role is the connection between the CNS and the different parts of human body. The PNS comprises two main divisions: the afferent or sensory division, responsible for transmitting electrical signals (called action potentials) from the sensory receptors to the CNS; the efferent or motor division, responsible for transmitting action potentials from the CNS to organs, such as muscles and glands.

2.1.1 Neurons

The nervous system is constituted by neurons and non-neural cells. The basic structural units of the nervous system are the neurons, which receive stimuli and transmits action potentials to other neurons or organs. They are organized as complex networks responsible for performing the functions of the nervous system (Seeley et al., 2008). Each neuron is constituted by a cell body (or soma) and two types of cell elongations: dendrites and axons.

Dendrites are filaments of the neurons that receive information in the form of nervous stimulus. When stimulated, they generate small electrical current which is then conducted to the cell body. The axon is the part of the neuron responsible for conducting action potentials from the cell body to the axon terminals, where they stimulate the release of neurotransmitters (Seeley et al., 2008).

Neurons are classified according to their function, considering the direction of the action potentials they conduct. Thus, afferent (or sensory) neurons conduct action potentials to the CNS and efferent (or motor) neurons conduct action potentials from the CNS to muscles or glands. Interneurons conduct action potentials from one neuron to another, within the CNS (Sherwood, 2008).

There are two types of motor neurons: upper motor neurons and lower motor neurons. Upper motor neurons are present in the motor cortex. These neurons connect with lower motor neurons in the brain and the spinal cord. Lower motor neurons connect with the muscles on face, chest and limbs, exerting direct control over muscle contraction.

¹Sensory receptors are specialized nerve endings cells, which may detect light, sound, pressure, pain, among other stimuli. These receptors may be located in the skin, muscles, joints, eyes and ears, for example.

²Nerves are sets of axons and dendrites, linking the CNS to the sensory receptors, muscles and glands. Definitions and descriptions of axons and dendrites are given in subsection 2.1.1.

³Agglomerations of neural cellular bodies located outside the CNS.

Thus, upper motor neurons are involved in the initiation of voluntary movements and the maintenance of appropriate muscle tone. If the upper motor neurons are damaged, the limbs will become spastic and the reflexes will be exaggerated. On the other hand, if the lower motor neurons are damaged, muscles will become weak and reflexes may disappear ([Mitsumoto, 2009](#)).

2.1.2 Spinal cord and central pattern generators

Spinal cord is of main importance for the global functioning of the nervous system, being the link between the brain and the PNS below the head level, integrating information the PNS receives and producing responses through reflex mechanisms. Spinal cord is also of great clinical importance, because it is a typical site of traumatic injury and a locus for many disease processes ([Seeley et al., 2008](#)).

Two consecutive lines of nerve roots (one for each side of the body) are present in the spinal cord and there are 31 pairs of spinal nerves. Spinal cord is divided into four regions, designated according to the spine location at which their nerves enter and leave: cervical (C), thoracic (T), lumbar (L) and sacral (S).

The role of the spinal cord in locomotor control has been mainly studied in animals ([Verma et al., 2012](#)). Mammals' locomotion is achieved by rhythmic activity of the central pattern generators (CPGs). CPGs have been described as networks of nerve cells that generate movements and include the required information to activate different motor neurons sequentially and with the necessary magnitude to generate motor patterns ([Belda-Lois et al., 2011](#)). CPGs are considered innate, despite the existence of further adaptation and improvement with experience.

The three fundamental principles that characterize CPGs are:

- (I) ability to generate rhythmic activity independent of sensory inputs;
- (II) the presence of a well-defined neuronal circuit;
- (III) the existence of influences from central and peripheral system capable of modulating these patterns.

Bipedal locomotion, typical of humans, is quite different from quadrupedal locomotion. However, CPGs are also hypothesized to exist in humans, as they are influenced by peripheral and central inputs ([Pons et al., 2013](#)).

2.1.3 Brain

Despite the considerable scientific progress made during the last years, we are still far from understanding in detail how human brain works.

It is common sense that brain injuries profoundly affect human gait (Reisman et al., 2007), which demonstrate the great cortical involvement in human walking. For example, in those patients who suffer a stroke, functions of cortex become weakened, while the spinal cord functions remain preserved. Thus, it can be argued that brain plays an extremely important role in the control of human gait, when compared with animals. As so, experimental data obtained in animals studies have to be analyzed with caution when it comes to studying the mechanisms controlling human gait (Verma et al., 2012). Current researches do not suggest any exclusive control of gait by the spinal cord neither that motor cortex alone is responsible to activate muscles during walking (Bowden et al., 2010).

It has been demonstrated the importance of peripheral sensory information (Field-Fote and Dietz, 2007) and inputs from motor cortex (Yang and Gorassini, 2006) to modulate CPGs' functions and particularly to lead to plasticity mechanisms after a brain injury. Thus, the hypothesis headed by scientific community is that human locomotion is the result of an interplay between the brain and the spinal cord (see Figure 2.1). Basic motor patterns of locomotion seem to be generated in the spinal cord, while the refinement of the control of those patterns is performed by different brain areas (Pons et al., 2013) (Belda-Lois et al., 2011).

2.2 Muscle activation

CNS controls human movements by generating central commands that activate muscles. The resulting muscle activation is directed to tendons, which, in turn, transmit forces to the connecting bones, pulling on them and causing movement.

2.2.1 Human Locomotor System

Locomotor system (also known as musculoskeletal system) is formed by the skeletal system and the muscular system. This system is highly optimized for efficient locomotion (Pons et al., 2013).

Skeletal system, made of 206 bones in adults, provides support to the body and protection for vital organs. It works together with the muscular system to move the

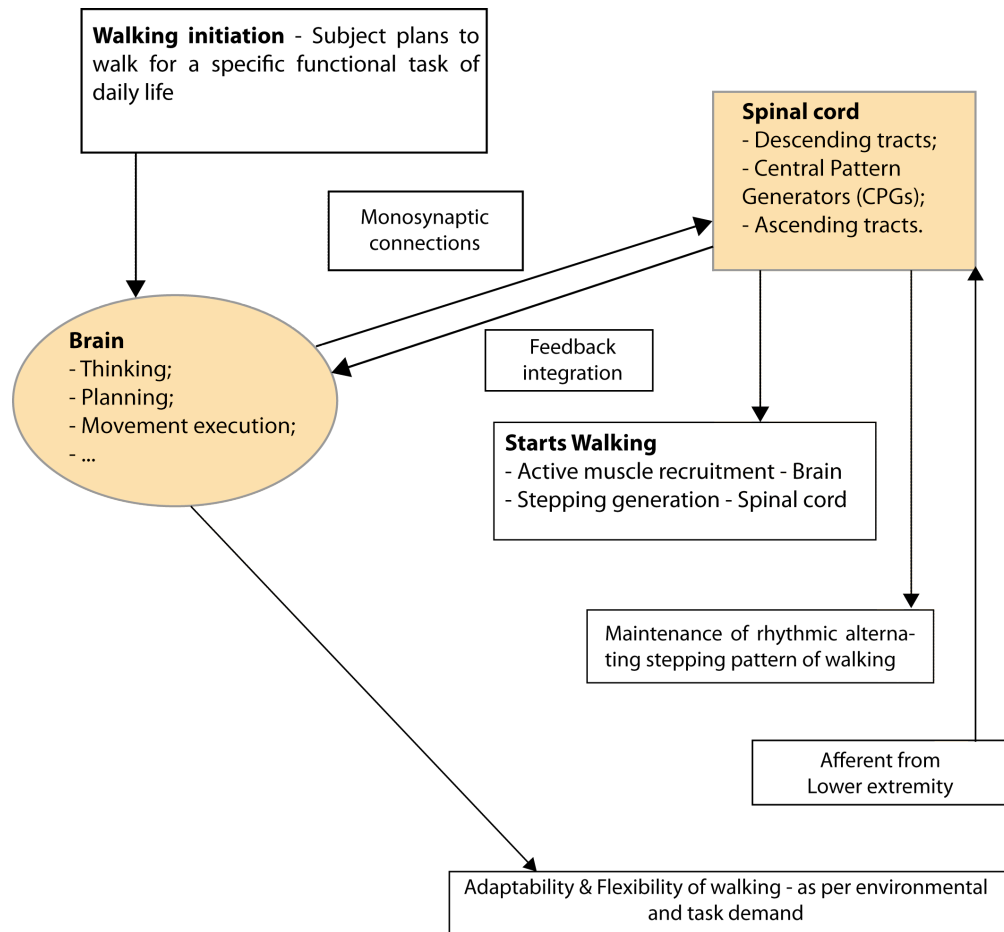


FIGURE 2.1: Role of brain and the spinal cord in human walking. Adapted from Verma et al. (2012).

body (Haywood, 2008). Skeletal muscles are those used for locomotion, for example, and their main function is to move the bones of the skeleton, which turn them into the “engines of the gait”. There are more than 600 skeletal muscles in humans (Lippincott, 2002), allowing us to move and stand erect. From all the skeletal muscles, there are 28 major muscles involved in the human gait (Bogey et al., 1992). Most of these major muscles for locomotion are represented in Appendix A.

2.2.2 Motor unit action potential

Central commands are sent to motor neurons innervating muscles through descending pathways. Motor units, made up of a motor neuron and the muscle fibers it innervates, are the smallest elements than can be controlled to produce muscle activation (Soderberg, 1992).

Every time a motor neuron is activated, an action potential goes in direction to the neuromuscular junctions, being propagated in both directions of muscle fibers towards the tendons (Barroso et al., 2013). The resulting muscle force is the result of the sum of small forces individually generated in each muscle fiber. Motor unit action potential (MUAP) is the sum of these muscle fiber action potentials. Neural drive is the ensemble of action potentials fired by spinal motor neurons (Farina et al., 2010).

2.3 Muscle synergies hypothesis

Motor coordination involves several regions of the CNS, including the motor cortex, red nucleus, basal ganglia, brainstem, cerebellum, peripheral sensory system and spinal neurons. The neural drive ultimately converge onto motor neuron pools that are each dedicated to controlling a single muscle of the body (Levine et al., 2014). However, the musculoskeletal system is redundant, as different combinations of muscle activation patterns may produce the same functional movements. The final result of individual muscle activation depends on the dynamic state of all body segments. Therefore, muscle activation must be thought as task-specific, *i.e.*, muscles activated in a coordinate way to execute a given task (Kirtley, 2006) (Bogey et al., 1992) (Prilutsky, 2000).

Given the redundancy of the musculoskeletal system, a long-standing idea is that CNS controls muscle activation by using a synergistic organization constituted by basic control elements, called synergies (also known as motor modules), which are combinations of motor neurons activation (Ivanenko et al., 2004) (Clark et al., 2010) (Neptune and McGowan, 2011) (Gizzi et al., 2011) (Levine et al., 2014) (Ting et al., 2015).

2.3.1 General concepts

In 1967, Nikolai Bernstein proposed the existence of muscle synergies as a simplified strategy of motor control (Bernstein, 1967). A muscle synergy is defined as a functional set formed by the co-activation of different muscles recruited by a common activation signal. Every muscle can belong to different synergies (Ivanenko et al., 2004) (Clark et al., 2010) (Gizzi et al., 2011). This synergistic control is represented in Figure 2.2.

Muscle synergies can be thought of as neural networks organized at the spinal or brainstem level, with each synergy specifying a weighted profile of activation for a set of muscles. Depending on the sensory information received, activation signals generated in higher neural centers selectively activate a repertoire of muscle synergies, resulting in a weighted distribution of the neural drive to different muscles (Barroso et al., 2014).

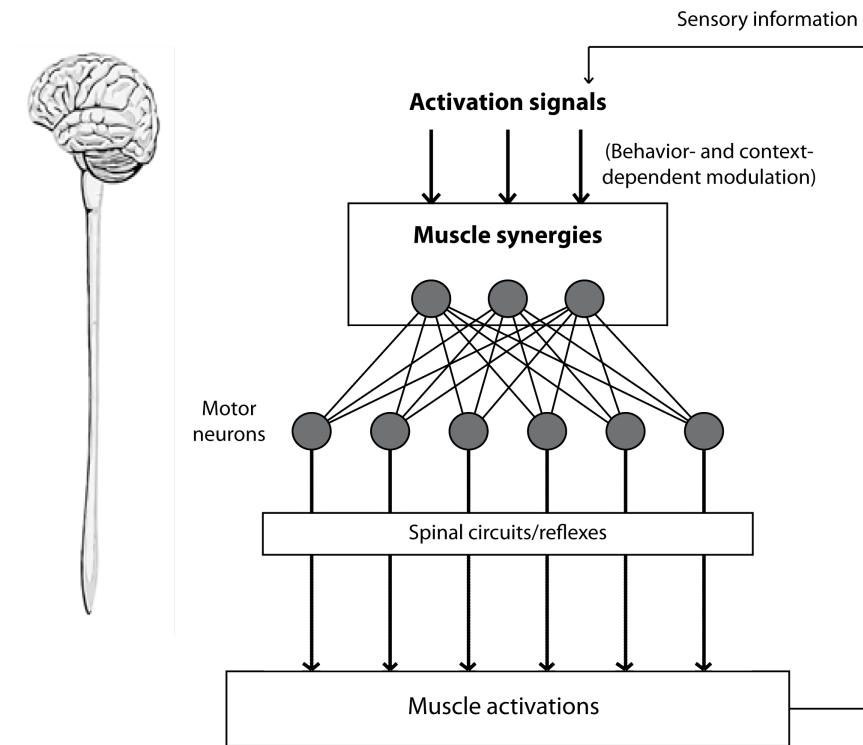


FIGURE 2.2: Conceptual model of motor coordination, in which motor neurons represent the motor output of the nervous system and activate muscles. Muscle activation patterns appear to be a superposition of muscle synergies activation and local circuitry, both subject to modulation dependent on the task and the context. Adapted from [Safavynia et al. \(2011\)](#).

The concept of muscle synergy has been used with different meanings, depending on the context. In neurorehabilitation, it refers to the stereotyped muscle activation observed after lesions and due to a loss of independent control, which results in abnormal and less flexible movement repertoires ([Howle, 2002](#)). In contrast, in motor neuroscience it indicates a strategy to simplify the motor control, in which a set of muscles are organized in functional groups ([Clark et al., 2010](#)). In the last fifteen years, the neuroscientific perspective has gained more and more relevance and will also be adopted along this Thesis. More specifically, this Thesis will adopt the hypothesis of “synchronous synergies” ([Tresch and Jarc, 2009](#)), in which groups of muscles are activated in a fixed balance to produce motor tasks. Within this hypothesis, every time a synergy is activated, all the muscles within that same synergy will be active.

[Ting et al. \(2015\)](#) proposed five neuromechanical principles underlying muscle synergies:

- (1) *Motor abundance*. There are several motor solutions that can produce similar or functionally equivalent behaviors. Thus, there is no better motor pattern,

but different solutions. This ability underlies the adaptability and robustness of biological systems.

- (2) *Motor structure*. For the same task, there are preferable movements than others. For instance, movements requiring less energy or neural control to be executed will be preferred. These movements, which are facilitated by body structure, shape the permissible structure and variability of muscle synergies.
- (3) *Motor variability*. If the effect on motor output is low, then the repertoire of solutions for motor control will be higher, *i.e.*, high variability in motor control will be found for those tasks without many constraints and biomechanical affordances.
- (4) *Individuality*. For the same task, each person may have his/her own synergies, shaped by experience and depending on evolutionary, developmental, and learning processes. This explains the inter-individual variability observed in muscle synergies among healthy subjects.
- (5) *Multifunctionality*. Muscle synergies may be combined in different ways to produce a wide range of motor tasks. Trial-by-trial variability can be explained by combining muscle synergies in different ways, which facilitates adaptation and learning.

2.3.2 The case for and against synergies

Several studies have examined the hypothesis that CNS produces movement through the flexible combination of muscles synergies, providing evidence both in support and in opposition to it (Tresch and Jarc, 2009). Whether muscle synergies are directly related to specific kinematic or kinetic goals (Ivanenko et al., 2003) or are shared between different motor tasks is still under investigation. In fact, it is very difficult to prove or challenge the muscle synergies hypothesis.

Low dimensionality of electromyography (EMG) signals may reflect factors such as biomechanical and task constraints, reflex control, or experimental protocols, rather than a neural control strategy (Kutch and Valero-Cuevas, 2012). These constraints require some groups of muscles to be co-activated to execute a given task (Steele et al., 2015). Based on analyses of the variability in motor patterns, some studies have provided evidence against muscle synergies. For instance, by analyzing the endpoint fingertip force fluctuations during isometric force generation at a multiple degree-of-freedom joint to examine muscle recruitment properties, Kutch et al. (2008) suggested an independent recruitment of individual muscles within the task, rather than the control of muscle synergies. According to Valero-Cuevas et al. (2009), muscle synergies cannot accurately

describe muscle activity when applying force with the index finger. These findings can be explained by the motor variability principle described by [Ting et al. \(2015\)](#). For isometric force production tasks like those analyzed by [Kutch et al. \(2008\)](#) and [Valero-Cuevas et al. \(2009\)](#), the degree of variation in muscle activity in the finger is relatively constrained, allowing for little variability.

On the other hand, evidence for the hypothesis of muscle synergies has been mainly indirect, based on the observation of low dimensionality in the muscle activity patterns recorded during a variety of motor behaviors ([Bizzi and Cheung, 2013](#)) ([Cheung et al., 2012](#)) ([Chvatal and Ting, 2013](#)) ([Clark et al., 2010](#)) ([Moreno et al., 2013](#)) ([Routson et al., 2013](#)) ([Torres-Oviedo and Ting, 2007](#)). Studies performed in animal models with monkeys ([Overduin et al., 2012](#)), cats ([Yakovenko et al., 2011](#)) and frogs ([Hart and Giszter, 2010](#)) support that activation signals are expressions of neural activities. [Bizzi et al. \(1991\)](#) found that the co-stimulation of two different loci in frogs produced a force field very similar to the summation of the resulting force fields from independent stimulus of each locus. Additional evidence for the muscle synergies hypothesis has been given by using biomechanical models to demonstrate that complex behaviors can be produced using combinations of muscle synergies ([Pons et al., 2013](#)). For instance, [Neptune et al. \(2009\)](#) used muscle synergies extracted from real EMG data from human locomotion to drive a complex musculoskeletal simulation of the human leg during locomotion, obtaining effective locomotion with only minor adjustments. Using these biomechanical models, [Neptune et al. \(2009\)](#), [Neptune and McGowan \(2011\)](#) and [McGowan et al. \(2010\)](#) demonstrated that four muscle synergies are capable of producing different locomotion activities, such as normal walking, walking with body weight support (BWS), walking with body mass increased/decreased, kicking and stepping. Each synergy was found to be associated with specific biomechanical task. Interestingly, some of these synergies are available at birth, with additional synergies being created throughout development and refined with age ([Dominici et al., 2011](#)). Additionally, muscle synergies are very similar between body sides ([Clark et al., 2010](#)) ([Gizzi et al., 2011](#)).

More direct evidence for the muscle synergies hypothesis might come by testing an experimental manipulation that can distinguish a synergistic control from a non-synergistic one ([d'Avella and Pai, 2010](#)). In this regard, [Berger et al. \(2013\)](#) manipulated the mapping between muscle activations and hand forces that could make such a distinction. Results showed that learning to perform a novel task is faster if it can be achieved by altering recruitment of a smaller number of muscle synergies rather than learning new control strategies for individual muscles, which support the existence of muscle synergies.

2.3.3 EMG factorization into muscle synergies

Researches on muscle synergies are usually based on statistical analysis of surface electromyography (sEMG) during specific behaviors (Tresch and Jarc, 2009). First, EMGs are recorded from a large number of muscles during the behavior (or more than one behavior) under analysis (*e.g.*, walking or cycling); secondly, it is performed a computational analysis using some factorization algorithm to identify a set of muscle synergies from EMGs; thirdly, it is usual to evaluate whether the recorded EMGs can be well described as a combination of the identified synergies; and fourthly, muscle synergies can be associated with specific biomechanical tasks (Tresch and Jarc, 2009).

2.3.3.1 Recording EMG

Surface EMG is the electrical recording of muscle activity using surface electrodes. As muscle fibers of a given motor unit are scattered randomly on the muscle, the recorded signal is reasonably representative of total muscle activity (Farina et al., 2004). It has been demonstrated that the structure of the extracted synergies depends on the muscles selected for analysis (Steele et al., 2013). As the analysis of muscle synergies intends to unveil motor control strategies, it is important to record the muscular activation of as many muscles as possible. It is recommended to at least record those muscles that play an important role in the studied motor task (Hug, 2011).

The SENIAM project developed recommendations for sEMG recordings, including the placement of electrodes on each muscle, and also the appropriate skin preparation to optimize the quality of the EMG signal (Hermens et al., 1999) (Hermens, 2000). After placing the electrodes, it is of main importance do perform some preliminary tests to check for cross talk and artifacts to ensure electrodes are correctly positioned. If needed, electrodes should be repositioned.

2.3.3.2 Processing the EMG

Recorded EMG signals consist of muscle activation signal affected by disturbances that do not relate to muscle activation. An example of a recorded raw EMG signal of gastrocnemius medialis during cycling is represented in Figure 2.3-(A).

Although it is impossible to guarantee a perfect removal of all these undesired disturbances without affecting the signal, a series of methodologies can be adopted to minimize them. A digital high-pass filter can eliminate most of the the associated motion artifacts (disturbances derived either from movements between the electrodes and the

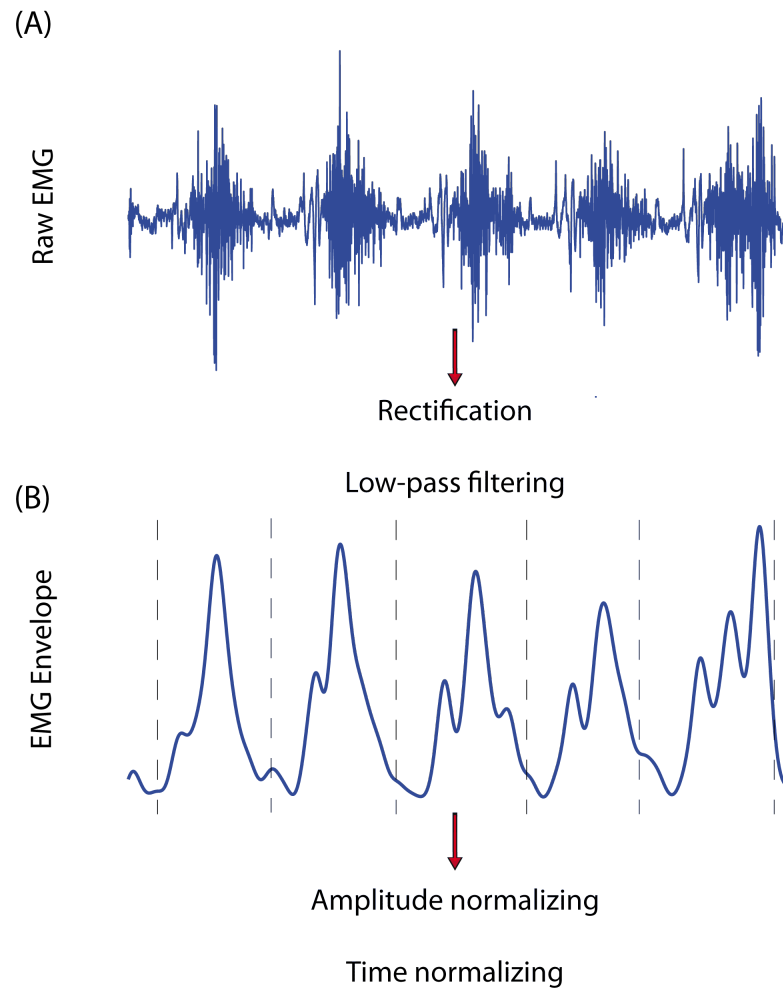


FIGURE 2.3: Example of sEMG signal processing. Panel (A) depicts a raw sEMG signal recorded from the gastrocnemius medialis during pedaling. The linear envelope is computed by rectification and low-pass filtering (at 5 Hz) (panel (B)). All pedaling cycles are determined based on the crank position. Dashed lines represent the beginning of a cycle (angle 0° , corresponding to the lowest position of the crank). Linear envelope is then amplitude and time normalized.

skin, or movements of the cables connecting the electrodes to the EMG amplifier). For the cutoff frequency of the filter, there must be a trade-off, because the higher the cutoff frequency, the higher the likelihood of degrade the signal (Hug, 2011). When the raw signal contains significant electromagnetic noise, a *Notch* filter might be used to remove part of the signal composed by frequencies near the power line frequency (usually 50 or 60 Hz).

After filtering the raw EMG signal, the next step is to obtain the EMG envelope, which is a more useful way of representing the level of muscle activation. This is done by first rectifying the filtered signal and then applying a digital low-pass filter to smooth the signal. The smoothness of the EMG envelope depends on the cutoff frequency of the filter, which must be adjusted to the analyzed task (*e.g.*, walking) and its speed of

execution. Depending on the desired smoothness, a cutoff frequency of 4-10 Hz is often used (Neptune et al., 2009) (Clark et al., 2010) (Gizzi et al., 2011) (Hug, 2011) (Routson et al., 2014). An example of an EMG envelope of *gastrocnemius medialis*, obtained after using a low-pass filter of 5Hz, is represented in Figure 2.3-(B).

For the same task under analysis, the amplitude of the EMG signal changes from person to person, between different measurements for the same person and between different muscles. Factors such as the electrical impedance of the skin or the amount of subcutaneous fat also interfere with the signal amplitude. For this reason, it is important to normalize the amplitude of the EMG signal to allow for comparisons between muscles, subjects and different studies. Notwithstanding, there is still no consensus on the best way to normalize the amplitude of EMG envelopes. Different methods described in literature range from isometric maximal voluntary contraction to sub-maximal isometric efforts (Hug, 2011). Nevertheless, to extract muscle synergies, it is sufficient to just normalize the envelope amplitude with respect to the peak or the mean of different cycles or trials (Hug, 2011).

For a given cyclical task like walking, each cycle will have different duration, especially if considering trials at different times or executed by different people. To eliminate inherent variability, a method called time normalization is applied. The first step is to define biomechanical events that may be considered the beginning or the end of a cyclical task (*e.g.*, heel strike in walking). After that, each cycle is interpolated to a defined number of points. Thus, it is possible to obtain cycles with the same number of points and also their corresponding mean and standard deviation.

2.3.3.3 Algorithms to extract muscle synergies

Most of the computational methods for the extraction of muscle synergies assume that individual muscle activation is the result of a linear combination of weighted activation coming from each synergy (Tresch et al., 2006) (Ting et al., 2015). These computational techniques are useful but may not fully capture the true complexity of muscle synergies (Ting et al., 2015). Advances in computational methods are ongoing and can bring new insight in the future. Among the actual algorithms used, there are principal component analysis (PCA) (Krishnamoorthy et al., 2003) (Weiss and Flanders, 2004), factor analysis (FA) (Ivanenko et al., 2003) (Ivanenko et al., 2004), independent component analysis (ICA) (Hart and Giszter, 2004) (Kargo and Nitz, 2003) and nonnegative matrix factorization (NNMF) (Clark et al., 2010) (Dominici et al., 2011) (Gizzi et al., 2011) (Hug et al., 2011) (Routson et al., 2013). Although each of these algorithms has

different restrictions on the outcomes, they all converge on a similar output related to the temporal structure of the EMG activity pattern (Hug et al., 2010).

The most frequently used algorithm is the NNMF (Lee and Seung, 1999), which will also be used in the studies performed in this Thesis. Before running the NNMF, it is first necessary to combine the normalized EMG envelopes from each recorded muscle into an $m \times t$ matrix (EMG_0), where m indicates the number of recorded muscles and t is the time base (see Figure 2.4-A).

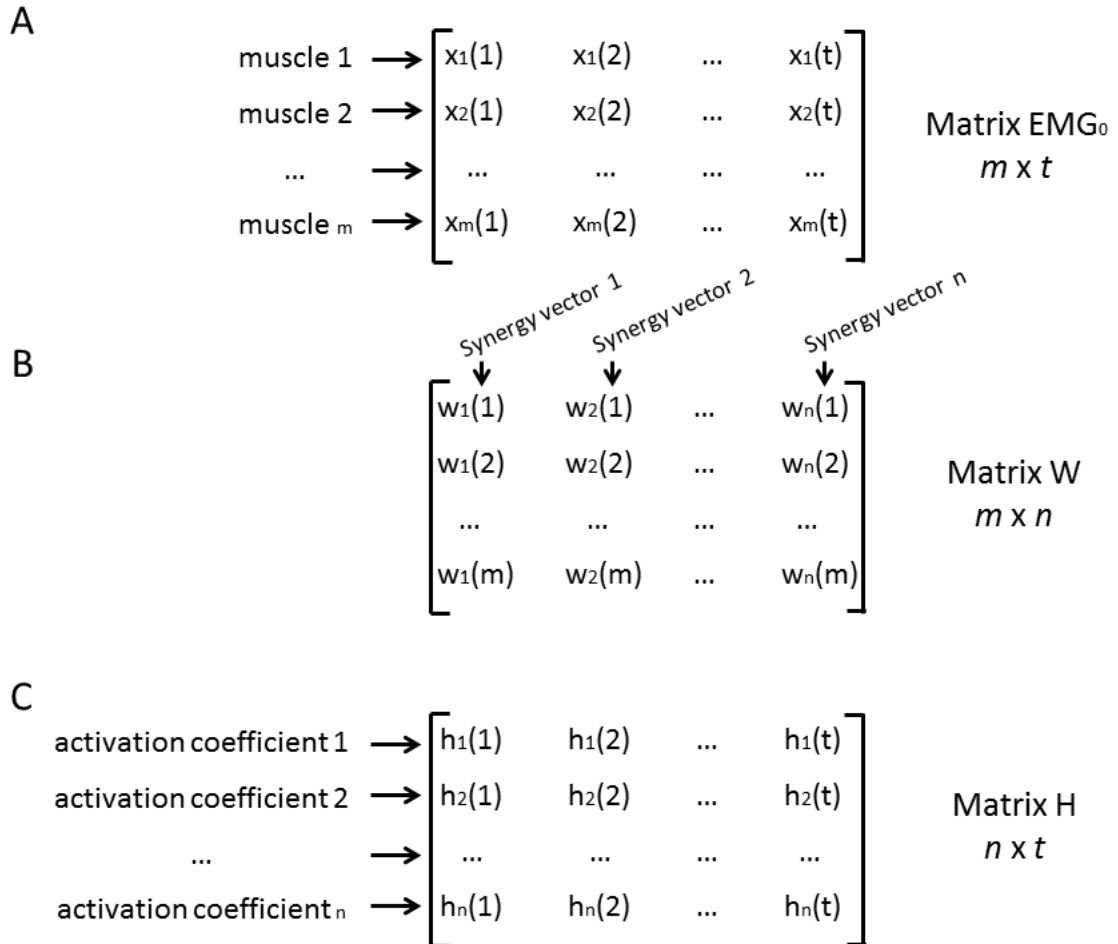


FIGURE 2.4: Representation of (A) matrix EMG_0 , (B) matrix W and (C) matrix H .

Mathematically, the output of the NNMF algorithm is represented in Equation 2.1.

$$EMG_0 = WH + e = EMG_r + e \quad (2.1)$$

, where W is an $m \times n$ matrix (n is the number of synergies) that specifies the relative weighting of each muscle within each synergy (hereafter, each column of matrix W will be referred to as *muscle synergy vector* - see Figure 2.4-B); H is an $n \times t$ matrix

that specifies the time-varying *activation coefficients* of each synergy (relative contribution of each synergy for each muscular pattern - see Figure 2.4-C); EMG_r is an $m \times t$ matrix that represents the reconstructed EMG envelopes of each muscle, as a result of the multiplication of W by H ; e is the residual error between EMG_0 and EMG_r . NNMF assumes that both synergy vectors and activation coefficients are non-negative. At each iteration, NNMF updates matrices W and H in order to minimize the residual Frobenius norm between EMG_0 and EMG_r , assuming a Gaussian distribution of error (Lee and Seung, 1999). As input for the NNMF, the number of synergies (n) has to be defined. One can start by using one synergy and increasing up to a maximum number, which is the number of recorded muscles. All this process of extracting muscle synergies from very basic raw EMG is schematically represented in Figure 2.5.

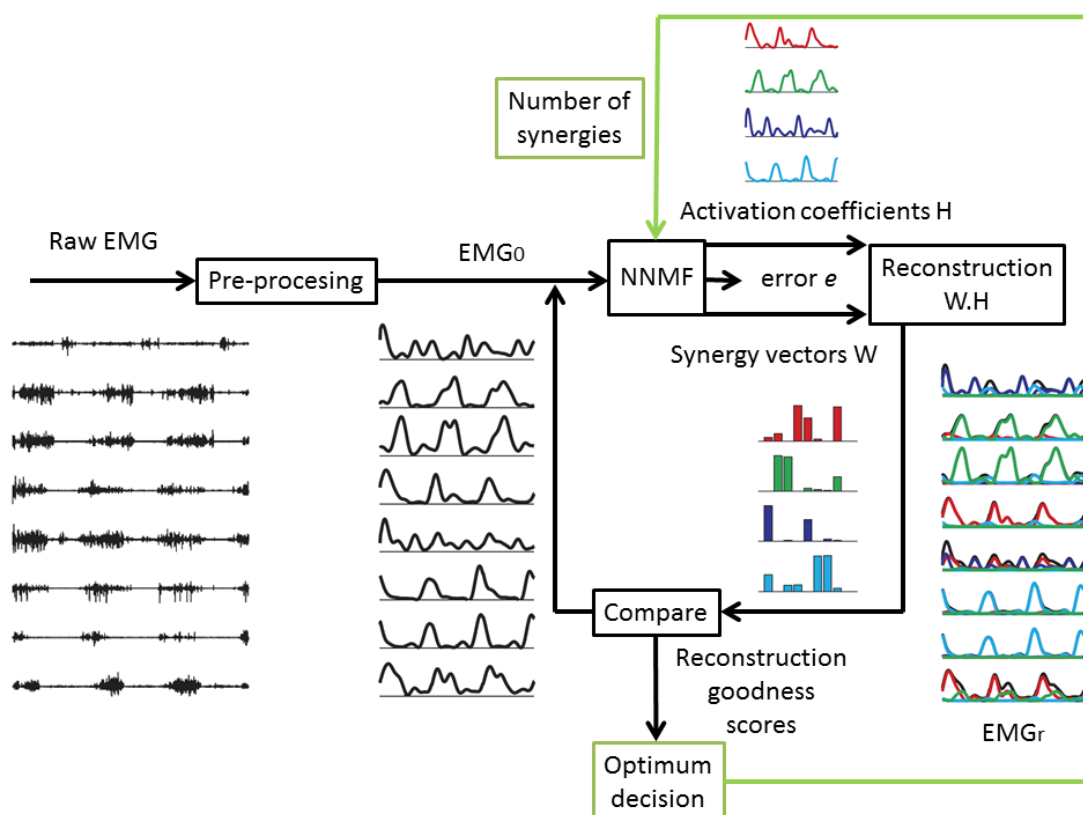


FIGURE 2.5: Process of estimating the activation coefficients (matrix H) and synergy vectors (matrix W) from eight experimental EMG signals.

In summary, each muscle synergy receives as input a modulation signal (activation coefficients) from higher neural centers, and gives as output a weighted activation signal to a set of muscles. The activation of each muscle is the sum of the weighted activation signals coming from each synergy. This mechanism eases the control of the high dimensional space of muscle activation by means of a lower dimensional set of neural commands.

2.3.3.4 Reconstruction goodness scores

At last, it is necessary to assess the quality of the reconstructed EMG envelopes, *i.e.*, whether the recorded EMGs can be well described as a combination of the identified synergies. For a given number of synergies, the similarity between EMG_0 and EMG_r is usually assessed with one of the following metrics: the variability accounted for (VAF_{total}) (Clark et al., 2010) or the coefficient of determination (r^2) (Torres-Oviedo et al., 2006). Low values of similarity cast doubt on the extracted synergies, indicating that they do not explain a large part of of EMG variance, suggesting that additional synergies are used. Different thresholds of similarity can be found in the literature, which makes the comparison of studies a difficult task.

2.3.4 Implications for the clinical setting

During the last fifteen years, the analysis of muscles synergies has received considerable attention from the neuroscience community as a way to interpret, in a quantitative way, the neural strategy adopted by the CNS to simplify the coordination of muscles. Experimental evidences has shown that the synergistic control is visibly affected in neurologically impaired people, leading to the verified impaired walking performance. For instance, according to Clark et al. (2010), poststroke patients need less muscle synergies to account for global muscle activation during walking at their preferred speed compared with healthy subjects. Participants requiring fewer muscle synergies present more muscle co-activation, resulting in less locomotor output complexity and impaired walking performance. Thus, the analysis of muscle synergies can be explored as a novel tool for the assessment of underlying neural strategies of movement and functional outcomes of muscle activity (Safavynia et al., 2011).

Assessment of spinal cord injury and stroke

Walking is a very complex task, which needs to be objectively assessed in people with gait impairments. A proper diagnosis and assessment of motor impairments is important to prescribe appropriate rehabilitation strategies ([DeLisa and States, 1998](#)). To understand impaired gait, it is first required to understand the basic biomechanics of the normal gait. Recent researches on pathological conditions strongly recommend gait analysis to adequately assess and follow-up patients and to support clinical decision on the best treatment ([Nadeau et al., 2011](#)).

There are two main groups of patients that suffered neurological damages and, as a consequence, present pathological gait: poststroke survivors and spinal cord injured (SCI). These two main groups of patients are the focus of this Ph.D. Thesis.

This Chapter starts by introducing the main biomechanical mechanisms underlying human walking, as well as the most used instrumented gait analysis systems. It continues by presenting general concepts of SCI and stroke, as well as the assessment of sensorimotor mechanisms underlying impaired walking in these neurological diseases.

3.1 Biomechanics of normal gait

Human gait refers to the locomotion achieved through the forward movement of limbs, in which the body moves from one place to another, changing alternately and repetitively the location of the feet ([Perry, 1992](#)). There are many types of human gait, like the walking, the skipping, and the running, among others. This Thesis focus on human

walking. A simplified diagram of the human gait during normal walking is represented in Figure 3.1.

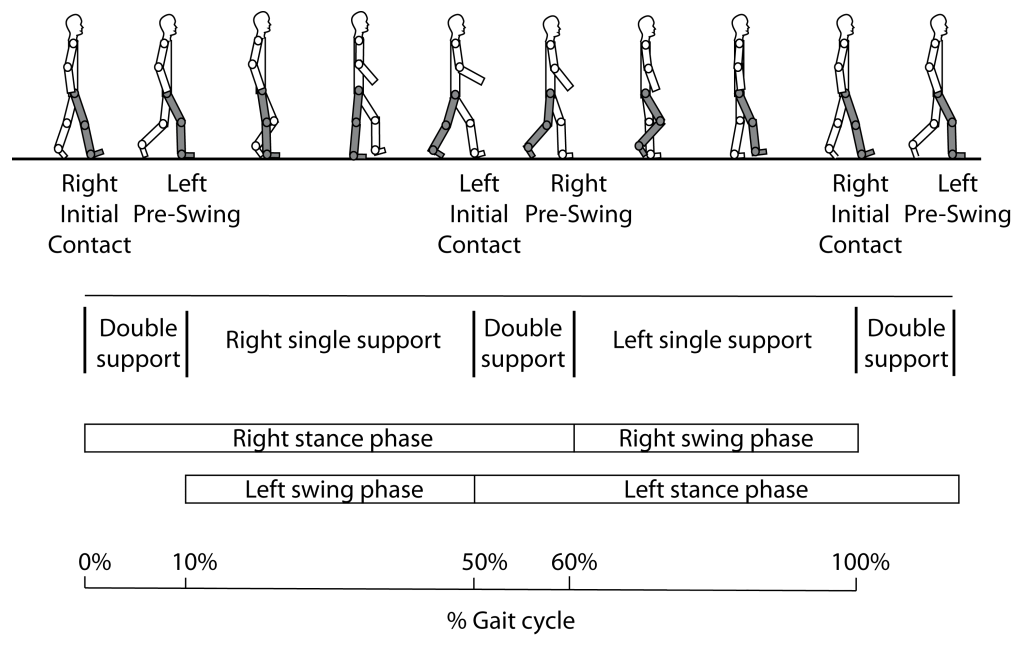


FIGURE 3.1: Main divisions of the human gait cycle. Gait cycle has two main phases: stance and swing. Swing phase is where the action takes place: toes are cleared; limbs move forward.

The gait cycle is the interval of time spent between the occurrence of two similar locomotion movements. Usually, the first contact (often called heel strike) of one foot represents the beginning (0%) of gait cycle, so that the final of the cycle (100%) happens when the same (*ipsilateral*) foot contacts the ground, which will also be the initial contact of the next cycle. Gait cycle can be divided in two global periods: *stance* and *swing*. Stance is the period in which the ipsilateral foot is on the ground (weight bearing) and lasts approximately 60% of the gait cycle at an average walking speed. Swing is the period in which the ipsilateral foot is in the air (limb is not weight bearing) (Perry, 1992) and lasts approximately 40% of the gait cycle. Since there are two lower limbs, alternating their movements in a sinusoidal way, the events of the opposite (*contralateral*) limb are offset by 50% in non-injured people, in a way that initial contact of contralateral limb occurs at 50% of the cycle.

As stance phase lasts approximately 60% of the gait cycle in a normal person, and $2 \text{ (legs)} \times 60 = 120$, it follows that both feet are on the ground during 20% of the cycle. This period is called *double support* and is divided into two parts: initial and final double support (see Figure 3.1). The remaining part of the stance phase, when only the ipsilateral foot is on the ground, is called *single support*.

Depending on the author, human gait can be divided into different number of phases. According to Perry (Perry, 1992), gait can be divided into eight phases, each one presenting a typical pattern and a functional objective. Those phases are:

- Phase 1 - *Initial contact* (or heel strike), occurring at 0-2% of the gait cycle. In this phase, it is done the initial contact of the ipsilateral foot with the ground and the goal is to obtain the correct alignment of the lower limb in order to begin the stance (Perry, 1992).
- Phase 2 - *Loading response*, occurring at 2-10% of the gait cycle. In this phase, both feet are on the ground (initial double support). The main events of this phase are the shock absorption and progress of the walking. This phase ends when the contralateral foot leaves the ground and starts its swing movement.
- Phase 3 - *Mid-stance*, which takes place at the 10-30% interval. The aim of this phase is the progression of the foot on the ground as well as to keep the stability of the limb and the trunk. This phases ends when the body weight is aligned with the forefoot.
- Phase 4 - *Terminal stance*, which happens at 30-50% gait cycle. The support of the limb ends in this phase and the goal is to progress the body in addition to the foot support. This phase starts with heel lifting and ends when the contralateral foot strikes the ground.
- Phase 5 - *Pre-swing*, which involves the 50-60% interval of gait cycle. The aim of this phase is to prepare the lower limb for the swing phase. This is the final phase of stance (final double support): it begins with the initial strike of the contralateral foot with the floor and ends when the ipsilateral leaves the floor.
- Phase 6 - *Initial swing*, which happens at 60-73% gait cycle. The aim of this phase is to lift the foot from the ground and move the lower limb. This phase starts when the ipsilateral foot lifts the ground and ends when it is opposite to the contralateral.
- Phase 7 - *Mid-swing*, which involves the 73-87% interval of gait. This second phase of the swing has the aim of moving the ipsilateral limb and free the foot from the ground. This phase starts when the ipsilateral limb is opposite to the contralateral limb and ends when the tibia of this limb in swing is in a vertical position (the moment when the knee and hip flexion are similar).
- Phase 8 - *Terminal swing*, which involves the 87-100% interval of gait cycle. This phase starts when the tibia is in vertical position and ends when the foot strikes the ground.

3.1.1 Spatio-temporal parameters

Spatio-temporal parameters of gait are important functional measures used to describe gait.

Every time the leg moves forward, it produces a *step* (Kirtley, 2006). If the left leg moves forward, it is a left step. Contrariwise, a right step happens when the right leg is the one that moves forward. *Step time* is the time spent from the moment the contralateral foot hit the ground until the ipsilateral foot hit the ground too, and the *step length* is the distance between the heel of the trailing limb to the heel of the leading one (Kirtley, 2006) (see Figure 3.2). When two steps occur (one left and one right), it makes a *stride* (or gait cycle).

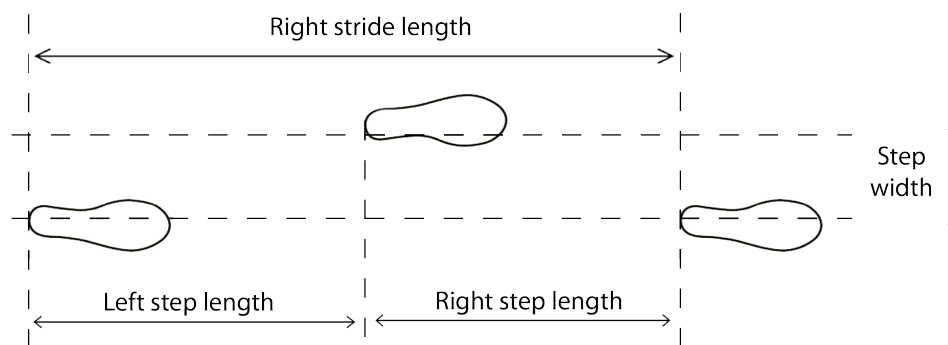


FIGURE 3.2: Representation of step length and step width.

Stride time is the time spent to execute two steps (one stride). *Step width* is the mediolateral distance between the midpoints of the two heels while in double support (see Figure 3.2). Another important spatio-temporal parameter is the cadence, which is usually the name given to the number of steps per minute. Natural cadence is about 120 steps/minute, which is the same of 60 strides/minute. Cadence usually does not change with age (Kirtley, 2006).

At last, another important spatio-temporal variable to describe gait is speed. Natural walking speed is relatively constant until age 70, after which it decreases about 15% per decade (Kirtley, 2006).

3.1.2 Kinematics

When it comes to the study of the gait, kinematics is the description of angles, positions, velocities and accelerations of body segments and joints (Kirtley, 2006). It is very important to measure kinematic patterns, as they are the basis for interpreting other

data like electromyography (EMG), force and stride characteristics, for example (DeLisa and States, 1998).

To describe kinematic patterns, a system of planes and axes is usually used. Three cardinal planes, intersected at the center of mass of the body, are represented in Figure 3.3-(A). Movement takes place in these planes (Hamill and Knutzen, 2006).

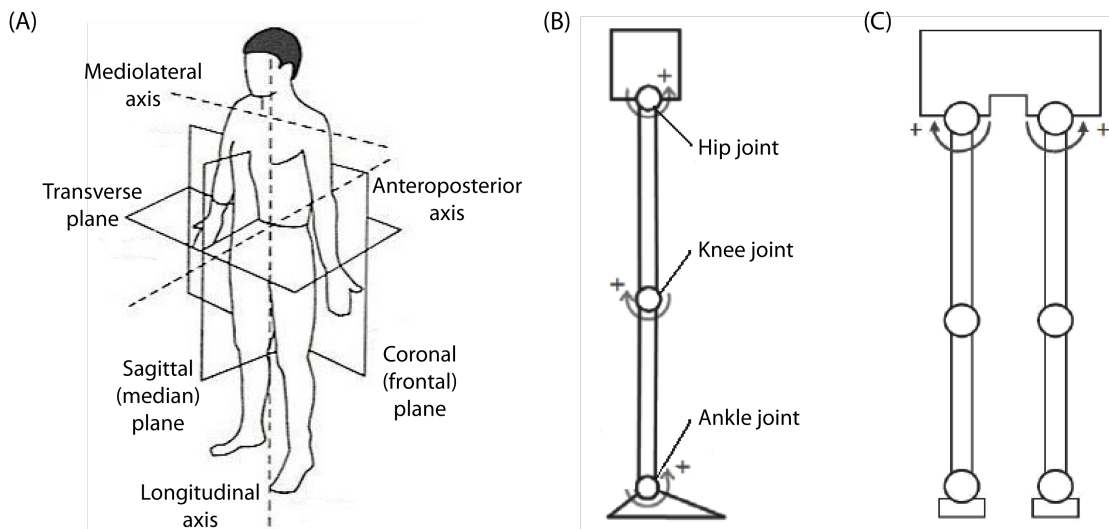


FIGURE 3.3: References for human kinematics. (A) Human planes and axes of reference. Three main planes originate at the center of gravity: the sagittal plane, which divides the body into right and left; the coronal plane, dividing the body into front and back; the transverse plane, dividing the body into top and bottom. Movement takes place in or parallel to the planes about a mediolateral axis (sagittal plane), an anteroposterior axis (coronal plane), or a longitudinal axis (transverse plane). (B) Diagram of the leg (lateral vision) shown in the rest position (0° at all joints) with the positive direction of movement indicated. (C) Diagram of both legs (frontal vision) shown in the rest position (0° at all joints) with the positive direction of movement indicated.

Sagittal plane virtually divides the body into right and left halves. Movements in this plane occur around the mediolateral axis, which goes side to side, passing through the center of mass of the body. The coronal (or frontal) plane divides the body in two halves: front and back. Movement on this plane occurs around the anteroposterior axis, which runs anterior and posterior from the plane. Transverse plane divides the body into upper and lower halves. Movement on this plane occurs around the longitudinal axis (Hamill and Knutzen, 2006).

Movements around the joints can be classified into different types, depending on the joint and the plane of movement. Most common movements are:

- *Flexion and extension.* In these movements, there is a decrease (positive direction in 3.3-(B)) or increase of the angle between the limb's segment that moves and the segment that stays fixed, respectively, in the sagittal plane. In relation to the ankle

joint, the decrease of the angle between the segments is usually called dorsiflexion and the increase of the angle is called plantarflexion (Barroso, 2011).

- *Adduction* and *abduction*, which are movements in the coronal plane. Abduction (positive direction in 3.3-(C)) is the motion of the hip away from the center of the body and adduction is the motion of the hip in direction to the center of the body (Barroso, 2011).
- *Medial* and *lateral rotation* in the transverse plane. Medial rotation happens towards the midline of the body, while lateral rotation is the movement away from the midline.

Kinematic patterns of normal gait in the sagittal plane are very well documented and studied (Perry, 1992) (Nymark et al., 2005) (Hidler et al., 2008) (van Asseldonk et al., 2008). Examples from an healthy subject are represented in Figure 3.4 and angles were obtained in relation to the joints references represented in Figure 3.3-(B) sagittal plane.

Hip joint is usually in flexion at the beginning of the gait cycle. Then it extends until approximately the end of terminal stance (50% of the gait cycle) and it finally flexes until the end of the gait cycle, performing a sinusoidal movement during the gait cycle (Barroso, 2011).

The movement of knee joint present two peaks of flexion along the gait cycle: one in stance and the other during swing phase, with the second peak being much larger than the former. Knee is always in a positive position (angle higher than 0°).

Ankle joint is usually at neutral position (0°) at the initial contact, after which it slightly dorsiflexes. After that, it plantarflexes through the remaining of stance phase. Approximately at the end of terminal stance, the ankle dorsiflexes again. During swing, it plantarflexes until reaching the neutral position.

3.1.3 Kinetics

Kinetics is the study of forces and moments that cause a movement, like ground reaction, gravitation, or forces produced by muscle contractions, for example (Rueterborries et al., 2010).

According to Newton's Third Law, if one body exerts a force on another body, there is a simultaneous force equal in magnitude and opposite in direction applied in the first body by the other body. Ground Reaction Force (GRF) is a force equal in

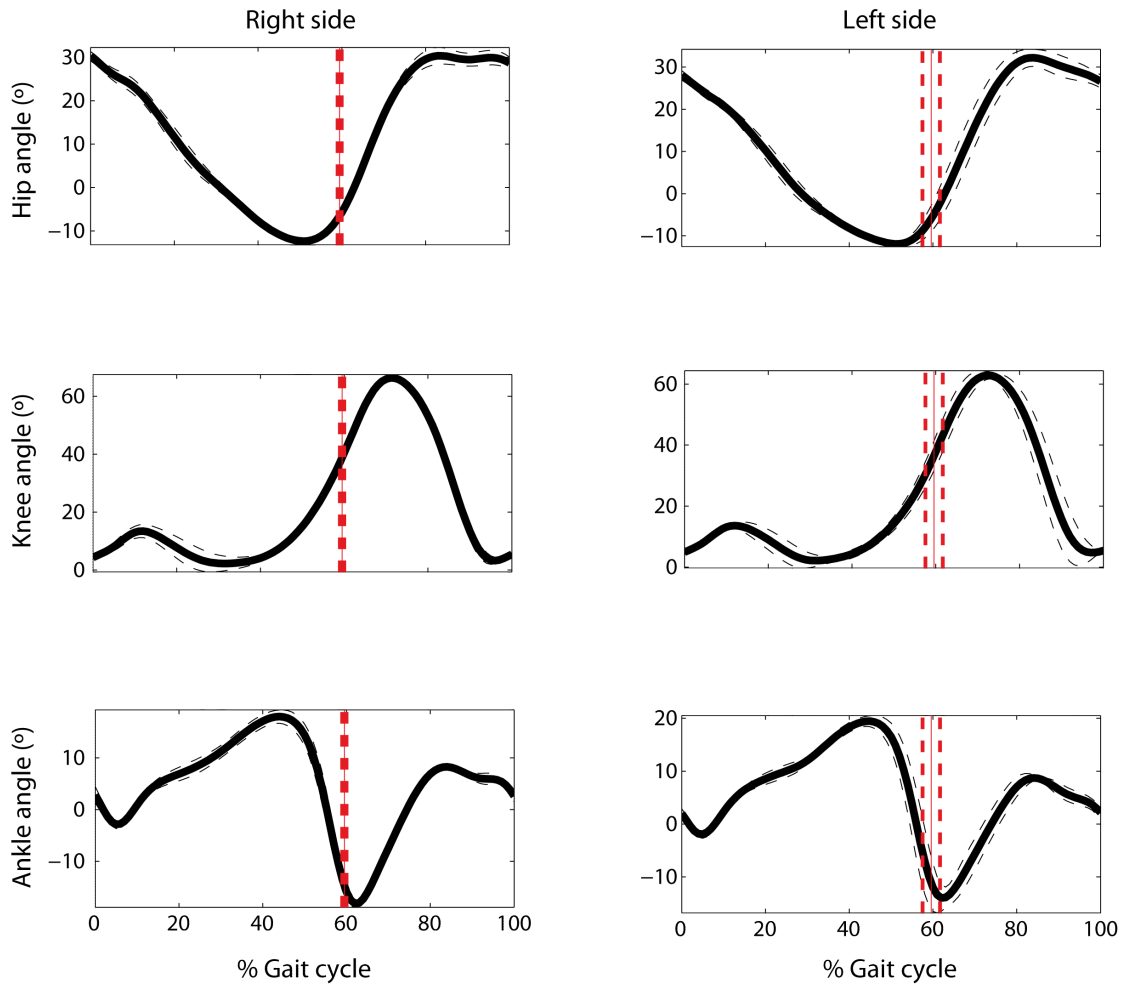


FIGURE 3.4: Comparison of time-normalized kinematics between the right and left side of a healthy subject, for the hip, knee and ankle joints in the sagittal plane. Thick black lines indicate the mean and the standard deviation (SD) is indicated in dashed black lines. Mean stance phase is indicated in red vertical lines, while dashed red vertical lines indicate the SD of the stance phase.

magnitude and opposite in direction to the applied by the foot on the ground. The understanding of GRF is very important in the clinical setting, as this force acts in the body during walking (DeLisa and States, 1998). The only other external force acting on the body in movement (if we do not consider the wind resistance) is the gravity force. 3D components of GRF are represented in Figure 3.5-A, whereas 3D components of the force applied by the body to the ground are represented in Figure 3.5-B.

According to Newton's Second Law, the vector sum of the forces F acting on an object is equal to its mass m multiplied by its acceleration vector a : $F = m \cdot a$. In Figure 3.5-C, vector $F = ma$ represents the instantaneous inertial force acting on an object. On the contrary, $F = mg$ is the vector representing the force of gravity acting on an object. The sum of gravitational and inertial forces is the resultant vector (F_r). Therefore, GRF

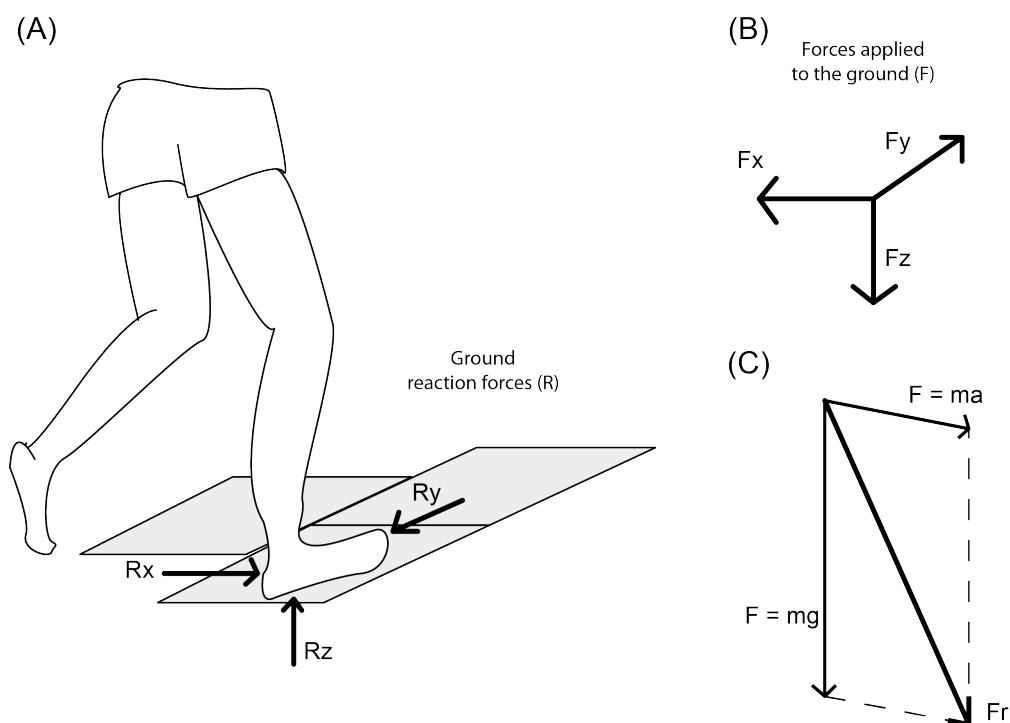


FIGURE 3.5: 3D representation of ground reaction forces (GRF). (A) 3D components of GRF. (B) 3D components of the force applied by the body to the ground. (C) Instantaneous inertial force and force of gravity acting on an object.

combines both body's movement and acceleration, as well as gravity's effect on the body, in three dimensions.

The largest component of GRF is the vertical and is related to the body's center of mass in the vertical direction of walking. In Figure 3.6-A, it is represented an example of the GRF vertical component of an healthy subject in motion. The force is normalized in relation to the weight of the subject. At the beginning of stance, force magnitude amounts to 120% of the BW during the double support. During this sub-phase of stance, vertical GRF is superior than gravity force due to body acceptance, which lowers the center of mass and consequently, the acceleration of the body (human body in this case) increases. After that, contralateral leg starts swing phase and vertical GRF decreases during this single period support. It may seem strange that this force decrease to less than the body weight when there is only one foot on the ground. Again, this is explained by the displacement of center of mass. This center of mass, which is located around the center of the pelvis, performs a sinusoidal movement and falls about 10 cm in space during gait (DeLisa and States, 1998).

Another component of the GRF is the anteroposterior (AP) component (see Figure 3.6-B). Initially it is a braking force and then it is a propulsion force, presenting a sinusoidal motion of about 25% BW (50% peak-to-peak) amplitude in healthy people.

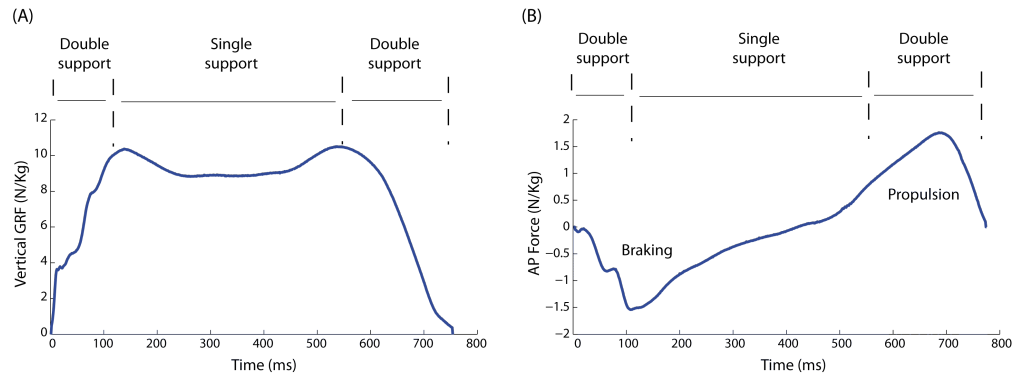


FIGURE 3.6: GRF acting on a healthy subject during walking. (A) Vertical GRF. (B) Anteroposterior (AP) GRF.

Typically, the first 50% of the stance phase correspond to braking and the remaining 50% of stance correspond to propulsion. The integral of each phase represents the force impulse. The braking impulse should be approximately equal to the propulsion impulse in a balanced gait. Thus, the integral of the forces must be equal to 0.

The third component of GRF is the mediolateral, which is the smallest of the three components. It is usually related to the balance while walking. This force acts usually towards medial direction during initial stance, with a magnitude of about 10% BW and then acts laterally during the balance of stance phase (DeLisa and States, 1998).

3.2 Instrumented gait analysis systems

Gait parameters are difficult to be assessed by naked eye. Thus, reliable instruments should be used to measure these variables accurately. The measurement of human gait has come a long way in the past decades. Modern gait analysis started with the work of Inman et al. (1952) in the 1950s and became a useful clinical tool after the pioneering efforts of Perry (1967) and Sutherland (1964).

Modern technology has provided clinicians and researchers a wide variety of gait outcomes, most of them in real time, allowing for the possibility of critical judgments about an individual's gait. This section provides information on the types of gait instrumentation that are commercially available and are usually used to assess patients' impairments.

3.2.1 Spatio-temporal parameters

Footswitches are force sensitive resistors that present good sensibility and can be integrated with other platforms for the analysis of gait. They may be placed on the heel, toe or metatarsal region, detecting different gait events according to their location on the foot. These instruments usually work on a binary mode, being *on* or *off*, depending if the detected force surpasses or not a predefined threshold, respectively. The main problems of footswitches are the ideal threshold values for each person and also the impossibility of measuring spatial variables like step/stride length.

To measure spatial variables, other devices have to be used. Recently, instrumented walkways have gained popularity to assess spatio-temporal variables in gait labs (Kirtley, 2006). GaitMat IITM and GAITRITETM are two examples of popular instrumented walkways, made of switches or pressure-sensing arrays, respectively. The major drawback of walkways are the impossibility of measuring long-distance locomotion.

At last, the most complex instruments to measure spatio-temporal variables are video motion systems, usually incorporated in gait analysis laboratories. Commercially available systems include *Vicon Motion Systems* (Oxford, UK), *CODA mpx30* (Charnwood Dynamics Ltd, Loughborough, UK), *BTS* (Milan, Italy) and *Motion Analysis Corp.* (Santa Rosa, CA, USA), among others. The working principle of most of the video motion systems relies on video-based photogrammetry (Kirtley, 2006). Bright markers placed over several locations on the person being tested are then tracked by video cameras. This way, it is possible to obtain 3D coordinates and each individual spatio-temporal parameter.

3.2.2 Kinematics

There are several types of measurement systems to assess human kinematics. Two of them are probably the most used nowadays: electrogoniometers and video motion systems (DeLisa and States, 1998).

Electrogoniometers are the simplest (can be used in different environments and outside the laboratories or clinics) and cheapest method to assess human kinematics, despite presenting limitations to obtain accurate results. The most basic model consists in a potentiometer mounted on two brackets strapped to the body segments either side of the joint. On the other hand, modern versions are more flexible, without the need for alignment with joint center. With these modern electrogoniometers, it is possible to

obtain three-dimensional information, despite they have been used mainly for 2D analysis. The main drawback of electrogoniometers is the impossibility to record absolute motion of the body segments, but simply the relative motion of body segments.

If the purpose of some research study is to measure absolute motion of body segments, measurements must be taken with respect to a fixed global reference system. Video motion systems (like those already mentioned in subsection 3.2.1) are the most popular for kinematic analysis. To obtain angles from position data, each body segment must be defined by at least three markers and joint centers have to be defined. Therefore, these systems compute inverse dynamics, which may introduce some errors due to markers position. Due to *digitization noise* of the markers position, kinematics data need to be filtered. Digitization noise tends to be high frequency, whereas markers position is usually low frequency. Therefore, a low pass filtered should be used. The choice of the cutoff frequency of the low pas filter is empirical. There is no consensus on the optimal value, ranging from 6 Hz to 20 Hz, depending on the authors (Allen and Neptune, 2012) (Sinclair et al., 2013) (Hidler et al., 2008) (Moreno et al., 2008). If the cutoff frequency is too high, much of the noise will remain; contrariwise, a low cutoff value will over-smooth the signal.

3.2.3 Kinetics

GRF is usually assessed using force platforms, which are devices used for measuring the force between and object or a body and the ground. Thus, force platforms are the most used force transducers in biomechanics (Robertson et al., 2013) and may be used to assess gait and balance, for example. More advanced platforms measure 3D components and its point of application, as well as moment of force and center of pressure.

Raw GRF data recorded by force platforms is usually filtered offline using a low-pass filter. Also, it should be normalized by each individual's body weight (BW) (Bowden et al., 2010). After this processing, the three components of GRF (vertical, anteroposterior and mediolateral) can be studied.

3.3 General Concepts of Stroke

Stroke, which may also be referred to as cerebrovascular accident (CVA), is a sudden dysfunction in the cerebral blood flow, which alters the function of a given brain region. There are two main types of stroke: ischemic and hemorrhagic. Ischemic strokes are caused by a significant decrease of blood flow in a part of the brain due to an occlusion

of a cerebral artery through a clot or other particle (Bendok and Naidech, 2011). These are the most common type of stroke (approximately 85%), whose the main consequence is the death of brain cells that did not receive enough oxygen and nutrients carried by the blood. Hemorrhagic stroke occur when the brain is filled with blood due to rupture of a cerebral vessel. These are less common but have a much higher mortality rate. However, patients who survive to this type of stroke usually present less serious sequelae in long term.

Stroke disproportionately affects the elderly, where it is more likely to be fatal or lead to long-term supportive care (Sohrabji et al., 2013). Stroke has an important impact in patients' life and also represents considerable costs for social and health care systems associated with patients' hospitalization and treatment. It is the the world's second most common cause of death (Gradil and Sá, 2015), being a major cause of mortality and morbidity in adults all over the world (Baghshomali and Bushnell, 2014). Moreover, it is expected that stroke incidence will increase 25% by 2030 (Ramsay et al., 2014).

About 80% of the patients survive to the acute phase poststroke. The period of greatest potential for recovery seems to be between the second and the fifth month poststroke, where patients may regain and learn new functions, as well as compensate for impairments. After the sixth month, functional changes are more limited (Jørgensen et al., 1995). It has been demonstrated that motor recovery poststroke is related to neural plasticity, which is the mechanism responsible for developing new neuronal interconnections (Takeuchi and Izumi, 2013).

After the first 6 months of evolution, between 70% to 85% of stroke survivors present a residual hemiparesis (slight paralysis or weakness on one side of the body) or impaired motor control on one side of the body, as well as a variety of neurological deficits, communication disorders, cognitive deficits or even impaired spatial-visual perception (Belda-Lois et al., 2011). Hemiplegia (paralysis of one side of the body) is a very common poststroke dysfunction and contributes significantly to reduce walking performance. Thus, hemiplegic gait has been a matter of enormous research during the last decades, with researchers aiming at developing novel methods of rehabilitation (Olney and Richards, 1996). After completing a traditional rehabilitation program, approximately 50%- 60% of poststroke patients remain with some degree of motor impairment and approximately 50% are at least partially dependent or restricted in daily activities (Schaechter, 2004).

3.3.1 Abnormal gait after stroke

As a consequence of the neurological injury, ambulatory poststroke patients usually present muscle weakness and poor balance, which lead to reduced walking ability and mobility restrictions (Eng and Tang, 2007), mainly on the side of the body contralateral to the injured hemisphere (Molina Rueda et al., 2012), usually called the hemiparetic side. Patients frequently develop compensatory motor strategies to overcome limitations of paretic side movement, but the repetitive use of these strategies may cause musculoskeletal disorders.

Problems in muscular activation are often associated with abnormal kinematics and kinetics. For instance, ambulatory poststroke patients with abnormal muscular coordination, reduced activation of hip flexors and extensors, as well as ankle plantarflexors (necessary for the propulsion) eventually walk slower (Nadeau et al., 2011). In fact, individuals frequently exhibit reduced walking speed after stroke. While healthy population usually walks with a mean speed of 1.3 m/s, poststroke patients walk within the range from 0.23 to 0.73 m/s (Verma et al., 2012). Stride length and cadence are also decreased in ambulatory poststroke patients (Roche et al., 2015) (Bonnyaud et al., 2014). Duration of double support is longer in post stroke patients (Olney and Richards, 1996). These spatiotemporal parameters are often related to kinematic alterations (*e.g.*, decreased active range of motion around lower limb joints and increased step width, if compared with healthy controls) (Bonnyaud et al., 2014) (Reissman and Dhaher, 2015).

Poststroke patients usually present a very asymmetrical and unstable gait (Nadeau et al., 2011), with affected temporal and kinematic parameters between the paretic and non-paretic side (Reissman and Dhaher, 2015). For instance, non-paretic side usually has increased stance phase if compared with the paretic side (Olney and Richards, 1996) (DeLisa and States, 1998). Decreased peak hip flexion, peak knee flexion and ankle dorsiflexion on the paretic side are frequently described (Roche et al., 2015) (Bonnyaud et al., 2014). In fact, decreased peak ankle dorsiflexion seems to be a key parameter affecting the quality of walking (Lamontagne et al., 2002). Hyperextension of the paretic leg during stance is usually associated with different types of impairments in motor control. If the main cause is muscle weakness, there is a tendency for this hyperextension to occur throughout the entire stance phase, which is accompanied by compensatory circumduction of the leg to achieve toe clearance in the swing phase (Nadeau et al., 2011). In the case of decreased peak ankle dorsiflexion during swing, compensatory mechanisms such as increasing peak hip flexion may be adopted as a strategy to increase foot clearance (Roche et al., 2015). Kinetic asymmetries have been also described in these patients (Bonnyaud et al., 2014). For instance, hemiparetic poststroke patients present decreased propulsion force generated by the paretic leg during walking (Clark

et al., 2010) (Bowden et al., 2010) (Awad et al., 2014). All these asymmetries lead to inefficient energy expenditure, joint damage, pain and falls (Verma et al., 2012) (Gaviria et al., 1996).

Spasticity syndrome is a very common disorder that may contribute to motor impairment after neurological injury (Bravo-Esteban et al., 2013). Despite the ease to recognize spasticity by a trained clinician, it has been difficult to achieve consensus on its definition and quantification (Gómez-Soriano et al., 2012). Perhaps the most common definition of spasticity is the one proposed by Lance (1980), defining spasticity as a “motor disorder characterized by a velocity dependent increase in tonic stretch reflexes (muscle tone) with exaggerated tendon jerks, resulting from hyper-excitability of the stretch reflexes, as one component of the upper motor neuron syndrome”. More recently, spasticity syndrome has been considered a complex set of clinical conditions including hypertonia¹, spasms², clonus³, hyperreflexia⁴ and muscle co-activation⁵ (Burrige et al., 2005) (Dietz and Sinkjaer, 2007) (Bennett, 2008) (Arene and Hidler, 2009). Co-activation is usually increased in people suffering from CNS disorders, in order to walk longer (Rosa et al., 2014). Nevertheless, this abnormal muscle activation may provoke fatigue and muscle pain (Rosa et al., 2014). In the case of poststroke patients, spasticity is characterized by high levels of muscle tone and a relative absence of spasms (Bennett, 2008).

Spasticity that occurs after stroke may alter walking patterns and, consequently, reduce walking ability. For instance, spasticity of rectus femoris is one of the main causes of residual peak knee flexion in swing in poststroke patients (Roche et al., 2015). Also, when the plantarflexion angle in the transition from stance to swing is low, it can be associated with spasticity of plantarflexors muscles (soleus, gastrocnemius medialis or gastrocnemius lateralis) (Nadeau et al., 2011).

3.3.2 Assessment of sensorimotor impairments poststroke

It is difficult to quantify motor recovery poststroke (Bowden et al., 2010). Traditionally, motor impairments poststroke have been assessed using clinical scales, which have been used to quantify the level of impairment, to predict further improvements, to assess the effectiveness of a given therapy or treatment and to support the clinical practice. More recently, emerging measures based on biomechanical and electromyographic features

¹Abnormal increase of muscle tone (Gómez-Soriano, 2012).

²Sudden involuntary muscle contraction (Gómez-Soriano, 2012).

³Involuntary rhythmic muscle contraction that causes oscillations in the distal joints, usually at a characteristic frequency of between 4 to 8 Hz (Gómez-Soriano, 2012).

⁴Exaggerated reflex of the muscles (Gómez-Soriano, 2012).

⁵Unintentional and simultaneous contraction of opposing muscle groups (Gómez-Soriano, 2012).

have been proposed to overcome some of the drawbacks of clinical scales (Bowden et al., 2010) (Routson et al., 2013). The following subsections present the most used clinical scales for the assessment of poststroke patients, as well as emerging measures that have been proposed as the key step toward a better quantitative assessment of this group of patients.

3.3.2.1 Clinical scales

Some of the most used scales in the clinical setting to assess functional walking poststroke are: Fugl-Meyer Assessment (FMA), Functional Ambulatory Classification (FAC) and Timed Up and Go (TUG) test.

Fugl-Meyer (Fugl-Meyer et al., 1975) is the gold standard in the assessment and classification of poststroke patients. For studies of walking, it is recommended to use the *Lower Extremity* subscale of the FMA (Fugl-Meyer assessment for lower extremity, FMA-LE). This assessment method is a cumulative numerical scoring system composed by four domains: motor function of the lower extremity (maximum score = 34 points), sensory function (maximum of 12 points), joint range of motion (maximum of 20 points) and joint pain (maximum of 20 points), resulting in a maximum motor score of 86 points for the lower extremity (Fugl-Meyer et al., 1975). For each item assessed, there is a 3-point ordinal scale: 0) the task cannot be performed, 1) the task can be partially performed, and 2) the task can be fully performed.

FMA-LE relies almost on isolated voluntary tasks performed in the bedside, which are not always representative of the walking performance. For instance, walking is a complex motor behavior, highly dependent on sensory feedback, which cannot be evaluated through FMA. For those reasons, it has been shown some concern with the ability of the FMA scale to evaluate the performance and the underlying impairments of such a complex activity like walking (Bowden et al., 2010).

FAC is a functional test that evaluates the walking ability and can be used to assess any motor disorder (Holden et al., 1986). It is a 6-point scale scored from 0 (no functional / unable) to 5 (patient can walk independently anywhere), determining the level of support required by the patient when walking, regardless of whether or not they use a personal assistive device. It presents excellent test-retest and inter-rater reliability in acute poststroke patients (Mehrholtz et al., 2007).

TUG test was designed as a screening tool to detect balance problems. This test incorporates a series of tasks, all of which are critical for independent mobility: stand up from a seated position on a chair, walk three meters, turn around, return to the

chair and sit down (Wall et al., 2000). The final score depends on the time required to perform the test.

In relation to the assessment of spasticity, the difficulty to classify a subject as spastic or not is a well-known problem (Reichenfelser et al., 2012). The modified Ashworth scale (MAS) (Bohannon and Smith, 1987) is commonly used to measure spasticity, although this scale specifically measures hypertonia (Gómez-Soriano et al., 2012), which is one of the clinical conditions of spasticity. The major drawbacks of MAS scale are the qualitative and subjective information provided as output, which raises concerns about its validity and reliability (Ansari et al., 2006).

3.3.2.2 Emerging measures of sensorimotor impairments poststroke

It is crucial to understand specific patient's impairments to prescribe effective customized treatments and target a reduction of compensatory motor strategies (Molina Rueda et al., 2012). Setting goals according to the rehabilitation objectives for a particular patient may also improve results (Belda-Lois et al., 2011). To do that, there is a need for reliable assessment and prognosis techniques that may detect and analyze early phenomenon of neuroplasticity, both adaptive and maladaptive.

Muscle coordination for task execution is compromised in poststroke patients (Reisman and Dhaher, 2015). As introduced in Section 2.3.4, the analysis of muscle synergies may be used to assess sensorimotor impairments specific to an individual and define targets for the rational development of novel rehabilitation therapies (Ting et al., 2015). According to Clark et al. (2010), poststroke patients need less muscle synergies to account for global muscle activation during walking at their preferred speed compared with healthy subjects. In addition, the number of muscle synergies seems to be a superior predictor of walking performance than the FMA (Bowden et al., 2010) (Clark et al., 2010), especially in the case of low intermuscular coordination, resulting from the co-activation of different muscle groups that are usually independently activated (Clark et al., 2010) (Routson et al., 2013). Very recently, the analysis of muscle synergies has been also used to measure motor recovery following therapeutic interventions. According to Routson et al. (2013), the combination of the analysis of the synergistic muscle control with the application of functional metrics could represent the key step toward a better quantitative assessment of stroke-related diseases. Notwithstanding, the analysis of muscles synergies has not been recommended yet as an outcome of these clinical conditions, being confined to the research environment.

Gait analysis is also a powerful tool to adequately assess and follow-up the patient and to support clinical decision on the best treatment (Wren et al., 2009). Some parameters derived from gait analysis may be useful to assess hemiparetic gait. For instance, meaningful gait speed improvement (Tilson et al., 2010), which is the meaningful increase of gait speed, has been used and proposed as an outcome of walking performance (Bowden et al., 2013). Responders (those patients with meaningful gait speed improvement) usually present higher FMA scores (Bowden et al., 2013). Metrics like paretic step ratio (PSR), *i.e.*, the percentage of the stride length performed by the paretic leg, has been proposed to assess patient's progress along the rehabilitation process (Bowden et al., 2010), being closer to 50% as the gait improves (right step length should be equal to left step length in healthy people). Paretic propulsion (PP), which is the percentage of propulsion performed by the paretic leg, has been also used to assess motor control poststroke (Bowden et al., 2010). This metric is based on the fact that hemiparetic poststroke patients usually present decreased propulsion force generated by the paretic leg during walking (Clark et al., 2010) (Bowden et al., 2010) (Awad et al., 2014).

The emerging measures presented in this section should be explored as novel metrics to assess walking poststroke. In particular, the analysis of muscle synergies, combined with behavioral and biomechanical measures, can give clinically relevant evidence on the cause-effect relationships between impaired neuromuscular activity and pathological movement (Safavynia et al., 2011).

3.4 General Concepts of Spinal Cord Injury

Spinal cord injury (SCI) is defined as any disturbance of the spinal cord that interrupt the normal transmission of nerve impulses from the brain to the PNS and vice versa (Finnerup, 2013). A trauma to the spinal cord may result in serious functional consequences affecting the health and quality of life of patients, including sensorimotor and autonomic functions below the level of injury, sexual function, bowel and bladder control, pain and spasticity syndrome (Bravo-Esteban et al., 2013) (Gómez-Soriano et al., 2012) (Kennedy et al., 2012) (van Middendorp et al., 2014).

SCI can be classified according to the degree of severity: it can be complete (when the spinal cord below the lesion is completely disconnected to the higher centers of the Nervous System) or incomplete (when part of the spinal cord preserves, to some extent, its continuity across the lesion) (Gómez-Soriano et al., 2012). In the case of incomplete spinal cord injury (iSCI), some level of motor recovery has been observed (Fawcett et al., 2007) (Duffell et al., 2015), although little is known about the sensorimotor mechanisms driving this improvement (Bravo-Esteban et al., 2014).

With the modernization of society, SCI incidence increases year after year (Yang et al., 2014). SCI incidence changes from country to country and from different regions, with higher prevalence in people between 18 and 32 years old, in both developed and developing countries (Lee et al., 2014) (Yang et al., 2014). For instance, it has been reported an estimated annual incidence of 40 per million in North America, 16 per million in Western Europe and 15 per million in Australia (Lee et al., 2014). Wirz (2013) reported that the proportion of incomplete SCI (iSCI) incidents was 52.8% in Europe and 44.3% in North America. One of the most important milestones in the rehabilitation process of iSCI patients is to improve gait function (Benito-Penalva et al., 2012). To improve customized therapy of iSCI patients, it is important to understand the neuromuscular and biomechanical features underlying abnormal gait after spinal cord injury.

3.4.1 Abnormal gait after spinal cord injury

There is a great variability in walking patterns across different iSCI subjects with ambulation capacity (Ting et al., 2015), with subjects presenting an impaired walking. For instance, iSCI patients tend to walk slowly, with poor balance and with the knee and hip hyperflexed in the stance phase (Gil-Agudo et al., 2013). Some iSCI patients also remain with the ankle dorsiflexed through the stance phase, which compromises an effective push-off (Ditunno and Scivoletto, 2009). Other iSCI patients walk with excessive plantarflexion and present impaired foot contact (van der Salm et al., 2005).

According to Krawetz and Nance (1996), the quality of gait in SCI patients with ambulation capacity is related to the level and completeness of the injury, as well as the spasticity affecting them. Moreover, symptoms like muscular weakness, co-activation of antagonist muscles and altered muscle mechanics also provoke abnormal gait and postural movements (Dietz, 2008). However, the relationship between hypertonia and gait function is still controversial (Duffell et al., 2015). Spasticity in SCI patients is mainly associated with the presence of flexor and extensor spasms triggered by cutaneous stimulation (Bennett, 2008).

3.4.2 Assessment of sensorimotor impairments after spinal cord injury

Nowadays, the assessment of SCI patients is based on physical examination and complementary tests, aiming to define the level, extent and evolutionary phase of injury. On the other hand, emerging measures have been proposed as the key step toward a better quantitative assessment of this group of patients. The following subsections present the most used clinical scales for the assessment of SCI patients, as well as these novel

TABLE 3.1: American Spinal Injury Association (ASIA) Impairment Scale (AIS).

ASIA grade	Description
A	Complete . No sensory or motor function is preserved in the sacral segments S4-S5.
B	Sensory incomplete. Sensory but not motor function is preserved below the neurological level and includes the sacral segments S4-S5. No motor function is preserved more than three levels below the motor level on either side of the body.
C	Motor incomplete. Motor function is preserved below the neurological level, and more than half of key muscle functions below the single neurological level of injury have a muscle grade less than 3 (Grades 0–2).
D	Motor incomplete. Motor function is preserved below the neurological level, and at least half of key muscle functions below the neurological level of injury have a muscle grade > 3 .
E	Normal motor and sensory function. Someone without a SCI does not receive an AIS grade.

proposed measures to quantitatively assess gait functioning, as well as spasticity and related symptoms of iSCI patients.

3.4.2.1 Clinical scales

Despite the existence of several functional scales to assess SCI patients, the American Spinal Injury Association (ASIA) Impairment Scale (AIS) is the gold standard to assess and quantify the neurologic level and the extension (complete or incomplete) of the lesion (see Appendix B). To quantify the sensory level, ASIA proposes the bilateral assessment of twenty-eight dermatomes using pinprick and light touch sensation. To quantify the motor level, ASIA proposes the bilateral assessment of ten key muscles with manual muscle testing. Figure B.1 shows how this sensory and motor assessment is done. The sum of the motor and sensory scores, used in combination with evaluation of anal sensory and motor function, determines the overall degree of functional impairment (AIS classification). AIS is an ordinal 5-point scale, ranging from A (no motor or sensory function is preserved in the sacral segments S4-S5) to E (normal motor and sensory function) (see Table 3.1) (Kirshblum et al., 2011). A major drawback of AIS scale is its inability to detect small changes in neurophysiological improvements (Awai, 2014) (Bravo-Esteban et al., 2014).

Apart from AIS scale, some of the most used scales in the clinical setting to assess functional walking after SCI are: Walking Index for Spinal Cord Injury (WISCI II), the aforementioned TUG test, the 10-Meter Walk Test (10MWT) and the 6-Minute Walk Test (6MWT).

WISCI II is SCI-specific test. It is used to assess the amount of physical assistance needed by the patient to walk 10 meters. This is a 21-point scale that ranges from 0 (patient unable to stand and/or participate in assisted walking) to 20 (patient ambulates 10 meters with no devices, no braces and no physical assistance) ([Dittuno and Ditunno, 2001](#)).

10MWT measures the time a person takes to walk 10 meters (with or without assistive devices). For that, the person walks 14 meters and the time spent in the intermediate 10 meters is counted. This test can be administered in iSCI patients the first, third, sixth and twelfth month after the injury ([van Hedel et al., 2005](#)) ([Forrest et al., 2014](#)).

6MWT is a sub-maximal test of endurance initially proposed by [Balke \(1963\)](#), measuring the total distance covered by a person to walk over a total of six minutes on a hard, flat surface ([Jackson et al., 2008](#)).

In addition, comprehensive rating scales like the Spinal Cord Independence Measure (SCIM), which is a disability scale specific for SCI ([Benito-Penalva et al., 2012](#)) ([Gil-Agudo et al., 2013](#)) ([Kapadia et al., 2014](#)), measure the ability of SCI patients to perform everyday tasks according to their value for the patient ([Catz and Itzkovich, 2007](#)). This scale can be used as a compact guide for determining certain treatment goals and for outcome assessment following interventions designed to promote recovery after SCI ([Catz and Itzkovich, 2007](#)).

In addition to the aforementioned modified Ashworth scale (MAS), other scales are usually used to assess clinical conditions of spasticity in SCI patients. Those scales are the Penn scale and the Spinal Cord Assessment Tool for Spastic Reflexes (SCATS). Penn scale is a self-report measure that assess a patient's perception of spasticity frequency and severity by assessing the frequency of spasms ([Penn et al., 1989](#)). On the other hand, SCATS scale measures three types of spastic reflexes in SCI patients: clonus, flexor spasms and extensor spasms, each of them rated from 0 (no reaction) to 3 (severe) ([Benz et al., 2005](#)).

3.4.2.2 Emerging measures of sensorimotor impairments after spinal cord injury

Novel metrics for a more detailed comprehension of neuromuscular control in terms of degree of voluntary motor control have been recently proposed. Those include the analysis of EMG coherence and muscle synergies.

Lower limb EMG coherence analysis has been used as an indirect measure of voluntary motor control, gait function ([Hansen et al., 2005](#)) and spasticity ([Bravo-Esteban et al., 2014](#)) after iSCI. This is a frequency-domain measure of the similarity between two independent EMG signals, having the potential to assess the descending motor drive ([Boonstra, 2013](#)). The fact that it just needs EMG recording to be calculated makes it suitable for clinical applications. Despite its ability to provide information about disturbances and changes in motor control, which can be very valuable to understand compensation strategies and for further rehabilitation processes, EMG is still rarely employed in the clinical setting to assess SCI patients ([Wang et al., 2013](#)).

On the other hand, the analysis of muscle synergies may be also used to assess sensorimotor impairments after SCI. For instance, [Hayes et al. \(2014\)](#) showed that the muscle synergy responsible for eccentric braking was absent in all individuals with iSCI, which is consistent with foot drop or slap that is often observed clinically. In general, muscle synergies of iSCI also exhibit abnormal co-activation of muscles and much broader temporal recruitment across the gait cycle ([Hayes et al., 2014](#)) ([Ting et al., 2015](#)), which may also be explored as a measure of sensorimotor impairment.

Chapter 4

Study 1 - Shared synergies in human walking and cycling

Abstract

Background. Biomechanical tasks may reflect synergistic control of muscles (*i.e.*, groups of muscles are co-activated to perform a given task). Due to similarities in kinematics and muscle control with walking, cycling may be explored as a novel framework for the assessment of motor performance.

Objective. The main goal of this Chapter is to investigate similar features of walking and cycling in healthy subjects, using the muscle synergies hypothesis. Thus, three hypotheses were tested: I) muscle synergies extracted from walking are similar to those extracted during cycling; II) muscle synergies extracted from one of these two motor tasks can be used to mathematically reconstruct the EMG patterns of the other task; III) muscle synergies of cycling can result from merging synergies of walking. The secondary goal of this study was to identify at what speed (and cadence) higher similarities emerged.

Methods. The EMG of eight muscles of the dominant leg was recorded in eight healthy participants while they walked and cycled at four matching cadences. NNMF algorithm was applied to extract individual muscle synergies.

Results. Results corroborated hypothesis II, showing that four synergies from walking and cycling can successfully explain most of the EMG variability of cycling and walking, respectively; and also corroborated hypothesis III, showing that two out of four synergies from walking appear to merge together to reconstruct one individual synergy of cycling, with best reconstruction values found for higher speeds. The direct

comparison of the synergies of walking and synergies of cycling (hypothesis I) produced moderated values of similarity.

Conclusion. This first study of the Ph.D. Thesis provides supporting evidences to the hypothesis that cycling and walking share common neuromuscular mechanisms. These results support the use of cycling as a novel tool to assess walking in people with impaired neuromotor control.

4.1 Introduction

Recent experimental results in animals and humans (Cheung et al., 2012) (De Marchis et al., 2013) (Dominici et al., 2011) (Gizzi et al., 2012) (Hug et al., 2011) (Moreno et al., 2013) (Routson et al., 2013), as well as simulations (Allen and Neptune, 2012) (Neptune et al., 2009) have supported the idea that motor system uses a synergistic organization to control biomechanical tasks.

There is still no agreement on the origin of muscle synergies: whether they are neurophysiological entities orchestrated by both supraspinal and afferent pathways to facilitate motor control (Berger et al., 2013) (Bizzi and Cheung, 2013) (Cheung et al., 2012) (Chvatal and Ting, 2013) (Clark et al., 2010) (Moreno et al., 2013) (Routson et al., 2013) (Torres-Oviedo and Ting, 2007) or muscular co-activation is rather a result of biomechanical constraints (Kutch and Valero-Cuevas, 2012) (Valero-Cuevas et al., 2009) (Kutch et al., 2008).

Some authors have provided evidence that the same muscle synergies are shared across different biomechanical conditions, such as speed (Cappellini et al., 2006) and loads (Ivanenko et al., 2004) in human walking, and multidirectional postural responses in humans and cats (Torres-Oviedo et al., 2006) (Torres-Oviedo and Ting, 2007). Additional evidence for the hypothesis that movement is a result of the synergistic control of the nervous system can be obtained by extracting similar synergies in different kinematic and biomechanical motor tasks (Tresch and Jarc, 2009). Hug et al. (2010) highlighted that two of the three synergies extracted during cycling in trained cyclists were similar to two of the four synergies presented by Neptune et al. (2009) in a simulation study of the motor control in human walking. Also, Chvatal and Ting (2013) showed that a common set of muscle synergies mediate reactive balance and walking. At the beginning of the Ph.D. Thesis, it was performed a preliminary study, where muscle synergies of cycling and walking of seven healthy subjects were compared at one matching speed, showing that these two motor tasks may in fact share similar muscle synergies (Barroso et al., 2013). However, the processes underlying this similarity must be studied in more

detail. For instance, as pedaling has fewer mechanical degrees-of-freedom (Raasch and Zajac, 1999) with respect to walking (Zajac et al., 2002), it is expected that the number of synergies in cycling may in fact be lower than in walking.

4.2 Goals

The first goal of this chapter is to provide additional evidences for the hypothesis that human walking and cycling share similar muscle synergies. The similarity analysis was investigated across four different speeds, using a threefold methodology. First, muscle synergies were extracted independently for each tested speed and motor task (walking and cycling), to be further compared. Second, it was tested if the EMG patterns from one motor task (e.g. walking) could be reconstructed by using the synergies of the other motor task (e.g. cycling). Finally, it was tested if reference set of matrices W_0 from cycling could be obtained by merging different walking synergies.

The secondary goal of this chapter is to identify the condition (cadence) at which similarity between tasks mostly emerged. This secondary goal is motivated by the idea of using cycling as a new scenario for the diagnosis and neurorehabilitation of walking in neurologically injured people.

4.3 Materials and Methods

4.3.1 Subjects

Eight healthy subjects (6 men and 2 women, age 27.3 ± 1.3 , height 1.77 ± 0.07 m, weight 75.9 ± 7.4 Kg) volunteered to participate in this study. They were informed about all the procedures and possible discomforts before giving their informed consent. A local committee provided ethical approval for this research.

4.3.2 Experimental protocol

Each participant was instructed to refrain from intense physical activities during the two days before the experiments. For each participant, the experiment was divided into three sessions.

In the first session, participants walked on a treadmill (DOMYOS TC-450 Motorised Treadmill, Decathlon, Villeneuve d'Ascq, France) in order to determine four specific speeds. These speeds were: maximum walking speed (MWS, set as 0.1 Km/h

less than the transition speed from walking to running); the speed at which each participant walked with a cadence of 42 strides per minute (S42); and two intermediate speeds at which each participant walked with a cadence of 70% (70%MWS) and 80% (80%MWS) of the MWS cadence. S42 condition was included to allow for an absolute comparison across subjects. Except for MWS condition, a metronome was used to synchronize participants' cadence in the other three conditions (70%MWS, 80%MWS and S42).

In the second session, each participant performed four walking trials, each one at the speeds previously determined. In the third session, each participant performed four pedaling trials on an electronically braked cycle ergometer (MOTOmed viva2, RECK, Betzenweiler, Germany - see Figure 4.1) in the passive mode, each one at matching cadences with respect to walking. For the pedaling trials, a metronome was used to help participants to synchronize with the target cycling frequency.



FIGURE 4.1: MOTOmed viva2, Reck, Betzenweiler, Germany.

To match cycling and walking cadences, the walking cadence (strides per minute) corresponding to each speed was calculated and then applied to the corresponding cycling trial, in terms of cycling frequency (expressed in rpm, revolutions per minute). To avoid biased results, the order of walking and cycling sessions, as well as the order of intra-session trials, was randomized.

The three sessions were performed during the same day. In the second and third sessions, each subject was first asked to warm-up during five minutes at a self-selected speed, and then to execute each trial during 30s (see Figure 4.2), with 30s resting between trials (Hidler and Wall, 2005). The first session took approximately 5 minutes, while the other two sessions lasted approximately 15 minutes each. A 15 minutes rest between sessions was respected, in order to prevent muscle fatigue.

EMG recordings

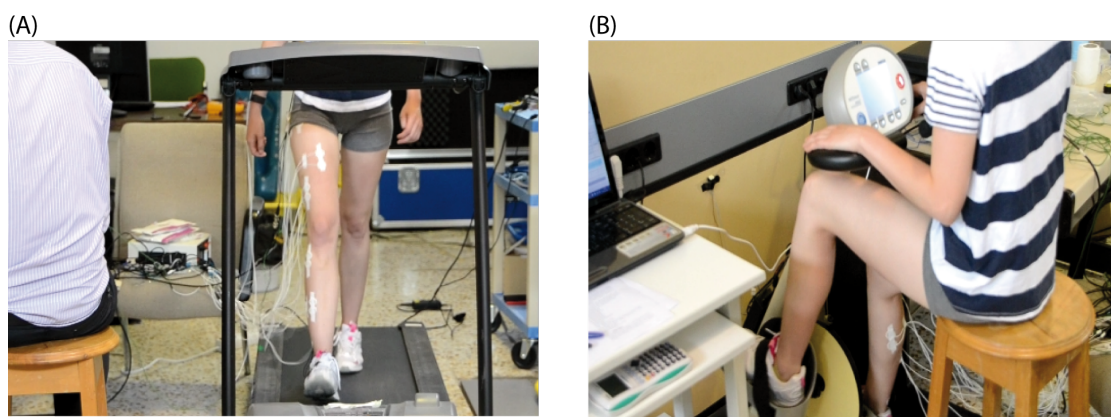


FIGURE 4.2: EMG recordings during a A) walking trial and a B) pedaling trial.

In the second and third sessions, an EMG amplifier (EMG-USB, OT Bioelettronica, Torino, Italy) with recording bandwidth of 10Hz - 750Hz, overall gain of 1000 V/V and acquisition frequency of 2048 Hz was used to record surface electromyography (sEMG) activity of eight muscles of the dominant leg. Before starting the sEMG recordings, the skin was shaved and cleaned with alcohol, to minimize the skin impedance. Bipolar EMG electrodes (Ag-AgCl, Ambu® Neuroline 720, Ambu, Ballerup, Denmark) were placed on the following muscles, according to the SENIAM recommendations (Hermens et al., 1999): Gluteus Medius (GMed), Rectus Femoris (RF), Vastus Lateralis (VL), Biceps Femoris (BF), Semitendinosus (Sem), Gastrocnemius Medialis (GaM), Soleus (Sol) and Tibialis Anterior (TA). A 2-cm inter-electrode distance was ensured, as recommended by SENIAM (Hermens et al., 1999). After being placed, electrodes were wrapped with bandages to ensure that the wires did not impede participants' movements and also to avoid movement-induced artifacts. Some preliminary tests were performed to check for crosstalk and artifacts. When needed, electrodes and cables were repositioned. One

footswitch (NORAXON©, Scottsdale, Arizona, U.S.A.) was placed beneath the heel of the dominant leg, in order to record heel strike moments during walking.

The cycling resistance (gear) was set to a constant and comfortable value for all the trials performed by each subject, so that they could cycle with some resistance. A potentiometer (Vishay, Malvern, PA, U.S.A.) was mounted on the crank to allow for pedal angle measurement. Data from potentiometer (acquisition frequency of 50 Hz) and footswitch (acquisition frequency of 1000 Hz) were used for further segmentation of pedaling and stride cycles, respectively. As the participants of this study were all right-leg dominant, each pedaling cycle started at the lowest pedal position (BDC) of the right crank and finished after completing a revolution. On the other hand, each walking cycle started at each right heel strike. EMG, potentiometer and footswitch data were synchronized by applying a trigger signal. Data were analyzed offline with Matlab R2011a (The Mathworks, Natick, MA) and IBM SPSS Statistics 20 software (IBM).

4.3.3 EMG analysis

A user-friendly GUI called SynergiesLAB (see Appendix C) was created to extract muscle synergies from raw EMG. SynergiesLAB is Matlab-based software tool developed along the Ph.D. period, which contains functions that allow for the detailed analysis and comprehension of all the computational steps to process multiple EMG channels, from the raw EMG processing, up to the calculation of activation coefficients and synergy vectors. This software can be customized to a wide range of motor tasks, different algorithms for synergies extraction, filtering options and number of muscles.

Using SynergiesLAB, for each trial, ten continuous non-corrupted stride/cycling cycles were selected for analysis. Raw EMG signals were high-pass filtered (cutoff frequency of 20Hz) (Moreno et al., 2013). Trials contaminated with 50Hz electromagnetic interference were additionally filtered by a 50Hz notch filter. After that, all the filtered signals were demeaned, rectified and low pass filtered at 5Hz, resulting in the EMG envelopes (Clark et al., 2010) (Hug et al., 2010) (Moreno et al., 2013).

For each participant, EMGs from each muscle were normalized by the average of its peaks from the ten cycles, and resampled at each 1% of the stride/cycling cycle. For each cycle, we subtracted the minimum of that cycle, in order to obtain a minimum value of zero for all the cycles. For each subject, motor task and speed, normalized EMGs were combined into an $m \times t$ matrix (EMG_0), where m indicates the number of muscles (eight in this case) and t is the time base ($t = \text{no. of strides (10)} \times 100 \text{ samples}$)).

Differences between mean EMG envelopes of iSCI patients and the mean EMG envelopes of the healthy group were assessed using two criteria proposed by [Hug et al. \(2011\)](#): the lag time and r_{max} coefficient. The lag time quantifies the time shift between EMG patterns and is calculated as the time shift needed to get the maximum (r_{max}) of the cross correlation between two signals. The cross correlation is calculated by the Matlab `xcorr` function for centered data (option = “coeff”), and the output values as the maximum of the cross-correlation function, which gives an indication on the similarity of shape of the EMG envelopes.

4.3.4 Muscle synergies analysis

The NNMF algorithm (see equation 2.1) ([Lee and Seung, 1999](#)) was chosen in Synergies-LAB (see the Matlab code in Appendix D) to extract the muscle synergy vectors and the corresponding activation coefficients. NNMF was applied over the 10 consecutive walking/pedaling cycles of the EMG envelopes, for each subject and speed. The algorithm was run from two to seven synergies. For each number of synergies and to avoid local minima, NNMF was run 40 times and the run with the lowest reconstruction error was selected.

Muscle synergy vectors (columns of matrix W) were normalized by the maximum of each column, and the corresponding activation coefficients (lines of matrix H) were scaled by the same quantity. The similarity between EMG_0 and EMG_r was calculated using the variability accounted for (VAF_{total}) as reconstruction goodness score coefficient, as represented in Equation 4.1.

$$VAF_{total} = 1 - \frac{\sum_{i=1}^m \sum_{j=1}^t (EMG_0(i, j) - EMG_r(i, j))^2}{\sum_{i=1}^m \sum_{j=1}^t (EMG_0(i, j))^2} \quad (4.1)$$

The quality of reconstruction was also computed for each muscle individually using VAF_{muscle} . A minimum value of 90% for VAF_{total} ([Hug et al., 2010](#)) and 75% for VAF_{muscle} were defined to consider the quality of reconstruction acceptable ([Hug et al., 2011](#)).

A reference set of matrices (hereafter called W_0 and H_0) were obtained for each speed and motor task, by concatenating the EMG envelopes from all the subjects and then applying the NNMF algorithm. W_0 corresponding to the MWS condition was also used as the reference to order the synergies extracted independently from each subject. This was done by comparing each individual muscle synergy vector (column of matrix W) with muscle synergy vectors from matrix W_0 , by using normalized scalar product ([Gizzi et al., 2011](#)), with the less similar being the last ordered.

Data analysis was divided in 3 sections: I) Independent analysis of walking, II) Independent analysis of cycling, and III) Comparison between walking and cycling. Sections I and II aimed to compare the results with literature on walking and cycling, respectively. Section III aimed to test the hypotheses of this study. To this aim, section III consisted on a threefold analysis. The first analysis was done by comparing muscle synergy vectors of walking with those of cycling, using normalized scalar product. Normalized scalar products = 0.75 were taken as similarity threshold, as proposed by [Cheung et al. \(2012\)](#). The second analysis was done by testing the hypothesis that EMG envelopes of cycling could be reconstructed using synergy vectors (columns of matrix W) extracted from walking, and vice versa, for each speed and subject. VAF_{total} values were used to evaluate the quality of this reconstruction. The third analysis tested if reference set of matrices W_0 from cycling could be obtained by merging different walking synergies. To determine which synergies extracted at cycling could be reconstructed by linear combinations of synergies extracted at walking, nonnegative least squares were used as described in ([Cheung et al., 2012](#)). This procedure is described in Equation 4.2 and detailed in Figure 4.3.

$$w_i \approx \sum_{k=1}^{n_{walking}} m_k^i w_k, m_k^i \geq 0, i = 1, \dots, n_{cycling} \quad (4.2)$$

where w_i is the i -th muscle synergy vector (column of matrix W_0) from cycling, w_k is the k -th muscle synergy vector from walking, $n_{walking}$ is the number of synergies at walking (four in this case), $n_{cycling}$ is the number of synergies at cycling (three in this case), and m_k^i is a nonnegative coefficient denoting the degree of contribution of the k^{th} synergy from walking to the structure of the i^{th} synergy from cycling. This algorithm was applied through nonnegative least squares implemented using the *lsqnonneg* option in Matlab. A walking synergy was considered to significantly contribute to the corresponding cycling synergy if the merging coefficient m_k^i was higher than 0.3. According to this method, and for matching speeds, each synergy extracted at walking could contribute to the reconstruction of one or more synergies at cycling. After selecting the walking synergies that could contribute for the reconstruction of cycling synergies, similarity between reconstructed w_i and the initially extracted synergy of cycling was assessed by using the normalized scalar product between corresponding columns.

In addition to the analysis of muscle synergy vectors, a simple analysis of temporal activations (H_0) was also performed, in order to identify the periods of activation and no activation of each synergy along the gait and pedaling cycle. This analysis was done by defining an onset threshold calculated as the triple SD range of activation for each activation coefficient, as performed before in a previous work (([Moreno et al., 2013](#))).

$$\begin{array}{c}
 \begin{array}{c} \text{Synergy vector 1} \\ \downarrow \text{of cycling} \\ \begin{bmatrix} w_1(1) \\ w_1(2) \\ \dots \\ w_1(m) \end{bmatrix} \end{array} \\
 \approx m_1^1 \cdot \begin{array}{c} \text{Synergy vector 1} \\ \downarrow \text{of walking} \\ \begin{bmatrix} w_1(1) \\ w_1(2) \\ \dots \\ w_1(m) \end{bmatrix} \\
 + m_2^1 \cdot \begin{array}{c} \text{Synergy vector 2} \\ \downarrow \text{of walking} \\ \begin{bmatrix} w_2(1) \\ w_2(2) \\ \dots \\ w_2(m) \end{bmatrix} \\
 + m_3^1 \cdot \begin{array}{c} \text{Synergy vector 3} \\ \downarrow \text{of walking} \\ \begin{bmatrix} w_3(1) \\ w_3(2) \\ \dots \\ w_3(m) \end{bmatrix} \\
 + m_4^1 \cdot \begin{array}{c} \text{Synergy vector 4} \\ \downarrow \text{of walking} \\ \begin{bmatrix} w_4(1) \\ w_4(2) \\ \dots \\ w_4(m) \end{bmatrix} \\
 \\
 \begin{array}{c} \text{Synergy vector 2} \\ \downarrow \text{of cycling} \\ \begin{bmatrix} w_2(1) \\ w_2(2) \\ \dots \\ w_2(m) \end{bmatrix} \\
 \approx m_1^2 \cdot \begin{array}{c} \downarrow \\ \begin{bmatrix} w_1(1) \\ w_1(2) \\ \dots \\ w_1(m) \end{bmatrix} \\
 + m_2^2 \cdot \begin{array}{c} \downarrow \\ \begin{bmatrix} w_2(1) \\ w_2(2) \\ \dots \\ w_2(m) \end{bmatrix} \\
 + m_3^2 \cdot \begin{array}{c} \downarrow \\ \begin{bmatrix} w_3(1) \\ w_3(2) \\ \dots \\ w_3(m) \end{bmatrix} \\
 + m_4^2 \cdot \begin{array}{c} \downarrow \\ \begin{bmatrix} w_4(1) \\ w_4(2) \\ \dots \\ w_4(m) \end{bmatrix} \\
 \\
 \begin{array}{c} \text{Synergy vector 3} \\ \downarrow \text{of cycling} \\ \begin{bmatrix} w_3(1) \\ w_3(2) \\ \dots \\ w_3(m) \end{bmatrix} \\
 \approx m_1^3 \cdot \begin{array}{c} \downarrow \\ \begin{bmatrix} w_1(1) \\ w_1(2) \\ \dots \\ w_1(m) \end{bmatrix} \\
 + m_2^3 \cdot \begin{array}{c} \downarrow \\ \begin{bmatrix} w_2(1) \\ w_2(2) \\ \dots \\ w_2(m) \end{bmatrix} \\
 + m_3^3 \cdot \begin{array}{c} \downarrow \\ \begin{bmatrix} w_3(1) \\ w_3(2) \\ \dots \\ w_3(m) \end{bmatrix} \\
 + m_4^3 \cdot \begin{array}{c} \downarrow \\ \begin{bmatrix} w_4(1) \\ w_4(2) \\ \dots \\ w_4(m) \end{bmatrix}
 \end{array}
 \end{array}
 \end{array}$$

FIGURE 4.3: Representation of the merging process using linear combinations of synergy vectors from walking to reconstruct synergy vectors from cycling. m_k^i is a non-negative coefficient denoting the degree of contribution of the k^{th} synergy vector from walking to the structure of the i^{th} synergy vector from cycling. m_k^i lower than 0.3 counted as zero for the linear combination.

4.3.5 Statistical analysis

Paired Student's t -tests were performed to compare cadences between motor tasks, for each different speed. Statistical significance was set by a p -value of 0.05.

4.4 Results

4.4.1 Independent analysis of walking

4.4.1.1 EMG envelopes

The group averaged EMG envelopes of each of the eight recorded muscles, for all walking conditions, are represented in Figure 4.4.

For each participant, the shapes of EMG envelopes during walking correlated well across conditions. The lowest correlation value when compared with MWS was obtained for RF at S42 speed (0.79 ± 0.08 , range 0.69-0.92) and the higher correlation was obtained for Sol at 80%MWS (0.98 ± 0.01 , range 0.96-0.99). On the other hand, it can be observed by visual inspection of Figure 4.4 that the peak of activation of some muscles (*e.g.*, RF and TA.) occurred slightly earlier in the gait cycle as the speed increased. The lower the speed, the later this peak occurred.

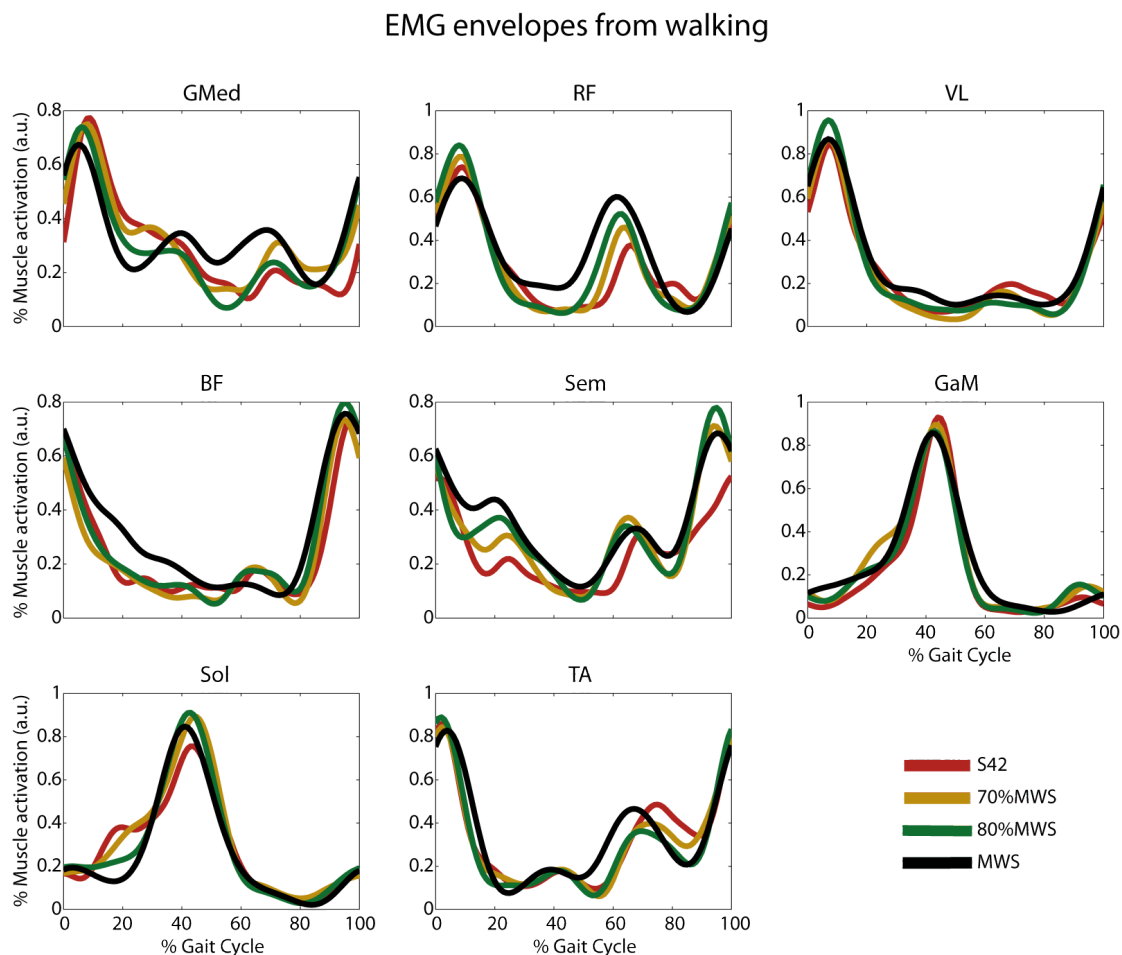


FIGURE 4.4: Group averaged EMG envelopes of the eight recorded muscles, for each of the four studied conditions in walking. A total of 80 cycles (ten individual cycles of each of the eight subjects) were averaged and expressed as a function of the gait cycle. Each walking cycle started at each right heel strike. For each subject, EMG envelopes from each muscle were previously normalized by the average of its peaks throughout the ten cycles. Muscle abbreviations: GMed - Gluteus Medius, RF - Rectus Femoris, VL - Vastus Lateralis, BF - Biceps Femoris, Sem - Semitendinosus, GaM - Gastrocnemius Medialis, Sol - Soleus and TA - Tibialis Anterior. Speed conditions abbreviations: MWS - maximum walking speed; S42 - speed at which each subject walked at 42 strides per minute; 70%MWS - speed at which each subject walked with a cadence of 70% of MWS cadence; 80%MWS - speed at which each subject walked with a cadence of 80% of MWS cadence.

4.4.1.2 Muscle synergies

Four muscle synergies were sufficient to reconstruct the original EMG envelopes for all the subjects and walking conditions, according to the criteria previously defined (VAF_{total} higher than 90% and VAF_{muscle} higher than 75% for each individual muscle). A minimum VAF_{total} value of 90.7% for subject 8 at S42 condition and a maximum of 96% for subject 3 at MWS condition were obtained. Nevertheless, three synergies were also sufficient to fit these criteria in one of the participants.

As a general trend among all the subjects, higher VAF_{total} values were obtained for higher speeds, as represented in Figure 4.5A. Reconstruction of EMG envelopes with five synergies did not improve considerably the reconstruction quality when compared with the reconstruction with four synergies.

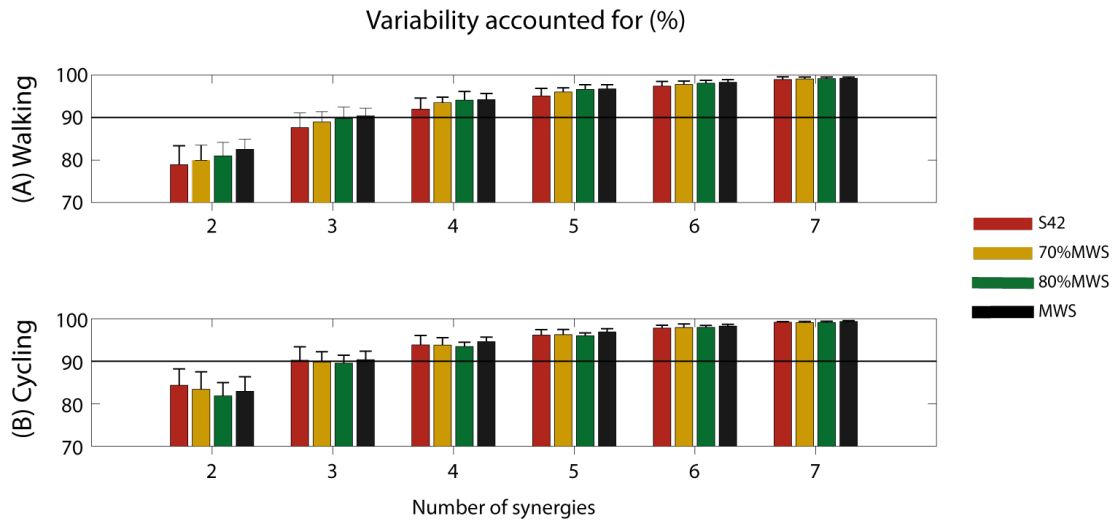


FIGURE 4.5: Variability accounted for (VAF_{total}) values (mean \pm SD) according to the number of muscle synergies used to reconstruct EMG envelopes with the NNMF algorithm, for each speed condition in (A) walking and (B) cycling. The quality of reconstruction of EMG data was considered good for VAF_{total} values $\geq 90\%$. An increment of the number of synergies led to higher VAF_{total} values.

When analyzing the variability accounted for each muscle (VAF_{muscle}) with 3 synergies (see Figure 4.6A), some muscles were not so well reconstructed. For instance, Sem presented a VAF_{muscle} value of 78.3 ± 13.6 at S42 and BF presented a VAF_{muscle} value of 77.3 ± 10.7 at 70%MWS. On the other hand, when analyzing VAF_{muscle} values with 4 synergies (see Figure 4.6B), all the muscles presented mean VAF_{muscle} values higher than 87%, and most of them present VAF_{muscle} values higher than 92%. As it happened with VAF_{total} , also VAF_{muscle} values increased, in general, with the increase of speed, for 3 and 4 synergies, as represented in Figure 4.6A and 4.6B, respectively.

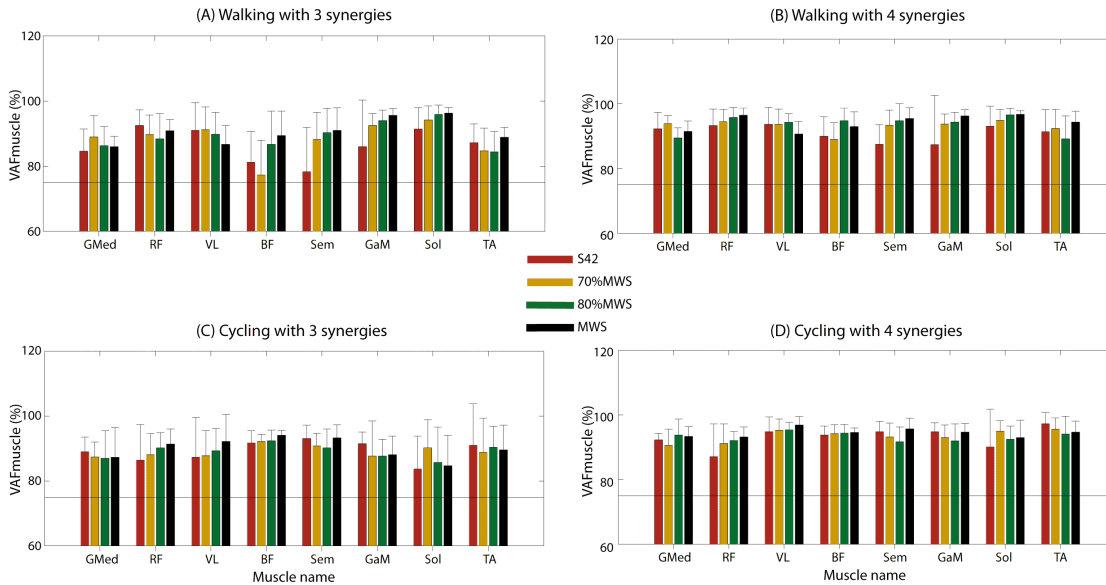


FIGURE 4.6: Variability accounted for (VAF_{muscle}) values (mean \pm SD) for each muscle; (A) Walking with 3 synergies; (B) Walking with 4 synergies; (C) Cycling with 3 synergies; (D) Cycling with 4 synergies. A minimum value of 75% for VAF_{muscle} was used to consider the quality of reconstruction of each muscle good.

Reference sets of muscle synergy vectors (columns of matrix W_0) and the corresponding activation coefficients (lines of matrix H_0) at MWS condition are represented in Figures 4.7A-II and 4.7A-I, respectively. Matrices W_0 and H_0 for each speed condition (see Figure 4.7A-III,IV) were extracted by using the NNMF algorithm after concatenating 10 cycles from all the eight subjects. The quality of reconstruction when using four synergies to reconstruct the pooled EMG envelopes from all the subjects was quite good. In fact, except for S42 condition ($VAF_{\text{total}} = 87.7\%$), it was possible to obtain VAF_{total} values higher than 90%. These results improved for higher speeds (90.2% for 70%MWS, 90.7% for 80%MWS and 90.9% for MWS). In the case of the reconstruction of pooled EMGs with three synergies, the quality of reconstruction was lower. VAF_{total} values ranged from 83.7% at S42 condition to 87.3% at MWS condition.

When analyzing matrices W_0 and H_0 from Figure 4.7A, some properties of muscle synergies during cycling can be identified. Synergy 1 consisted mainly of the co-activation of GMed (hip abductor and hip flexor) and TA (ankle dorsiflexor) (see Figure 4.7A-IV). In the case of higher speeds, this synergy was also responsible for the co-activation of VL (mainly a knee extensor). Synergy 1 was mainly activated during loading response and mid-stance. Synergy 2 consisted mainly of the co-activation of RF (hip flexor, also knee extensor) and, in minor extent, of VL and TA. This synergy

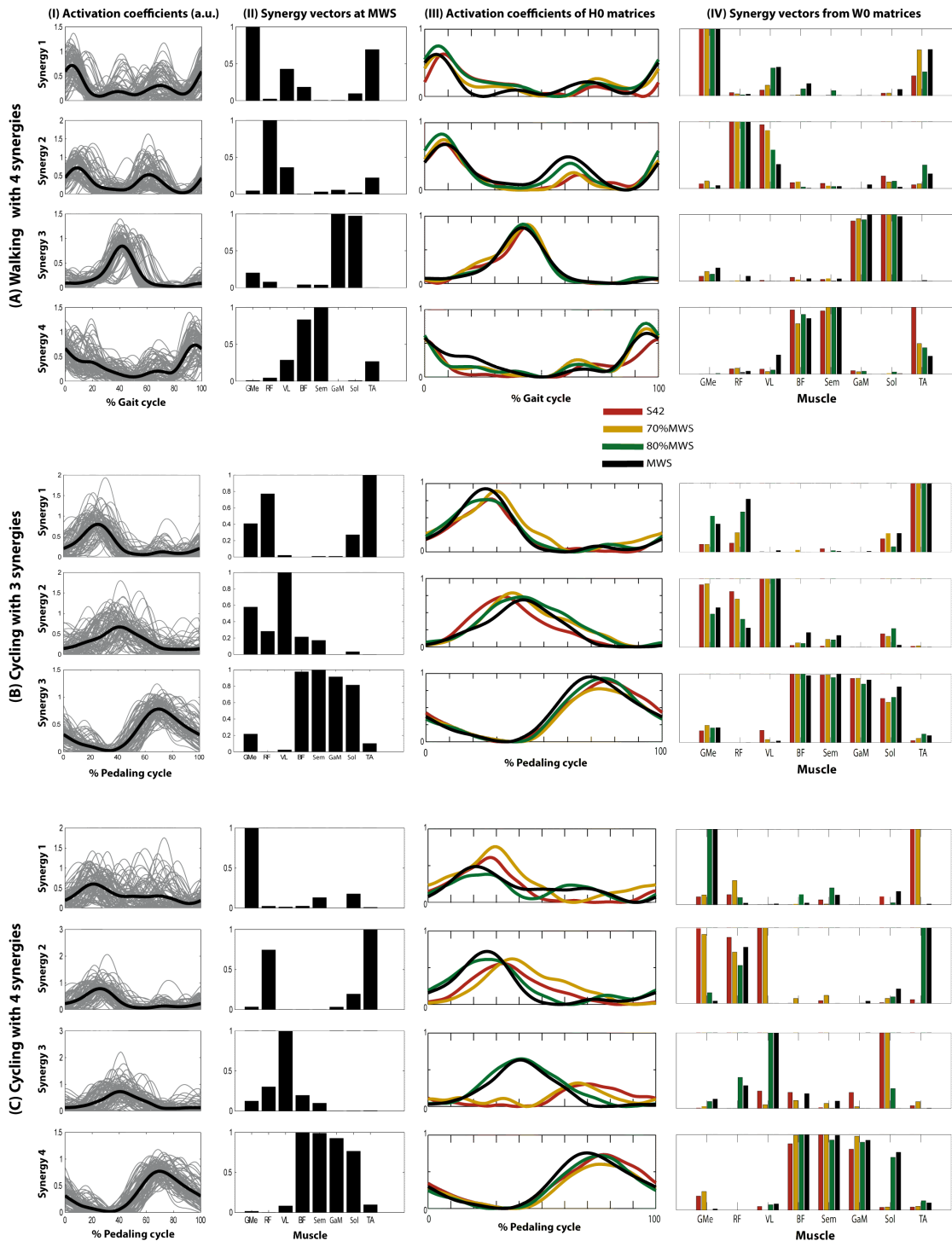


FIGURE 4.7: Reconstruction of concatenated EMGs from the 8 subjects with the NNMF algorithm, when using (A) 4 synergies for walking, (B) 3 synergies for cycling and (C) 4 synergies for cycling. (I) Normalized activation coefficients (lines of matrix H_0) for MWS condition indicate the time-variant profiles responsible to activate each synergy. Thin grey lines represent activation coefficients of each of the 80 cycles (10 cycles per subject), with each black thick line representing the average of those cycles. (II) Each muscle synergy vector (columns of matrix W_0) of MWS condition has a time-invariant profile of activation, representing the relative contribution of each synergy for each muscular pattern. Muscle synergy vectors were normalized by their maximum value. (III) Averaged activation coefficients for all the speeds were calculated, in order to compare periods of activation responsible for important biomechanical tasks of each type of movement. (IV) Muscle synergy vectors for all the speeds are represented with different grey scales.

contributed in a lower extent for VL activation with the increase of speed, in opposition to the synergy 1 influence. This synergy 2 presented two peaks of activation: one at mid-stance phase and the other at initial swing phase. The peak at initial swing phase was lower for lower speeds. Synergy 3 consisted mainly of the co-activation of GaM (knee flexor and ankle plantarflexor) and Sol (ankle plantarflexor) during terminal stance. Synergy 4 consisted mainly of the co-activation of BF (hip extensor and knee flexor), Sem (hip extensor and knee flexor) and, in minor extent, by TA muscles at terminal swing and initial stance. The contribution of this synergy for TA overall activity was higher for decreasing speeds.

4.4.2 Independent analysis of cycling

4.4.2.1 EMG envelopes

The group averaged EMG envelopes of each of the eight recorded muscles, for all cycling conditions, are represented in Figure 4.8. The shapes of EMG envelopes during cycling correlated well across speeds. This is corroborated by the high correlation values across speeds. When compared with MWS, the lowest correlation value was 0.91 ± 0.06 (range 0.80-0.99) for Sol at 70%MWS.

4.4.2.2 Muscle synergies

Four muscle synergies were sufficient to reconstruct the original EMG envelopes for all the subjects and walking conditions, according to the first inclusion criterion ($\text{VAF}_{\text{total}}$ higher than 90%), as represented in Figure 4.5B. A minimum $\text{VAF}_{\text{total}}$ value of 92% for subject 1 at 80%MWS condition and a maximum of 96% for subject 4 at 70%MWS condition were obtained. $\text{VAF}_{\text{muscle}}$ values were higher than 90% for all the muscles and speed conditions of cycling, when using four synergies to reconstruct original EMG envelopes (see Figure 4.6D).

When analyzing EMG reconstruction with three synergies, $\text{VAF}_{\text{total}}$ values oscillated around 90%. Three synergies were sufficient to fit the criterion of $\text{VAF}_{\text{muscle}}$ higher than 90% in six out of the eight subjects. A minimum of 87% for subject 1 at 80%MWS condition and a maximum of 94% for subject 7 at S42 condition were obtained for $\text{VAF}_{\text{total}}$. Conversely, $\text{VAF}_{\text{muscle}}$ values were higher than 83% for all the muscles, which fit the second inclusion criterion, based on $\text{VAF}_{\text{muscle}} > 75\%$ (see Figure 4.6C). Interestingly, $\text{VAF}_{\text{total}}$ did not increase with the increase of speed. The inclusion of a fifth synergy did not improve considerably the reconstruction quality (see Figure 4.5B).

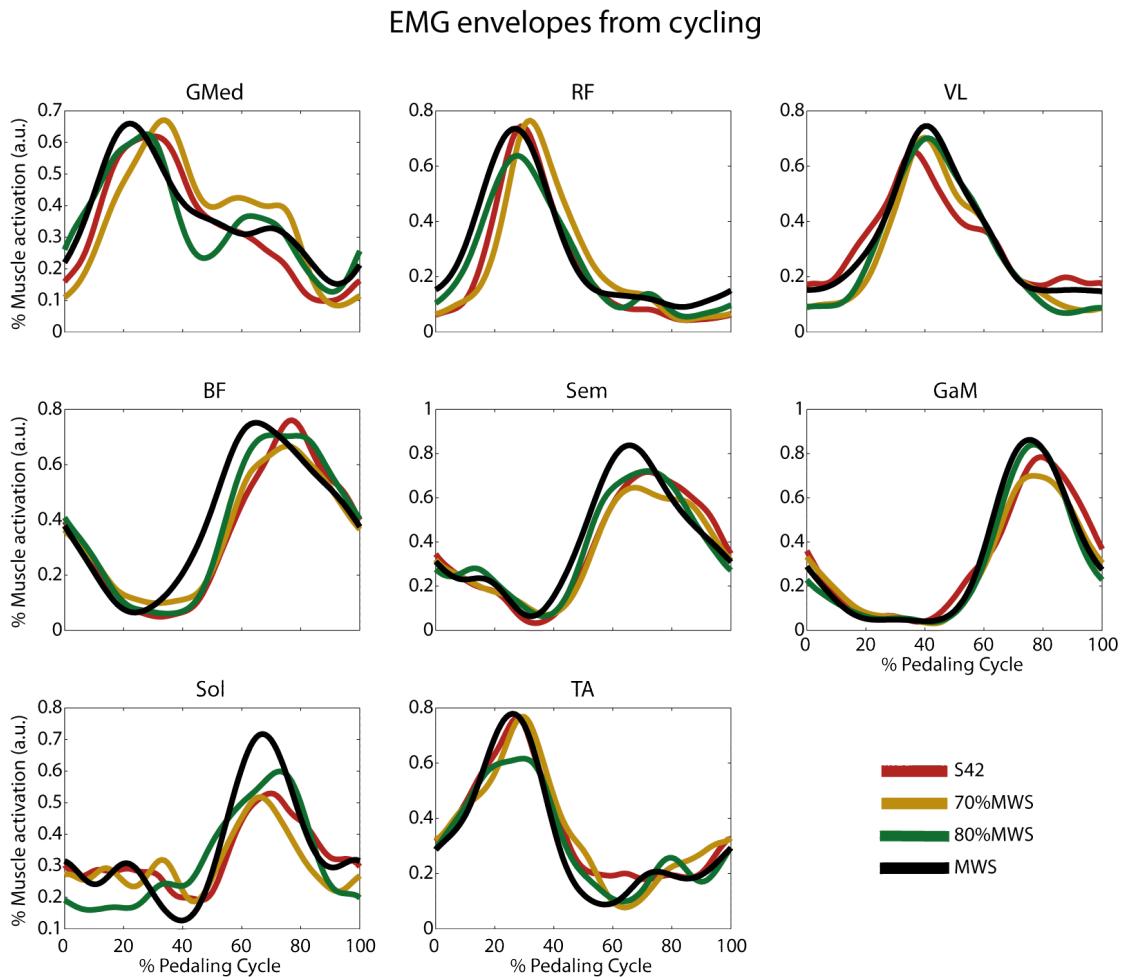


FIGURE 4.8: Group averaged EMG envelopes of the eight recorded muscles, for each of the four studied conditions in cycling. A total of 80 cycles (ten individual cycles of each of the eight subjects) were averaged and expressed as a function of the pedaling cycle. Each pedaling cycle started at the lowest position of the right pedal. For each subject, EMG envelopes from each muscle were previously normalized by the average of its peaks throughout the ten cycles.

Reference sets of three and four muscle synergy vectors (columns of matrix W_0) and the corresponding activation coefficients (lines of matrix H_0) of the entire group while cycling at MWS condition are represented in Figure 4.7B-I,II and Figure 4.7C-I,II, respectively. For all the speed conditions, matrices W_0 and H_0 (see Figure 4.7B-III,IV and 4.7C-III,IV) were also extracted. This representation allowed to have a global template of the synergistic control of cycling for the different speeds and compare it with literature.

When analyzing matrices W_0 and H_0 with three synergies from Figure 4.7B, some properties can be identified. Synergy 1 consisted mainly of the co-activation of TA and, to a lower extent, RF, GMed and Sol (see Figure 4.7B-IV). The contribution of this synergy to the total activity of RF and GMed decreased drastically with the speed.

This synergy was mainly active during initial upstroke phase of cycling (see Figure 4.7B-III). Synergy 2 consisted mainly of the co-activation of RF, GMed and VL and, to a lower extent, of Sol, being mainly active during the final upstroke phase and initial downstroke phase of cycling. Synergy 3 is clearly represented by the activity of BF, Sem, GaM and Sol. Its contribution to Sol activity decreased with the speed. This synergy was active during downstroke phase of cycling.

Considering the case of four muscle synergies, as represented in Figure 4.7C, it can be observed that two different synergistic profiles were obtained: one for lower speeds (S42 and 70%MWS conditions) and other for higher speeds (80%MWS and MWS conditions). When comparing matrix W_0 with four synergies for higher speeds and matrix W_0 with three synergies, it can be observed that, respectively, synergy vector 4 corresponds to synergy vector 3, synergy vector 3 has practically the same morphology of synergy vector 2, and synergy vectors 1 and 2 are fractions of synergy vector 1. On the other hand, synergy vectors from matrix W_0 with four synergies for S42 and 70%MWS conditions were very different from higher speed conditions, mainly because synergy 3 was only responsible for the activation of Sol.

The quality of reconstruction (VAF_{total}) of EMG profiles with concatenated data from all the subjects was higher than 84% when using 3 synergies and higher than 89% when using 4 synergies.

4.4.3 Comparison between walking and cycling

4.4.3.1 Cadence

Subjects maintained a very similar cadence between matching speeds, with no significant differences ($p > 0.05$ for all the speeds). In particular, p -values of 0.229, 0.704, 0.988 and 0.093 were obtained for S42, 70%MWS, 80%MWS and MWS speed conditions, respectively. Walking trials were performed at a mean cadence of 42.1 ± 3.0 strides/minute for S42 condition, 50.1 ± 3.6 strides/minute for 70%MWS condition, 56.7 ± 4.6 strides/minute for 80%MWS condition and 67.7 ± 3.3 strides/minute for MWS condition. On the other hand, cycling trials were performed at a mean cadence of 43.0 ± 2.7 revolutions/minute for S42 condition, 46.6 ± 4.8 revolutions/minute for 70%MWS condition, 56.7 ± 5.1 revolutions/minute for 80%MWS condition and 70.0 ± 4.0 revolutions/minute for MWS condition.

The following subsections present the results of the threefold analysis of similarity between walking and cycling synergies based on the following approaches: 1) direct comparison of muscle synergy vectors, 2) cross-reconstruction of the EMG of

TABLE 4.1: Normalized scalar product between matching synergy vectors from walking and cycling, for each participant (ID01 - ID08).

	ID01	ID02	ID03	ID04	ID05	ID06	ID07	ID08	Mean	Mean (each speed)
S42										0.722
Synergy 1	0.99	0.61	0.67	0.85	0.85	0.61	0.72	0.66	0.75	
Synergy 2	0.92	0.88	0.51	0.92	0.47	0.75	0.82	0.69	0.75	
Synergy 3	0.91	0.75	0.99	0.68	0.79	0.78	0.87	0.96	0.84	
Synergy 4	0.76	0.11	0.48	0.78	0.63	0.52	0.78	0.39	0.56	
70%MWS										0.723
Synergy 1	0.79	0.47	0.89	0.71	0.89	0.84	0.76	0.67	0.75	
Synergy 2	0.94	0.8	0.36	0.91	0.83	0.81	0.78	0.89	0.79	
Synergy 3	0.73	0.64	0.93	0.6	0.76	0.7	0.42	0.56	0.67	
Synergy 4	0.75	0.61	0.65	0.69	0.76	0.43	0.65	0.91	0.68	
80%MWS										0.66
Synergy 1	0.27	0.66	0.85	0.76	0.85	0.75	0.57	0.69	0.68	
Synergy 2	0.71	0.83	0.09	0.96	0.95	0.24	0.69	0.83	0.66	
Synergy 3	0.56	0.12	0.71	0.65	0.91	0.69	0.57	0.23	0.56	
Synergy 4	0.73	0.64	0.93	0.82	0.75	0.53	0.68	0.91	0.75	
MWS										0.738
Synergy 1	0.7	0.84	0.82	0.93	0.68	0.84	0.74	0.87	0.80	
Synergy 2	0.79	0.84	0.31	0.95	0.52	0.15	0.81	0.97	0.67	
Synergy 3	0.75	0.85	0.7	0.79	0.85	0.75	0.72	0.36	0.72	
Synergy 4	0.78	0.83	0.84	0.81	0.75	0.64	0.66	0.78	0.76	

Similarity was calculated between the four extracted synergies for both motor tasks. The similarity threshold was set to 0.75.

cycling by means of walking synergy vectors and vice-versa, and 3) merging walking synergy vectors in order to obtain cycling synergy vectors.

4.4.3.2 Direct comparison of muscle synergy vectors

The four extracted synergies of walking were compared with the four extracted synergies of cycling, by using the normalized scalar product between matching synergy vectors for each subject and speed. Results (see Table 4.1) showed a mean similarity of 0.738 for the MWS condition, 0.66 for the 80%MWS condition, 0.723 for the 70%MWS condition, and 0.722 for the S42 condition. For each subject and speed, at least one of the synergies had, generally, a normalized scalar product lower than 0.75.

Taking into account that EMG envelopes during cycling in trained cyclists can be also well reconstructed using three synergies (Hug et al., 2010) (Hug et al., 2011), a similar comparison of muscle synergy vectors as described before was done, but this time

TABLE 4.2: Normalized scalar product between the three synergy vectors from cycling and the three most similar synergy vectors from walking, for each participant (ID01 - ID08), according to their similarity values.

	ID01	ID02	ID03	ID04	ID05	ID06	ID07	ID08	Mean	Mean (each speed)
S42										0.737
Synergy 1	0.91	0.62	0.66	0.85	0.47	0.76	0.71	0.7	0.71	
Synergy 2	0.92	0.93	0.51	0.92	0.76	0.66	0.83	0.76	0.79	
Synergy 3	0.77	0.71	0.56	0.87	0.63	0.48	0.78	0.92	0.72	
70%MWS										0.778
Synergy 1	0.79	0.81	0.88	0.7	0.84	0.84	0.79	0.67	0.79	
Synergy 2	0.93	0.62	0.98	0.81	0.81	0.85	0.62	0.82	0.81	
Synergy 3	0.72	0.66	0.65	0.66	0.77	0.86	0.69	0.91	0.74	
80%MWS										0.737
Synergy 1	0.67	0.64	0.85	0.77	0.92	0.79	0.76	0.86	0.78	
Synergy 2	0.8	0.83	0.2	0.96	0.97	0.49	0.55	0.79	0.70	
Synergy 3	0.72	0.7	0.64	0.75	0.8	0.67	0.68	0.88	0.73	
MWS										0.777
Synergy 1	0.79	0.85	0.82	0.93	0.67	0.84	0.73	0.88	0.81	
Synergy 2	0.75	0.74	0.35	0.96	0.93	0.84	0.82	0.92	0.79	
Synergy 3	0.79	0.8	0.68	0.7	0.72	0.61	0.75	0.78	0.73	

The similarity threshold was set to 0.75.

comparing the three muscle synergy vectors extracted in cycling with the three muscle synergy vectors extracted in walking (from the total of four muscle synergy vectors) that best correlated with them (see Table 4.2). Activation coefficient 3 of cycling was the one with less similarity values when compared with walking activation coefficients. Normalized scalar product values of synergy vector 3 from cycling and the corresponding synergy vector from walking varied considerably across subjects. Nonetheless, normalized scalar product values were higher in the case of three synergies than those obtained with four synergies, across all speed conditions. Mean correlation values of 0.777 for the MWS condition, 0.737 for the 80%MWS condition, 0.778 for the 70%MWS condition, and 0.737 for the S42 condition were obtained.

4.4.3.3 Cross-reconstruction of EMG envelopes

For each speed and subject, the NNMF algorithm was applied using the walking synergy vectors (columns of matrices W), to reconstruct the cycling EMG envelopes, and vice-versa, at each corresponding matching speed. An individual example of the reconstruction of the cycling EMG envelopes at MWS condition is represented in Figure 4.9A.

The activation coefficients (lines of matrices H) that best fit the walking synergy vectors (represented in Figure 4.9C) are depicted in Figure 4.9B.

Average VAF_{muscle} values when reconstructing cycling EMG envelopes with the corresponding 4 synergy vectors from walking are represented in Figure 4.10A. These values were quite similar across muscles and presented a high inter-subject variability. When analyzing VAF_{total} values of this reconstruction using four synergies from walking (Figure 4.10B), a minimum value of $80.4 \pm 6.1\%$ for S42 condition and a maximum value of $84.5 \pm 3.4\%$ for MWS condition were obtained. When analyzing VAF_{total} values of this reconstruction but with 3 synergies (Figure 4.10B), a minimum value of $71.6 \pm 5.4\%$ for S42 condition and a maximum value of $79.7 \pm 3.4\%$ for MWS condition were obtained. Mean VAF_{total} values of this reconstructed data (with 3 and 4 muscle synergies) increased with the increase of speed, with the best reconstruction values achieved for the MWS conditions.

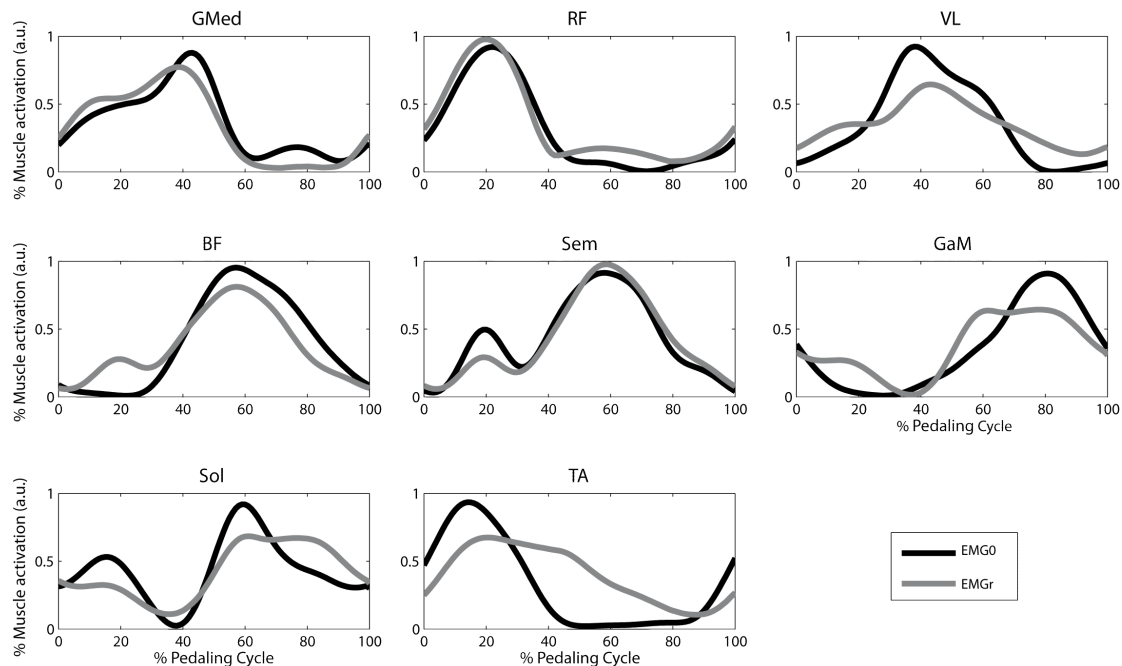
Average VAF_{muscle} values when reconstructing walking EMG envelopes with the corresponding 4 synergies from cycling are represented in Figure 4.10C. These values were high for GMed, RF, VL and TA; on the other hand, low VAF_{muscle} values were found for BF, Sem, GaM and Sol. When analyzing VAF_{total} values of this reconstruction with four synergies (Figure 4.10D), a minimum value of $77.9 \pm 4.3\%$ for S42 condition and a maximum value of $81.5 \pm 0.9\%$ for MWS condition were obtained. When analyzing VAF_{total} values of this reconstruction but with 3 synergies (Figure 4.10D), a minimum value of $71.9 \pm 5.6\%$ for S42 condition and a maximum value of $77.5 \pm 2.4\%$ for MWS condition were obtained. Mean VAF_{total} values of this reconstructed data also increased with the increase of speed (with 3 and 4 muscle synergies), with the best reconstruction values achieved for the MWS conditions.

When comparing the two types of reconstruction, similar VAF_{total} values were achieved when using 3 synergies. On the other hand, the reconstruction of cycling envelopes with walking synergies was better than the other reconstruction, when using 4 synergies.

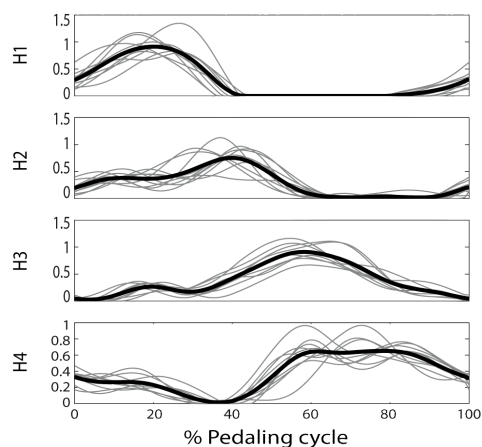
4.4.3.4 Merging of muscle synergy vectors

Muscle synergy vectors extracted from concatenated data of walking (those represented in Figure 4.7A-IV) were merged, by linear combination, in order to reconstruct similar synergy vectors to those extracted from concatenated data in cycling (represented in Figure 4.7B-IV), according to Equation 4.2. The schematic of this merging process for MWS condition is represented in Figure 4.11. The merging coefficients of the merging process are presented in Table 4.3.

(A) Cross-reconstruction of EMGs - Individual example



(B) Activation coefficients (a.u.) obtained in the cross-reconstruction - Individual example



(C) Muscle synergy vectors used for the cross-reconstruction - Individual example

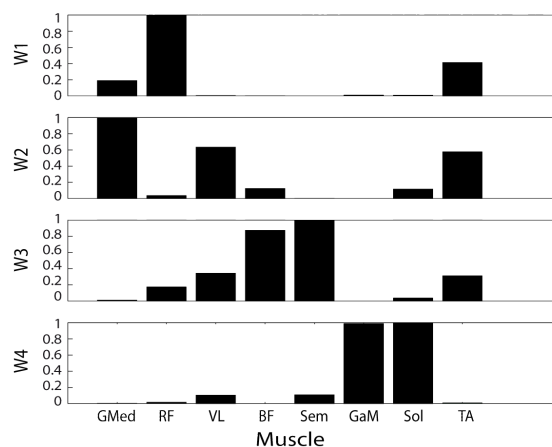


FIGURE 4.9: Individual example of the cross-reconstruction of the cycling EMG envelopes at MWS condition. (A) Black lines represent the original average EMG envelopes (EMG_0) and grey lines represent the reconstructed EMG envelopes (EMG_r) of the eight recorded muscles. NNMF algorithm was applied using the four walking synergies coefficients (matrix W) to reconstruct the cycling EMG envelopes. (B) Normalized activation coefficients (matrix H) indicate the time-variant profile responsible to activate each synergy. Thin grey lines represent activation coefficients of each of the 10 cycles, with each black thick line representing the average of those cycles. (C) Each synergy coefficient extracted at walking (columns of matrix W) is represented by a vector (time-invariant profile of activation), representing the relative contribution of each synergy for each muscular pattern. Muscle synergy vectors were normalized by their maximum value.

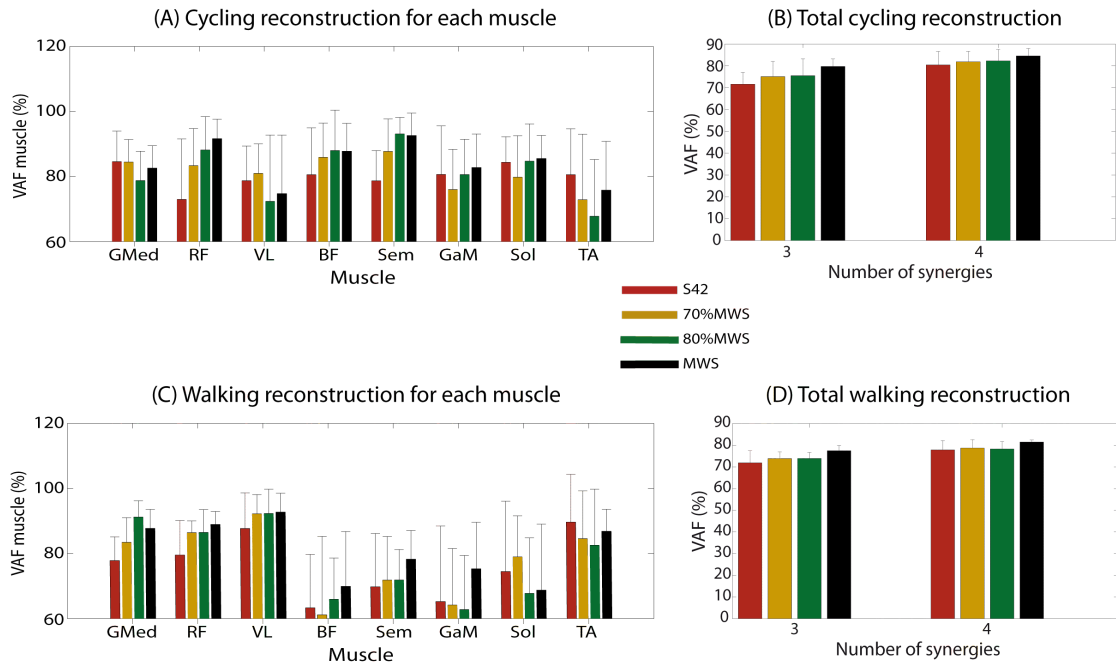


FIGURE 4.10: Quality of cross-reconstruction of EMG envelopes. (A) Group variability accounted for (mean \pm SD) values for each muscle (VAF_{muscle}) when the NNMF algorithm was applied with 4 synergy vectors (matrix W) from walking to reconstruct the cycling EMG envelopes, for all the speeds. (B) Group variability accounted for (VAF_{total}) results (mean \pm SD) when the NNMF algorithm was applied with fixed synergy vectors (3 and 4, respectively) from walking to reconstruct the cycling EMG envelopes, for all the speeds. (C) Group VAF_{muscle} values (mean \pm SD) when the NNMF algorithm was applied with 4 synergy vectors (matrix W) from cycling to reconstruct the walking EMG envelopes, for all the speeds. (D) Group VAF_{total} results (mean \pm SD) when the NNMF algorithm was applied with fixed synergy vectors (3 and 4, respectively) from cycling to reconstruct the walking EMG envelopes, for all the speeds.

A synergy vector of walking was considered to significantly contribute to the merging of a synergy vector of cycling if the merging coefficient was higher than 0.3. After selecting the contribution of the selected synergies and merging them, similarity between reconstructed and original synergy vectors of cycling was assessed. The results are presented in Table 4.4.

MWS and 80%MWS were the speeds at which more similarities were found in the merging process. Synergy vector 3 of cycling was always very well reconstructed with linear combinations of synergy vectors 3 and 4 from walking, for all the speeds (see similarity values in Table 4.4). Also, for MWS and 80% MWS conditions, synergy vectors 1 and 2 from cycling could be both reconstructed by merging synergy vectors 1 and 2 from walking (see Table 4.3 and Table 4.4). For S42 and 70%MWS, synergy vector 2 from cycling could be well reconstructed by merging synergy vectors 1 and 2

TABLE 4.3: Representation of the merging coefficients.

	Cycling		
	Synergy 1	Synergy 2	Synergy 3
S42 walking			
Synergy 1	0.28	0.78	0.00
Synergy 2	0.02	0.86	0.03
Synergy 3	0.07	0.00	0.82
Synergy 4	0.34	0.00	0.66
70%MWS walking			
Synergy 1	0.47	0.56	0.00
Synergy 2	0.10	0.84	0.00
Synergy 3	0.09	0.05	0.77
Synergy 4	0.17	0.00	0.97
80%MWS walking			
Synergy 1	0.51	0.52	0.02
Synergy 2	0.50	0.55	0.00
Synergy 3	0.01	0.11	0.75
Synergy 4	0.07	0.00	0.96
MWS walking			
Synergy 1	0.51	0.49	0.00
Synergy 2	0.69	0.38	0.00
Synergy 3	0.07	0.00	0.88
Synergy 4	0.00	0.18	0.96

Merging coefficients > 0.3 (bold) were considered to contribute to the merging procedure.

TABLE 4.4: Similarity between reconstructed synergy vectors resulting from the merging process and corresponding synergy vectors of cycling.

	Synergy 1	Synergy 2	Synergy 3
S42	0.61	0.98	0.89
70%MWS	0.62	0.93	0.95
80%MWS	0.76	0.84	0.98
MWS	0.85	0.75	0.98

Similarity was assessed by using the normalized scalar product between corresponding synergy vectors. Values > 0.75 (representing good similarity) appear in bold.

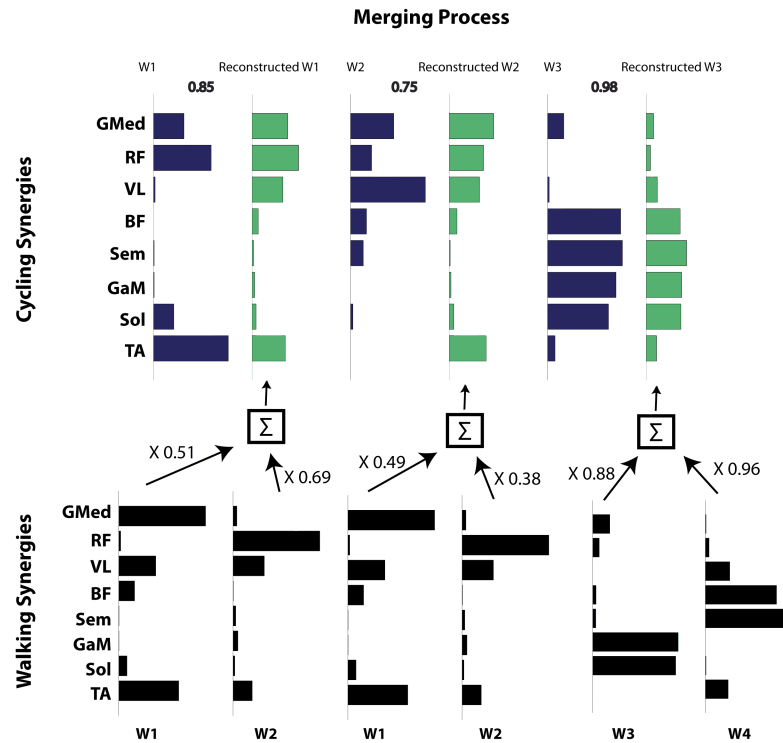


FIGURE 4.11: Cycling synergy vectors reconstructed as a merging (linear combination) of walking synergy vectors for MWS condition. Each of the four walking synergy vectors was considered to significantly contribute to the merging of a cycling synergy vector if its merging coefficient was higher than 0.3 (See Table 4.3). Each synergy vector extracted at walking could contribute to the reconstruction of one or more synergy vectors at cycling. After selecting the contribution of the selected synergy vectors for the merging model, similarity between reconstructed and original cycling synergy vectors was assessed by using the normalized scalar product between corresponding columns. For instance, at MWS, synergy vector 1 (W1) and 2 (W2) from cycling could be well reconstructed by merging synergies 1 (W1) and 2 (W2) from walking; synergy 3 (W3) from cycling could be well reconstructed by merging synergy vectors 3 (W3) and 4 (W4) of walking. The reconstructed synergy vectors presented high degrees of similarity when compared with original synergy vectors of cycling: 0.85 for W1, 0.75 for W2 and 0.98 for W3.

from walking. Finally, synergy vector 1 from cycling at S42 and 70%MWS conditions could not be well reconstructed by merging synergy vectors from walking.

4.5 Discussion

4.5.1 Novelty of the work

The most remarkable finding of this study is that, in healthy subjects, muscle synergies extracted from cycling trials can be reconstructed applying a merging process of muscle

synergies extracted from walking trials. In the preliminary study done at the beginning of the Ph.D. Thesis (Barroso et al., 2013), a direct comparison between synergy vectors of cycling and walking at one selected speed (MWS) was performed, with results suggesting that both tasks may share a similar synergistic control. For the present study, the experiments were performed with different subjects and bigger sample size, three more speeds and investigated the additional merging hypothesis, as well as the cross-reconstruction of EMG patterns.

4.5.2 Cadence

One of the premises to compare the synergistic control of different motor tasks is to assure similar cadences between matching speeds. As no statistically significant differences (p -values > 0.05 for all the speeds) between matching speeds for walking and cycling were verified, the rhythmic activity generated by central pattern generators (CPGs) (Lacquaniti et al., 2012) did not biased the comparison.

4.5.3 Electromyographic patterns in walking and cycling

According to a large number of previous studies (Clark et al., 2010) (Dominici et al., 2011) (Gizzi et al., 2011) (Hug et al., 2011) (Gizzi et al., 2012), EMG envelopes from both legs of healthy people present high similarity. For this reason, muscles from the right were chosen for analysis.

To further compare muscles synergies between walking and cycling, the first goal was to verify the visual similarity both in shape and timing of the EMG envelopes obtained in this study and those presented in literature (Clark et al., 2010) (Dominici et al., 2011) (Gizzi et al., 2012) (Hidler and Wall, 2005) (Ivanenko et al., 2004) (Moreno et al., 2013) (Nymark et al., 2005) (Ricamato and Hidler, 2005). Regarding EMG envelopes for walking trials, the similarity was confirmed. The peak of activation of some muscles occurred earlier in the gait cycle as the speed increased, in agreement with other authors (Ivanenko et al., 2004) (Hof et al., 2002). This behavior seems to be related with changes in the duration of stance (Ivanenko et al., 2004) (*i.e.*, decreased % of stance as the speed increases). As the walking speed increases, the activations are played faster, with no change in the relative timing of activation of EMG envelopes (Hof et al., 2002).

In what concerns the cycling trials, EMG envelopes were also similar to those presented in literature (Wakeling and Horn, 2009) (Hug et al., 2010) (Hug et al., 2011) (De Marchis et al., 2013), with the exception of some muscles (*e.g.*, RF, BF and Sem),

whose activations occurred earlier within the pedaling cycle. This might be due to the slightly different seating position of the subjects in this study: whereas the individuals analyzed in the referred studies seated in an ergometer, with the seat above the axis of rotation, a conventional chair with a seating position closer in height to the axis of rotation was used for this study. The correlations between the EMG envelopes at MWS condition and the other speed conditions were higher than those observed for walking. Best correlation values were obtained for higher speeds, which is in accordance that cadence affects EMG profiles of some muscles of the lower limb (Marsh and Martin, 1995) (Baum and Li, 2003) (Wakeling and Horn, 2009).

4.5.4 Dimensionality of synergistic control

The results presented in this study show that a low-dimensional and impulsive synergistic control is sufficient to control both walking and cycling. Four synergies were sufficient to explain more than 90% of total variability of electromyographic activity of the eight studied muscles, for all subjects and speeds during both motor tasks. For cycling trials, this dimensionality seems to be reduced if compared with walking (see Figures 4.5 and 4.6). Six out of the eight subjects just needed three synergies to fit the criteria defined to consider the quality of reconstruction acceptable ($\text{VAF}_{\text{total}} \geq 90\%$ and $\text{VAF}_{\text{muscle}} \geq 75\%$) for cycling. On the other hand, seven out of the eight subjects needed four synergies to fit these criteria in walking trials. Apparently, three synergies are sufficient to represent most of the electromyographic activity of non-trained cyclists with the subset of 8 muscles analyzed. In the preliminary study done at the beginning of the Ph.D. Thesis (Barroso et al., 2013), four synergies were also sufficient to explain more than 90% of $\text{VAF}_{\text{total}}$ for both walking and cycling, at MWS condition. In the case of cycling, two of the four synergies (one related with the main activation of hamstrings and the other mainly responsible for GaM and Sol activation) were activated by similar activation coefficients (both in time and in shape). This observation provides additional evidence for the hypothesis of lower dimensionality of synergistic control of cycling, when compared with walking. According to d'Avella and Bizzi (2005) and Bizzi and Cheung (2013), muscle synergies may act to constrain the possibilities of motor output. As cycling is a motor task with fewer degrees of freedom than walking (Raasch and Zajac, 1999) (Zajac et al., 2002), it is expected that a higher or at least the same number of synergies are needed to adequately reconstruct EMG envelopes of walking when compared with cycling.

There are many factors that can influence the number of extracted synergies. One main issue that is rarely referred to is the cutoff frequency of the low-pass filter to obtain EMG envelopes, as explained in Subsection 2.3.3. This value should be adapted

to the type of motor task and frequency of movement (Hug, 2011). For the study presented in this chapter, the same cutoff frequency was applied for all the trials and motor task. Another important aspect is the number of muscles considered, which can affect the number of extracted synergies (Clark et al., 2010) (Monaco et al., 2010) (Steele et al., 2013). Contrarily to what was performed in Barroso et al. (2013), the study here presented did not analyze EMG activity from gluteus maximus and tensor fasciae latae; also, a different processing methodology was applied to obtain EMG envelopes. All these factors may explain small differences in the dimensionality. Finally, little is known about the influence of the normalization procedures on the number of extracted synergies, as well as on their composition (Hug et al., 2011). Nonetheless, as referred by Gizzi et al. (2012), the small differences in dimensionality found in different studies are not in disagreement with the hypothesis that motor coordination can be represented by a small set of muscle synergies, robust to explain differences between subjects and conditions.

4.5.5 Reconstruction quality

For walking trials, VAF_{total} increased with the speed for most of the subjects, which is in accordance with the results presented by Ivanenko et al. (2004). According to Tresch et al. (2006), lower signal-to-noise ratio of EMG envelopes in lower speeds may result in lower VAF_{total} values. On the other hand, VAF_{total} of cycling was constant across speeds, for the same number of synergies.

The quality of reconstruction of EMG data obtained by concatenating together all the subjects was also quite good when using 4 synergies for walking (VAF_{total} higher than 88% for all the speeds) and three synergies for cycling (VAF_{total} higher than 84% for all the speeds). These results show that intra and inter-subject variability can be represented by a unique and fixed set of muscle synergies.

4.5.6 Functional interpretation of muscle synergies

The correct execution of biomechanical tasks depends on coordinated muscle activation, because individual muscle action cannot, in general, result in a functional biomechanical function (Zajac et al., 2002). Due to the articulated nature of the body, the activation of a muscle may be reverberated in other muscles and joints that are not connected to that muscle. Thus, it has been suggested that muscle synergies may incorporate knowledge of both musculoskeletal dynamics and other biomechanical properties of the limb (Berniker et al., 2009). The set of all existing synergies should be thought as a compendium of coordinative patterns to execute several movements under different

biomechanical conditions (Bizzi and Cheung, 2013). Nevertheless, other mechanisms as feedback-related activities (Kutch and Valero-Cuevas, 2012) and monosynaptic stretch reflexes may also contribute to individual muscular activity and muscle coupling.

By analyzing the representative sets of muscle synergy vectors (columns of matrices W_0) and the corresponding activation coefficients (lines of matrices H_0), extracted by concatenating EMG data from all the subjects (Figure 4.7-III,IV), it is possible to associate each synergy with a specific biomechanical function. In the case of walking, synergy 1 (involving primarily hip abductor and ankle dorsiflexor) is mainly related to the biomechanical function of body weight support during the early stance phase (Neptune et al., 2009) (Lacquaniti et al., 2012) (Moreno et al., 2013). Synergy 2 (hip flexor and knee extensors) contributed to the control of ankle during initial stance and initial swing (foot lift off) (Neptune et al., 2009) (Lacquaniti et al., 2012) (Moreno et al., 2013). Synergy 3 (knee flexors and ankle plantarflexors) mainly contributed to the forward propulsion of the foot during terminal stance phase (Neptune et al., 2009) (Lacquaniti et al., 2012) (Moreno et al., 2013). Synergy 4 (hip extensors and knee flexors) was a major responsible of leg movement during terminal swing (deceleration of the leg in preparation to heel contact) and preparation towards initial stance (stabilizing the leg after heel contact) (Neptune et al., 2009) (Lacquaniti et al., 2012) (Moreno et al., 2013).

In what concerns the three muscle synergies extracted for cycling trials, they were very similar to those already published by Hug et al. (2010) (see 4.7B). Specifically, synergy 1 (involving primarily hip flexor, knee extensor, and ankle dorsiflexor) mainly provided force to start the upstroke phase of cycling (Barroso et al., 2013). The energy generated by RF in this phase of cycling is transmitted to the crank by the activation of TA (Raasch and Zajac, 1999). TA is excited early in this phase due to its participation in flexion of the limb. Synergy 2 (hip abductor, hip flexor, knee extensors and ankle plantarflexor) contributed to the second part of upstroke phase and also to the initial downstroke phase. Despite being activated to a lower extent, Sol was found to be necessarily co-activated with hip and knee flexors during initial downstroke phase, to facilitate energy transfer from the limb to the crank (Raasch and Zajac, 1999). Finally, synergy 3 (hip extensors, knee flexors and ankle plantarflexors) activated muscles responsible for downstroke phase of cycling (Barroso et al., 2013), including the plantarflexion needed to transfer energy produced by gluteus maximus to the crank (Zajac et al., 2002). Moreover, GaM and Sol act to oppose the strong acceleration of the leg verified during this phase (Zajac et al., 2002). In summary, Sol and TA play a very important role in the proper positioning of the feet to transfer energy from the limb to the crank, preventing ankle dorsiflexion during limb extension and controlling excessive plantarflexion during limb flexion (Raasch and Zajac, 1999) (Zajac et al., 2002).

Considering the case of four synergies extracted for cycling trials (see Figure 4.7C), two different synergistic profiles were obtained: one for lower speeds (S42 and 70%MWS conditions) and other for higher speeds (80%MWS and MWS conditions). For the late one, synergies 3 and 4 presented the same periods of activation (H_0) of synergies 2 and 3 from Figure 4.7B (three synergies). Therefore, these synergies can be considered the same synergy. Synergies 1 and 2 were fractions of synergy 1 from Figure 4.7B. Interestingly, synergies composition (W_0) for S42 and 70%MWS conditions were very similar to those presented by De Marchis et al. (2012). This may indicate a speed effect on synergistic composition in cycling, when using four synergies.

4.5.7 Comparison between walking and cycling

Based on the neural-mechanical components that are thought to be shared between walking and cycling (Raasch and Zajac, 1999) (Zehr et al., 2007) (Hug et al., 2010), this study tested the general hypothesis that pedaling should at least share some similar neural mechanisms involved in the coordination of walking. This was done using a threefold methodology.

The first similarity test was performed by correlating the four synergy vectors of walking with the four synergy vectors of cycling (see Table 4.1). Maximum correlation values were obtained for MWS condition (mean correlation of 73.8%), in accordance with the values presented previously (Barroso et al., 2013) (mean $r = 79.8\% \pm 6\%$). Moreover, the 3 synergy vectors extracted for cycling were correlated with the 3 synergy vectors of walking (from the set of 4 synergies) that best correlated with the cycling synergy vectors (see Table 4.2). In this case, correlation values varied considerably for synergy 3. Four muscles (BF, Sem, GaM and Sol) that are usually activated by synergy 3 of cycling (see Figure 4.7B-IV) are generally activated by synergies 3 and 4 in walking (see Figure 4.7A-IV). As synergy vectors 1 and 2 from cycling usually were similar to synergy vectors 1 and 2 from walking, the synergy vectors of walking that better correlated with synergy vector 3 of cycling were synergy vectors 3 or 4. This explains the lower correlation values for synergy vector 3, when compared with the other two synergy vectors (see Table 4.2). Nevertheless, the correlation values in this case were better than those obtained with four synergies, across all conditions, which may indicate a possible lower dimensionality for cycling.

The second similarity test was performed by testing the hypothesis that EMG envelopes obtained in cycling trials could be reconstructed with the four synergy vectors extracted from walking, and vice-versa. The reconstruction of cycling EMG patterns by using the four walking synergy vectors resulted in slightly higher VAF_{total} values than

the opposite reconstruction. Average $\text{VAF}_{\text{muscle}}$ values when reconstructing walking EMG envelopes with the corresponding four synergy vectors from cycling were high for GMed, RF, VL and TA. On the other side, low $\text{VAF}_{\text{muscle}}$ values were found for BF, Sem, GaM and Sol, because these muscles are activated by the same synergy in cycling (see Figure 4.7B-IV), and by two synergies in walking (see Figure 4.7A-IV). In the future, caution should be used when using just $\text{VAF}_{\text{total}}$ as a metric to decide the number of synergies to use. A combination of $\text{VAF}_{\text{total}}$ with $\text{VAF}_{\text{muscle}}$ (and maybe other metrics) will introduce more reliability. These results support the hypothesis that synergies extracted from walking can be used to reconstruct cycling EMG patterns.

Finally, the hypothesis that synergy vectors of cycling can result from merging synergy vectors of walking was tested. According to the results presented in Table 4.3, synergy vectors 1 and 2 from walking could generally be merged in cycling. When synergy vectors 1 and 2 of both motor tasks were compared for matching speeds, mean normalized scalar products ranged from 0.66 to 0.80 (see Table 4.1). Moreover, there is evidence that two synergies from walking, normally activated independently, can be merged (thus co-activated) into one synergy during cycling (see Table 4.3). This is the case of synergy vector 3 of cycling, which was always very well reconstructed with linear combinations from synergy vectors 3 and 4 from walking (see Tables 4.3 and 4.4), across all the speed conditions. MWS and 80%MWS were the conditions at which more similarities were found in the merging process (see Table 4.4). Apparently, CNS may choose the appropriate subset of synergies from a larger set, and depending on the motor function, use them independently or in a merging state to cope with the required biomechanical task. Merging coefficients higher than 0.3 were chosen for the merging process, which is a slightly higher values than the threshold of 0.2 used by Cheung et al. (2012). As they recorded EMG activity from 10-16 muscles, it is reasonable to use a higher threshold once the study presented in this chapter analyzed a set of 8 muscles. If a lower threshold had been chosen, similarity between reconstructed and original cycling synergies would be even higher.

Globally, the results presented in this study corroborate previous evidences defending that both walking and cycling result from a modular control architecture (Clark et al., 2010) (Gizzi et al., 2012) (Hug et al., 2011) (Moreno et al., 2013) (Routson et al., 2013). Nonetheless, muscle synergies should not be interpreted as completely invariant profiles of spatial activation. As referred by Lacquaniti et al. (2012), this hypothesis may be too rigid to be physiologically plausible for human locomotion. Muscles belonging to the same anatomical group may have different biomechanical properties, which introduce competing demands on the appropriate way of activation of each one (Wakeling and Horn, 2009). Therefore, it is thought that muscle synergies can incorporate the biomechanical properties of the limbs (Bizzi and Cheung, 2013).

4.5.8 Methodological considerations

Muscular activity from gluteus maximus was recorded during the experiment, but some data were corrupted due to the contact of this muscle with the chair. Therefore, the set of muscles presented in this study did not include this muscle.

Other interesting muscles could have been analyzed, *i.e.*, gracilis (as hip and knee flexor), psoas or vastus medialis (monoarticular muscle in the knee, but very similar to vastus lateralis). For comparison with previous work on motor control of walking ([Clark et al., 2010](#)) ([Gizzi et al., 2012](#)) and cycling ([De Marchis et al., 2012](#)) ([Hug et al., 2010](#)), a subset with the same number of muscles (except for [Hug et al. \(2010\)](#)) and functionally matching muscular groups was chosen.

[Baum and Li \(2003\)](#) referred that load changes have an effect on EMG profiles during cycling. [Hug et al. \(2011\)](#) also reported a moderated similarity between EMG patterns in two different load conditions, despite the extracted synergies presented higher similarity between the two conditions. Therefore, it was used a fixed resistance value in the ergometer, in order to guarantee equal biomechanical constraints across subjects.

Study 2 - Muscle synergies during cycling as a measure of sensorimotor function in SCI

Abstract

Background. After incomplete spinal cord injury (iSCI), patients suffer important sensorimotor functional consequences, including motor impairments and maladaptive symptoms associated with spasticity. Complementary to current diagnostic procedures, novel outcome measures that reflect small changes of antagonist neuromuscular control over several joints are required. The analysis of muscle synergies can be used to quantify the spatiotemporal muscle co-activation, identified as an important clinical characteristic of spasticity. Moreover, muscle synergies have been related to both gait performance and speed.

Objective. Based on the findings presented in Chapter 4, confirming the hypothesis that similar synergistic features are shared between walking and cycling, the research presented in this Chapter tests two hypothesis: I) iSCI patients preserve synergistic control of muscles during cycling; II) muscle synergies outcomes extracted during cycling correlate with clinical measurements of gait performance and/or spasticity.

Methods. The EMG of 13 muscles of the lower limb was recorded in a group of ten healthy individuals and ten iSCI subjects while they cycled at four different cadences. NNMF algorithm was applied to extract muscle synergy components. Two reconstruction goodness scores (VAF_{total} and r^2 , both introduced at section 2.3.3.4)

were used to evaluate the ability of a given number of synergies to reconstruct the EMG envelopes.

Results. iSCI patients preserved a synergistic control of muscles during cycling. However, muscle synergies composition of more impaired patients was less similar to the healthy controls if compared with the less impaired iSCI patients. A stepwise multiple regression analysis indicated that $\text{VAF}_{\text{total}}$ and r^2 at 42 rpm were good predictors of gait performance, accounting for at least 63% of the variance of clinical scales of gait performance (*i.e.*, TUG, 10-Meter Walk Test (10MWT) and WISCI II). Similarly, two metrics based on the similarity between the healthy and affected synergies were able to predict spasticity symptoms measured by Penn, Modified Ashworth, and SCATS scales.

Conclusions. The results presented in this Chapter provide supporting evidences for the hypothesis that iSCI patients preserve synergistic control of muscles during cycling and also evidences that the analysis of muscle synergies during cycling can be used for a detailed quantitative assessment of gait performance and symptoms of spasticity. This analysis can complement current assessment procedures.

5.1 Introduction

One of the main goals of rehabilitation of SCI patients is to promote the recovery of gait after injury (van Middendorp et al., 2014). The development of the spasticity syndrome is one of the crucial contributors to motor impairment (Bravo-Esteban et al., 2013). Although the most common clinical definition of the spasticity syndrome is based on the detection of velocity-dependent stretch reflex activity (Lance, 1980), this syndrome has also been considered as a complex set of symptoms including hypertonia, spasms, clonus, hyperreflexia and muscle co-activation (Arene and Hidler, 2009) (Bennett, 2008) (Burridge et al., 2005) (Dietz and Sinkjaer, 2007). While some levels of co-activation are important to guarantee joint stability, movement accuracy and energy efficiency (Rosa et al., 2014), poststroke patients show abnormal co-activation of both agonist and antagonist muscles during the execution of certain motor tasks, which in turn may reflect adaptive and maladaptive mechanisms of motor recovery (Gómez-Soriano et al., 2012). The analysis of multi-joint muscle activation would support clinical decisions based on residual useful motor function, help to assess the effects of standard and novel therapies, and guide the prescription of standard anti-spastic medications (Bowden and Stokic, 2009) (Reichenfelser et al., 2012). As such, an improvement in the estimation of agonist and antagonist muscle activity may represent an important outcome measure of rehabilitation after SCI (Awai and Curt, 2014).

Based on the premise that the estimation of co-activation of both agonist and antagonist muscles may improve the assessment of spasticity, the analysis of muscle synergies can be explored as a reliable method to estimate muscle coordination (Berger et al., 2013) (Bizzi et al., 2008) (Cheung et al., 2012) (Clark et al., 2010) (d'Avella and Bizzi, 2005) (Oliveira et al., 2014), as they define weights of co-activated muscles. Recent studies in healthy subjects demonstrated that the combination of three to four muscle synergies can explain most of the activation of lower limb muscles during walking and cycling (Barroso et al., 2013) (Clark et al., 2010) (De Marchis et al., 2012) (Gizzi et al., 2011) (Hug et al., 2010) (Hug et al., 2011). In the case of poststroke patients, the number of muscle synergies have been related to gait performance and seems to be a superior predictor of walking performance, if compared with the gold-standard scales (Clark et al., 2010). Also in the case of poststroke patients, Routson et al. (2013) used both synergy vectors and activation coefficients to measure motor recovery following therapeutic interventions. In the case of SCI patients, it has been observed that a disruption of muscle coordination plays a major role in iSCI patients during overground walking (Hayes et al., 2014), with less impaired SCI subjects presenting more similar synergy vectors to the healthy controls than those of the most affected SCI subjects (Ivanenko et al., 2003). Thus, the analysis of muscle synergies can be explored as a method to assess gait performance and/or spasticity of iSCI patients.

Not all the patients have the required muscle strength to walk during the early stage of rehabilitation, even with an amount of body weight support. Thus, the prediction of their walking performance is compromised. As proposed in Chapter 4, cycling may be explored as a novel framework for the assessment of motor performance in people with impaired neuromotor control, given the similar synergistic control of walking and pedaling. Specifically, it was demonstrated that 1) the four synergy vectors extracted from walking can be used to reconstruct cycling EMG envelopes; 2) synergies 1 and 2 from walking could generally be merged in cycling; 3) synergy 3 from cycling was always very well reconstructed with linear combinations from synergies 3 and 4 from walking.

5.2 Goals

This Chapter aims to test two main hypotheses: I) iSCI patients preserve synergistic control of muscles during cycling; II) muscle synergies outcomes extracted during cycling correlate with clinical measurements of gait performance and/or spasticity. The confirmation of hypothesis I) will provide additional evidence for the hypothesis that different types of movement can be achieved using a low-dimensional synergistic control and will give new insight on the impaired mechanisms underlying cycling in iSCI patients. The

confirmation hypothesis II) will be relevant to choose the most efficient experimental setup (*e.g.*, different cycling velocities and different number of tested muscles) for extracting reliable results in the clinical context.

This study is motivated by the potential use of cycling exercises as a mean to assess the affected sensorimotor mechanisms involved in pathologic locomotion, as well as an alternative tool to monitor patients' recovery.

5.3 Materials and Methods

5.3.1 Subjects

All recruited subjects gave their written consent to participate in the study and for data publication, after being informed about the procedures and possible discomfort associated with the experiments, in accordance with the Declaration of Helsinki (see Appendix E.1). The local Toledo Paraplegics Hospital Clinical Ethical Committee approved this study (07/05/2013 N°47). Ten healthy subjects (6 men and 4 women), with an age of 33.9 ± 8.48 yr (25.75-44.5, 25th percentile – 75th percentile), with no diagnosed neural injury, neither central nor peripheral, were recruited to participate as controls. Ten iSCI patients (6 men and 4 women), with an age of 43.08 ± 14.32 yr (25.69-59.31), 7.23 ± 4.86 months (2.72-9.66) post-SCI, volunteered to participate in this study. All of them received the standard rehabilitation program of the hospital. Inclusion criteria were: aged between 18 and 80 yr; motor incomplete spinal lesion (AIS C-D) of traumatic and non-traumatic etiology, with prognosis of recovery of the walking function; evolution of at least 1.5 months. Exclusion criteria were: supraspinal or peripheral neurological involvement; history of epilepsy; musculoskeletal involvement of lower limbs or spasticity higher than 3 (measured with the Modified Ashworth Scale) for each joint, either for extension or flexion. Detailed information of the patients is presented in Table 5.1.

5.3.2 Experimental protocol

Prior to the experiment, a trained physiotherapist performed a set of clinical evaluations in order to inform about the clinical and functional status of the patients. The hypertonia of the muscles of the ankle and knee joints was evaluated using the Modified Ashworth scale (MAS, see Table 5.2) (Bohannon and Smith, 1987). The frequency of spasms was assessed using the Penn scale (Penn et al., 1989). Patients were also assessed with the Spinal Cord Assessment Tool for Spastic Reflexes (SCATS), which measures three types of spastic reflexes in SCI patients: clonus, flexor spasms and extensor spasms, each of

TABLE 5.1: Individual iSCI patients' description.

Patient ID	Age (Years)	Gender	Time post-SCI (months)	Level of Lesion	Most affected side	AIS
1	25	M	9	C5	Right	C
2	46	M	6	T9	Left	D
3	61	M	4	T10	Right	D
4	25	M	5	T4	Left	D
5	37	M	25	C3	Left	D
6	19	F	2	C6	Right	D
7	36	F	3	T3	Left	D
8	58	F	2	C5	Right	D
9	77	M	13	C7	Right	D
10	44	F	5	C4	Left	C

M, male; F, female; Level of Lesion: C – Cervical, T – Thoracic; AIS, American Spinal Injury Association (ASIA) Impairment Scale.

them rated from 0 (no reaction) to 3 (severe) (Benz et al., 2005). Patients showing a Total MAS higher than 1 or a Penn score greater or equal to 1 were characterized as presenting spasticity (see Table 5.2), as done by Bravo-Esteban et al. (2014).

The gait performance of seven out of the ten iSCI patients was evaluated using the Timed Up and Go (TUG) test (Wall et al., 2000) and the 10-Meter test (Forrest et al., 2014). The other three patients were unavailable to perform these tests. The Walking Index for Spinal Cord Injury (WISCI II) was used to assess the amount of physical assistance needed by the patients to walk 10 meters. This is a 21-point scale that ranges from 0 (patient unable to stand and/or participate in assisted walking) to 20 (patient ambulates 10 meters with no devices, no braces and no physical assistance) (Dittuno and Dittuno, 2001).

On the day of the experiment, patients received their standard rehabilitation therapy in the morning, and performed the cycling trials in the afternoon. For both iSCI patients and healthy subjects, four cycling trials (at 30, 42, 50 and 60 rpm, revolutions per minute) of 30 s duration each, with 60 s resting between trials, were performed on an electronically braked cycle ergometer (MOTOmed viva2, Reck, Betzenweiler, Germany) in the passive mode. For each participant, the order of the trials was randomized to avoid biased results. All participants were asked to perform the experiment while sat on a regular chair. Patients who felt more comfortable doing the experiments on their own wheelchair were allowed to remain sat on it (see Figure 5.1). When this occurred, a pillow was placed on the backside to maintain the pedaling position similar to the regular chair position.

TABLE 5.2: Amount of physical assistance needed, gait performance and spasticity syndrome scores of iSCI patients.

Patient ID	WISCI II	TUG (s)	10-Meter (s)	MAS				MAS Knee	MAS Ankle	Total MAS	Penn scale	SCATS		
				KF	KE	DF	PF					C	F	E
1†	16	22.0	23.0	1	1	1	1	2	2	4	2	1	0	1
2	20	23.0	12.0	0	0	0	0	0	0	0	0	0	0	0
3†	16	44.7	50.8	0	1+	1+	0	2	2	4	1	1	0	0
4†	15	29.3	27.7	2	1	3	0	4	4	8	1	1	0	1
5†	20	N.A.	N.A.	0	1+	3	0	2	4	6	1	0	1	1
6†	0	N.A.	N.A.	1+	2	3	0	5	4	9	2	3	1	0
7†	16	31.0	30.0	1+	0	1+	0	2	2	4	0	2	0	0
8	13	27.0	23.0	0	0	0	0	0	0	0	0	0	0	0
9	19	25.1	10.2	0	0	0	0	0	0	0	0	0	0	0
10†	8	N.A.	N.A.	0	0	3	0	0	4	4	3	3	0	3

WISCI II, Walking Index for Spinal Cord Injury; TUG, Timed Up and Go; MAS, Modified Ashworth Scale; KF, knee flexion; KE, knee extension; DF, dorsiflexion; PF, plantarflexion. MAS Knee, sum of KF and KE. In order to sum, 1+ counts as 2, 2 counts as 3, 3 counts as 4 and 4 counts as 5; MAS Ankle, sum of DF and PF; Total MAS, sum of MAS Knee and MAS Ankle; Penn, Penn scale; SCATS, Spinal Cord Assessment Tool for Spastic Reflexes; Types of spastic reflexes: C, clonus; F, flexion; E, extension; N.A., measure not available; †, patients characterized as presenting spasticity.



FIGURE 5.1: EMG recordings during cycling trials of a iSCI patient (ID 6) who performed the cycling trials on her own wheelchair.

In order to synchronize participants' cycling frequency with the desired cadence, an auditory metronome was used. The cycling resistance (gear) of the ergometer was individually chosen by each iSCI patient, in order to cycle comfortably with the same gear across the four cadences. A constant gear was set for all control subjects.

An EMG amplifier (EMG-USB, OT Bioelettronica, Torino, Italy) with recording bandwidth of 10-750 Hz, overall gain of 1,000 V/V, and acquisition frequency of 2,048 Hz was used to record surface electromyography (sEMG) of 13 muscles of the most affected leg of patients, and the dominant leg of healthy subjects. The recorded muscles were: Gluteus Medius (GMe), Adductor Longus (AL), Sartorius (Sar), Tibialis Anterior (TA), Rectus Femoris (RF), Tensor Fascia Latae (TFL), Vastus Lateralis (VL), Vastus Medialis (VM), Biceps Femoris (BF), Semitendinosus (Sem), Soleus (Sol), Gastrocnemius Lateralis (GaL) and Gastrocnemius Medialis (GaM). The most affected side of each patient was determined based on the muscle score (Seddon, 1976) of quadriceps, hamstrings, TA and gastrocnemius for both limbs.

SENIAM recommendations for sEMG recording procedures (Hermens et al., 1999) were followed before placing the electrodes: shaving the places where the electrodes were placed; cleaning the skin with alcohol to minimize impedance; allowing the alcohol to vaporize in order to dry the skin before placing the electrodes. After that, bipolar EMG electrodes (Ag-AgCl, Ambu® Neuroline 720, Ambu, Ballerup, Denmark) were fastened with a 2-cm inter-electrode distance on each recorded muscle. Finally, the electrodes and cables were wrapped with bandages to ensure that the wires did not impede cycling movements and also to avoid movement-induced artifacts. Preliminary tests were performed to check for cross-talk and contact artifacts, giving special attention to the hamstrings of those patients that cycled on their own wheelchair. When needed, electrodes were repositioned.

Crank angle was measured with a potentiometer (Vishay, Malvern, PA), and digitalized with a sampling frequency of 100 Hz. The bottom dead center (BDC) position of the pedal of the analyzed leg was used to segment data into pedaling cycles. EMG and angular data were synchronized by means of a common synchronization signal. For each subject, each recording session lasted approximately 10 minutes, in addition to the donning and doffing of the EMG recording setup (15-30 minutes, depending on the subject and level of impairment).

Data were analyzed offline with MATLAB R2011a (The MathWorks, Natick, MA) and IBM SPSS Statistics 20 software (IBM).

5.3.3 EMG analysis

Using SynergiesLAB (see Appendix C), for each trial and participant, ten continuous non-corrupted pedaling cycles were selected for analysis. The selected raw EMG signals were high-pass filtered at 20 Hz, demeaned, rectified, and smoothed with a low-pass filter at 5 Hz, resulting in the EMG envelopes, according to the procedures performed by Clark et al. (2010) Hug et al. (2010).

EMG envelopes from each muscle were then normalized by the average of the maximum of each of the ten cycles, and resampled at each 1% of the pedaling cycle. For each participant and trial, normalized EMG envelopes were combined into an $m \times t$ matrix (EMG_0), where m is the number of muscles (thirteen in this case) and t is the time base ($t = \text{no. of cycles} (10) \times 100$).

Differences between mean EMG envelopes of iSCI patients and the mean EMG envelopes of the healthy group were assessed using two criteria proposed by Hug et al. (2011): the lag time and r_{max} coefficient, as performed in section 4.3.3. The lag time quantifies the time shift between EMG patterns and is calculated as the time shift needed to get the maximum (r_{max}) of the cross correlation between two signals.

5.3.4 Muscle synergies analysis

Muscle synergy vectors and the corresponding activation coefficients were extracted using the NNMF algorithm in SynergiesLAB (see equation 2.1) (Lee and Seung, 1999). For each EMG_0 , the NNMF algorithm was run four times, considering as input 2 to 5 synergies ($n = 2, 3, 4, 5$). In order to avoid local minima, for each run, the NNMF was repeated 40 times and the repetition with the lowest reconstruction error was selected.

Each muscle synergy vector (column of matrix W) was normalized by the maximum value of the muscle in the synergy to which they belong, which also helps the visual comparisons among subjects, as performed by Hug et al. (2010) and Muceli et al. (2010). Then, the corresponding activation coefficients were scaled by the same quantity, as done by De Marchis et al. (2012).

The similarity between EMG_0 and EMG_r was calculated based on two indicators: the variability accounted for (VAF_{total} , see Equation 4.1) (Clark et al., 2010) and the coefficient of determination (r^2) (Torres-Oviedo et al., 2006). The coefficient of determination was calculated by the MATLAB function 'rsquare'. Both VAF_{total} and r^2 have been adopted in most studies on muscle synergies (Clark et al., 2010) (Torres-Oviedo

et al., 2006). $\text{VAF}_{\text{total}}$ has been suggested to be more stringent than r^2 , since it is sensitive to both shape and amplitude of the signals, whereas r^2 only addresses similarity in shape.

VAF was also computed for each muscle individually ($\text{VAF}_{\text{muscle}}$).

For each cadence, reference set of matrices (W_0 and H_0) were obtained by concatenating the EMG envelopes from all the healthy subjects, and applying the NNMF algorithm, constrained to a fixed number of synergies. This fixed number was defined as the minimum number of synergies needed to obtain $\text{VAF}_{\text{total}}$ values $\geq 85\%$ in at least half of the healthy participants. Synergy vectors of each patient were ordered according to their similarity with columns of W_0 , at the corresponding matching speeds. This was done by means of the normalized scalar product and corresponds mathematically to the scalar product of pairs of columns from matrices W , each one previously normalized by its norm, providing output values ranging from 0 to 1. After being ordered, muscle synergy vectors and activation coefficients of each patient were compared with the reference healthy set (W_0 and H_0) using the normalized scalar product.

In order to study the sensitivity of the method to the number of muscles, the overall process was repeated on two muscle datasets, the first including all (13) muscles recorded in the experiment, and the second including the eight muscles considered in Chapter 4. These eight muscles are marked with an asterisk in Figure 5.3.

5.3.5 Statistical analysis

Independent Student's t -tests were computed to test the similarity between the cadences achieved by both groups, at each matching speed. Independent Student's t -tests were also performed to test the similarity of the $\text{VAF}_{\text{total}}$ and r^2 scores between the two groups and between spastic and non-spastic patients, when using 2 to 5 synergies. Statistical significance was set by a p -value of 0.05.

Stepwise multiple regression analyses were carried out to identify a small set of variables that could predict motor performance or spasticity scales scores. Multiple regression analysis is a predictive model that uses two or more predictors (independent variables) as input to predict the result of a dependent variable, according to the equation 5.1

$$Y = b_0 + b_1X_1 + b_2X_2 + \dots + b_nX_n \quad (5.1)$$

,where Y is the dependent variable, X_1 to X_n are the n different independent variables used as input for the model, b_0 is a constant and b_1 to b_n are the estimated regression coefficients. A significance of $p < 0.05$ was used, as performed by Roche et al. (2015).

To predict the value of each gait scale score (WISCI II, TUG and 10-Meter tests), the VAF_{total} and r^2 values obtained for each different number of muscle dataset and speed were considered as input to the model. To predict the value of each spasticity scale score (Total MAS, Penn and spastic reflexes from SCATS), the normalized scalar products between H and H_0 and between W and W_0 (hereafter denoted with “ $H \cdot H_0$ ” and “ $W \cdot W_0$ ”, respectively), were considered as input to the model. In both cases (gait performance and spasticity scales), preliminary linear regressions between each independent variable and the corresponding scale were performed in order to minimize the number of independent variables used as input, including only those with a p -value ≤ 0.05 , as represented in Figure 5.2.

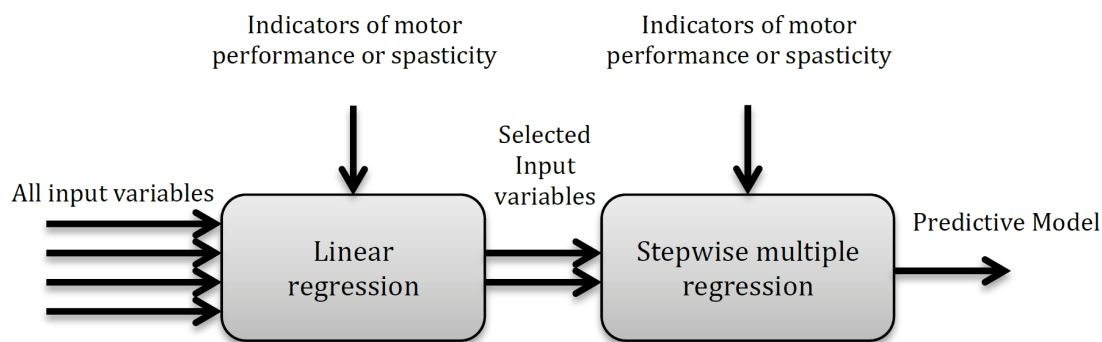


FIGURE 5.2: Schematic representation of the steps included in the stepwise multiple regressions to predict motor performance or spasticity scales scores.

5.4 Results

5.4.1 Cadence

SCI group cycled with a cadence of (mean \pm SD) 30.26 ± 0.87 , 41.89 ± 1.04 , 49.71 ± 1.91 and 57.73 ± 3.57 rpm for the desired speeds of 30, 42, 50 and 60 rpm, respectively. The healthy group cycled with a cadence of 30.21 ± 0.34 , 42.21 ± 1.15 , 49.25 ± 0.76 and 59.79 ± 0.90 rpm, respectively. The tests of equality of means from Independent Student’s t -tests revealed no significant differences between the two groups, in any of the four speeds considered. In particular, p -values of 0.868, 0.516, 0.492 and 0.093 were obtained for speeds of 30, 42, 50 and 60 rpm, respectively.

5.4.2 Individual EMG profiles

The average EMG envelopes of each group, for each of the 13 recorded muscles, are represented in Figure 5.3. Average activations of GMed, AL, Sar, TA and, to a lower extent, RF, occurred during the initial upstroke phase. Average activations of TFL, VL and VM were observed during the final upstroke phase and initial downstroke. Average activation of BF, Sem, Sol, GaL and GaM occurred mostly during the downstroke phase of cycling.

For each muscle, the shape and activation timing of average EMGs were very similar across speeds and also between the two groups (see Figure 5.4), except for TA, VM, Sol and GaL. In the case of these muscles, the timing of maximum activation occurred earlier in the pedaling cycle in the iSCI patients, as indicated by the vertical arrows in Figure 5.3 and represented in Figure 5.4A. On the other hand, maximum values of the cross-correlation function were lower for Sol and GaL, when compared with the other muscles (Figure 5.4B). For these two muscles, maximum correlations were lower than 0.85 for higher speeds, while maximum correlations were higher than 0.95 for the other muscles at most of the speed conditions.

5.4.3 Muscle synergies

5.4.3.1 Reconstruction goodness

Three synergies were sufficient to describe most of the variance of the two different sets of muscles in the two groups of participants analyzed, according to the criterion previously defined ($\text{VAF}_{\text{total}}$ values $\geq 85\%$ for at least half of the healthy participants). Hence, the following analysis of this chapter is based on three synergies.

For the set of 8 muscles, both groups reached their minimum values of $\text{VAF}_{\text{total}}$ at the speed of 60 rpm. $\text{VAF}_{\text{total}}$ values in such condition were $86.7 \pm 2.0\%$ (Figure 5.5AI) for the healthy group and $86.6 \pm 3.1\%$ (Figure 5.5AII) for the iSCI group. The maximum $\text{VAF}_{\text{total}}$ was obtained at the speed of 30 rpm, reaching values of $88.5 \pm 4.2\%$ and $88.2 \pm 3.9\%$ for the healthy and iSCI groups, respectively.

When analyzing $\text{VAF}_{\text{muscle}}$ values with 3 synergies for the same set of 8 muscles, all the muscles presented values higher than 75%. For instance, in the case of the healthy group, a minimum $\text{VAF}_{\text{muscle}}$ value of $83.0 \pm 13.0\%$ was obtained for Sem at the speed of 30 rpm; a maximum $\text{VAF}_{\text{muscle}}$ value of $91.9 \pm 4.7\%$ was obtained for VL at the speed of 50 rpm. In the case of the iSCI group, a minimum $\text{VAF}_{\text{muscle}}$ value of $75.6 \pm 8.4\%$ was

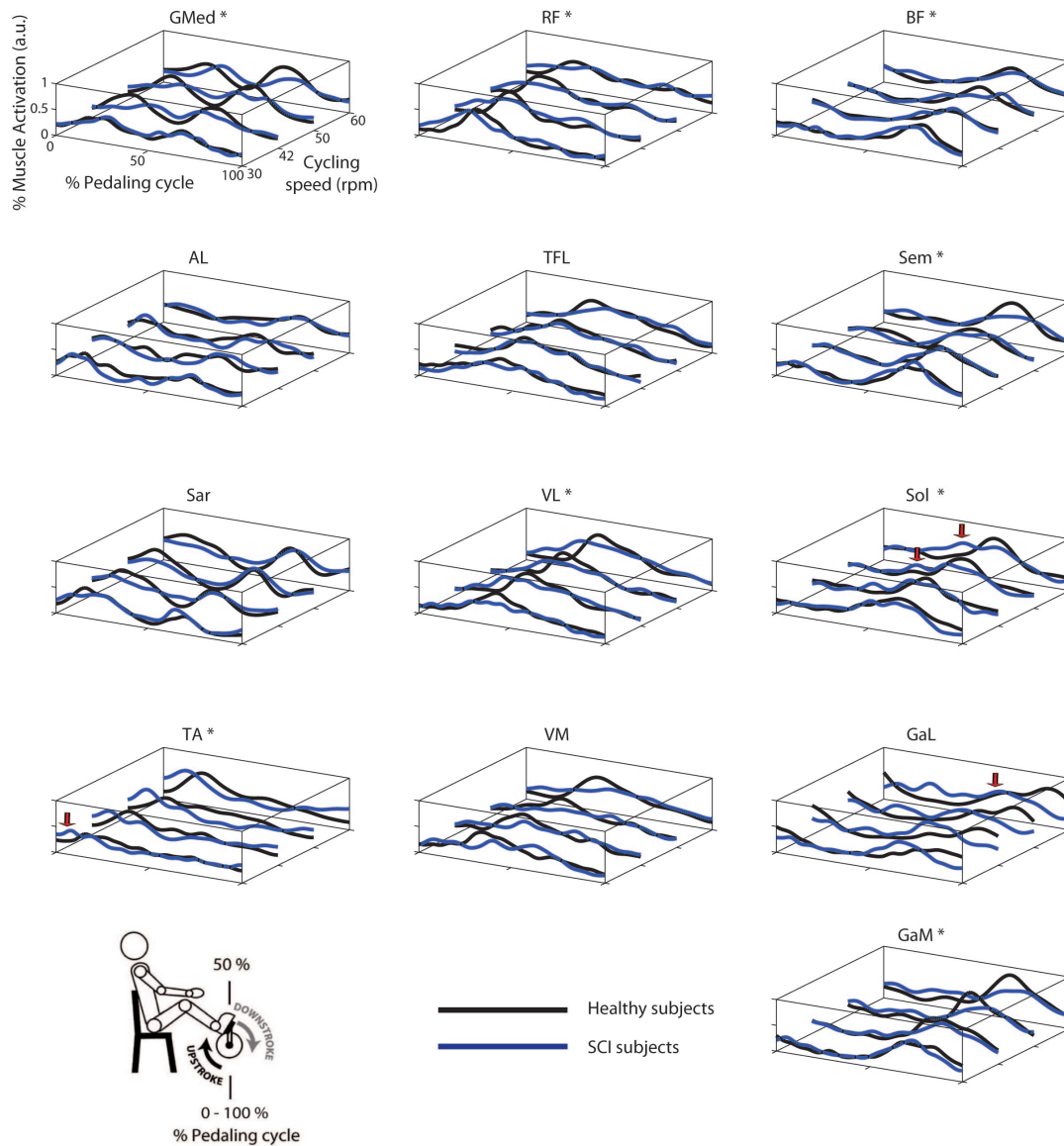


FIGURE 5.3: Group average electromyographic (EMG) envelopes of the 13 recorded muscles for each of the 4 speeds during cycling (30, 42, 50 and 60 rpm). For each group (healthy subjects, black lines; iSCI patients, grey lines), a total of 100 cycling cycles (10 cycles by subject) were averaged and expressed as a function of the pedaling cycle. Pedaling cycle is divided into two phases: upstroke and downstroke. Upstroke begins when the pedal corresponding to the dominant leg (in healthy subjects) or the most affected leg (in iSCI subjects) is at the lowest position and ends when the pedal is at the top position. The end of upstroke phase corresponds to the beginning of downstroke phase, and ends when the pedal reaches the lowest position again. EMGs from each subject and muscle were previously normalized by the average of its maximum values throughout the 10 cycles. a.u., arbitrary unit. *, muscles belonging to the 8 muscles set used in parallel analysis. Red arrows indicate the early timing of maximum activation observed in the average EMGs of iSCI group.

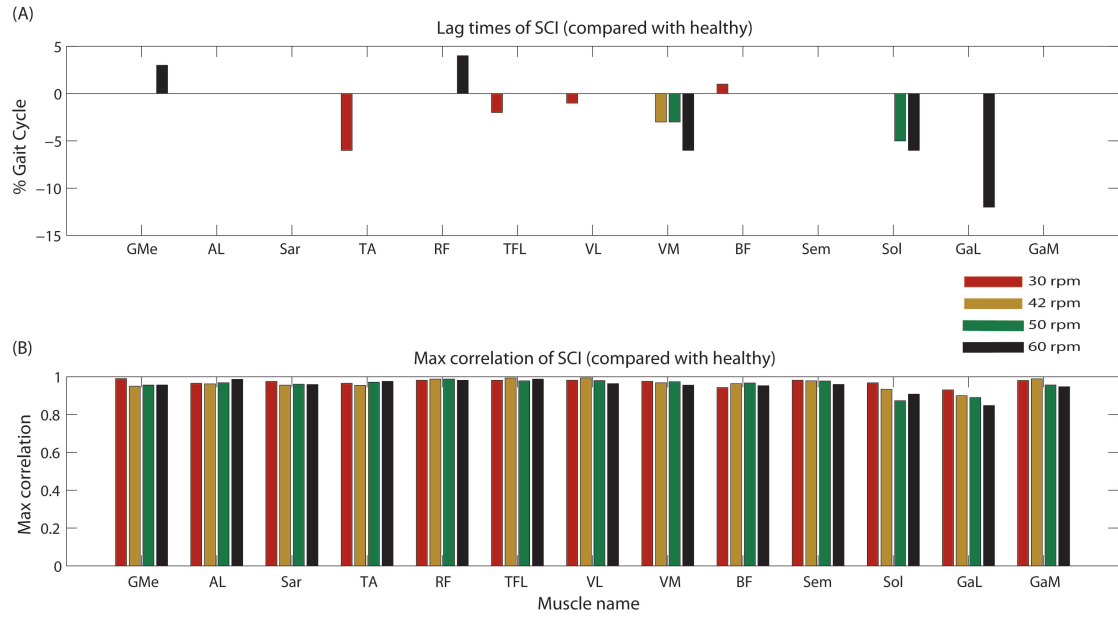


FIGURE 5.4: Comparison of mean EMG envelopes from iSCI patients and the mean EMG envelopes from the healthy group for the 13 recorded muscles for each of the 4 speed conditions (30, 42, 50 and 60 rpm). (A) The lag time quantifies the time shift between EMG patterns and is calculated as the time shift needed to get the maximum of the cross correlation (r_{max}) between two signals. A negative value indicates that mean EMG envelopes from iSCI patients shifted earlier in the cycle relative to the mean EMG envelopes from the healthy group. (B) Maximum of the cross correlation (r_{max}) between the two signals.

obtained for GMe at the speed of 60 rpm; a maximum VAF_{muscle} value of $91.0 \pm 2.4\%$ was obtained for GaM at the speed of 30 rpm.

VAF_{total} values decreased when considering the set of 13 muscles. Minimum values of $84.0 \pm 2.2\%$ (Figure 5.5AIII) and $83.1 \pm 4.0\%$ (Figure 5.5AIV) were obtained for the healthy and iSCI group, respectively. In this case, the healthy group reached minimum VAF_{total} values at the speed of 60 rpm, whereas iSCI group reached its minimum at the speed of 50 rpm. The maximum values of $86.0 \pm 4.6\%$ and $85.2 \pm 4.2\%$ were obtained for the healthy and iSCI group, respectively, both at 30 rpm.

When considering 3 synergies for the set of 13 muscles, all the muscles presented VAF_{muscle} values higher than 75%, except for one muscle and condition in the iSCI group. Specifically, a minimum VAF_{muscle} value of $73.8 \pm 10.8\%$ was obtained for GMe at 60 rpm; a maximum VAF_{muscle} value of $87.4 \pm 3.3\%$ was obtained for BF at 60 rpm. In the case of the healthy group, a minimum VAF_{muscle} value of $77.2 \pm 11.1\%$ was obtained for AL at 42 rpm; a maximum VAF_{muscle} value of $91.9 \pm 4.6\%$ was obtained for VL at 30 rpm.

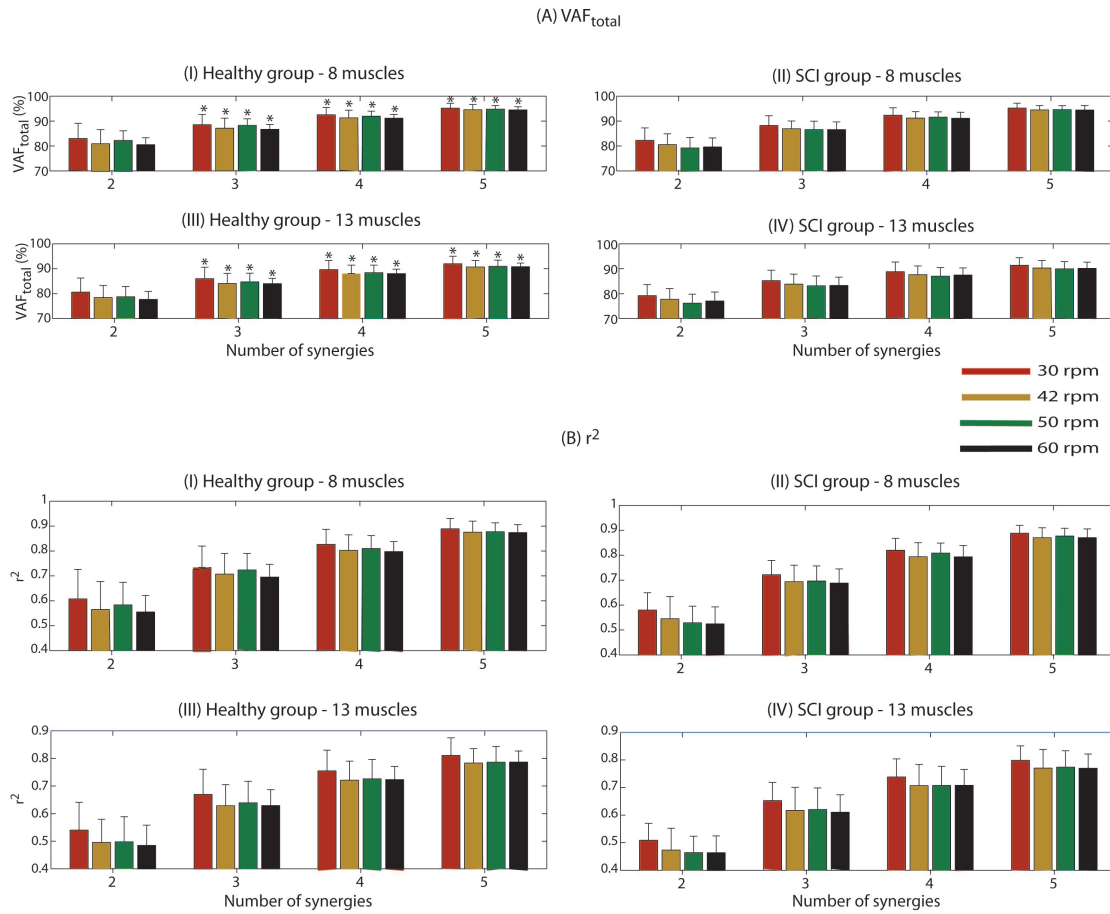


FIGURE 5.5: (A) Variability accounted for (VAF_{total}) and (B) coefficient of determination (r^2), according to the number of synergies, for each of the 4 speeds (30, 42, 50 and 60 rpm). Values are given in means \pm SD. These reconstruction goodness indexes were calculated after running the NNMF algorithm to reconstruct a set of 8 EMG envelopes for the healthy group (I) and the iSCI group (II), as well as a set of 13 EMG envelopes (III and IV for the healthy group and iSCI group, respectively). A VAF_{total} value of 100% and a r^2 value of 1 mean perfect reconstruction of the EMG set. *, Number of synergies sufficient to describe VAF_{total} values $\geq 85\%$ for at least half of the healthy participants.

Independent Student's t -tests revealed no significant differences for the VAF_{total} scores between the two groups and also between spastic and non-spastic patients, for the 4 studied speeds, when using 2 to 5 synergies as input to the NNMF algorithm to reconstruct EMG signals.

In the case of the r^2 coefficient with 3 synergies, a minimum of 0.70 ± 0.05 (Figure 5.5BI) and 0.69 ± 0.06 (Figure 5.5BII) were obtained for the healthy and iSCI group, respectively, for the set of 8 muscles. Both values were obtained for the speed of 60 rpm. On the other hand, a maximum of 0.73 ± 0.09 and 0.72 ± 0.06 were obtained for

the healthy and iSCI group, respectively. Both values were obtained for the speed of 30 rpm.

As it happened in the case of VAF_{total} , also r^2 values decreased in the case of 13-muscle dataset. A minimum of 0.63 ± 0.08 (Figure 5.5BIII) and 0.61 ± 0.06 (Figure 5.5BIV) were obtained for the healthy (at 42 rpm) and iSCI group (at 60 rpm), respectively. A maximum of 0.67 ± 0.09 and 0.65 ± 0.07 were obtained for the healthy and iSCI group, respectively, both at 30 rpm.

Independent Student's t -tests indicated no significant differences for the r^2 scores between the two groups and also between spastic and non-spastic patients, for all speeds and input number of synergies.

5.4.3.2 Synergy vectors and activation coefficients

The reference sets of three muscle synergy vectors (W_0) and the corresponding activation coefficients (H_0) of the healthy group at the four different speeds are represented in Figure 5.6AI and Figure 5.6AII, respectively. Synergy 1, activated predominantly during the upstroke phase of cycling (see Figure 5.6AII), was represented by the activity of GMed, AL, Sar, TA and RF. Synergy 2, activated during the final upstroke phase and initial downstroke phase of cycling, was represented by the activity of TFL, VL, VM and, to a lower extent, TA and RF. Synergy 3, activated during the downstroke phase of cycling, was composed by the activity of BF, Sem, Sol, GaL and GaM.

Results from a representative iSCI patient (ID 4) with spasticity are represented in Figure 5.6BI and Figure 5.6BII. In the case of this patient, it was verified high variability of muscle synergy vectors and activation coefficients across speeds. This is reflected by the normalized scalar product values between muscle synergy vectors W extracted with the set of 13 muscles, and the reference matrices W_0 ($W \cdot W_0$). Those values ranged from 0.41 to 0.69 in synergy 1, from 0.57 to 0.78 in synergy 2, and from 0.74 to 0.90 in synergy 3 (see Table 5.3). In the case of activation coefficients, $H \cdot H_0$ values ranged from 0.63 to 0.91 for activation coefficient 1, from 0.59 to 0.90 for activation coefficient 2, and from 0.50 to 0.87 for activation coefficient 3. When only 8 muscles were considered, $W \cdot W_0$ ranged from 0.41 to 0.66 for synergy vector 1, from 0.70 to 0.73 for synergy vector 2, and from 0.74 to 0.96 for synergy vector 3 (see Table 5.4). Normalized scalar product ranged from 0.60 to 0.81 for activation coefficient 1, from 0.58 to 0.88 for activation coefficient 2, and from 0.61 to 0.90 for activation coefficient 3.

Results from a representative iSCI patient (ID 9) without spasticity are represented in Figure 5.6CI and Figure 5.6CII. In this case, muscle synergy vectors and activation

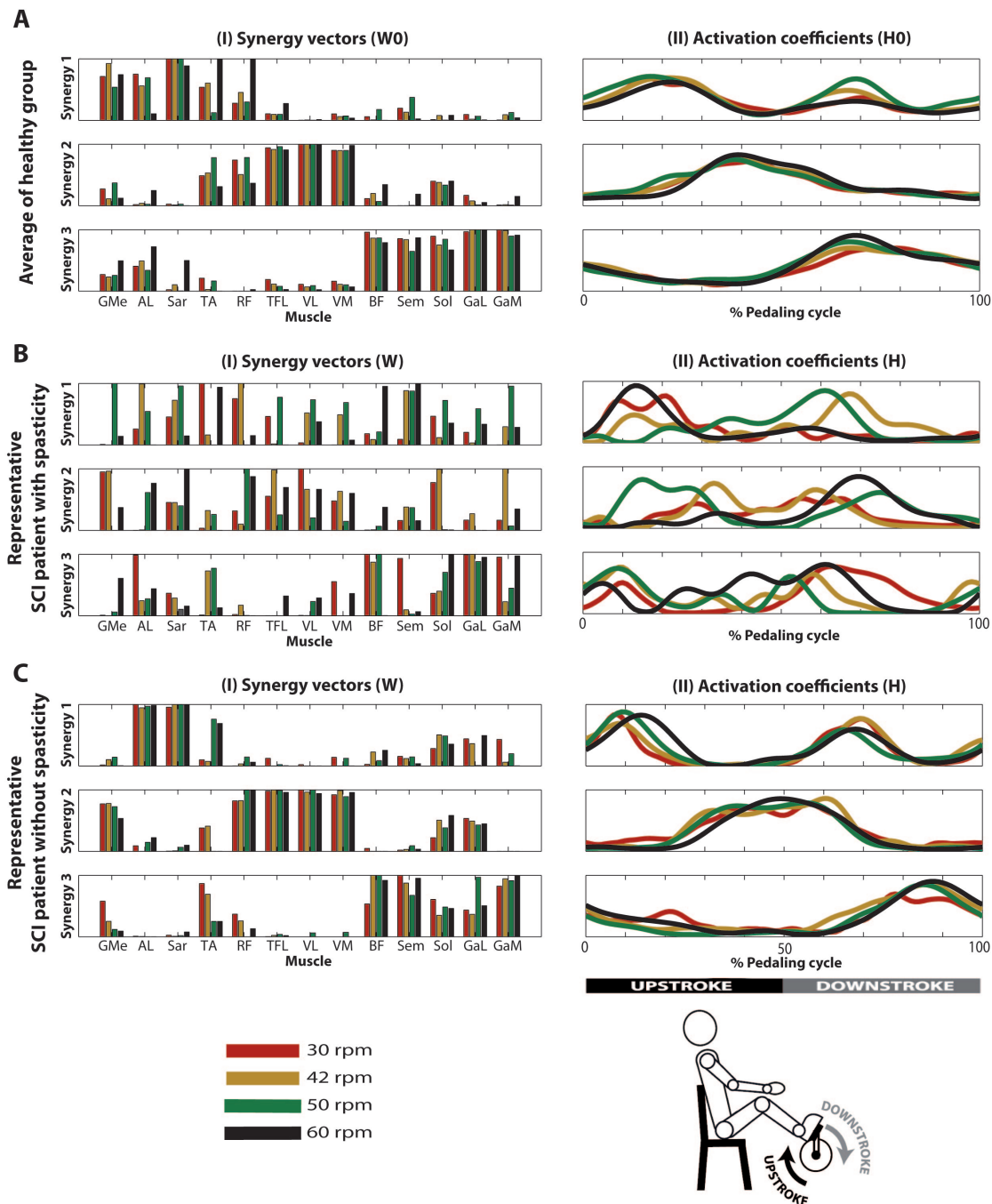


FIGURE 5.6: Reconstruction of EMG envelopes in four speeds (30, 42, 50 and 60 rpm) using concatenated data from (A) the 10 healthy subjects, and (B) individual data from a patient with spasticity - ID 04 and (C) a patient without spasticity - ID 09, applying the NNMF algorithm with 3 synergies. I: muscle synergy vectors. Each muscle synergy vector has a time-invariant profile, representing the relative contribution of each synergy for each muscular pattern. Muscle synergy vectors were normalized by their maximum value. II: averaged activation coefficients, indicating time-variant profiles responsible to activate each synergy.

TABLE 5.3: Normalized scalar product between matching muscle synergy vectors from matrices W of each patient and the matrix W_0 obtained from all healthy subjects pooled together, considering the set of 13 muscles and 3 synergies.

Patient ID	$W \cdot W_0$ at 30rpm			$W \cdot W_0$ at 42rpm			$W \cdot W_0$ at 50rpm			$W \cdot W_0$ at 60rpm		
	1	2	3	1	2	3	1	2	3	1	2	3
1†	0.48	0.71	0.79	0.64	0.67	0.78	0.60	0.78	0.68	0.74	0.68	0.78
2	0.91	0.89	0.99	0.92	0.81	0.91	0.87	0.73	0.90	0.87	0.79	0.88
3†	0.55	0.83	0.96	0.58	0.84	0.95	0.40	0.78	0.91	0.46	0.73	0.95
4†	0.62	0.78	0.90	0.61	0.68	0.74	0.69	0.57	0.85	0.41	0.71	0.79
5†	0.79	0.88	0.94	0.78	0.80	0.90	0.75	0.77	0.93	0.93	0.90	0.88
6†	0.73	0.54	0.73	0.45	0.58	0.67	0.73	0.65	0.61	0.67	0.76	0.76
7†	0.96	0.96	0.96	0.93	0.97	0.94	0.88	0.77	0.68	0.86	0.89	0.85
8	0.70	0.69	0.86	0.50	0.75	0.85	0.70	0.31	0.66	0.74	0.39	0.78
9	0.76	0.95	0.83	0.68	0.92	0.83	0.81	0.89	0.96	0.57	0.88	0.85
10†	0.54	0.80	0.93	0.71	0.78	0.97	0.44	0.83	0.85	0.40	0.88	0.82
Mean	0.71	0.80	0.89	0.68	0.78	0.85	0.69	0.71	0.80	0.67	0.76	0.83
(SD)	(0.13)	(0.10)	(0.07)	(0.12)	(0.09)	(0.08)	(0.12)	(0.12)	(0.12)	(0.16)	(0.11)	(0.05)

The scalar product was abbreviated with the notation “ $W \cdot W_0$ ”. Values ≥ 0.9 appear in bold. †, patients characterized as presenting spasticity.

TABLE 5.4: Normalized scalar product between matching muscle synergy vectors from matrices W of each patient and the matrix W_0 obtained from all healthy subjects pooled together, considering the set of 8 muscles and 3 synergies.

Patient ID	$W \cdot W_0$ at 30rpm			$W \cdot W_0$ at 42rpm			$W \cdot W_0$ at 50rpm			$W \cdot W_0$ at 60rpm		
	1	2	3	1	2	3	1	2	3	1	2	3
1†	0.37	0.74	0.84	0.73	0.67	0.71	0.69	0.87	0.81	0.59	0.78	0.75
2	0.83	0.73	0.98	0.87	0.72	0.86	0.82	0.51	0.87	0.95	0.70	0.84
3†	0.80	0.76	0.97	0.79	0.81	0.96	0.81	0.89	0.95	0.68	0.83	0.97
4†	0.66	0.73	0.96	0.60	0.70	0.86	0.46	0.72	0.82	0.41	0.71	0.74
5†	0.76	0.73	0.98	0.73	0.65	0.78	0.39	0.74	0.82	0.95	0.83	0.70
6†	0.36	0.58	0.71	0.52	0.89	0.85	0.79	0.86	0.69	0.56	0.83	0.88
7†	0.68	0.87	0.81	0.96	0.93	0.99	0.70	0.56	0.87	0.94	0.75	0.93
8	0.54	0.70	0.78	0.84	0.91	0.95	0.93	0.57	0.81	0.94	0.79	0.85
9	0.75	0.89	0.88	0.70	0.81	0.91	0.77	0.85	0.97	0.75	0.76	0.93
10†	0.22	0.80	0.83	0.12	0.88	0.85	0.15	0.88	0.78	0.23	0.78	0.84
Mean	0.60	0.75	0.87	0.69	0.80	0.87	0.65	0.74	0.84	0.70	0.78	0.84
(SD)	(0.18)	(0.06)	(0.08)	(0.16)	(0.09)	(0.06)	(0.19)	(0.12)	(0.06)	(0.20)	(0.04)	(0.07)

The scalar product was abbreviated with the notation “ $W \cdot W_0$ ”. Values ≥ 0.9 appear in bold. †, patients characterized as presenting spasticity.

coefficients were very similar across the speeds, as it happened with the healthy group. In particular, $W \cdot W_0$ ranged from 0.57 to 0.81 for synergy 1, from 0.88 to 0.95 for synergy 2, and from 0.83 to 0.96 for synergy 3 (see Table 5.3). In the case of activation coefficients, $H \cdot H_0$ ranged from 0.65 to 0.87 for activation coefficient 1, from 0.92 to 0.95 for activation coefficient 2, and from 0.78 to 0.92 for activation coefficient 3. For the set of 8 muscles, $W \cdot W_0$ ranged from 0.70 to 0.77 for synergy vector 1, from 0.76 to 0.89 for synergy vector 2, and from 0.88 to 0.97 for synergy vector 3 (see Table 5.4). As for the activation coefficients, $H \cdot H_0$ ranged from 0.78 to 0.95 for synergy 1; 0.91 to 0.97 for synergy 2; 0.72 to 0.93 for synergy 3.

When comparing these similarity values between spastic and non-spastic patients, most of the metrics presented a lower mean in spastic patients, despite those differences were not statistically significant. Just in the case of $H_2 \cdot H_{02}$ at 30 rpm for the dataset of 13 muscles, differences were significant (p -value = 0.036), with spastic patients (0.9 ± 0.04) presenting lower similarity than non-spastic (0.94 ± 0.02).

Normalized scalar products between synergy vector 3 (W_3) from each iSCI patients and the corresponding synergy vector from the healthy group (W_{03}) were, on average, higher than those obtained for W_1 and W_2 , for all speeds (see Tables 5.3 and 5.4), in both sets of 13 and 8 muscles. In general, normalized scalar products were higher at lower speeds. Also, normalized scalar products using the set of 13 muscles were higher than those observed with the set of 8 muscles at 30 rpm, and lower for the other speeds.

Normalized scalar products of activation coefficient 3 from each iSCI patient (H_3) and activation coefficient 3 from the healthy group (H_{03}) were, on average, higher than those obtained for H_1 and H_2 , for all speeds and sets of muscles.

5.4.4 Stepwise regressions to predict gait performance

One of the goals of this study was to find some correlations between synergies outcomes extracted during cycling in iSCI patients and clinical measurements of gait performance. Stepwise multiple linear regressions showed that r^2 scores obtained at 42 rpm with the dataset of 8 muscles could alone account for approximately 64% of the variance of TUG scores ($R^2 = 0.635$, Adjusted $R^2 = 0.563$) and approximately 71% of the variance of 10-Meter scores ($R^2 = 0.711$, Adjusted $R^2 = 0.653$). Both predictions were statistically significant ($F = 8.715$, $p = 0.032$, in the case of TUG test; $F = 12.310$, $p = 0.017$, in the case of 10-Meter test). Resulting models are:

$$\text{TUG score} = 89.813 - 85.698 \times (r^2 \text{ with 8 muscles at 42 rpm})$$

$$\text{10-Meter score} = 138.517 - 159.3 \times (r^2 \text{ with 8 muscles at 42 rpm})$$

Multiple linear regression models for TUG and 10-Meter tests are represented in Figures 5.7A and 5.7B, respectively.

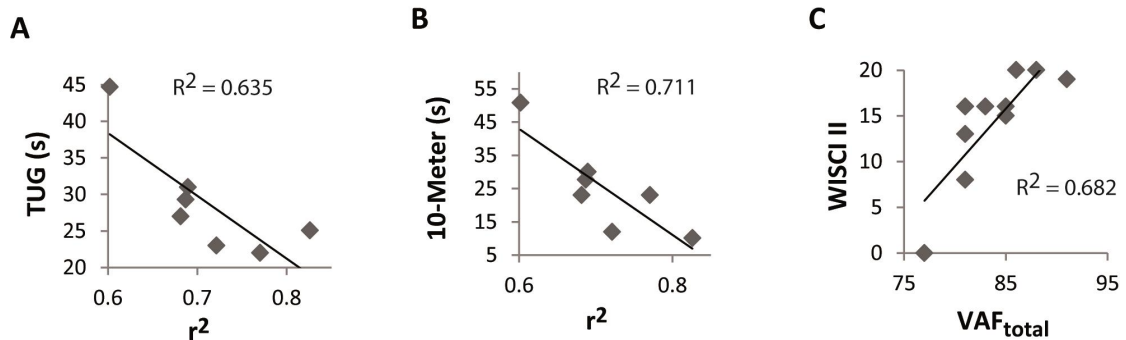


FIGURE 5.7: Stepwise multiple linear regressions using reconstruction goodness indexes as predictors of gait performance. r^2 scores using the dataset of 8 muscles at 42 rpm predicted the time to perform TUG (A) and 10-Meter test (B); $\text{VAF}_{\text{total}}$ scores using the dataset of 13 muscles at 42 rpm predicted the WISCI II score (C).

$\text{VAF}_{\text{total}}$ score obtained at 42 rpm, when using the dataset of 13 muscles, was statistically significant ($F = 17.174$, $p = 0.003$) and accounted for approximately 68% of the variance of WISCI II scores ($R^2 = 0.682$, Adjusted $R^2 = 0.642$). Resulting model is:

$$\text{WISCI II score} = -91.075 + 1.257 \times (\text{VAF}_{\text{total}} \text{ with 13 muscles at 42 rpm})$$

This linear regression is represented in Figure 5.7C.

5.4.5 Stepwise regressions to predict spasticity

Another goal of this study was to find some correlations between synergies outcomes extracted during cycling in iSCI patients and clinical measurements of spasticity. $\text{H}_2 \cdot \text{H}_{02}$ score obtained at 30 rpm, when using the dataset of 13 muscles, was statistically significant ($F = 13.186$, $p = 0.007$) and accounted for approximately 62% of the variance of Total MAS scores (see Figure 5.8A) ($R^2 = 0.622$, Adjusted $R^2 = 0.575$). Resulting model is:

$$\text{Total MAS score} = 56.448 - 58.09 \times (\text{H}_2 \cdot \text{H}_{02} \text{ with 13 muscles at 30 rpm})$$

Scores obtained at Penn scale, as well as the clonus and extensor spasms assessed with SCATS, could be predicted using $\text{W}_1 \cdot \text{W}_{01}$ scores when using the dataset of 8

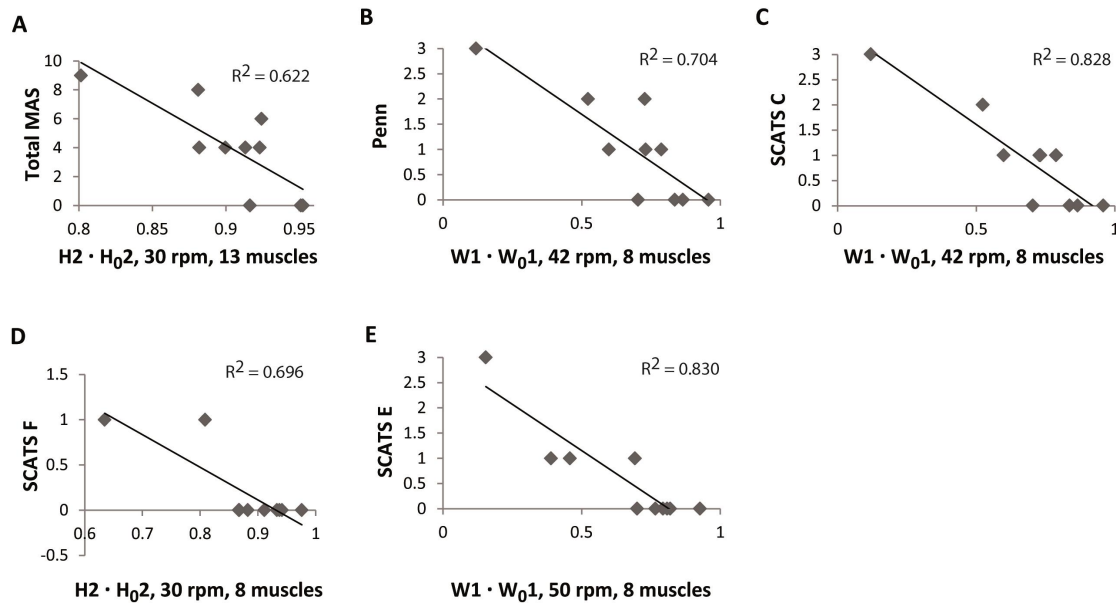


FIGURE 5.8: Multiple linear regressions using similarity scores as input to predict the score of some spasticity scales. $H2 \cdot H_02$ score obtained at 30 rpm, when using the dataset of 13 muscles, predicted Total MAS scores (A); scores obtained with Penn scale (B), as well as the clonus spasms assessed with SCATS (C), could be predicted using $W1 \cdot W_01$ scores with the dataset of 8 muscles at 42 rpm; flexor spasms assessed with SCATS (D) could be predicted using $H2 \cdot H_02$ scores with the dataset of 8 muscles at 30 rpm; extensor spasms assessed with SCATS (E) could be predicted using $W1 \cdot W_01$ scores with the dataset of 8 muscles at 50 rpm.

muscles, at two different speeds: 42 rpm in the case of Penn scale (see Figure 5.8B) and clonus spasms assessed with SCATS (see Figure 5.8C); 50 rpm in the case of extensor spasms assessed with SCATS (see Figure 5.8E). These three predictions were statistically significant ($F = 19.038$, $p = 0.002$, in the case of Penn scale; $F = 38.429$, $p < 0.001$, in the case of clonus spasms assessed with SCATS; $F = 38.983$, $p < 0.001$, in the case of extensor spasms assessed with SCATS) and accounted for approximately 70% of the variance of Penn scale scores ($R^2 = 0.704$, Adjusted $R^2 = 0.667$); approximately 83% of the variance of clonus spasms assessed with SCATS ($R^2 = 0.828$, Adjusted $R^2 = 0.806$); approximately 83% of the variance of extensor spasms assessed with SCATS ($R^2 = 0.830$, Adjusted $R^2 = 0.808$). Resulting models are:

$$\text{Penn score} = 3.576 - 3.759 \times (W1 \cdot W_01 \text{ with 8 muscles at 42 rpm})$$

$$\text{Clonus spasms assessed with SCATS} = 3.535 - 3.845 \times (W1 \cdot W_01 \text{ with 8 muscles at 42 rpm})$$

$$\text{Extensor spasms assessed with SCATS} = 2.984 - 3.665 \times (W1 \cdot W_01 \text{ with 8 muscles at 50 rpm})$$

At last, $H_2 \cdot H_{02}$ scores obtained at 30 rpm, when using the dataset of 8 muscles, was statistically significant ($F = 18.297$, $p = 0.003$) and accounted for approximately 70% of the variance of flexor spasms assessed with SCATS (see Figure 5.8D) ($R^2 = 0.696$, Adjusted $R^2 = 0.658$). Resulting model is:

$$\text{Flexor spasms assessed with SCATS} = 3.360 - 3.607 \times (\text{H}_2 \cdot \text{H}_{02} \text{ with 8 muscles at 30 rpm})$$

5.5 Discussion

Two main findings were provided by this study: I) iSCI patients (with and without spasticity symptoms) preserve a synergistic control of muscles during cycling, evidence that was not previously reported in the literature; II) gait performance and spasticity can be predicted by muscle synergies outcomes extracted during cycling. In particular, gait performance of iSCI patients may be predicted by synergy reconstruction goodness scores, whereas spasticity can be predicted by the degree of similarity between iSCI and healthy synergies. The following sections provide a detailed discussion on the main findings of this work, as well as additional reasoning for their correct interpretation.

5.5.1 Electromyographic patterns in iSCI patients during cycling

According to several studies, the EMG activity of lower limb muscles is similar between sides, during tasks like walking and cycling in healthy subjects (Clark et al., 2010) (Gizzi et al., 2011) (Hug et al., 2011). Hence, only the dominant leg of healthy participants was chosen for analysis in this study. In the case of iSCI patients, the most affected side was the one chosen for analysis, in order to extract more relevant information on the underlying impairments.

In addition to the eight muscles studied previously in healthy subjects and presented in Chapter 4, five additional muscles (mono and bi-articular) were recorded to test the influence of the number of muscles on the correlations between muscle synergies outcomes and clinical scales of gait performance and spasticity.

As part of the standard rehabilitation program of the hospital, patients were already familiarized with cycling on MOTomed viva2. With the exception of TA, VM, Sol and GaL, the average EMG envelopes of all muscles presented very similar activation timing and shape between the two groups, for the four matching speeds. In the case of the three distal muscles (TA, Sol and GaL), which are usually affected by spasticity (Bravo-Esteban et al., 2013) and co-activation (Gómez-Soriano et al., 2010), the differences

in the average activation timing and shape might be explained by the hypertonia and clonus presented by some of the patients recruited.

5.5.2 Reconstruction goodness scores

To assess the reconstruction goodness scores of reconstructed EMG envelopes with a given number of synergies, two different coefficients were used: $\text{VAF}_{\text{total}}$ and the coefficient of determination (r^2). Both coefficients have been used in most studies on muscle synergies (Clark et al., 2010) (Torres-Oviedo et al., 2006). $\text{VAF}_{\text{total}}$ has been suggested to be more stringent than r^2 , since it is sensitive to both shape and amplitude of the signals, whereas r^2 only addresses similarity in shape.

In Chapter 4, $\text{VAF}_{\text{total}}$ values of approximately 90% were obtained when using three synergies to reconstruct a set of eight lower limb muscles in eight healthy subjects, for cycling speeds ranging from 43 ± 2.7 to 70 ± 4.0 rpm. In this study, similar $\text{VAF}_{\text{total}}$ values ($86.7 \pm 2.0\%$ to $88.5 \pm 4.2\%$) were obtained for the same set of muscles in ten healthy subjects. As expected, both $\text{VAF}_{\text{total}}$ and r^2 values decreased when using 3 synergies to reconstruct the set of 13 muscles, when compared with the case of 8 muscles. As referred by Steele et al. (2013), Clark et al. (2010) and Monaco et al. (2010), the higher the number of muscles, the lower is the reconstruction goodness score. No significant differences were found in the $\text{VAF}_{\text{total}}$ and r^2 scores neither between the iSCI group and the healthy group nor between spastic and non-spastic patients, for the 4 speeds, when using 2 to 5 synergies. This result may be explained by the low complexity of cycling (few degrees of freedom), which seems to be executed by the same number of synergies by both healthy and iSCI subjects.

Differently from previous studies, in which $\text{VAF}_{\text{total}}$ is used to define the optimal number of synergy for each subject, here it was introduced a global criterion ($\text{VAF}_{\text{total}}$ values $\geq 85\%$ in at least 50% of the subjects) in order to fix a “globally optimum” number of synergies for all subjects. This criterion allowed to i) use $\text{VAF}_{\text{total}}$ values as a continuous quantitative metric of motor performance with a fixed number of synergies, and ii) perform a direct comparison between patients’ synergies and a reference dataset from healthy subjects (W_0 and H_0).

5.5.3 Similarity of synergy vectors and activation coefficients

Little is known about the effect of iSCI on muscle synergies organization. The few studies that investigated this synergistic control focused on gait (Hayes et al., 2014) (Ivanenko et al., 2003) (Ivanenko et al., 2009). These studies suggested that the training post-SCI

and the underlying plasticity lead to a reorganization of interneuronal networks, this way modifying and creating new muscle synergies. Notwithstanding, the synergistic control of iSCI patients during cycling has not been described yet, to our best knowledge.

When using the set of 13 muscles, the activation coefficients were very similar to those obtained with the set of 8 muscles (see Figure 5.6AII), and similar to those presented in Chapter 4 (see Figure 4.7B). Synergy vectors were also very similar between the 8- and 13-muscle datasets, with the additional five muscles being incorporated within the 3 synergy vectors (see Figure 5.6AI).

In the healthy group, antagonist muscles were not activated by the same synergy (e.g., the quadriceps and hamstrings, the TA and the Triceps Surae), in accordance with the literature on walking (Clark et al., 2010) and cycling (Hug et al., 2011). As expected, patients with no diagnosed spasticity presented similar synergy vectors to the healthy people (levels of co-activation of agonists/antagonists very low) (see representative patient from Figure 5.6CI). However, this was not the case of some iSCI patients diagnosed with spasticity (see representative patient from Figure 5.6BI). In this case, there was high variability of muscle synergy vectors and activation coefficients across the speeds, and also antagonist muscles were activated by the same synergy (e.g., TA and Sol activated by synergy 3 in Figure 5.6BI). Although spastic patients presented, on average, lower similarity values ($W \cdot W_0$ and $H \cdot H_0$) than non-spastic patients, differences were not statistically significant, except for the case of $H_2 \cdot H_{02}$ at 30 rpm for the dataset of 13 muscles. This metric could also predict Total MAS scores.

When considering the whole iSCI group, similarity with the healthy reference set was higher for the activation coefficients than for the synergy vectors. These results may indicate less disruption of the corticospinal drive (represented by activation coefficients) than the disruption of the spinal organization (represented by the synergy vectors) after SCI (Ting et al., 2015) (Ivanenko et al., 2003).

Synergy 3 (activated during the downstroke phase of cycling) from iSCI patients was the one with higher similarity with the corresponding synergy of the healthy group, for both spastic and non-spastic patients. This was observed both for the synergy vectors ($W_3 \cdot W_{03}$) and activation coefficients ($H_3 \cdot H_{03}$), indicating less variability for this synergy composition and activation. Taking into account the higher similarity of synergy 3, it can be hypothesized that the similarity scores for W_1 and W_2 , as well as H_1 and H_2 , which present lower correlation values with the healthy group, would better distinguish the spasticity levels of each patient.

5.5.4 Predictions of gait performance

Gait speed is an important variable assessed in the clinical setting. For instance, the criteria used to include similar patients in a group are usually based on classic clinical evaluations and walking speed (Nadeau et al., 2011). By analyzing muscle synergies during walking in poststroke subjects, Clark et al. (2010) reported that the number of synergies correlated with the preferred walking speed. Also, Routson et al. (2013) referred that poststroke patients that improved the activation coefficients (more similar to the healthy group) also improved walking performance. Based on the observed common muscle synergies between cycling and walking (Barroso et al., 2014), one of the hypothesis of this study was that the analysis of muscle synergies during cycling correlates with gait performance scales.

When assessing iSCI subjects, van Hedel et al. (2005) reported that the 10-Meter test was more sensitive than the WISCI II in demonstrating improvements on walking performance. In the study presented in this Chapter, after performing individual linear correlation with WISCI II, both goodness scores (VAF_{total} and r^2) at different speeds were selected as input for the Multiple Regression Model. As output of the model, VAF_{total} score at 42 rpm with the dataset of 13 muscles could alone predict most of the variance of WISCI II. r^2 values using the dataset of 8 muscles, also at 42 rpm, could predict alone the time to perform TUG and 10-Meter tests. Thus, 42 rpm seems to be the most appropriate speed to assess motor performance in iSCI patients.

5.5.5 Predictions of spasticity

The difficulty to classify a subject as spastic or not is a well-known problem (Reichenfeller et al., 2012). In the case of poststroke patients, spasticity is characterized by high levels of muscle tone and a relative absence of spasms, whereas in iSCI patients, spasticity is mainly associated with the presence of flexor and extensor spasms triggered by cutaneous stimulation (Bennett, 2008). Ashworth and modified Ashworth scales are commonly used to assess spasticity, although they specifically measure hypertonia (Gómez-Soriano et al., 2012). It has been suggested that the combination of these scales with a spasms frequency scale may be useful to obtain more information about the spasticity of iSCI patients (Priebe et al., 1996).

Despite the valuable information of pathophysiological mechanisms involved in spasticity (Biering-Sørensen et al., 2006), there is still need for novel tools capable of providing quantitative metrics of spasticity, with low intra and inter-rater variability (Gómez-Soriano et al., 2012). As shown by the results presented in this Chapter, the use of EMG analysis may provide solutions to this problem.

Similarity scores for synergies 1 and 2 could predict spasticity and spasms frequencies. In particular, $H2 \cdot H_02$ at 30 rpm for the dataset of 13 muscles predicted Total MAS scores. $W1 \cdot W_01$ with the dataset of 8 muscles could alone predict most of the variance of Penn and the spasms of SCATS scale. These results indicate that $H2 \cdot H_02$ at low speeds may be useful to assess the level of hypertonia, whereas $W1 \cdot W_01$ may be used to assess and predict the spasms frequency. On the other hand, these results also encourage a wider use of Penn and SCATS scale to assess spasticity syndrome in iSCI patients.

Study 3 - Combining biomechanical and neuromuscular analysis to assess walking symmetry post iSCI

Abstract

Background. To improve customized therapy of iSCI patients, it is important to understand the neuromuscular and biomechanical features underlying the motor control of both sides, as iSCI may lead to an asymmetric motor control and functional behavior. The analysis of muscle synergies, as well as the study of biomechanics, may detect differences between the most and less affected sides in iSCI patients.

Objective. The research presented in this Chapter tests two hypothesis: I) some biomechanical features can differentiate most and less affected side of iSCI patients; II) the analysis of muscle synergies can also differentiate most and less affected side of iSCI patients.

Methods. Eight iSCI patients and eight healthy subjects completed ten walking trials at matching speed. For each trial, three-dimensional (3D) motion analysis, as well as the recording of the electrical activity of seven leg muscles from both limbs using surface electromyography (sEMG) were performed. Muscle synergies were further extracted using the NNMF algorithm, with the number of synergies being defined as the minimum number needed to obtain variability accounted for ($VAF_{total} \geq 90\%$).

Results. Six kinematic variables and one spatio-temporal variable showed significant differences between the most and the less affected side of SCI patients. Fewer

muscle synergies were needed to account for the muscle activity of the most affected side of iSCI. Differences of similarity with the healthy reference were also observed in synergy 2 between both sides of patients.

Conclusions. Biomechanical analysis was more effective to detect differences between most and less affected side of iSCI patients than the analysis of muscle synergies, maybe due to the reduced number of muscles assessed in this study.

6.1 Introduction

The progressive adaptation to the patient-specific reorganization of sensorimotor functions is one of the main challenges in gait training (Wang et al., 2013). A central issue to achieve this goal is to accurately measure the locomotor responses after neurological disease (Ivanenko et al., 2013).

Biomechanical measures obtained with gait analysis systems may provide detailed and a quantitative description of motor behavior of iSCI patients. It has been referred that iSCI patients present an impaired walking and tend to walk slowly (Ditunno and Scivoletto, 2009). Moreover, Gil-Agudo et al. (2011) and Gil-Agudo et al. (2013) showed remarkable kinematic differences localized at the knee and ankle level, in the sagittal plane, between iSCI patients and healthy subjects. The understanding of how iSCI affects kinematics of lower limbs during walking is of great importance to help the physician to set a customized rehabilitation program.

In addition to the biomechanical analysis, surface electromyography (EMG) may also provide valuable information about disturbances and changes in motor control in neurological diseases, which can be used to further guide the rehabilitation process (Wang et al., 2013). Neurological impairments such as iSCI may alter the normal functioning of the synergistic control typically observed in healthy subjects, and lead to gait disturbances (Fox et al., 2013).

The few existing reports on the synergistic control of iSCI patients suggest that muscle synergies are altered after the injury. However, it is very complicated to compare the results presented in these studies, since different age groups have been analyzed and also the sites of injuries are highly variable in location and magnitude (Ting et al., 2015). For instance, Fox et al. (2013) reported that less number of muscle synergies were needed to account for most of the variability of EMG envelopes of lower limb muscles of children who suffered iSCI in comparison with healthy children. However, these results should be analyzed with caution, as children's nervous system is still immature and developing, which may represent a different synergistic control of walking than the observed in adults

(Fox et al., 2013). Other authors have studied heterogeneous populations, including patients with complete motor SCI, and analyzed different conditions of weight loading and treadmill speed (Grasso et al., 2004) (Ivanenko et al., 2003) (Ivanenko et al., 2009). Hayes et al. (2014) conducted a study to quantify neuromuscular deficits in muscle coordination during overground walking in iSCI subjects, concluding that iSCI patients presented significant reduced muscle coordination if compared with healthy controls, with neuromuscular constraints contributing to person-specific deficits in overground walking.

One limitation of most of these studies is that they assess only one side of the body or average data from both sides. As iSCI may affect both sides differently, leading to an asymmetric motor control and functional behavior, it is important to understand which biomechanical and EMG features may detect differences between the two sides in patients with iSCI, to further improve customized therapy.

6.2 Goals

The main goal of this Chapter is to test two hypotheses: I) some biomechanical features can differentiate most and less affected side of iSCI patients; II) muscle synergies can also differentiate most and less affected side of iSCI patients. The confirmation of these two hypotheses would support the importance of studying the bilateral control of lower limb functions in iSCI patients, as well as to combine biomechanical features and the analysis of the synergistic muscle control.

6.3 Materials and Methods

6.3.1 Subjects

All recruited subjects gave their written consent to participate in the study and for data publication, after being informed about the procedures and possible discomfort associated with the experiments, in accordance with the Declaration of Helsinki (see Appendix E.2). The National Hospital for Spinal Cord Injury Ethical Committee approved this study.

Eight healthy subjects (4 men, 4 women), with an age of 31.50 ± 6.61 yr, with similar demographic and anthropometric characteristics, and with no diagnosed neural injury, neither central nor peripheral, were recruited to participate as controls (CG - control group). Eight iSCI patients (5 men, 3 women), with an age of 38.38 ± 10.45 yr,

TABLE 6.1: Individual iSCI patients' information.

Patient ID	Gender	Age (Years)	Level of Lesion	AIS	Time post-SCI (months)	WISCI II	Assistive device	LEMS (L/R, total)	10MWT (s)	TUG (s)	SCIM	Cadence (steps/min) (L/R)	Most affected side
1	M	25	C4	D	4	19	One crutch (R)	16/21, 27 37	32	68	42.3/53.5	L	
2	M	36	C7	D	154	20	None	21/25, 12.5 46	10	93	73.8/76.5	L	
3	M	51	T12	D	216	20	None	21/20, 8 41	8	93	103.4/101.8	R	
4	M	41	C6	D	6	20	None	24/24, 9 48	10	83	95/86.7	R	
5	M	31	C6	D	3	19	One crutch (R)	18/24, 10 42	11	83	85.7/91.8	L	
6	F	48	C5	D	3	20	None	24/25, 7 49	6.15	99	101/99.2	R	
7	F	26	T10	D	6	19	One crutch (R)	22/22, 8 44	9	83	84.4/79.5	R	
8	F	49	T7	D	7	12	Two crutches and braces	17/22, 18 39	21	85	68.9/74.8	L	

M, male; F, female; Level of Lesion: C – Cervical, T – Thoracic; AIS, American Spinal Injury Association (ASIA) Impairment Scale; WISCI II, Walking Index for Spinal Cord Injury; R, right; L, left; LEMS, Lower Extremity Motor Score; 10MWT, 10-Meter Walk Test; TUG, Timed Up and Go; SCIM, Spinal Cord Independence Measure.

volunteered to participate in this study. All of them received the standard rehabilitation program of the hospital. Inclusion criteria were: aged between 18 and 65 years, motor incomplete spinal lesion (AIS C-D), evolution of at least 1.5 months, absence of any other pathological condition, ability to walk 10 meters unassisted with or without technical aids. Exclusion criteria were: history of epilepsy, passive restriction of the joints and diagnosis of any other disease associated with memory, concentration and/or visual deficits. Detailed information of the patients is presented in Table 6.1.

6.3.2 Experimental protocol and data collection

The research presented in this Chapter was carried out in the Biomechanical and Technical Aids Department of the National Hospital for Spinal Cord Injury (Toledo, Spain).

Patients underwent two different types of assessment: clinical evaluation and 3D gait analysis. Clinical evaluation was not performed for the control group.

Clinical evaluation was performed by a trained physiatrist and consisted on a set of evaluations to examine the clinical and functional status of the patients. In order to minimize inter-rater variability, one physiatrist carried out the entire assessment procedure, evaluating the following scales (see Table 6.1): Lower Extremity Motor Score (LEMS), which test five key muscles in each leg with a score from 0 to 5, with the accumulative score for each extremity being between 0 and 25 and a total score from 0 to 50; Walking Index for Spinal Cord Injury II (WISCI II), which assesses the amount of physical assistance needed by the patient to walk 10 meters (0 indicates that the patient cannot stand and walk, whereas 20 means that the patient can walk 10 meters without any kind of assistance); 10-Meter Walk Test, which measures the time a person takes to walk 10 meters using the usual walking devices; the Timed Up and Go (TUG) test, which measures the time spent to stand up from a chair, walking 3 meters, turn around, return to the chair and sit down again at self-selected speed and using the habitual walking devices; and the Spinal Cord Independence Measure (SCIM), which is a disability scale specific for SCI (Benito-Penalva et al., 2012) (Gil-Agudo et al., 2013) (Kapadia et al., 2014).

Gait analysis was performed using a 3D motion analysis system with two scanner units (CODA System6, Charnwood Dynamics, Ltd, UK) and a force platform embedded in the walking path, which allowed the study of ground reaction forces. An acquisition frequency of 200 Hz was used to record data with CODA and from the force platform. Each participant completed ten walking trials along a 10 m walkway at self-selected speed, resting one minute between trials to avoid fatigue (see Figure 6.1). Eleven active markers were positioned and attached to anatomic landmarks, as described by Kadaba et al. (1990). All the iSCI patients walked with their usual footwear. CG participants were asked to walk within the range of speeds of iSCI group, following the same criterion performed by Ochi et al. (1999) and Gil-Agudo et al. (2013).

For all iSCI patients, surface electromyography (sEMG) data were recorded bilaterally using an EMG recording system (Noraxon®, Scottsdale, Arizona, U.S.A.), with an acquisition frequency of 1500 Hz, being synchronized online with CODA data. In the case of the CG, just the right side was evaluated. Surface EMG electrodes were positioned as described in Cram (2011), on the following seven muscles: Gluteus Medius (GMe), Gluteus Maximus (GMa), Rectus Femoris (RF), Adductor Longus (AL), Biceps Femoris (BF), Tibialis Anterior (TA) and Gastrocnemius Medialis (GaM).

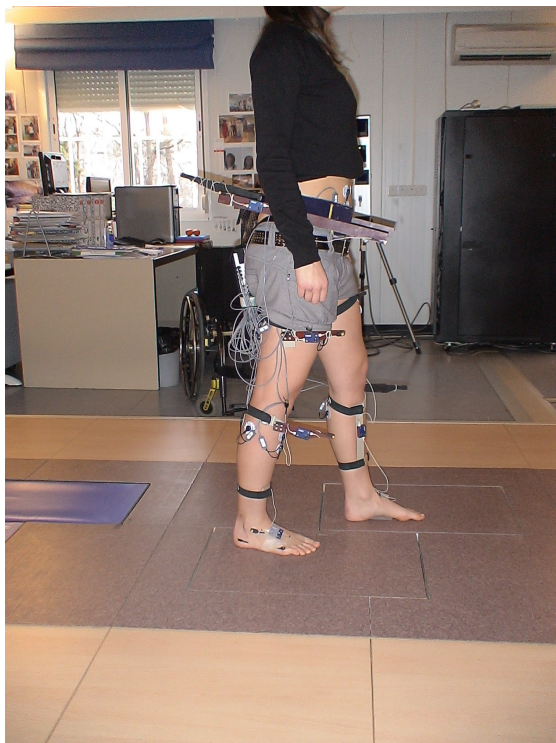


FIGURE 6.1: Incomplete SCI patient walking during one trial.

For each subject, the recording session lasted approximately 20 minutes, in addition to the donning and doffing of the EMG recording setup and the markers for 3D gait analysis (15-30 minutes, depending on the subject and level of impairment).

Data were analyzed offline with MATLAB R2011a (The MathWorks, Natick, MA) and IBM SPSS Statistics 20 software (IBM).

6.3.3 Data analysis

Heel strike events were determined by visual inspection of the heel marker trajectory. Each walking stride started at the heel strike of the corresponding leg. Cadence and speed were calculated independently for each side, according to the time spent and distance walked during a step. Cadence values of each side were used to tag sides as being the most or the less affected side, with the most affected side (iSCIa) defined as the one achieving a lower cadence (see Table 6.1). For each one of the ten trials performed by each subject, the central left stride and the central right stride were selected for analysis. Finally, for each side, data from the chosen strides were concatenated.

6.3.3.1 Analysis of muscle synergies

Using SynergiesLAB software (see Appendix C), concatenated raw EMG signals from each participant and side analyzed were high-pass filtered at 20 Hz, demeaned, rectified, and smoothed with a low-pass filter at 5 Hz, resulting in the EMG envelopes, according to the procedures performed by Clark et al. (2010) and Hug et al. (2010). EMG envelopes were then normalized by the average of the maximum of each of the ten strides, and resampled at each 1% of the stride cycle. For each participant and analyzed side, normalized EMG envelopes were combined into an $m \times t$ matrix (EMG_0), where m is the number of muscles (seven in this case) and t is the time base ($t = \text{no. of cycles (10) x 100}$)).

Muscle synergy vectors and the corresponding activation coefficients were extracted using the NNMF algorithm in SynergiesLAB (see equation 2.1) (Lee and Seung, 1999). For each EMG_0 , the NNMF algorithm was run six times, considering as input 2 to 7 synergies ($n = 2, 3, 4, 5, 6, 7$). In order to avoid local minima, for each run, the NNMF algorithm was repeated 40 times and the repetition with the lowest reconstruction error was selected.

Each muscle synergy vector (column of matrix W) was normalized by the maximum value of the muscle in the synergy to which they belong, which also helps the visual comparisons among subjects, as performed by Hug et al. (2010) and Muceli et al. (2010). Then, the corresponding activation coefficients were scaled by the same quantity, as done by De Marchis et al. (2012).

The similarity between EMG_0 and EMG_r was calculated using the variability accounted for (VAF_{total} , see Equation 4.1) (Clark et al., 2010). The number of synergies was defined as being the minimum number needed to obtain VAF_{total} values $\geq 90\%$ (Routson et al., 2014).

At last, two reference sets of matrices (W_0 and H_0) were obtained by concatenating the EMG envelopes from all the CG subjects, and applying the NNMF algorithm constrained to four muscle synergies, regardless the VAF_{total} criterion, as done previously by Clark et al. (2010) and Routson et al. (2014). Hence, it was possible to compare muscle synergy vectors and activation coefficients of iSCI with the four synergies described in literature for healthy subjects while walking (Clark et al., 2010) (Routson et al., 2014). After that, previously extracted muscle synergy vectors (columns of matrix W) of each patient were ordered according to their similarity with columns of W_0 . This was done by means of the normalized scalar product and corresponds mathematically to the scalar product of pairs of columns from matrices W , each one previously normalized by its

norm, providing output values ranging from 0 to 1. After being ordered, muscle synergy vectors and activation coefficients of each patient were compared with the reference healthy sets (W_0 and H_0), using the normalized scalar product. In this Chapter, the normalized scalar products between H and H_0 and between W and W_0 are denoted “ $H \cdot H_0$ ” and “ $W \cdot W_0$ ”, respectively.

6.3.3.2 Kinematics

Raw kinematic data of each analyzed side and subject were low-pass filtered at 6 Hz (Allen and Neptune, 2012). From the mean profile over the ten selected strides (Bowden et al., 2010), it was possible to extract the following joint kinematic parameters usually used to describe gait (Schutte et al., 2000) (Moreno et al., 2013) (Bonnyaud et al., 2014) (Roche et al., 2015):

- Hip joint parameters: peak flexion ($^{\circ}$), peak extension ($^{\circ}$), range of flexion ($^{\circ}$), pre-swing angle (min) ($^{\circ}$), peak of abduction in swing ($^{\circ}$), range of abduction ($^{\circ}$), mean rotation in stance ($^{\circ}$);
- Knee joint parameters: flexion at initial contact ($^{\circ}$), time of peak flexion (% gait cycle), peak flexion ($^{\circ}$), time of peak extension (% gait cycle), peak extension ($^{\circ}$), range of flexion ($^{\circ}$);
- Ankle joint parameters: peak dorsiflexion during stance ($^{\circ}$), peak dorsiflexion during swing ($^{\circ}$), peak dorsiflexion ($^{\circ}$), peak plantarflexion ($^{\circ}$), range of flexion ($^{\circ}$);
- Pelvis joint parameters: mean tilt ($^{\circ}$), range of tilt ($^{\circ}$), mean rotation ($^{\circ}$);

6.3.3.3 Spatio-temporal parameters

Based on the 3D position of the foot markers, it was possible to extract the mean of the following spatio-temporal parameters (Schutte et al., 2000) (Bowden et al., 2010) (Boudarham et al., 2013) (Bonnyaud et al., 2014) (Arnold et al., 2014): speed (m/s), stride length (m), stride duration (s), strides/minute, step length (m), step duration (s), cadence (steps/minute), % stance, duration of stance (s), duration of single support (s), % single support, duration of double support (s).

6.3.3.4 Kinetics

Raw data from the force platform were low-pass filtered at 20 Hz and normalized by subject's weight (Bowden et al., 2010). The mean over the ten trials was calculated and the following parameters were extracted (Bonnyaud et al., 2014) (Bowden et al., 2010): vertical ground reaction force (GRF) during single support phase (N/Kg), peak of propulsion (N/Kg), peak of braking (N/Kg), peak medio-lateral force (N/Kg).

6.3.4 Statistical analysis

After verifying the normality of the samples with the Kolmogorov-Smirnov test, it was used one-way ANOVA with post-hoc Bonferroni for multiple comparisons between the three groups (control group, most affected side of iSCI patients and less affected side of iSCI patients) in terms of speed, cadence, VAF_{total} scores and the number of synergies.

Paired Student's *t*-tests were performed to test significant differences between most and less affected side of iSCI patients on the following variables: synergy similarity indicators ($H \cdot H_0$ and $W \cdot W_0$), kinematic, spatio-temporal and kinetic variables.

Statistical significance was set by a *p*-value of 0.05.

6.4 Results

6.4.1 Biomechanical differences between sides

Patients walked at very heterogeneous speed, ranging from 0.30 to 1.05 m/s. When considering each side independently (using data from independent strides), patients showed an average speed of 0.71 ± 0.24 m/s for the most affected side and 0.73 ± 0.25 m/s for the less affected side. The CG walked with an average of 0.92 ± 0.20 m/s, which fits the range of motion of iSCI patients. Differences in speed were not statistically significant when comparing the speed of the three groups (iSCI, iSCIa and CG) ($p = 0.158$).

Regarding patients' cadence, values ranged from 42.28 to 103.40 steps/min. When considering each side independently (using data from independent strides), an average cadence of 80.49 ± 18.55 for the most affected side and 84.32 ± 17.16 for the less affected side was obtained. CG walked with a cadence of 89.29 ± 12.40 steps/min, which fits the range of motion of iSCI patients. No statistically significant differences were found comparing the cadence of the three analyzed groups ($p = 0.565$).

Six kinematic variables (peak of hip flexion, range of hip flexion, peak of hip abduction in swing, range of hip abduction, peak of knee flexion and peak of ankle plantarflexion) showed significant differences between the most and the less affected side of iSCI patients ($p < 0.05$), with the most affected side presenting lower values than the less affected side, except for peak of hip abduction in swing (see Table 6.2). For these six kinematic variables, CG presented the following values (mean \pm SD) (see Figure 6.2A-F): $40.97 \pm 10.70^\circ$ for peak of hip flexion, $38.36 \pm 5.89^\circ$ for range of hip flexion, $0.45 \pm 2.47^\circ$ for peak of hip abduction in swing, $10.80 \pm 4.29^\circ$ for range of hip abduction, $64.03 \pm 3.22^\circ$ for peak of knee flexion and $19.54 \pm 2.23^\circ$ for peak of ankle plantarflexion. Mean \pm SD values of these six variables for the most affected side of iSCI patients were less than or equal to those verified for the CG. On the other hand, data from the less affected side of iSCI patients were greater than or equal to those verified for the CG, except for the peak of hip abduction in swing, which was lower for the less affected side of iSCI patients than the CG.

Step length was the only spatio-temporal variable that showed significant differences between the most and the less affected side of iSCI patients ($p = 0.027$), with the most affected side presenting lower values (0.50 ± 0.12) than the less affected side (0.56 ± 0.09) (see Table 6.3). Both the most and less affected side of iSCI patients presented lower values than those verified for the CG (0.65 ± 0.068) (see Figure 6.2G).

No significant differences were found between the most and the less affected side of iSCI patients when analyzing kinetic variables.

6.4.2 Synergistic control of gait

Fewer muscle synergies were needed to account for the whole muscle activity of the seven analyzed muscles in the most affected side (2.88 ± 0.64) than the less affected side (3.38 ± 0.52) of iSCI patients and the CG (3.62 ± 0.52) (see Table 6.4). The difference between the number of synergies needed to account for the whole muscle activity of the most affected side of iSCI patients (iSCIa) and the CG was statistically significant (p -value = 0.042).

Considering the most affected side, two patients (25%) required two synergies, five patients (62.5%) required three synergies and one patient (12.5%) required four synergies to obtain VAF_{total} values $\geq 90\%$. In the case of the less affected sides, five patients (62.5%) required three synergies, whilst three patients (37.5%) required four synergies to obtain VAF_{total} values $\geq 90\%$. Three healthy subjects (37.5%) required three synergies, while the other five healthy participants (62.5%) needed four synergies to obtain VAF_{total} values $\geq 90\%$.

TABLE 6.2: Comparison of kinematic indicators between most and less affected sides of iSCI patients. Values are given in mean \pm SD.

Kinematic variables	Side	Mean \pm SD	<i>p</i> -value
Peak of hip flexion ($^{\circ}$)	most affected	30.21 \pm 10.72	0.044*
	less affected	43.23 \pm 11.08	
Peak of extension ($^{\circ}$)	most affected	-3.07 \pm 11.67	0.427
	less affected	0.31 \pm 12.32	
Range of hip flexion ($^{\circ}$)	most affected	37.28 \pm 4.19	0.011*
	less affected	42.93 \pm 4.94	
Pre-swing angle of hip (min) ($^{\circ}$)	most affected	-3.08 \pm 11.67	0.427
	less affected	0.31 \pm 12.32	
Peak of hip abduction in swing ($^{\circ}$)	most affected	-0.08 \pm 3.05	0.022*
	less affected	-5.80 \pm 4.93	
Range of hip abduction ($^{\circ}$)	most affected	10.80 \pm 3.71	0.003**
	less affected	14.43 \pm 3.69	
Mean rotation of hip in stance ($^{\circ}$)	most affected	12.26 \pm 4.13	0.754
	less affected	11.72 \pm 4.18	
Knee flexion at initial contact ($^{\circ}$)	most affected	5.58 \pm 5.62	0.357
	less affected	8.49 \pm 3.85	
Time of peak knee flexion (% gait cycle)	most affected	77.75 \pm 5.99	0.697
	less affected	78.88 \pm 4.29	
Peak of knee flexion ($^{\circ}$)	most affected	50.10 \pm 11.62	0.011*
	less affected	61.35 \pm 8.96	
Time of peak knee extension (% gait cycle)	most affected	53.13 \pm 29.50	0.198
	less affected	74.13 \pm 38.74	
Peak of knee extension ($^{\circ}$)	most affected	-1.19 \pm 6.46	0.122
	less affected	3.48 \pm 6.09	
Range of knee flexion ($^{\circ}$)	most affected	51.30 \pm 10.30	0.169
	less affected	57.86 \pm 8.98	
Peak of ankle dorsiflexion during stance ($^{\circ}$)	most affected	-10.41 \pm 6.50	0.121
	less affected	-6.28 \pm 2.89	
Peak of ankle dorsiflexion during swing ($^{\circ}$)	most affected	-5.59 \pm 8.59	0.263
	less affected	-1.31 \pm 5.38	
Peak of ankle dorsiflexion ($^{\circ}$)	most affected	-10.55 \pm 6.65	0.132
	less affected	-6.46 \pm 2.88	
Peak of ankle plantarflexion ($^{\circ}$)	most affected	13.66 \pm 7.00	0.042*
	less affected	18.48 \pm 5.20	
Range of ankle flexion ($^{\circ}$)	most affected	24.21 \pm 5.18	0.668
	less affected	24.94 \pm 4.02	
Mean pelvic tilt ($^{\circ}$)	most affected	14.34 \pm 7.44	0.371
	less affected	16.77 \pm 8.58	
Range of pelvic tilt ($^{\circ}$)	most affected	8.48 \pm 4.24	0.110
	less affected	6.94 \pm 3.84	
Mean pelvic rotation ($^{\circ}$)	most affected	-0.57 \pm 3.61	0.215
	less affected	2.23 \pm 3.61	

* Values are significantly different between sides ($p < 0.05$). ** Values are significantly different between sides ($p < 0.01$). For those indicators with significant differences between sides, the side with higher values is evidenced in bold.

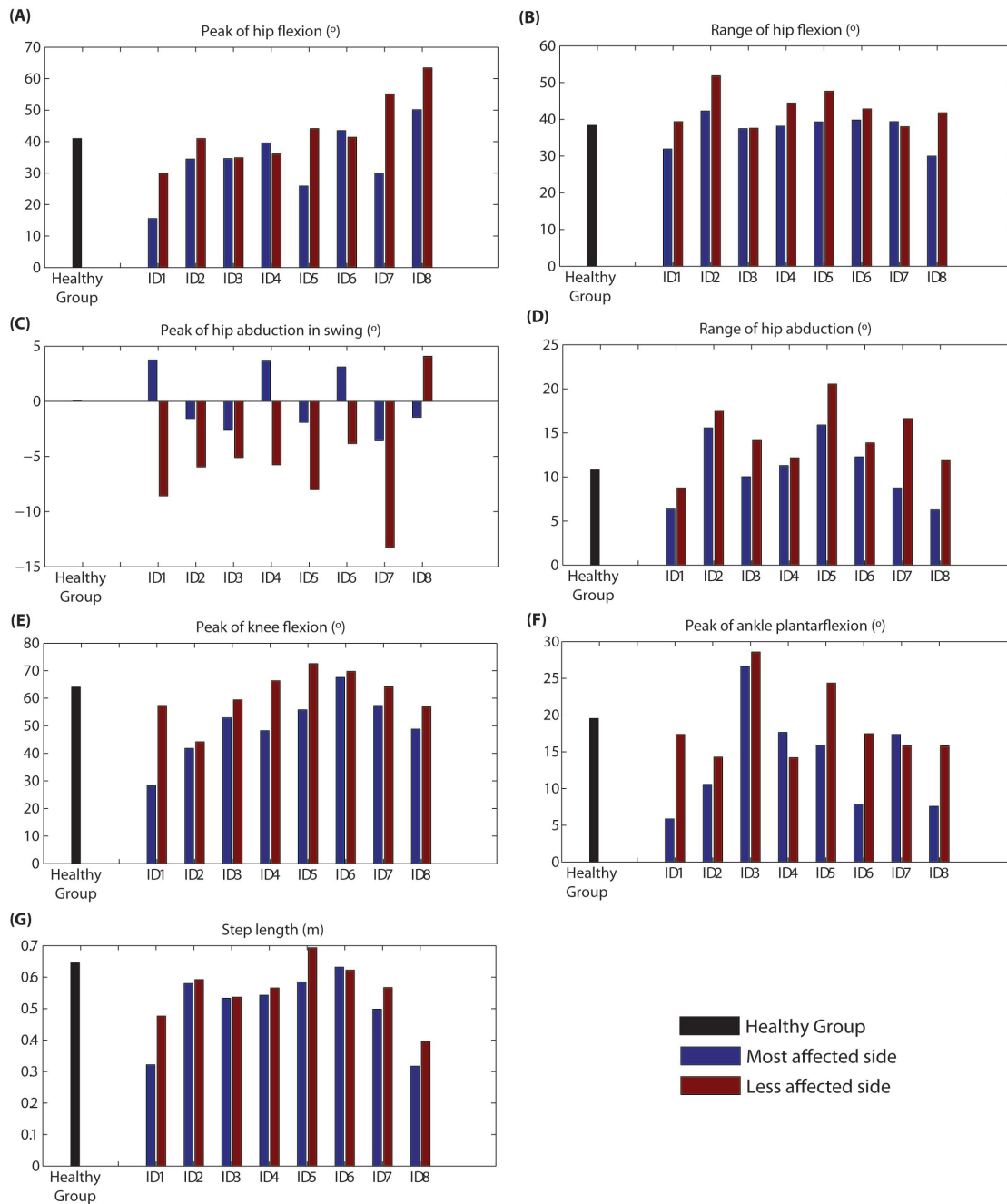


FIGURE 6.2: Biomechanical indicators that showed significant differences between most and less affected side in iSCI patients.

TABLE 6.3: Comparison of spatio-temporal and kinetic indicators between most and less affected sides of iSCI patients. Values are given in mean \pm SD.

Variables	Side	Mean \pm SD	<i>p</i> -value
Spatio-temporal			
Speed (m/s)	most affected	0.71 \pm 0.24	0.466
	less affected	0.73 \pm 0.25	
Stride length (m)	most affected	1.02 \pm 0.19	0.588
	less affected	1.03 \pm 0.18	
Stride duration (s)	most affected	1.55 \pm 0.45	0.773
	less affected	1.55 \pm 0.47	
Strides/minute	most affected	41.18 \pm 9.19	0.952
	less affected	41.16 \pm 9.12	
Step length (m)	most affected	0.50 \pm 0.12	0.027*
	less affected	0.56 \pm 0.09	
Step duration (s)	most affected	0.80 \pm 0.27	0.186
	less affected	0.75 \pm 0.18	
Cadence (steps/minute)	most affected	80.49 \pm 18.55	0.073
	less affected	84.32 \pm 17.16	
% Stance	most affected	69.71 \pm 3.21	0.138
	less affected	72.10 \pm 5.42	
Duration of stance (s)	most affected	1.09 \pm 0.36	0.233
	less affected	1.14 \pm 0.46	
Duration of single support (s)	most affected	0.41 \pm 0.36	0.163
	less affected	0.46 \pm 0.09	
% Single support	most affected	27.87 \pm 5.28	0.103
	less affected	30.28 \pm 3.33	
Duration of double support (s)	most affected	0.34 \pm 0.17	0.837
	less affected	0.34 \pm 0.18	
Kinetics			
Vertical ground reaction force(N/Kg)	most affected	10.05 \pm 1.30	0.332
	less affected	10.31 \pm 0.86	
Peak of propulsion (N/Kg)	most affected	0.86 \pm 0.31	0.175
	less affected	1.04 \pm 0.51	
Peak of braking (N/Kg)	most affected	-1.03 \pm 0.61	0.397
	less affected	-0.91 \pm 0.37	
Peak of medio-lateral force (N/Kg)	most affected	0.71 \pm 0.14	0.276
	less affected	0.67 \pm 0.19	

* Values are significantly different between sides ($p < 0.05$). For those indicators with significant differences between sides, the side with higher values is evidenced in bold.

TABLE 6.4: Number of muscle synergies and $\text{VAF}_{\text{total}}$ values obtained for the three groups, when using two to four synergies to reconstruct overall muscle activity. Values are expressed as mean \pm SD. iSCI, less affected side; iSCIa, most affected side; CG, control group.

Variable	iSCI	iSCIa	CG	p -value
Number of synergies	3.38 \pm 0.52	2.88 \pm 0.64	3.62 \pm 0.52	0.042
$\text{VAF}_{\text{total}}$ (2 synergies)	83.44 \pm 4.60	85.20 \pm 5.40	81.80 \pm 2.75	0.321
$\text{VAF}_{\text{total}}$ (3 synergies)	90.25 \pm 2.58	91.88 \pm 1.66	90.39 \pm 2.12	0.269
$\text{VAF}_{\text{total}}$ (4 synergies)	94.51 \pm 1.35	95.48 \pm 1.00	94.83 \pm 1.49	0.332

Bold values indicate significant differences.

When considering $\text{VAF}_{\text{total}}$ values, no significant differences were found among the three groups (p -value $>$ 0.05), despite iSCIa had presented higher mean values (see Table 6.4).

Reference sets of muscle synergy vectors (W_0) and activation coefficients (H_0) were consistent with those described in literature (see Figure 6.3) using eight muscles and similar functional muscle groups (Clark et al., 2010) (Routson et al., 2014) and qualitatively similar to previous studies that recorded a larger set of muscles (Ivanenko et al., 2004) (Cappellini et al., 2006). Synergy 1 consisted mainly on the activity of biceps femoris (BF) (knee flexors and hip extensors) at the end of swing and initial heel contact. Synergy 2 consisted on the activity of GMe (hip abductor) and GMa (hip extensor and abductor), RF (knee extensor and hip flexor) and TA (ankle dorsiflexor) during early stance. Synergy 3 consisted mainly on the activity of GaM (ankle plantarflexor), and to a lower extent, GMe, during late stance. Finally, synergy 4 consisted in the activation of AL (hip adductor), TA, and to a lower extent, RF, during initial swing phase.

The similarity of synergy vectors ($W \cdot W_0$) and activation coefficients ($H \cdot H_0$) from iSCI patients with the control group (CG) reference was calculated by means of normalized scalar product (see Table 6.5). Both muscle synergy vectors (W) and activation coefficients (H) were very heterogeneous for both sides of patients. A significant difference between sides was found for $H_2 \cdot H_0$ ($p = 0.046$). Specifically, H_2 from the less affected side was more similar to the healthy reference than the most affected side of iSCI patients (see Figure 6.4). No more significant differences were found for the other similarity indicators.

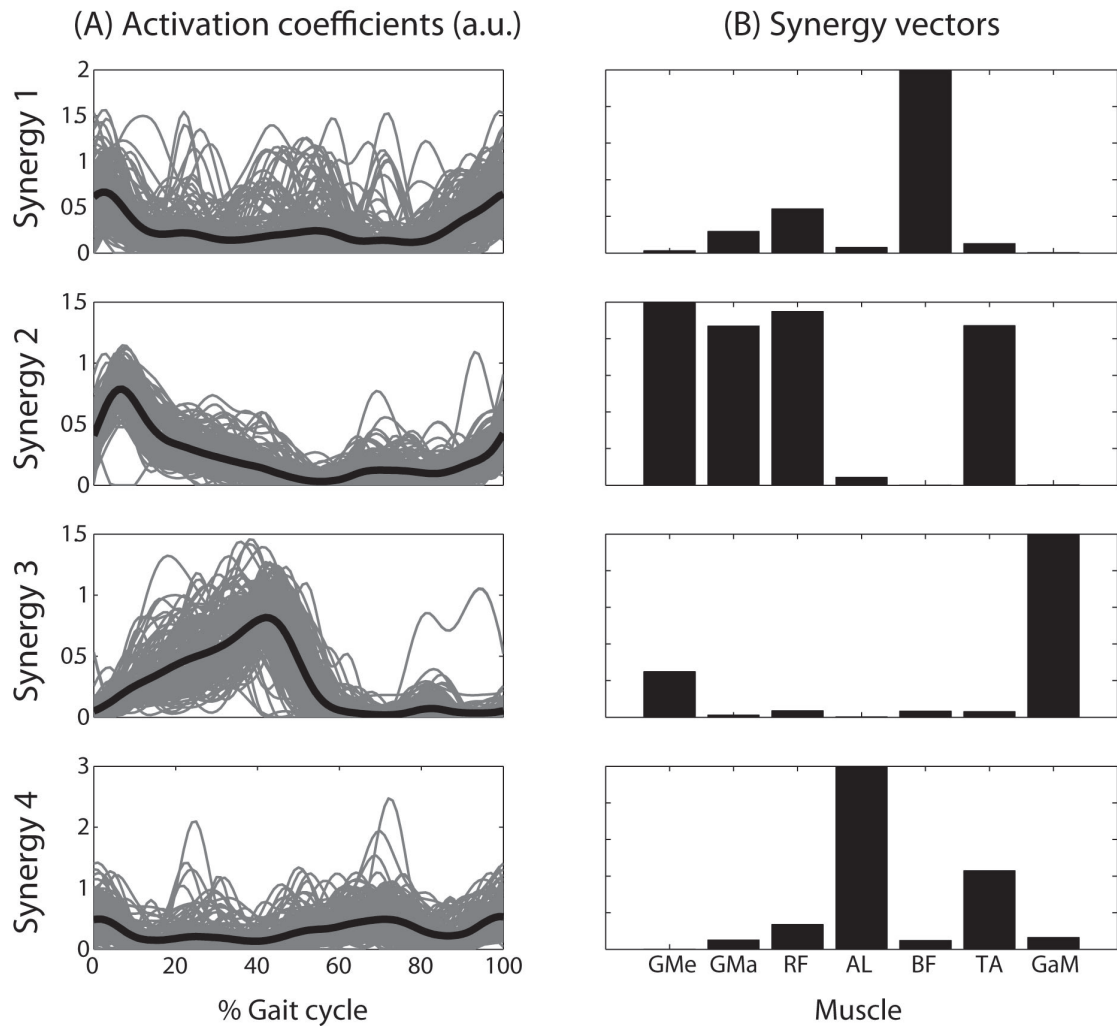


FIGURE 6.3: Reconstruction of EMG envelopes using concatenated data from the 8 healthy subjects and 4 muscle synergies. (A) Activation coefficients (rows of matrix H_0) of the reference set indicate time-varying profiles of activation responsible to activate each synergy. Thin gray lines represent activation coefficients of each of the 80 strides (10 stride cycles/ healthy subject), with each black thick line representing the average of those cycles. (B) Synergy vectors (columns of matrix W_0) of the reference set indicate the relative weighting of each synergy for each muscular pattern. GMe, Gluteus Medius; GMa, Gluteus Maximus; RF, Rectus Femoris; AL, Adductor Longus; BF, Biceps Femoris; TA, Tibialis Anterior (TA); GaM, Gastrocnemius Medialis.

TABLE 6.5: Similarity of synergy vectors ($W \cdot W_0$) and activation coefficients ($H \cdot H_0$) with the control group (CG) reference, using four synergies to reconstruct the EMG envelopes of the less affected side (iSCI) and the most affected side (iSCIa) of iSCI patients.

Subject ID	W1·W ₀ 1	W2·W ₀ 2	W3·W ₀ 3	W4·W ₀ 4	H1·H ₀ 1	H2·H ₀ 2	H3·H ₀ 3	H4·H ₀ 4
iSCI1	0.99	0.86	0.98	0.91	0.87	0.59	0.79	0.93
iSCI2	0.88	0.92	0.81	0.84	0.73	0.91	0.96	0.89
iSCI3	0.17	0.74	0.98	0.64	0.88	0.82	0.50	0.61
iSCI4	0.15	0.76	1.00	0.90	0.76	0.95	0.94	0.94
iSCI5	0.87	0.77	0.94	0.55	0.85	0.93	0.89	0.80
iSCI6	0.91	0.99	0.96	0.98	0.88	0.92	0.99	0.78
iSCI7	0.45	0.64	0.99	0.82	0.77	0.88	0.98	0.80
iSCI8	0.17	0.76	0.78	0.97	0.84	0.94	0.84	0.90
mean±SD	0.57±0.38	0.81±0.11	0.93±0.08	0.83±0.15	0.82±0.06	0.87±0.12	0.86±0.16	0.83±0.11
iSCIa1	0.98	0.80	0.71	0.65	0.82	0.54	0.93	0.75
iSCIa2	0.88	0.80	0.80	0.66	0.73	0.78	0.87	0.86
iSCIa3	0.76	0.83	0.93	0.47	0.94	0.85	0.53	0.94
iSCIa4	0.91	0.91	0.96	0.83	0.93	0.93	0.94	0.90
iSCIa5	0.79	0.70	0.86	0.88	0.90	0.71	0.94	0.43
iSCIa6	0.88	0.99	0.91	0.94	0.81	0.94	0.84	0.79
iSCIa7	0.70	0.65	0.92	0.81	0.78	0.80	0.96	0.88
iSCIa8	0.46	0.79	0.81	0.85	0.86	0.83	0.82	0.74
mean±SD	0.79±0.16	0.81±0.11	0.86±0.09	0.76±0.15	0.85±0.08	0.79±0.13	0.86±0.14	0.79±0.16
<i>p</i> -value	0.089	0.949	0.070	0.321	0.370	0.046	0.816	0.561

Values close to 1 mean mean high similarity with the healthy reference. Similarity lower than 0.75 appear in bold. Bold values in the last row indicate significant or marginally significant differences between sides.

6.5 Discussion

This Chapter had two main goals: to compare the biomechanical and the synergistic control of walking between the two lower limbs in iSCI patients. Underlying these goals is the fact that walking patterns after a SCI are not always symmetrical between limbs, *i.e.*, one side may be more affected than the other, as it happens, for instance, in the case of hemiparesis following stroke.

As higher walking speeds may contribute to the identification of more muscle synergies (Clark et al., 2010), healthy subjects were asked to walk within the range of speeds

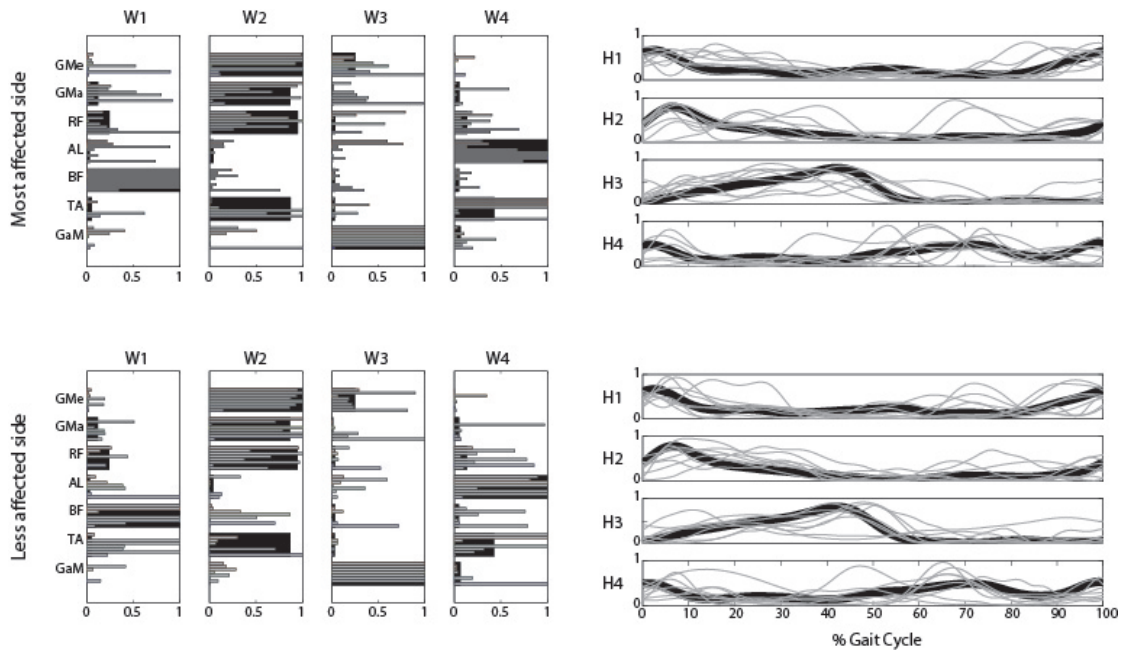


FIGURE 6.4: Muscle synergies components for the iSCI patients. Upper plot: Synergy vectors (W) and activation coefficients (H) extracted for the most affected side of iSCI patients, considering four synergies. Low plot: Synergy vectors (W) and activation coefficients (H) extracted for the less affected side of iSCI patients using four synergies. For the synergy vectors (W1-W4), each gray bar represents each iSCI patient, and the reference from the control group is represented in black. In relation to the activation coefficients (H1-H4), grey lines represent the results of each iSCI patient, and black lines represent the reference from the control group.

of the iSCI group. Moreover, the trials were performed overground, because comfortable speed may differ in populations with motor impairments if walking on a treadmill (Bowden et al., 2010).

LEMS score is usually employed in the clinical practice to assess patients' most affected side (van Middendorp et al., 2010) (Gil-Agudo et al., 2013). Nevertheless, four out of the eight iSCI patients presented equal or very similar LEMS score between sides. In order to distinguish between most and less affected side, we used another criterion: the cadence achieved by each side independently, according to the time spent to perform a step, with the most affected side being the one that needed more time. This additional criterion seems to be robust and useful to determine the most affected side in iSCI patients, as further differences were found between sides.

6.5.1 Biomechanical differences between sides

It has been reported that iSCI patients present an impaired walking, with poor balance and decreased walking speed, if compared with healthy subjects (Ditunno and Scivoletto,

2009). By assessing only one side of the body or average data from both sides, some other biomechanical features have shown differences in relation to the normality: kinematic differences localized at the knee and ankle level, in the sagittal plane (Gil-Agudo et al., 2011) (Gil-Agudo et al., 2013), with the knee and hip hyperflexed in the stance phase. The effective push-off in the transition between stance to swing is also compromised in some of these patients due to the excessive ankle plantarflexion through the stance phase (Ditunno and Scivoletto, 2009).

As presented in the Results section, some biomechanical variables showed significant differences between the most and the less affected side of iSCI patients. In particular, four variables associated with the hip (peak of hip flexion and abduction in swing, range of hip flexion and abduction), as well as peak of knee flexion, peak of ankle plantarflexion and step length differed between sides. These differences may represent compensatory strategies applied by these patients, which are not usually reported in literature.

6.5.2 Synergistic control of gait

There is evidence that SCI patients need less muscle synergies than healthy subjects to explain the EMG variability of lower limbs (Fox et al., 2013) (Hayes et al., 2014), though these reports had analyzed only the right limb of patients. When using the cadence criterion to tag each side as being more or less affected, the results of this Chapter showed that less muscle synergies were needed to explain the EMG variability of the most affected side during walking overground if compared with the less affected side, suggesting less complexity in the patterned activity of the most affected side. In fact, the identification of less muscle synergies is associated with lower independence among the activation patterns of each muscle, suggesting coupling of muscles across the limb or a possible merging of existing muscle synergies (Cheung et al., 2012). Similar results were reported by Clark et al. (2010) when comparing the paretic and non-paretic sides of poststroke patients.

When analyzing the healthy group, four synergies were needed to obtain $VAF_{total} \geq 90\%$. Synergy 1 consisted mainly of BF activation (hip extensor and knee flexor), which was activated in the terminal swing phase and initial heel contact to decelerate the lower limb during the final gait cycle and prepare for the initial contact (Neptune et al., 2009) (Clark et al., 2010) (Lacquaniti et al., 2012). Synergy 2 consisted on the activation of GMe (hip abductor), GMa (hip extensor and abductor), RF (hip flexor and knee extensor) and TA (ankle dorsiflexor), which were activated during the loading response phase to support the body and accept the body weight during initial contact (Neptune et al., 2009) (Clark et al., 2010) (Lacquaniti et al., 2012). Synergy 3 consisted

mainly of GaM (ankle plantarflexor) activation during mid and terminal stance phase, contributing to body support and forward propulsion (Neptune et al., 2009) (Clark et al., 2010) (Lacquaniti et al., 2012). GMe was also activated by this synergy, which might prevent pelvic drop during the monopodal stance and also the Trendelenburg gait pattern¹. Synergy 4 was mainly composed by AL activation, which might have provided stability in the frontal plane of hip during the terminal stance (Hayes et al., 2014). This synergy also consisted on the activation of TA and RF during initial swing phase, contributing to foot clearance (Neptune et al., 2009) (Clark et al., 2010) (Lacquaniti et al., 2012).

Both muscle synergy vectors (W) and activation coefficients (H) were very heterogeneous for both sides of patients. When testing the similarity with the healthy reference, a significant difference between sides was found just for $H_2 \cdot H_0$. One possible explanation for these results is the reduced number of muscles assessed from each side of the body. The assessment of more muscle could eventually reveal more neural control differences between sides.

6.5.3 Limitations of the study

The study presented in this Chapter has some limitations. First of all, the number of assessed iSCI patients (eight) limits the ability to detect statistical significance. Another limitation was the the range of speeds at which patients walked (0.30 to 1.05 m/s), as speed may influence the number of extracted synergies (Clark et al., 2010). To ease this effect, the control group was asked to walk within the range of speeds of iSCI patients, despite this decrease of their normal speed may had also altered their usual gait patterns. Another possible limitation was the recording of seven representative muscles of each side. It is possible to find or identify additional synergies if the repertoire of analyzed muscles is larger (Ivanenko et al., 2004) or the chosen muscles are different (Steele et al., 2013). However, taking into account that both sides were analyzed, in addition to the markers for 3D gait analysis, it was reached a good compromise between measurement completeness and minimal experimental burden, with the latter being a critical factor when analyzing SCI patients, similar to what has been performed by others when measuring both lower limbs (Clark et al., 2010) (Bowden et al., 2010) (Fox et al., 2013).

¹Trendelenburg gait is an abnormal walking pattern caused either by weak hip abductor muscles or an unstable hip fulcrum (Benson et al., 2010).

Study 4 - Combining biomechanical and neuromuscular analysis to assess walking poststroke

Abstract

Background. Gait analysis laboratories have been increasingly integrated into the clinical practice, as they provide crucial data to understand pathological gait. However, there is a need to reduce the typical large amount of data provided by gait analysis into a small and meaningful set of gait features able to assess walking performance poststroke.

Objective. Based on the findings presented in Chapter 5, showing that muscle synergies during cycling can be used to assess functional motor impairments in iSCI patients, the purpose of this research was to test whether the combination of a small set of gait features (kinematics, kinetics and spatiotemporal parameters) and the analysis of muscle synergies can better predict walking function poststroke than Fugl-Meyer Assessment (FMA), which is one of the most used quantitative measures of motor impairment.

Methods. Nine poststroke hemiparetic patients were assessed with FMA and 3D gait analysis, in order to extract synergies outcomes, kinematic, kinetic and spatiotemporal variables bilaterally during walking.

Results. Stepwise multiple regression analyses using parameters from the non-paretic side indicated that early time of peak knee flexion, high VAF_{total} values and prolonged stance phase predicted impaired walking function. At the same time, stepwise multiple regression analyses using parameters from the paretic side indicated that

reduced propulsion force, range of hip flexion and also prolonged stance phase predicted impaired walking function. All these predictors have shown better prediction of walking function than FMA.

Conclusions. Therapies focused on improving these predictors may improve functional gait. Specifically, therapies targeted to reduce spasticity, as well as to sculpt plantarflexion or dorsiflexion muscle synergies will improve the independent activation of ankle and knee muscles, therefore improving poststroke walking performance.

7.1 Introduction

The occurrence of a stroke may result in a series of motor impairments contralateral to the brain lesion (DeLisa and States, 1998), such as muscle weakness or hemiparesis (Ramsay et al., 2014). Clinical assessment of motor impairments in post-stroke patients is usually quantified by the Fugl-Meyer Assessment (FMA) (Bowden et al., 2010), which can be divided into upper-extremity (FMA-UE) and lower-extremity (FMA-LE). FMA-LE may be used for prognosis and to quantify the results of a given therapy. This test focuses on isolated voluntary tasks, which are not always representative of the walking performance. For instance, walking is a complex motor behavior, controlled by spinal cord, in coordination with both supraspinal control and peripheral afferent input (Bowden et al., 2010). As such, FMA may have limited relevance to assess walking performance. Duncan et al. (1983) have recommended using FMA in conjunction with other assessments (e.g., activities of daily living, gait, and perceptual motor skills), allowing therapists to plan appropriate treatment programs and measure progress.

Despite the usefulness of FMA to assess motor recovery, small improvements in neurological and biomechanical mechanisms may be not detected by this scale. The latest researches on pathological conditions strongly recommend gait analysis to adequately assess and follow-up the patient and to support clinical decision on the best treatment (Wren et al., 2009). Gait analysis systems usually provide a complete description of the main biomechanical features of walking, as well as the neuromuscular state. However, it is difficult to interpret the typical large amount of data produced, favoring the use of the classical clinical scales. Therefore, several gait summary scales have been proposed to quantify the degree of deviation from normal gait (Cimolin and Galli, 2014). The major goal of rehabilitation should not be a complete normalization of gait (Andrés et al., 2013), but an increase of functionality and improvement of walking performance (and not clinical scales). To achieve that goal, it is necessary to treat some features of gait that will improve walking performance, *i.e.*, some variables that predict walking performance.

Experimental evidences have shown that the synergistic control is visibly affected in poststroke patients (Clark et al., 2010) (Cheung et al., 2012) (Gizzi et al., 2011). Hence, the analysis of muscles synergies has gained relevance as a tool to describe the neuromuscular coordination during the execution of multi-limb movements. Compared to the FMA, the analysis of muscle synergies seems to be a superior predictor of walking performance (Clark et al., 2010) (Bowden et al., 2010), especially in the case of patients with poor intermuscular coordination. According to Routson et al. (2013), the combination of the analysis of the synergistic muscle control with the application of functional metrics could represent the key step toward a better quantitative assessment of stroke-related diseases.

7.2 Goals

The main goal of this Chapter is to test the hypothesis that the combination of muscle synergies analysis and a small set of biomechanical features (gait kinematics, kinetics and spatiotemporal parameters) will improve the functional assessment of walking performance poststroke. Specifically, it is hypothesized that the new set of features will provide more meaningful information about walking function than the one provided by FMA.

7.3 Materials and Methods

7.3.1 Subjects

Nine hemiparetic patients with stroke (Table 7.1) were recruited by the Movement Analysis, Ergonomics, Biomechanics and Motor Control Laboratory of Rey Juan Carlos University. All patients provided written informed consent to participate in this study (see Appendix E.3). The local Ethics Committee (EC) approved this study. Inclusion criteria were: to present moderate disability (Rankin scale ≤ 3); Mini-mental state examination (MMSE) score > 24); NIH Stroke Scale (NIHSS) score < 20 . Exclusion criteria were: to present severe cognitive impairment, mixed aphasia, unilateral spatial neglect, important visual deficits, joint stiffness (irreducible contractures and arthrodesis), convulsive crisis and alterations of the behavior (no cooperation).

TABLE 7.1: Individual description of nine hemiparetic stroke subjects.

Patient ID	Age, yrs	Gender	Height, m	Weight, Kg	Post, ms	Type of lesion, Affected hemisphere	FAC	FMA-LE	Side affected
01	41	M	1.76	71.5	158	Hem, R	5	68	L
02	76	M	1.69	64.0	18	Hem, L	4	63	R
03	60	F	1.62	101.8	18	Isch, L	5	81	R
04	54	M	1.79	83.0	55	Isch, R	5	70	L
05	55	M	1.78	75.7	119	Hem, L	5	67	R
06	54	F	1.59	61.3	192	Isch, R	5	66	L
07	53	F	1.55	48.2	60	Isch, L	5	75	R
08	40	M	1.68	64.8	6	Isch, R	5	77	L
09	44	M	1.69	93.7	54	Isch, R	4	45	L

M indicates male; F, female; Post ms, months poststroke; Hem, Hemorrhagic; Isch, Ischemic; FAC, Functional Ambulation Categories scores; FMA-LE, Fugl-Meyer assessment for lower extremity; L, left; R, right.

7.3.2 Experimental protocol and data collection

Patients underwent two different types of assessment: clinical evaluation and 3D gait analysis.

Clinical evaluation consisted on the Fugl-Meyer assessment for lower extremity (FMA-LE). This assessment method is a cumulative numerical scoring system composed by four domains: motor function of the lower extremity (maximum score = 34 points), sensory function (maximum of 12 points), joint range of motion (maximum of 20 points) and joint pain (maximum of 20 points), resulting in a maximum motor score of 86 points for the lower extremity (Fugl-Meyer et al., 1975). In order to minimize inter-rater variability, one physiatrist carried out the entire assessment procedure.

Gait analysis was performed using Vicon Motion Systems (Oxford Metrics, Oxford, UK) and three 3D AMTI force platforms (Watertown, USA) embedded in the walking path, which allowed the study of ground reaction forces. An acquisition frequency of 100 Hz was used to record data with Vicon and from force platforms. Each patient completed 10 walking trials, at their comfortable speed, on a plain path of 11-m length (see Figure 7.1). A 30-sec rest between trials was included to avoid muscle fatigue. Since it has been suggested to remove from the analysis the first three trials of walking in poststroke patients (in order to exclude the adaptation phase) (Boudarham et al., 2013), just the last six trials were analyzed. Sixteen special lightweight surface markers were attached on the skin over standardized landmarks on the lower limbs and trunk, according to the biomechanical model of Kadaba et al. (1990) and Davis et al. (1991).

Furthermore, patients wore a harness for body weight support attached to a moving rail to ensure stability and safety during walking. The percentage of body weight support was set to the minimum value that allowed the patient to walk independently, with no external support.



FIGURE 7.1: Poststroke patient walking during one trial.

Surface electromyography (sEMG) was recorded with the Cometa ZeroWire EMG system (Milan, Italy) from the following 11 muscles, bilaterally: erector spinae, gluteus maximus, gluteus medius, tensor fasciae latae, adductor longus, rectus femoris, vastus lateralis, biceps femoris, gastrocnemius medialis, soleus and tibialis anterior. The EMG amplifier had an acquisition frequency of 1,000 Hz. SENIAM recommendations for sEMG recording procedures were performed (Hermens et al., 1999). Synchronization between EMG and Vicon data was done automatically by the VICON MXControl Unit.

For each subject, each recording session lasted approximately 20 minutes, in addition to the donning and doffing of the EMG recording setup and the markers for 3D gait analysis (15-30 minutes, depending on the subject and level of impairment).

Data were analyzed offline with MATLAB R2011a (The MathWorks, Natick, MA) and IBM SPSS Statistics 20 software (IBM).

7.3.3 Data analysis

Heel strike events were determined by visual inspection after analyzing Vicon data. Each walking stride started at each heel strike event of the corresponding leg. At least two valid strides were obtained for each trial. For each subject, raw data corresponding to those valid trials were concatenated. The ten central strides were further selected for analysis (Barroso et al., 2014).

7.3.3.1 Analysis of muscle synergies

Using SynergiesLAB (see Appendix C), the selected raw EMG signals from each patient were high-pass filtered at 20 Hz, demeaned, rectified, and smoothed with a low-pass filter at 5 Hz, resulting in the EMG envelopes, according to the procedures performed by Clark et al. (2010) and Hug et al. (2010).

EMG envelopes from each muscle were then normalized by the average of the maximum of each of the ten strides, and resampled at each 1% of the walking stride. For each participant, normalized EMG envelopes were combined into an $m \times t$ matrix (EMG_0), where m is the number of muscles (eleven in this case) and t is the time base ($t = \text{no. of cycles (10) x 100}$).

Muscle synergy vectors and the corresponding activation coefficients were extracted using the NNMF algorithm in SynergiesLAB (see equation 2.1) (Lee and Seung, 1999). For each EMG_0 , the NNMF algorithm was run three times, considering as input 3 to 5 synergies ($n = 3, 4, 5$). In order to avoid local minima, for each run, the NNMF was repeated 40 times and the repetition with the lowest reconstruction error was selected.

Each muscle synergy vector (column of matrix W) was normalized by the maximum value of the muscle in the synergy to which they belong, as performed by Hug et al. (2010) and Muceli et al. (2010). Then, the corresponding activation coefficients were scaled by the same quantity, as done by De Marchis et al. (2012).

The similarity between EMG_0 and EMG_r was calculated based on two indicators: the variability accounted for (VAF_{total} , see Equation 4.1) (Clark et al., 2010) and the coefficient of determination (r^2) (Torres-Oviedo et al., 2006). The coefficient of determination was calculated by the MATLAB function 'rsquare'.

$VAF_{\text{total}} \geq 90\%$ was the criterion used to determine the optimal number of muscle synergies for each side and patient (Routson et al., 2014).

7.3.3.2 Kinematics

Raw kinematic data of each side and subject were low-pass filtered at 6 Hz (Allen and Neptune, 2012). From the mean profile over the ten selected strides (Bowden et al., 2010), it was possible to extract the following joint kinematic parameters usually used to describe gait (Schutte et al., 2000) (Moreno et al., 2013) (Bonnyaud et al., 2014) (Roche et al., 2015):

- Hip joint parameters: peak flexion ($^{\circ}$), peak extension ($^{\circ}$), range of flexion ($^{\circ}$), pre-swing angle (min) ($^{\circ}$), peak of abduction in swing ($^{\circ}$), range of abduction ($^{\circ}$), mean rotation in stance ($^{\circ}$);
- Knee joint parameters: flexion at initial contact ($^{\circ}$), time of peak flexion (% gait cycle), peak flexion ($^{\circ}$), time of peak extension (% gait cycle), peak extension ($^{\circ}$), range of flexion ($^{\circ}$);
- Ankle joint parameters: peak dorsiflexion during stance ($^{\circ}$), peak dorsiflexion during swing ($^{\circ}$), peak dorsiflexion ($^{\circ}$), peak plantarflexion ($^{\circ}$), range of flexion ($^{\circ}$);
- Pelvis joint parameters: mean tilt ($^{\circ}$), range of tilt ($^{\circ}$), mean rotation ($^{\circ}$);

7.3.3.3 Spatio-temporal parameters

Based on the 3D position of the foot markers, it was possible to extract the mean of the following spatio-temporal parameters (Schutte et al., 2000) (Bowden et al., 2010) (Boudarham et al., 2013) (Bonnyaud et al., 2014) (Arnold et al., 2014): speed (m/s), stride length (m), stride duration (s), strides/minute, step length (m), step width (m); step duration (s), cadence (steps/minute), % stance, duration of stance (s), duration of single support (s), % single support, duration of double support (s).

7.3.3.4 Kinetics

Raw data from the force platforms were low-pass filtered at 20 Hz and normalized by subject's weight (Bowden et al., 2010). The mean over the six selected trials was calculated and the following parameters were extracted (Bonnyaud et al., 2014) (Bowden et al., 2010): vertical ground reaction force (GRF) during single support phase (N/Kg), peak of propulsion (N/Kg), peak of braking (N/Kg), paretic propulsion, peak medio-lateral force (N/Kg).

7.3.4 Statistical analysis

Paired Student’s *t*-tests were performed to test significant differences between paretic and non-paretic sides on the following variables: quality of reconstruction indicators, kinematic, spatio-temporal and kinetic variables. FMA-LE values were correlated with the walking performance indicators using non-parametric Spearman’s correlations. As indicators of walking performance, the following indicators were used: speed (Bowden et al., 2010); percentage of stance of the paretic limb; paretic propulsion (PP), *i.e.*, percentage of total propulsion force performed by the paretic leg (Bowden et al., 2010); and the paretic step ratio (PSR), *i.e.*, the percentage of the stride length performed by the paretic leg (Bowden et al., 2010). Statistical significance was set by a *p*-value of 0.05.

Stepwise multiple regression analyses were carried out to identify variables that most correlated with walking performance, as done in Section 5.3.5. A significance of $p < 0.05$ was used, as performed by Roche et al. (2015).

As input of the model (independent variables), all the measured variables were considered, *i.e.*, quality of reconstruction indicators, kinematic, spatio-temporal and kinetic variables. To minimize the number of independent variables, a preliminary analysis was performed, using a liner regression between each considered independent variable and the walking performance indicator, selecting as input for the multiple regression analysis only those with a p -value ≤ 0.05 , as represented in Figure 7.2.

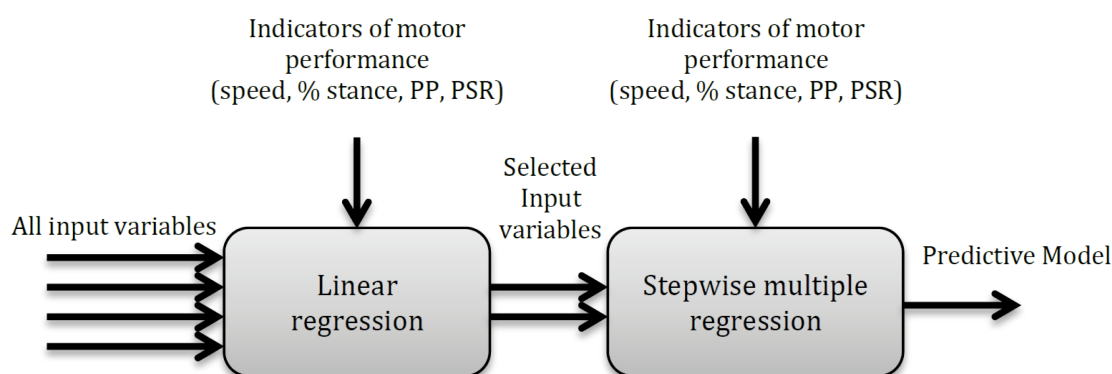


FIGURE 7.2: Schematic representation of the steps included in the stepwise multiple regressions to predict walking performance indicators.

7.4 Results

7.4.1 Synergistic control of gait

Fewer muscle synergies were needed to account for the whole muscle activity of the 11 analyzed muscles in the paretic side (3.67 ± 0.44) than the non-paretic side (4.11 ± 0.59). Three paretic sides required three synergies, while six paretic sides required four synergies. The non-paretic side demonstrated a more heterogeneous behavior: three synergies were required in two patients, four synergies in four patients, and five synergies in the remaining three patients to obtain $\text{VAF}_{\text{total}}$ values $\geq 90\%$.

For all the subjects and sides, the quality of reconstruction indicators ($\text{VAF}_{\text{total}}$ and r^2) were significantly lower in the non-paretic side compared to the paretic side (see Figure 7.3 and Table 7.2) (p -values < 0.05).

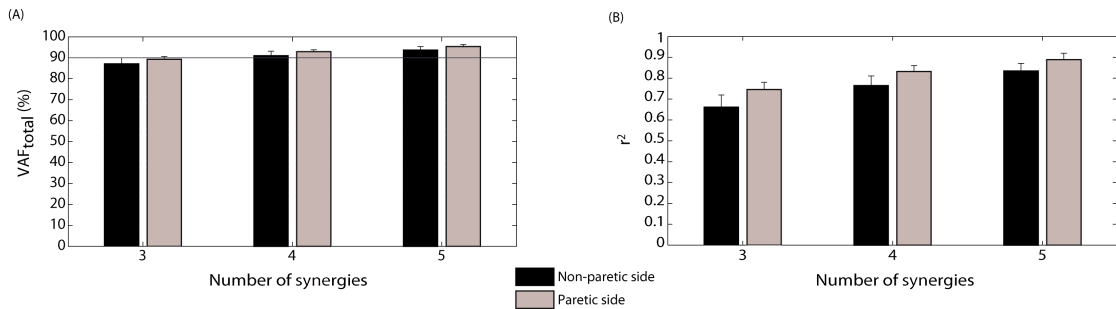


FIGURE 7.3: Variability accounted for ($\text{VAF}_{\text{total}}$) (A) and coefficient of determination (r^2) (B) according to the number of synergies, for both paretic and non-paretic sides. Values are given in mean \pm SD. These reconstruction goodness indexes were calculated after running the NMF algorithm to reconstruct a set of 11 EMG envelopes in a group of 9 poststroke patients. The quality of reconstruction of EMG data was considered good for values of $\text{VAF}_{\text{total}} \geq 90\%$. A $\text{VAF}_{\text{total}}$ value of 100% and a r^2 value of 1 indicate perfect reconstruction of the EMG set.

7.4.2 Biomechanical differences between sides

Five kinematic variables (time of peak knee flexion, peak knee flexion, range of knee flexion, range of ankle flexion and mean pelvic rotation) showed significant differences between paretic and non-paretic sides ($p < 0.05$), with the paretic side presenting lower values in all cases, as detailed in Table 7.3 and represented in Figure 7.4.

Significant differences between paretic and non-paretic sides were also found for six spatio-temporal variables (step duration, cadence, % stance, duration of stance, duration of single support and % single support) (see Table 7.3 and Figure 7.5), presenting all of these variables lower values in the paretic side, except for step duration.

TABLE 7.2: Comparison of quality of reconstruction indicators ($\text{VAF}_{\text{total}}$ and r^2) between paretic and non-paretic side, when using 3 to 5 synergies. Values are given in mean \pm SD.

Quality of reconstruction indicators		Mean \pm SD	p -value
$\text{VAF}_{\text{total}}$ with 3 synergies	paretic side	89.33 \pm 1.4	0.014*
	non-paretic side	87.00 \pm 2.8	
$\text{VAF}_{\text{total}}$ with 4 synergies	paretic side	93.00 \pm 0.8	0.012*
	non-paretic side	91.00 \pm 2.1	
$\text{VAF}_{\text{total}}$ with 5 synergies	paretic side	95.33 \pm 1.0	0.017*
	non-paretic side	93.67 \pm 1.9	
r^2 with 3 synergies	paretic side	0.75 \pm 0.04	0.005**
	non-paretic side	0.66 \pm 0.06	
r^2 with 4 synergies	paretic side	0.83 \pm 0.03	0.004**
	non-paretic side	0.77 \pm 0.05	
r^2 with 5 synergies	paretic side	0.89 \pm 0.03	0.005**
	non-paretic side	0.83 \pm 0.04	

* Values are significantly different between sides ($p < 0.05$). ** Values are significantly different between sides ($p < 0.01$). For those indicators with significant differences between sides, the side with higher values is evidenced in bold.

At last, significant differences were found between sides for two kinetic variables (peak of propulsion and peak medio-lateral force) (see Table 7.3 and Figure 7.5).

7.4.3 Correlation between FMA-LE and walking performance indicators

Patients walked at a speed of 0.52 ± 0.18 m/s, with stance phase of the paretic limb lasting $62.23 \pm 4.56\%$ of the gait cycle, a paretic propulsion ratio (PP) of 0.24 ± 0.14 , and a paretic step ratio (PSR) of 0.51 ± 0.05 . Except for PSR, the other three walking performance indicators presented significant correlations ($p < 0.01$) among themselves.

Spearman's correlation showed that, of the four motor indicators, only PP correlated significantly ($p = 0.045$) with FMA-LE (see Table 7.4). Correlation between FMA-LE and speed almost reached significance ($p = 0.088$).

7.4.4 Stepwise regressions to predict speed

When analyzing variables from the non-paretic side, the stepwise linear regression showed that time of peak knee flexion and $\text{VAF}_{\text{total}}$ with 4 synergies accounted together for approximately 91% of the variance of walking speed ($R^2 = 0.913$, Adjusted $R^2 = 0.885$) and were statistically significant ($F = 31.64$, $p = 0.001$). Resulting predictive model is:

TABLE 7.3: Comparison of biomechanical indicators that showed significant differences between paretic and non-paretic side. Values are given in mean \pm SD.

Variables with significant differences between sides		Mean \pm SD	<i>p</i> -value
Kinematics			
Time of peak knee flexion (% gait cycle)	paretic side	70.34 \pm 4.67	
	non-paretic side	81.15 \pm 4.66	<0.001**
Peak knee flexion ($^{\circ}$)	paretic side	34.90 \pm 10.94	
	non-paretic side	62.26 \pm 9.79	<0.001**
Range of knee flexion ($^{\circ}$)	paretic side	39.45 \pm 12.60	
	non-paretic side	60.51 \pm 10.12	<0.001**
Range of ankle flexion ($^{\circ}$)	paretic side	22.15 \pm 5.41	
	non-paretic side	26.02 \pm 2.65	0.018*
Mean pelvic rotation ($^{\circ}$)	paretic side	-5.9711 \pm 4.14	
	non-paretic side	5.4511 \pm 4.11	0.003**
Spatio-temporal			
Step duration (s)	paretic side	0.94 \pm 0.18	
	non-paretic side	0.64 \pm 0.08	<0.001**
Cadence (steps/minute)	paretic side	75.30 \pm 11.67	
	non-paretic side	80.55 \pm 13.00	<0.001**
% Stance	paretic side	62.23 \pm 4.56	
	non-paretic side	74.38 \pm 7.44	<0.001**
Duration of stance (s)	paretic side	0.99 \pm 0.22	
	non-paretic side	1.19 \pm 0.30	<0.001**
Single support (s)	paretic side	0.33 \pm 0.12	
	non-paretic side	0.57 \pm 0.08	0.001**
% Single support	paretic side	35.25 \pm 16.16	
	non-paretic side	50.41 \pm 12.71	0.013*
Kinetics			
Peak of propulsion (N/Kg)	paretic side	0.49 \pm 0.31	
	non-paretic side	0.94 \pm 0.31	<0.001**
Peak medio-lateral force (N/Kg)	paretic side	0.78 \pm 0.17	
	non-paretic side	0.65 \pm 0.14	0.031*

* Values are significantly different between sides ($p < 0.05$). ** Values are significantly different between sides ($p < 0.01$). For those indicators with significant differences between sides, the side with higher values is evidenced in bold.

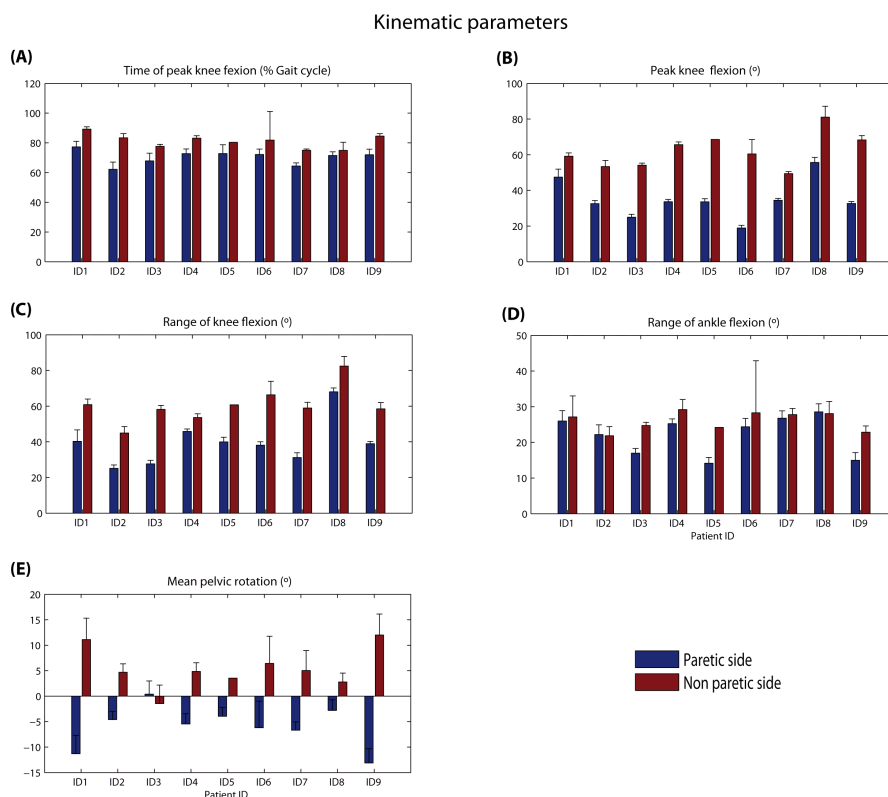


FIGURE 7.4: Kinematic variables that showed significant differences between paretic and non-paretic side.

TABLE 7.4: Spearman’s correlations between Fugl-Meyer assessment for lower extremity (FMA-LE) and walking performance indicators.

	Speed	% Stance paretic side	PP	PSR
	$r = 0.600$	$r = -0.217$	$r = \mathbf{0.678^*}$	$r = -0.185$
FMA-LE	$p = 0.088$	$p = 0.576$	$p = \mathbf{0.045}$	$p = 0.634$

PP, paretic propulsion; PSR, paretic step ratio. * Correlation is significant at the 0.05 level.

$$\text{Speed} = 7.785 - 0.048 \cdot (\text{time of peak non-paretic knee flexion}) - 3.672 \cdot (\text{non-paretic VAF}_{\text{total}} \text{ with 4 synergies})$$

When analyzing variables from the paretic side, peak of propulsion and range of hip flexion were statistically significant ($F = 77.32$, $p < 0.001$) and accounted for approximately 96% of the variance of walking speed ($R^2 = 0.963$, Adjusted $R^2 = 0.950$). Resulting model is:

$$\text{Speed} = -0.079 + 0.443 \cdot (\text{peak of paretic propulsion}) + 0.011 \cdot (\text{range of paretic hip flexion})$$

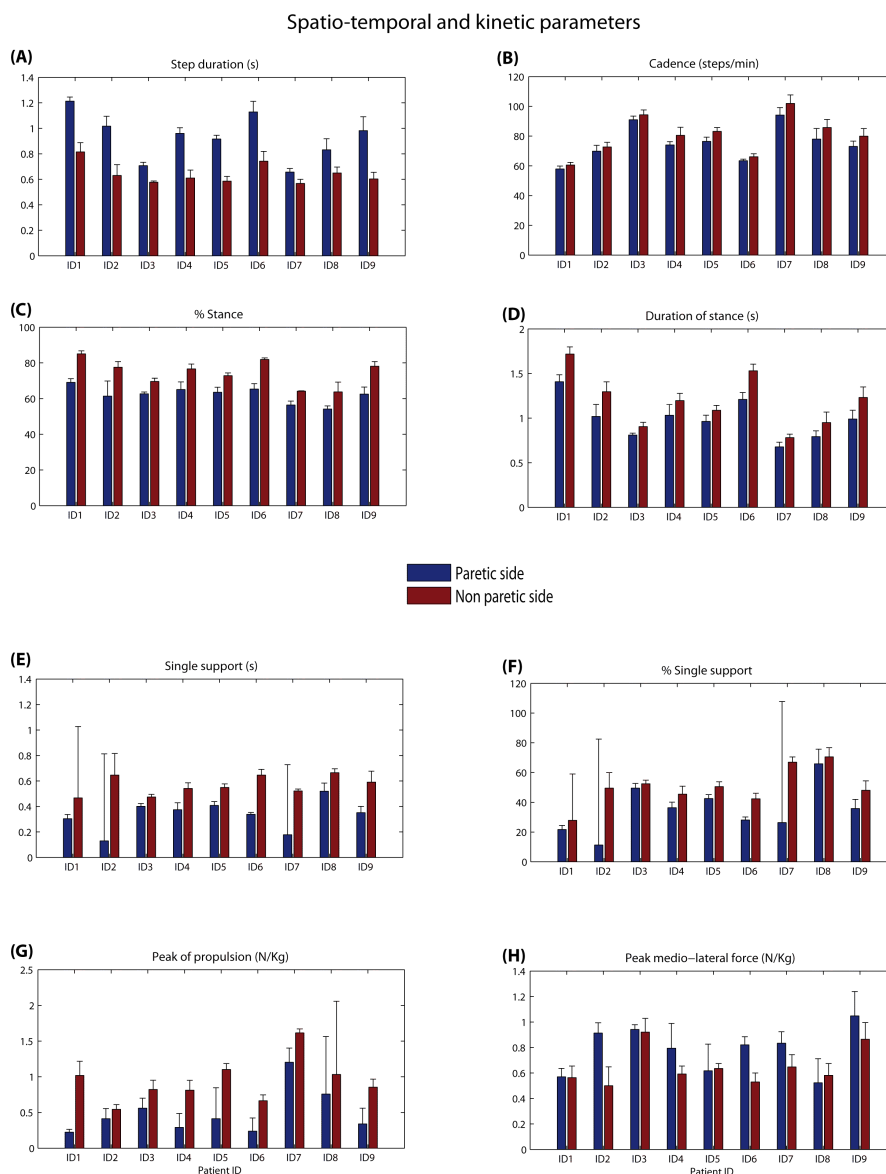


FIGURE 7.5: Spatio-temporal and kinetic variables that showed significant differences between paretic and non-paretic side.

7.4.5 Stepwise regressions to predict % stance of the paretic side

When analyzing variables from the non-paretic side, only the time of peak knee flexion was statistically significant ($F = 18.29$, $p = 0.004$) and accounted for approximately 72% of the variance of % stance of the paretic side ($R^2 = 0.723$, Adjusted $R^2 = 0.684$) (no other variables reached significance). Resulting model is:

$$\% \text{ stance of the paretic side} = -5.169 + 0.831 \cdot (\text{time of peak non-paretic knee flexion})$$

When analyzing variables from the paretic side, only the peak of propulsion was statistically significant ($F = 15.79$, $p = 0.005$) and could account for approximately 69% of the variance of % stance of the paretic side ($R^2 = 0.693$, Adjusted $R^2 = 0.649$) (no other variables reached significance). Resulting model is:

$$\% \text{ stance of the paretic side} = 68.171 - 12.060 \cdot (\text{peak of paretic propulsion})$$

7.4.6 Stepwise regressions to predict paretic propulsion

Most of the spatio-temporal variables from both non-paretic and paretic side correlated significantly with PP, when doing the preliminary analysis using linear regressions to predict PP. Therefore, the fit of the model was perfect and included several independent variables. This suggests that most of the chosen spatio-temporal variables are redundant, being the duration of stance of each side the one that presented the most significant correlation ($p < 0.001$, and negative correlation for both sides) with PP.

7.4.7 Stepwise regressions to predict paretic step ratio

When analyzing variables from the non-paretic side, none of the variables could predict paretic step ratio. On the other hand, when analyzing variables from the paretic side, peak hip flexion was the only statistically significant variable ($F = 6.21$, $p = 0.041$) and accounted for approximately 47% of the variance of PP ($R^2 = 0.470$, Adjusted $R^2 = 0.394$). Nevertheless, caution should be taken with these significance values. Resulting model is:

$$\text{PSR} = 0.616 - 0.003 \cdot (\text{Peak hip flexion})$$

7.5 Discussion

From the initial dataset of biomechanical features and muscle synergies outcomes assessed in this Chapter, it was possible to find a small set of variables that could predict walking performance. Those variables predicted the resulting walking speed, % stance of the paretic side and paretic propulsion (PP), and may be used to drive customized rehabilitation therapies. For instance, when assessing the non-paretic side, early time of peak knee flexion, high $\text{VAF}_{\text{total}}$ values and prolonged stance phase predicted impaired walking performance. When assessing the paretic side, reduced propulsion force, range of hip flexion and also prolonged stance phase predicted impaired walking performance.

It has been referred that poststroke patients may present decreased knee flexion as a result of increased ankle plantarflexion or quadriceps spasticity (DeLisa and States, 1998). Other patients may present reduced planterflexion and produce compensatory strategies based on reducing range of hip flexion (Roche et al., 2015). If patients walk with the excessive dorsiflexion, they will also present decreased propulsion. Taking the aforementioned predictors together, it seems that therapies targeted to reduce spasticity, as well as to sculpt plantarflexion or dorsiflexion muscle synergies (with FastFES, for example) (Ting et al., 2015) will improve the independent activation of ankle and knee muscles, therefore improving walking performance.

The number of muscle synergies is usually determined based on a reconstruction quality criterion (VAF_{total} or r^2) (Clark et al., 2010). The results presented in this Chapter showed that both reconstruction quality indicators are also valid to assess the neural control of both sides in poststroke patients. Quality of reconstruction indicators assessed in this study were significantly lower in the non-paretic side if compared with the paretic side, in accordance with the results reported by Clark et al. (2010). The results of these reconstruction quality indicators suggest less complexity in the patterned activity of the paretic limb during walking (Clark et al., 2010). The identification of less muscle synergies is associated with lower independence among the activation patterns of each muscle, associated with coupling of muscles across the limb or a possible merging of existing muscle synergies (Cheung et al., 2012). These impairments in muscle coordination result in walking deficits and asymmetry highlighted by kinematic, spatio-temporal and kinetic patterns.

As indicators of walking performance, the following indicators were used: speed, percentage of stance of the paretic limb, paretic propulsion (PP) and paretic step ratio (PSR). Walking speed is an important indicator of poststroke gait performance (Verma et al., 2012) (Clark et al., 2010). Healthy population usually walks with a mean speed of 1.3 m/s, while poststroke patients walk within the range from 0.23 to 0.73 m/s (Verma et al., 2012), which is in accordance with the values obtained in this study (0.52 ± 0.18 m/s). PP has been shown to be a crucial predictor of gait performance (Bowden et al., 2010) (Clark et al., 2010), with healthy population presenting values near to 0.5 (similar propulsion forces from both limbs). Poststroke patients assessed in this study presented PP values of 0.24 ± 0.14 , which indicates decreased propulsion executed by the paretic limb. Due to compensation mechanisms, patients presented reduced stance phase of the paretic limb in comparison with the non-paretic limb. PSR has been also proposed as a metric to assess walking performance (Bowden et al., 2010), with healthy population presenting values near to 0.5 (similar step length from both limbs). Poststroke patients assessed in this study presented PSR values of 0.51 ± 0.05 , which cast doubt about the usefulness of this metric to assess impaired gait. That

explains why PSR did not correlate significantly with the other three motor indicators. In fact, [Verma et al. \(2012\)](#) referred that different studies have reported that poststroke patients walk with either relatively longer paretic or non-paretic step length, which was the case of the population assessed in this study. The reasons for that have not been explained ([Verma et al., 2012](#)). These results suggest that walking performance poststroke may be assessed by looking at walking speed, PP and % stance of the paretic side.

From all the four motor indicators, only PP correlated significantly with FMA-LE. One possible reason for the low correlation between FMA-LE and the other walking performance indicators of the patients assessed in this study is the good recovery poststroke presented by them (minimum of 66 points out of 86 in the FMA-LE scale, except for one patient; FAC = 4,5). FMA-LE seems to present some restrictions to assess poststroke patients with improved function, despite presenting walking asymmetry. As referred by [Bowden et al. \(2010\)](#) and [Clark et al. \(2010\)](#), the number of muscle synergies seems to be a better predictor of walking performance than the FMA-LE. The explanation for this is that muscle synergies analysis are based on data collected from walking, while the tasks assess on FMA-LE are not similar to those performed while walking ([Bowden et al., 2010](#)).

At last, FMA-LE does not assess differences between sides. As suggested by the stepwise multiple regressions, both limbs present important features that can predict walking performance. Different compensation strategies may be applied by poststroke patients to improve functional performance, ranging from improved mechanical output from the paretic limb, or increased reliance on mechanical output from the non-paretic limb ([Routson et al., 2013](#)).

In the future, these experiments might be replicated, by assessing a wider sample of poststroke patients, with different levels of walking impairments, and compare the results with a control group of healthy subjects.

Concluding Remarks

Research on the assessment and management of recovery after neural damage is a constantly evolving area that today requires an early convergence of clinical and engineering perspectives. It is of utmost importance to understand specific patient's impairments in order to prescribe effective customized treatments at the very early stage of rehabilitation ([Molina Rueda et al., 2012](#)). In that sense, the main goal of this Ph.D. Thesis was to generate meaningful quantitative metrics to assess sensorimotor impairments of patients that suffered a stroke or an incomplete spinal cord injury (iSCI), which can complement current clinical assessment procedures. To achieve this main goal, four distinct but complementary studies were performed. For each study, metrics based on the analysis of muscle synergies, on the biomechanics of walking, or a combination of both, were used.

The analysis of biomechanics of walking can provide quantitative description and disclose impairments underlying abnormal walking. This can be used to extract important information to select a task-oriented rehabilitation approach that might enhance therapeutic response, which cannot be provided by clinical evaluation alone ([Nadeau et al., 2011](#)).

On the other hand, as the improvements on the design of future motor interventions should be based on the deep understanding of the neural function and plasticity, the analysis of muscle synergies has great potential for the assessment of neuromotor diseases, offering the clinician a simplified view on the neural structure underlying motor behaviors ([Bowden et al., 2010](#)). The analysis of muscle synergies can also provide valuable data to quantify spasticity. According to the review presented by [Rosa et al. \(2014\)](#), it is not possible to recommend the most appropriate way to quantify or access muscle co-activation, which is one of the spasticity symptoms. Given the potential of

co-activation as a target for gait rehabilitation, novel and recognized methods need to arise to quantitatively assess muscle co-activation. In that sense, the analysis of muscle synergies can provide valuable data. However, the analysis of muscles synergies has not been recommended as an outcome measure of motor performance neither spasticity yet, mainly because of the need for EMG data and complex mathematical analysis. Nevertheless, this tool might be integrated in clinical diagnosis, because it may help clinicians to understand gait motor control in patients that suffered neural damage (Bowden et al., 2010).

In summary, the use of quantitative metrics based on EMG and biomechanical features gave valuable information on the motor recovery mechanisms as well as the performance after neural damage in a population of patients that suffered a stroke or a SCI, which was the main goal of this Ph.D. Thesis. These analyses may complement current assessment procedures.

The next section present the main conclusions of each of the four individual studies performed along this research work.

8.1 General Conclusions

8.1.1 Study 1

Study 1 presented possible arrangements of existing muscle synergies which, when adequately combined, could result in the typical muscular patterns verified at walking and cycling in healthy controls. The results presented in this study provide evidences in line with the hypothesis of a neural meaning of muscle synergies to explain motor control in walking and cycling.

Dimensionality of motor control in cycling seems to be reduced if compared with walking. Four synergies from walking could explain most of the EMG variability of cycling trials and also be merged to cope with the required biomechanical demand of this motor task.

The main discovery of this study was that cycling and walking share common neuromuscular mechanisms. This evidence supported the use of cycling as a novel tool to assess walking in people with impaired neuromotor control.

8.1.2 Study 2

Study 2 was an explorative study that tested the ability of muscle synergy analysis during cycling movements, to quantitatively assess walking functionality, as well as to quantify hypertonia and spasms, which are important clinical conditions of spasticity present in iSCI patients (Bennett, 2008).

The main goal was to characterize the synergistic control of iSCI patients during cycling at different cadences. Results provided supporting evidences for the hypothesis that iSCI patients preserve synergistic control of muscles during cycling, evidence that was not reported previously in the literature. However, muscle synergies composition of more impaired patients was less similar to the healthy controls if compared with the less impaired iSCI patients.

As a secondary goal, it was found that the analysis of muscle synergies during cycling can be used for a detailed quantitative assessment of gait performance and symptoms of spasticity. In particular, reconstruction goodness indexes presented significant correlation with gait performance scales (TUG, 10MWT and WISCI II). Additionally, metrics based on the similarity between the healthy and affected synergies correlated with spasticity symptoms measured by Penn, MAS, and SCATS scales. The analysis of muscle synergies can, therefore, complement current assessment procedures performed in the clinical setting.

8.1.3 Study 3

Study 3 proposed the use of a new criterion to determine the most affected side in iSCI patients presenting similar LEMS scores for each side. This criterion is based on the cadence achieved by each side independently, according to the time spent to perform a step, with the most affected side being the one that needed more time. This criterion seems to be robust and useful to determine the most affected side in iSCI patients, as further differences were found between sides.

Incomplete SCI patients presented significant less muscle synergies in the most affected side when compared with the healthy group. Thus, the analysis of muscle synergies might be explored to detect differences between the two sides in patients with iSCI. Specifically, VAF_{total} can be used as neurophysiological metric to assess and monitor patients' condition through their specific gait rehabilitation program. However, the biomechanical analysis was more effective to detect differences between most and less affect side of iSCI patients than the analysis of muscle synergies, maybe due to the reduced number of muscles assessed in this study.

The results presented in this study support the importance of studying the bilateral control of lower limb functions in iSCI patients, as well as to combine biomechanical features and the analysis of the synergistic muscle control.

8.1.4 Study 4

Study 4 tested whether the combination of a small set of gait features and the analysis of muscle synergies could better predict walking function poststroke than Fugl-Meyer Assessment (FMA), which is one of the most used quantitative measures of motor impairment. Although scales like FMA do not present administrative expenses, they might present inter-rater variability. In addition, the tasks assessed by this scale are not quite similar to those executed during walking. FMA is a global motor function measure. This study aimed to find a small set of variables that could provide quantitative and objective information about the patient's motor status.

First of all, results showed that fewer muscle synergies were needed to account for the whole muscle activity of the analyzed muscles in the paretic side than the non-paretic side, *i.e.*, the quality of reconstruction indicators ($\text{VAF}_{\text{total}}$ and r^2) were significantly lower in the non-paretic side compared to the paretic side. Additionally, some biomechanical variables also differentiated between the paretic and the non-paretic side.

Second, results showed that some parameters associated to the non-paretic side (early time of peak knee flexion, high $\text{VAF}_{\text{total}}$ values and prolonged stance phase) predicted impaired walking function. At the same time, some parameters associated to the paretic side (reduced propulsion force, range of hip flexion and also prolonged stance phase) predicted impaired walking function. All these predictors have shown better prediction of walking function than FMA.

Therapies focused on improving these predictors may improve functional gait. Specifically, therapies targeted to reduce spasticity, as well as to sculpt plantarflexion or dorsiflexion muscle synergies may improve the independent activation of ankle and knee muscles, therefore improving poststroke walking performance.

8.2 Future Work

The assessment methods and tools developed in this Ph.D. Thesis pave the way for future research in the fields of wearable sensing and exoskeletons technologies, as well as the clinical assessment of patients that suffered a stroke or an iSCI. Subsequent phases of work include:

- Performing longitudinal studies from the acute to the chronic phase of iSCI, in order to test the intra and inter-rater variability of the analysis of muscle synergies during pedaling as a tool for the assessment of walking functionality. This is of main importance to validate this approach for long term monitoring and assessment of different therapeutic interventions, as well as to predict motor recovery.
- Exploring the ability of muscle synergy analysis to detect hypertonia and spasms online, which can be used in robotic-assisted rehabilitation. In this type of rehabilitation, it is important to identify spastic muscle activity, in order to protect patients against mechanical injury.
- Exploring cycling exercise as a novel approach to promote the re-learning process of locomotion, based on biofeedback. The use of biofeedback in cycling is gaining relevance in clinical applications, as a way to improve motor performance. This potential application should be further investigated by appropriate longitudinal studies.
- Using IMUs as a substitute to traditional motion capture systems for the real time assessment of gait in poststroke patients. Therefore, important biomechanical features could be assessed outside the laboratory (e.g., gait tracking at home) and improve poststroke training. However, additional efforts are needed in order to use these devices outside the lab, including better data processing, reduction of donning/doffing time, as well as a reduction of sensors' size ([Rueterbories et al., 2010](#)).

8.3 Technical Contributions

As a demonstration of the scientific quality of the work performed along the Ph.D., the main technical contributions are listed below:

- Development of the user-friendly GUI SynergiesLAB, which allows for both qualitative and quantitative diagnosis of synergistic control. Particular requirements of the software tool have been gathered to permit a practical and intuitive use by users non-familiarized with Matlab, like therapists and doctors. Functions that allow to perform detailed analysis and comprehension of all the computational steps to process multiple EMG channels are described, from the raw EMG processing, up to the calculation of activation coefficients and synergy vectors. The software can be customized to a wide range of motor tasks, different algorithms for synergies extraction, filtering options and number of muscles.

- Study of the neurophysiologic meaning of muscle synergies, by analyzing different tasks (*e.g.*, walking, pedaling and standing) in different populations that suffered neural injuries, as stroke, incomplete spinal cord injured (iSCI) and cerebral palsy.
- Assessment of pathological gait in terms of biomechanics and neuromuscular performance in the above-mentioned populations.
- Training of movement with biofeedback that was designed based on targeted neuromuscular patterns. Preliminary tests are in progress using an ergometer to train cycling movements of poststroke and iSCI patients.
- Use of ergometers as novel clinical tools to assess motor performance and spasticity in iSCI patients.

8.4 Publications

The work described along this Thesis allowed the publication and preparation of the following book chapters, journal papers and conference papers.

Book chapters

- **Barroso F**, Torricelli D, Moreno JC. Recovery of Motor Function in Spinal Cord Injury, Chapter *Emerging Techniques for Assessment of Sensorimotor Impairments after Spinal Cord Injury*. (In Preparation). InTech. 2016.
- **Barroso F**, Figueiredo J. Nuevas tecnologías en Neurorehabilitación, Chapter *Introducción a la Bioingeniería*. (In Preparation). Elsevier, 2016.
- Torricelli D, **Barroso F**, Coscia M, Alessandro C, Lunardini F, Bravo-Esteban E, d'Avella A. Emerging Therapies in Neurorehabilitation II, Chapter *Muscle synergies in clinical practice: theoretical and practical implications*. Springer Berlin Heidelberg. 2015.
- **Barroso F**, Torricelli D, Pons JL. Control y Aprendizaje Motor, Chapter *Evaluación de las sinergias musculares: aplicación al análisis de la organización modular de la marcha*. Editorial Médica Panamericana, Madrid, 2015.
- **Barroso F**, Ruiz Bueno D, Gallego JA, Jaramillo P, Kilicarslan A. Emerging Therapies in Neurorehabilitation, Chapter *Surface EMG in Neurorehabilitation and Ergonomics: State of the Art and Future Perspectives*. Springer Berlin Heidelberg. 2013.

Papers in journals

- **Barroso FO**, Torricelli D, Molina Rueda F, Alguacil Diego IM, Cano De La Cuerda R, Santos C, Moreno JC, Miangolarra JC, Pons JL. (In Revision). Combining biomechanical and neuromuscular analysis to assess walking poststroke.
- Pérez-Nombela S, **Barroso FO**, Torricelli D, de los Reyes-Guzmán A, del-Ama AJ, Gómez-Soriano J, Pons JL, Gil-Agudo A. (In Revision). Modular control of gait after incomplete spinal cord injury: differences between sides.
- Bravo-Esteban E, Taylor J, **Barroso FO**, Piazza S, Torricelli D, Avila-Martin G, Galan-Arriero I, Pons JL, Gómez-Soriano J. (In Preparation). Tibialis Anterior muscle coherence during cycling in patients with spinal cord injury: a new scenario for the diagnosis of residual walking recovery.
- **Barroso FO**, Torricelli D, Bravo-Esteban E, Taylor J, Gómez-Soriano J, Santos C, Moreno JC and José L. Pons. Muscle synergies in cycling after incomplete spinal cord injury: correlation with clinical measures of motor function and spasticity. *Front. Hum. Neurosci.* 9: 706, 2015.
- **Barroso FO**, Torricelli D, Moreno JC, Taylor J, Gomez-Soriano J, Bravo-Esteban E, Piazza S, Santos C, Pons JL. Shared muscle synergies in human walking and cycling. *J Neurophysiol*, 2014.
- Moreno JC, **Barroso F**, Farina D, Gizzi L, Santos C, Molinari M, Pons JL. Effects of robotic guidance on the coordination of locomotion. *J Neuroeng Rehabil* 10: 79, 2013. (2014 Top 5 Cited Articles from JNER).

International Conferences

- Loma-Ossorio M, Torricelli D, Moral Saiz B, Parra Mussín E, Martín Lorenzo T, **Barroso F**, Martínez Caballero I, Lerma Lara S. Changes in Modular Control of Gait Following SEMLS in Children with Cerebral Palsy. 24th Annual Meeting of the European Society for Movement Analysis in Adults and Children, Heidelberg, Germany, 2015.
- Gómez-Soriano J, Bravo-Esteban E, **Barroso F**, Piazza S, Torricelli D, Serrano-Muñoz D, Taylor J. Tibialis Anterior Muscle Coherence During Cycling. A New Measure for Incomplete Spinal Cord Injury. International Neurorehabilitation Symposium (INRS 2015), 2015.

- Pérez-Nombela S, **Barroso F**, Torricelli D, Gómez Soriano J, Reyes-Guzmán A, del-Ama AJ, Pons JL, Gil-Agudo A. Modular Control of Gait in Incomplete Spinal Cord Injury: Preliminary Results. Proceedings of the 2nd International Conference on NeuroRehabilitation (ICNR2014): 601-610, 2014.
- **Barroso F**, Torricelli D, Moreno JC, Taylor J, Gómez-Soriano J, Bravo-Esteban E, Santos C, Pons JL. Similarity of muscle synergies in human walking and cycling: preliminary results. EMBC'13 - 35th Annual International Conference of the IEEE Engineering in Medicine and Biology Society: 6933-6936, 2013.
- Torricelli D, Pajaro M, Lerma S, Marquez E, Martinez I, **Barroso F**, Pons JL. Modular Control of Crouch Gait In Spastic Cerebral Palsy. MEDICON 2013 - XIII Mediterranean Conference on Medical and Biological Engineering and Computing, 2013.
- Piazza S, Torricelli D, Alguacil Diego IM, Cano De La Cuerda R, Molina Rueda F, **Barroso F**, Pons JL. Muscle synergies underlying voluntary anteroposterior sway movements. MEDICON 2013 - XIII Mediterranean Conference on Medical and Biological Engineering and Computing, 2013.
- Asín G, **Barroso F**, Moreno JC, Pons JL. Assessment of the Suitability of the Motorized Ankle-Foot Orthosis as a Diagnostic and Rehabilitation Tool for Gait. Neurotechnix 2013; Special Session: Sensory Fusion for Diagnostics and Neurorehabilitation - SensoryFusion 2013, 2013.
- **Barroso F**, Santos C, Pons JL, Moreno JC. Muscular activation and kinetic effects of robotic guidance force on human walking. Proceedings of the International Conference on NeuroRehabilitation (ICNR2012): 787-791, 2012.

Local Conferences

- Miangolarra Page JC, **Barroso F**, Cano de la Cuerda R, Carratalá Tejada M, Iglesias Giménez J, Torricelli D. Evaluación de las sinergias musculares implicadas en la marcha en pacientes con ictus. 53 Congreso Nacional de la Sociedad Española de Rehabilitación y Medicina Física - SERMEF 2015, 2015.
- Alguacil Diego IM, Cano de la Cuerda R, Molina Rueda F, Rivas Montero FM, **Barroso F**, Torricelli D. Evaluación de las sinergias musculares en el control postural mediolateral en sujetos con ictus vs sujetos sanos. 52 Congreso Nacional de la Sociedad Española de Rehabilitación y Medicina Física - SERMEF 2014, 2014.

-
- **Barroso F**, Santos C, Moreno JC. Influence of the robotic exoskeleton Lokomat on the control of human gait: an electromyographic and kinematic analysis. *IEEE 3rd Portuguese Bioengineering Meeting*, 2013.

Bibliography

- Allen, J. L. and R. R. Neptune (2012). Three-dimensional modular control of human walking. *J Biomech* 45, 2157–2163.
- Andrés, D. G., I. P. Valdeolivas, J. A. Martín, J. López, and E. R. Tamayo (2013). Relationship among gillette gait index parameters and gmfcs. *Gait & Posture* 38(1), S10—S11.
- Ansari, N. N., S. Naghdi, H. Moammeri, and S. Jalaie (2006). Ashworth scales are unreliable for the assessment of muscle spasticity. *Physiother Theory Pract* 22(3), 119–125.
- Arene, N. and J. Hidler (2009). Understanding motor impairment in the paretic lower limb after a stroke: a review of the literature. *Top Stroke Rehabil* 16(5), 346–356.
- Arnold, J. B., S. Mackintosh, S. Jones, and D. Thewlis (2014). Differences in foot kinematics between young and older adults during walking. *Gait & Posture* 39(2), 689—694.
- Awad, L. N., D. S. Reisman, T. M. Kesar, and S. A. Binder-Macleod (2014). Targeting paretic propulsion to improve poststroke walking function: a preliminary study. *Arch Phys Med Rehabil* 95(5), 840–848.
- Awai, L. (2014). *Gait Control and Locomotor Recovery after Spinal Cord Injury*. Ph. D. thesis, Zürich, Switzerland.
- Awai, L. and A. Curt (2014). Intralimb coordination as a sensitive indicator of motor-control impairment after spinal cord injury. *Front Hum Neurosci* 8(148).
- Baghshomali, S. and C. Bushnell (2014). Reducing stroke in women with risk factor management: blood pressure and cholesterol. *Womens Health (Lond Engl)* 10, 5.
- Balke, B. (1963). A simple field test for the assessment of physical fitness. *Rep Civ Aeromed Res Inst US*, 1–8.

- Barbosa, D., C. P. Santos, and M. Martins (2015). The application of cycling and cycling combined with feedback in the rehabilitation of stroke patients: A review. *Journal of Stroke and Cerebrovascular Diseases* 24(2), 253—273.
- Barroso, F. (2011). Influence of the robotic exoskeleton Lokomat on the control of human gait: an electromyographic and kinematic analysis. Master's thesis, University of Minho.
- Barroso, F., D. Ruiz Bueno, J. A. Gallego, P. Jaramillo, and A. Kilicarslan (2013). *Emerging Therapies in Neurorehabilitation*, Chapter Surface EMG in Neurorehabilitation and Ergonomics: State of the Art and Future Perspectives. Springer Berlin Heidelberg.
- Barroso, F., D. Torricelli, J. C. Moreno, J. Taylor, J. Gómez-Soriano, E. B. Esteban, C. Santos, and J. L. Pons (2013). Similarity of muscle synergies in human walking and cycling: preliminary results. In *EMBC'13 - 35th Annual International Conference of the IEEE Engineering in Medicine and Biology Society*, pp. 6933–69360,.
- Barroso, F. O., D. Torricelli, J. C. Moreno, J. Taylor, J. Gomez-Soriano, E. Bravo-Esteban, S. Piazza, C. Santos, and J. L. Pons (2014). Shared muscle synergies in human walking and cycling. *Journal of Neurophysiology*.
- Baum, B. S. and L. Li (2003). Lower extremity muscle activities during cycling are influenced by load and frequency. *Journal of Electromyography and Kinesiology* 13, 181–190.
- Belda-Lois, J.-M., S. Mena-Del Horno, I. Bermejo-Bosch, J. C. Moreno, J. L. Pons, D. Farina, M. Iosa, M. Molinari, F. Tamburella, A. Ramos, A. Caria, T. Solis-Escalante, C. Brunner, and M. Rea (2011). Rehabilitation of gait after stroke: a review towards a top-down approach. *J Neuroeng Rehabil* 8(1).
- Bendok, B. R. and A. M. Naidech (2011). *Hemorrhagic and Ischemic Stroke: Medical, Imaging, Surgical and Interventional Approaches*. Thieme.
- Benito-Penalva, J., D. J. Edwards, E. Opisso, M. Cortes, R. Lopez-Blazquez, N. Murillo, U. Costa, J. M. Tormos, J. Vidal-Samsó, J. E. M. S. a. H. S. C. I. S. G. Valls-Solé, and J. Medina (2012). Gait training in human spinal cord injury using electromechanical systems: effect of device type and patient characteristics. *Arch Phys Med Rehabil* 93(3), 404–412.
- Bennett, D. J. (2008). Demystifying spasticity: Reply to dietz. *J Neurophysiol* 99, 1041–1043.

- Benson, M. ., J. Fixsen, M. Macnicol, and K. Parsch (2010). *Children's Orthopaedics and Fractures*. Springer Science & Business Media.
- Benz, E. N., T. G. Hornby, R. K. Bode, R. A. Scheidt, , and B. D. Schmit (2005). A physiologically based clinical measure for spastic reflexes in spinal cord injury. *Arch Phys Med Rehabil* 86(1), 52–59.
- Berger, D. J., R. Gentner, T. Edmunds, D. K. Pai, and A. d'Avella (2013). Differences in adaptation rates after virtual surgeries provide direct evidence for modularity. *The Journal of Neuroscience* 33(30), 12384–12394.
- Berniker, M., A. Jarc, E. Bizzi, and M. C. Tresch (2009). Simplified and effective motor control based on muscle synergies to exploit musculoskeletal dynamics. *Proceedings of the National Academy of Sciences* 106(18), 7601—7606.
- Bernstein, N. A. (1967). *The co-ordination and regulation of movements*. Pergamon Press.
- Biering-Sørensen, F., J. B. Nielsen, , and K. Klinge (2006). Spasticity-assessment: a review. *Spinal Cord* 44(12), 708–722.
- Bizzi, E. and V. C. Cheung (2013). The neural origin of muscle synergies. *Frontiers in Computational Neuroscience* 7.
- Bizzi, E., V. C. Cheung, A. d'Avella, P. Saltiel, and M. Tresch (2008). Combining modules for movement. *Brain Res Rev* 57(1), 125–133.
- Bizzi, E., F. A. Mussa-Ivaldi, and S. Giszter (1991). Computations underlying the execution of movement: a biological perspective. *Arch Phys Med Rehabil* 253(5017), 287–291.
- Bogey, R., L. Barnes, and J. Perry (1992). Computer algorithms to characterize individual subject emg profiles during gait. *Arch Phys Med Rehabil* 73, 835–841.
- Bohannon, R. W. and M. B. Smith (1987). Interrater reliability of a modified ashworth scale of muscle spasticity. *Phys Ther* 67(2), 206–207.
- Bonnyaud, C., R. Zory, J. Boudarham, D. Pradon, D. Bensmail, and N. Roche (2014). Effect of a robotic restraint gait training versus robotic conventional gait training on gait parameters in stroke patients. *Exp Brain Res* 232(1), 31–42.
- Boonstra, T. W. (2013). The potential of corticomuscular and intermuscular coherence for research on human motor control. *Front Hum Neurosci* 7(855).

- Boudarham, J., N. Roche, D. Pradon, C. Bonnyaud, D. Bensmail, and R. Zory (2013). Variations in kinematics during clinical gait analysis in stroke patients. *PLoS One* 8(6).
- Bowden, M. and D. S. Stokic (2009). Clinical and neurophysiologic assessment of strength and spasticity during intrathecal baclofen titration in incomplete spinal cord injury: single-subject design. *J Spinal Cord Med* 32(2), 183–190.
- Bowden, M. G., A. L. Behrman, R. R. Neptune, C. M. Gregory, and S. A. Kautz (2013). Locomotor rehabilitation of individuals with chronic stroke: difference between responders and nonresponders. *Arch Phys Med Rehabil*. 94(5), 856–862.
- Bowden, M. G., D. J. Clark, and S. A. Kautz (2010). Evaluation of abnormal synergy patterns poststroke: relationship of the fugl-meyer assessment to hemiparetic locomotion. *Neurorehabil Neural Repair* 24(4), 328–337.
- Bravo-Esteban, E., J. Taylor, J. Abián-Vicén, S. Albu, C. Simón-Martínez, D. Torricelli, and J. Gómez-Soriano (2013). Impact of specific symptoms of spasticity on voluntary lower limb muscle function, gait and daily activities during subacute and chronic spinal cord injury. *NeuroRehabilitation* 33(4), 531–543.
- Bravo-Esteban, E., J. Taylor, M. Aleixandre, C. Simon-Martínez, D. Torricelli, J. L. Pons, and J. Gómez-Soriano (2014). Tibialis anterior muscle coherence during controlled voluntary activation in patients with spinal cord injury: diagnostic potential for muscle strength, gait and spasticity. *J Neuroeng Rehabil* 11(23).
- Burrige, J. H., D. E. Wood, H. J. Hermens, G. E. Voerman, G. R. Johnson, F. van Wijck, T. Platz, M. Gregoric, R. Hitchcock, and A. D. Pandyan (2005). Theoretical and methodological considerations in the measurement of spasticity. *Disabil Rehabil* 27(1–2), 69–80.
- Cappellini, G., Y. P. Ivanenko, R. E. Poppele, and F. Lacquaniti (2006, June). Motor patterns in human walking and running. *J Neurophysiol* 95(6), 3426–3437.
- Catz, A. and M. Itzkovich (2007). Spinal cord independence measure: comprehensive ability rating scale for the spinal cord lesion patient. *J Rehabil Res Dev* 44(1), 65–68.
- Cheung, V. C. K., A. Turolla, M. Agostini, S. Silvoni, C. Bennis, P. Kasi, S. Paganoni, P. Bonato, and E. Bizzi (2012). Muscle synergy patterns as physiological markers of motor cortical damage. *Proc Natl Acad Sci U S A* 109(36), 14652–14656.
- Chvatal, S. A. and L. H. Ting (2013). Common muscle synergies for balance and walking. *Gait & Posture* 7.

- Cimolin, V. and M. Galli (2014). Summary measures for clinical gait analysis: A literature review. *Gait & Posture* 39(4), 1005–1010.
- Clark, D. J., L. H. Ting, F. E. Zajac, R. R. Neptune, and S. A. Kautz (2010, February). Merging of healthy motor modules predicts reduced locomotor performance and muscle coordination complexity post-stroke. *J Neurophysiol* 103(2), 844–857.
- Cram, J. R. (2011). *Electrode Placements*. In: Criswell E (eds). *Cram's Introduction to surface electromyography*. 2nd edn. PJones and Barlett Publishers.
- d'Avella, A. and E. Bizzi (2005). Shared and specific muscle synergies in natural motor behaviors. *Proc Natl Acad Sci U S A* 102(8), 3076–3081.
- d'Avella, A. and F. Lacquaniti (2013). Control of reaching movements by muscle synergy combinations. *Front Comput Neurosci* 7(42).
- d'Avella, A. and D. K. Pai (2010). Modularity for sensorimotor control: evidence and a new prediction. *J Mot Behav* 42(6), 361–369.
- Davis, R. B., S. Öunpuu, D. Tyburski, and J. R. Gage (1991). A gait analysis data collection and reduction technique. *Human Movement Science* 10(5), 575—587.
- De Marchis, C., A. M. Castronovo, D. Bibbo, M. Schmid, and S. Conforto (2012). Muscle synergies are consistent when pedaling under different biomechanical demands. *Conf Proc IEEE Eng Med Biol Soc*, 3308–3311.
- De Marchis, C., M. Schmid, D. Bibbo, I. Bernabucci, and S. Conforto (2013). Inter-individual variability of forces and modular muscle coordination in cycling: A study on untrained subjects. *Human Movement Science* 32(6), 1480—1494.
- De Mauro, A., E. Carrasco, D. Oyarzun, A. Ardanza, A. Frizera Neto, D. Torricelli, J. L. Pons, A. Gil, and J. Florez (2011). Virtual reality system in conjunction with neurorobotics and neuroprosthetics for rehabilitation of motor disorders. *Stud Health Technol Inform* 163, 163–165.
- DeLisa, J. A. and U. States (1998). *Gait analysis in the science of rehabilitation*. Dept. of Veterans Affairs, Veterans Health Administration, Rehabilitation Research and Development Service, Scientific and Technical Publications Section Washington, D.C.
- Dietz, V. (2008). Body weight supported gait training: from laboratory to clinical setting. *Brain Research Bulletin* 76, I–VI.
- Dietz, V. and T. Sinkjaer (2007). Spastic movement disorder: impaired reflex function and altered muscle mechanics. *Lancet Neurol* 6(8), 725–733.

- Dittuno, P. L. and J. F. J. Ditunno (2001). Walking index for spinal cord injury (wisci ii): scale revision. *Spinal Cord* 39(12), 654–656.
- Ditunno, J. and G. Scivoletto (2009). Clinical relevance of gait research applied to clinical trials in spinal cord injury. *Brain Research Bulletin* 78(1), 35–42.
- Dominici, N., Y. Ivanenko, G. Cappellini, A. d’Avella, V. Mondì, M. Cicchese, A. Fabiano, T. Silei, A. Di Paolo, C. Giannini, R. Poppele, and F. Lacquaniti (2011). Locomotor primitives in newborn babies and their development. *Science* 334(6058), 997–9.
- Duffell, L. D., G. L. Brown, and M. M. Mirbagheri (2015). Facilitatory effects of antispastic medication on robotic locomotor training in people with chronic incomplete spinal cord injury. *J Neuroeng Rehabil* 12(29).
- Duncan, P. W., M. Propst, and S. G. Nelson (1983). Reliability of the fugl-meyer assessment of sensorimotor recovery following cerebrovascular accident. *Phys Ther* 63(10), 1606–1610.
- Eng, J. J. and P. F. Tang (2007). Gait training strategies to optimize walking ability in people with stroke: a synthesis of the evidence. *Expert Rev Neurother* 7(10), 1417–1436.
- Farina, D., A. Holobar, R. Merletti, and R. M. Enoka (2010). Decoding the neural drive to muscle from the surface electromyogram. *Clin Neurophysiol* 10(121), 1616–1623.
- Farina, D., R. Merletti, and R. M. Enoka (2004). The extraction of neural strategies from the surface emg. *J Appl Physiol* 94(6), 1486–1495.
- Fawcett, J. W., A. Curt, J. D. Steeves, W. P. Coleman, M. H. Tuszynski, D. Lammertse, P. F. Bartlett, A. R. Blight, V. Dietz, J. Ditunno, B. H. Dobkin, L. A. Havton, P. H. Ellaway, M. G. Fehlings, A. Privat, R. Grossman, J. D. Guest, N. Kleitman, M. Nakamura, and D. Gaviria, M. Short (2007). Guidelines for the conduct of clinical trials for spinal cord injury as developed by the iccp panel: spontaneous recovery after spinal cord injury and statistical power needed for therapeutic clinical trials. *Spinal Cord* 45(3), 190–205.
- Field-Fote, E. and V. Dietz (2007). Single joint perturbation during gait: Preserved compensatory response pattern in spinal cord injured subjects. *Clin Neurophysiol*.
- Finnerup, N. B. (2013). Pain in patients with spinal cord injury. *Pain*.
- Forrest, G. F., K. Hutchinson, D. J. Lorenz, J. J. Buehner, L. R. Vanhiel, S. A. Sisto, and D. M. Basso (2014). Are the 10 meter and 6 minute walk tests redundant in patients with spinal cord injury? *PLoS One* 9(5).

- Fox, E. J., N. J. Tester, S. A. Kautz, D. R. Howland, D. J. Clark, C. Garvan, and A. L. Behrman (2013). Modular control of varied locomotor tasks in children with incomplete spinal cord injuries. *J Neurophysiol* 110(6), 1415–1425.
- Fugl-Meyer, A. R., L. Jääskö, L. I., S. Olsson, and S. Steglind (1975). The post-stroke hemiplegic patient. 1. a method for evaluation of physical performance. *Scand J Rehabil Med* 7(1), 13–31.
- Gaviria, M., M. D'Angeli, P. Chaveta, J. Pelissierb, E. Peruchona, and P. Rabischonga (1996). Plantar dynamics of hemiplegic gait: a methodological approach. *Gait & Posture* 4(4), 297—305.
- Gil-Agudo, A., S. Pérez-Nombela, A. Forner-Cordero, E. Pérez-Rizo, B. Crespo-Ruiz, and A. del Ama-Espinosa (2011). Gait kinematic analysis in patients with a mild form of central cord syndrome. *J Neuroeng Rehabil* 8(7).
- Gil-Agudo, A., S. Pérez-Nombela, E. Pérez-Rizo, A. del Ama-Espinosa, B. Crespo-Ruiz, and J. L. Pons (2013). Comparative biomechanical analysis of gait in patients with central cord and brown-séquad syndrome. *J Neuroeng Rehabil* 35(22), 1869–1876.
- Gizzi, L., J. Nielsen, F. Felici, Y. Ivanenko, and D. Farina (2011). Impulses of activation but not motor modules are preserved in the locomotion of subacute stroke patients. *J Neurophysiol* 106(1), 202–210.
- Gizzi, L., J. F. Nielsen, F. Felici, J. C. Moreno, J. L. Pons, and D. Farina (2012). Motor modules in robot-aided walking. *J Neuroeng Rehabil* 9(76).
- Gómez-Soriano, J. (2012). *Espasticidad después de la lesión medular: Fisiopatología, valoración cuantitativa y nuevos enfoques de tratamiento*. Ph. D. thesis, Madrid, Spain.
- Gómez-Soriano, J., R. Cano-de-la Cuerda, E. Muñoz-Hellin, R. Ortiz-Gutiérrez, and J. S. Taylor (2012). Evaluation and quantification of spasticity: a review of the clinical, biomechanical and neurophysiological methods. *Rev Neurol* 55(4), 217–226.
- Gómez-Soriano, J., J. M. Castellote, E. Pérez-Rizo, A. Esclarin, and J. S. Taylor (2010). Voluntary ankle flexor activity and adaptive coactivation gain is decreased by spasticity during subacute spinal cord injury. *Exp Neurol* 224(2), 507–516.
- Gradil, C. and M. C. Sá (2015). Management of stroke. *Surgery (Oxford)*. (in press).
- Grasso, R., Y. P. Ivanenko, M. Zago, M. Molinari, G. Scivoletto, V. Castellano, V. Macellari, and F. Lacquaniti (2004). Distributed plasticity of locomotor pattern generators in spinal cord injured patients. *Brain* 127(5), 1019–1034.

- Hamill, J. and K. M. Knutzen (2006). *Biomechanical Basis of Human Movement*. Lippincott Williams and Wilkins.
- Hansen, N. L., B. A. Conway, D. M. Halliday, S. Hansen, H. S. Pyndt, F. Biering-Sørensen, and J. B. Nielsen (2005). Reduction of common synaptic drive to ankle dorsiflexor motoneurons during walking in patients with spinal cord lesion. *J Neurophysiol* 94(2), 934–942.
- Hart, C. B. and S. F. Giszter (2004). Modular premotor drives and unit bursts as primitives for frog motor behaviors. *J Neurosci* 24(22), 5269–5282.
- Hart, C. B. and S. F. Giszter (2010). A neural basis for motor primitives in the spinal cord. *J Neurosci* 30(4), 1322–1336.
- Hayes, H. B., S. A. Chvatal, M. A. French, L. H. Ting, and R. D. Trumbower (2014). Neuromuscular constraints on muscle coordination during overground walking in persons with chronic incomplete spinal cord injury. *Clin Neurophysiol* 125(10), 2024–2035.
- Haywood, K. (2008). *Skeletal System (Amazing Human Body)*. Cavendish Square Publishing.
- Hermens, H. (2000, October). Development of recommendations for SEMG sensors and sensor placement procedures. *Journal of Electromyography and Kinesiology* 10(5), 361–374.
- Hermens, H., B. Freriks, and R. Merletti (1999). *European recommendations for surface electromyography: results of the SENIAM project*. Biomedical and health research program. Roessingh Research and Development.
- Hidler, J., W. Wisman, and N. Neckel (2008). Kinematic trajectories while walking within the lokomat robotic gait-orthosis. *Clin Biomech* 23(10), 1251–1259.
- Hidler, J. M. and A. E. Wall (2005). Alterations in muscle activation patterns during robotic assisted walking. *Clin Biomech* 20(2), 184–193.
- Hof, A. L., H. Elzinga, W. Grimmius, and J. P. Halbertsma (2002). Speed dependence of averaged emg profiles in walking. *Gait & Posture* 16(1), 78–86.
- Holden, M. K., K. M. Gill, and M. R. Magliozzi (1986). Gait assessment for neurologically impaired patients. standards for outcome assessment. *Phys Ther* 66(10), 1530–1539.
- Howle, J. M. (2002). *Neuro-developmental Treatment Approach: Theoretical Foundations and Principles of Clinical Practice*. NeuroDevelopmental Treatment.

- Hug, F. (2011). Can muscle coordination be precisely studied by surface electromyography? *Journal of Electromyography and Kinesiology* 21(1), 1 – 12.
- Hug, F., N. A. Turpin, A. Couturier, and S. Dorel (2011). Consistency of muscle synergies during pedaling across different mechanical constraints. *J Neurophysiol* 106(1), 91–103.
- Hug, F., N. A. Turpin, A. Guével, and S. Dorel (2010). Is interindividual variability of emg patterns in trained cyclists related to different muscle synergies? *J Appl Physiol* 108(6), 1727–1736.
- Inman, V. T., H. J. Ralston, J. B. d. C. M. Saunders, B. Feinstein, and E. W. J. Wright (1952). Relation of human electromyogram to muscular tension. *Electromyogr Clin Neurophysiol* 4, 187–194.
- Ivanenko, Y., G. Cappellini, N. Dominici, R. Poppele, and F. Lacquaniti (2005). Coordination of locomotion with voluntary movements in humans. *The Journal of Neuroscience* 25(31), 7238–7253.
- Ivanenko, Y., R. Grasso, M. Zago, M. Molinari, G. Scivoletto, V. Castellano, V. Macellari, and F. Lacquaniti (2003). Temporal components of the motor patterns expressed by the human spinal cord reflect foot kinematics. *J Neurophysiol* 90(5), 3555–65.
- Ivanenko, Y. P., G. Cappellini, I. A. Solopova, A. A. Grishin, M. J. Maclellan, R. E. Poppele, and F. Lacquaniti (2013). Plasticity and modular control of locomotor patterns in neurological disorders with motor deficits. *Front Comput Neurosci* 7(123).
- Ivanenko, Y. P., R. E. Poppele, and F. Lacquaniti (2004, April). Five basic muscle activation patterns account for muscle activity during human locomotion. *J Physiol* 556(Pt 1), 267–282.
- Ivanenko, Y. P., R. E. Poppele, and F. Lacquaniti (2009). Distributed neural networks for controlling human locomotion: Lessons from normal and sci subjects. *Brain Research Bulletin* 78(1), 13–21.
- Jackson, A. B., C. T. Carnel, J. F. Ditunno, M. S. Read, M. L. Boninger, M. R. Schmeler, S. R. Williams, W. H. Donovan, Gait, and A. Subcommittee (2008). Outcome measures for gait and ambulation in the spinal cord injury population. *J Spinal Cord Med* 31(5), 487–499.
- Jain, N. B., G. D. Ayers, E. N. Peterson, M. B. Harris, L. Morse, K. C. O'Connor, and E. Garshick (2015). Traumatic spinal cord injury in the united states, 1993-2012. *JAMA* 313(22), 2236–2243.

- Jørgensen, H. S., H. Nakayama, H. O. Raaschou, J. Vive-Larsen, M. Støier, and T. S. Olsen (1995). Outcome and time course of recovery in stroke. part i: Outcome. the copenhagen stroke study. *Arch Phys Med Rehabil* 76(5), 399–405.
- Kadaba, M. P., H. K. Ramakrishnan, and M. E. Wootten (1990). Measurement of lower extremity kinematics during level walking. *J Orthop Res* 8(3), 383–392.
- Kapadia, N., K. Masani, B. Catharine Craven, L. M. Giangregorio, S. L. Hitzig, K. Richards, and M. R. Popovic (2014). A randomized trial of functional electrical stimulation for walking in incomplete spinal cord injury: Effects on walking competency. *J Spinal Cord Med* 37(5), 511–524.
- Kargo, W. J. and D. A. Nitz (2003). Early skill learning is expressed through selection and tuning of cortically represented muscle synergies. *J Neurosci* 23(35), 11255–11269.
- Kennedy, P., E. F. Smithson, and L. C. Blakey (2012). Planning and structuring spinal cord injury rehabilitation: the needs assessment checklist. *Top Spinal Cord Inj Rehabil* 18(2), 135–137.
- Kirshblum, S. C., S. P. Burns, F. Biering-Sorensen, W. Donovan, D. E. Graves, A. Jha, M. Johansen, L. Jones, A. Krassioukov, M. J. Mulcahey, M. Schmidt-Read, and W. Waring (2011). International standards for neurological classification of spinal cord injury (revised 2011). *J Spinal Cord Med* 34(6), 535–546.
- Kirtley, C. (2006). *Clinical gait analysis: theory and practice*. Elsevier Health Sciences.
- Krawetz, P. and P. Nance (1996). Gait analysis of spinal cord injured subjects: Effects of injury level and spasticity. *Archives of Physical Medicine and Rehabilitation* 77(7), 635–638.
- Krishnamoorthy, V., M. L. Latash, J. P. Scholz, and V. M. Zatsiorsky (2003). Muscle synergies during shifts of the center of pressure by standing persons. *Exp Brain Res* 152(3), 281–92.
- Kutch, J. J., A. D. Kuo, A. M. Bloch, and W. Z. Rymer (2008). Endpoint force fluctuations reveal flexible rather than synergistic patterns of muscle cooperation. *Journal of Neurophysiology* 100(5), 2455–2471.
- Kutch, J. J. and F. J. Valero-Cuevas (2012). Challenges and new approaches to proving the existence of muscle synergies of neural origin. *PLOS Computational Biology* 8(5).
- Lacquaniti, F., Y. P. Ivanenko, and M. Zago (2012). Patterned control of human locomotion. *The Journal of Physiology* 590(10), 2189–2199.

- Lamontagne, A., F. Malouin, C. L. Richards, and F. Dumas (2002). Mechanisms of disturbed motor control in ankle weakness during gait after stroke. *Gait Posture* 15(3), 244–255.
- Lance, J. W. (1980). *Spasticity: Disordered Motor Control*. In: *Symposium synopsis*. Yearbook Medical Publishers.
- Lee, D. D. and H. S. Seung (1999, October). Learning the parts of objects by non-negative matrix factorization. *Nature* 401(6755), 788–791.
- Lee, P. P., R. A. Cripps, M. Fitzharris, and P. C. Wing (2014). The global map for traumatic spinal cord injury epidemiology: update 2011, global incidence rate. *Spinal Cord* 52(2), 110–126.
- Levine, A. J., C. A. Hinckley, K. L. Hilde, S. P. Driscoll, T. H. Poon, J. M. Montgomery, and S. L. Pfaff (2014). Identification of a cellular node for motor control pathways. *Nature Neuroscience* 17, 586—593.
- Lippincott (2002). *Anatomy and Physiology*. Lippincott Williams & Wilkins.
- Marsh, A. P. and P. E. Martin (1995). The relationship between cadence and lower extremity emg in cyclists and noncyclists. *Medicine & Science in Sports & Exercise* 27(2), 217–225.
- McGowan, C. P., R. R. Neptune, D. J. Clark, and S. A. Kautz (2010, February). Modular control of human walking: Adaptations to altered mechanical demands. *Journal of Biomechanics* 43(3), 412–419.
- Mehrholz, J., K. Wagner, K. Rutte, D. Meissner, and M. Pohl (2007). Predictive validity and responsiveness of the functional ambulation category in hemiparetic patients after stroke. *Arch Phys Med Rehabil* 88(10), 1314–1319.
- Mitsumoto, H. (2009). *Amyotrophic Lateral Sclerosis: A Guide for Patients and Families*. Demos Health Series. Demos Health.
- Molina Rueda, F., F. M. Rivas Montero, M. Pérez de Heredia Torres, I. M. Alguacil Diego, A. Molero Sánchez, and J. C. Miangolarra Page (2012). Movement analysis of upper extremity hemiparesis in patients with cerebrovascular disease: a pilot study. *Neurologia* 27(6), 343–347.
- Monaco, V., A. Ghionzoli, and S. Micera (2010). Age-related modifications of muscle synergies and spinal cord activity during locomotion. *J Neurophysiol* 104(4), 2092—2102.

- Moreno, J. C., F. Barroso, D. Farina, L. Gizzi, C. Santos, M. Molinari, and J. L. Pons (2013). Effects of robotic guidance on the coordination of locomotion. *Journal of NeuroEngineering and Rehabilitation* 10(79).
- Moreno, J. C., F. Brunetti, E. Rocon, and J. L. Pons (2008). Immediate effects of a controllable knee ankle foot orthosis for functional compensation of gait in patients with proximal leg weakness. *Med Biol Eng Comput* 41, 43–53.
- Muceli, S., A. T. Boye, A. d’Avella, and D. Farina (2010). Identifying representative synergy matrices for describing muscular activation patterns during multidirectional reaching in the horizontal plane. *J Neurophysiol* 103(3), 1532—1542.
- Nadeau, S., C. Duclos, L. Bouyer, and C. L. Richards (2011). Guiding task-oriented gait training after stroke or spinal cord injury by means of a biomechanical gait analysis. *Prog Brain Res* 192, 161–180.
- Nations, U. (2013). *World Population Prospects - The 2012 Revision*. United Nations.
- Neptune, R. R., D. J. Clark, and S. A. Kautz (2009). Modular control of human walking: a simulation study. *Journal of Biomechanics* 42(9), 1282–1287.
- Neptune, R. R. and C. P. McGowan (2011, January). Muscle contributions to whole-body sagittal plane angular momentum during walking. *J Biomech* 44(1), 6–12.
- Nymark, J. R., S. J. Balmer, E. H. Melis, E. D. Lemaire, and S. Millar (2005). Electromyographic and kinematic nondisabled gait differences at extremely slow over-ground and treadmill walking speeds. *J Rehabil Res Dev* 42(4), 523–34.
- Ochi, F., A. Esquenazi, B. Hirai, and M. Talaty (1999). Temporal-spatial features of gait after traumatic brain injury. *J Head Trauma Rehabil* 14(2), 105–115.
- Oliveira, A. S., L. Gizzi, D. Farina, and U. G. Kersting (2014). Motor modules of human locomotion: influence of emg averaging, concatenation, and number of step cycles. *Front. Hum. Neurosci* 8(33).
- Olney, S. J. and C. Richards (1996). Hemiparetic gait following stroke. Part I: Characteristics. *Gait Posture* 4(2), 136–148.
- Overduin, S. A., A. d’Avella, J. M. Carmena, and E. Bizzi (2012). Microstimulation activates a handful of muscle synergies. *Neuron* 76(6), 1071—1077.
- Page, M. I. B. R. (2016). Diagrams - muscular system. Available at <http://mriclassroom.weebly.com/diagrams-muscular-system.html>.

- Penn, R. D., S. M. Savoy, D. Corcos, M. Latash, G. Gottlieb, B. Parke, and J. S. Kroin (1989). Intrathecal baclofen for severe spinal spasticity. *N Engl J Med* 320(23), 1517–1521.
- Perry, J. (1967). The mechanics of walking: a clinical interpretation. *Phys Ther* 47(9), 777–801.
- Perry, J. (1992). *Gait analysis: normal and pathological function*. SLACK.
- Pons, J. L., J. C. Moreno, D. Torricelli, and J. S. Taylor (2013). Principles of human locomotion: A review. *EMBC'13 - 35th Annual International Conference of the IEEE Engineering in Medicine and Biology Society*, 6941–6944.
- Priebe, M. M., A. M. Sherwood, J. I. Thornby, N. F. Kharas, , and J. Markowski (1996). Clinical assessment of spasticity in spinal cord injury: a multidimensional problem. *Arch Phys Med Rehabil* 77(7), 713–716.
- Prilutsky, B. (2000). Coordination of two- and one-joint muscles: functional consequences and implications for motor control. *Motor Control* 4(1), 1–44.
- Raasch, C. C. and F. E. Zajac (1999). Locomotor strategy for pedaling: muscle groups and biomechanical functions. *Journal of Neurophysiology* 82(2), 515–525.
- Ramsay, J. W., T. S. Buchanan, and J. S. Higginson (2014). Differences in plantar flexor fascicle length and pennation angle between healthy and poststroke individuals and implications for poststroke plantar flexor force contributions. *Stroke Research and Treatment* 2014.
- Reichenfelser, W., H. Hackl, J. Hufgard, J. Kastner, K. Gestaltner, and M. Gföhler (2012). Monitoring of spasticity and functional ability in individuals with incomplete spinal cord injury with a functional electrical stimulation cycling system. *J Rehabil Med* 44(5), 444–449.
- Reisman, D. S., R. Wityk, K. Silver, and A. J. Bastian (2007). Locomotor adaptation on a split-belt treadmill can improve walking symmetry post-stroke. *Brain* 130(7), 1861–1872.
- Reissman, M. E. and Y. Y. Dhaher (2015). A functional tracking task to assess frontal plane motor control in post stroke gait. *J Biomech* 48(10), 1782–1788.
- Ricamato, A. L. and J. M. Hidler (2005). Quantification of the dynamic properties of emg patterns during gait. *Journal of Electromyography and Kinesiology* 15(4), 384–392.

- Robertson, G., G. Caldwell, J. Hamill, G. Kamen, and S. Whittlesey (2013). *Research Methods in Biomechanics, 2E*. Human Kinetics.
- Roche, N., C. Bonnyaud, M. Geiger, B. Bussel, and D. Bensmail (2015). Relationship between hip flexion and ankle dorsiflexion during swing phase in chronic stroke patients. *Clin Biomech* 30(3), 219–225.
- Rosa, M. C., A. Marques, S. Demain, C. D. Metcalf, , and J. Rodrigues (2014). Methodologies to assess muscle co-contraction during gait in people with neurological impairment - a systematic literature review. *J Electromyogr Kinesiol* 24(2), 179–191.
- Routson, R. L., D. J. Clark, M. G. Bowden, S. A. Kautz, and R. R. Neptune (2013). The influence of locomotor rehabilitation on module quality and post-stroke hemiparetic walking performance. *Gait Posture* 38(3), 511–517.
- Routson, R. L., S. A. Kautz, and R. R. Neptune (2014). Modular organization across changing task demands in healthy and poststroke gait. *Physiol Rep* 2(6).
- Rueterbories, J., E. G. Spaich, B. Larsen, and O. K. Andersen (2010). Methods for gait event detection and analysis in ambulatory systems. *Med Eng Phys* 32(6), 545–552.
- Russo, T., G. Felzani, and C. Marini (2011). Stroke in the very old: A systematic review of studies on incidence, outcome, and resource use. *Journal of Aging Research* 2011.
- Safavynia, S. A., G. Torres-Oviedo, and L. H. Ting (2011). Muscle synergies: Implications for clinical evaluation and rehabilitation of movement. *Top Spinal Cord Inj Rehabil* 17(1), 16–24.
- Schaechter, J. D. (2004, May). Motor rehabilitation and brain plasticity after hemiparetic stroke. *Prog Neurobiol* 73(1), 61–72.
- Schutte, L. M., U. Narayanan, J. L. Stout, P. Selber, J. R. Gage, and M. H. Schwartz (2000). An index for quantifying deviations from normal gait. *Gait Posture* 11(1), 25–31.
- Seddon, H. W. J. (1976). *Aids to the exam of the peripheral nervous system*. Medical Research Council - London: Her Majesty's Stationery Office.
- Seeley, R. R., P. Tate, and T. D. Stephens (2008). *Anatomy & Physiology*. McGraw-Hill.
- Sherwood, L. (2008). *Human physiology: from cells to systems*. Human Physiology. Brooks/Cole, Cengage Learning.
- Sinclair, J., P. J. Taylor, and S. J. Hobbs (2013). Digital filtering of three-dimensional lower extremity kinematics: an assessment. *J Hum Kinet* 39, 25–36.

- Soderberg, G. L. (1992). *Selected topics in surface electromyography for use in the occupational setting: expert perspectives*. U.S. Department of Health and Human Services.
- Sohrabji, F., S. Bake, and D. K. Lewis (2013). Age-related changes in brain support cells: Implications for stroke severity. *Neurochem Int* 63(4), 291–301.
- Steele, K. M., M. C. Tresch, and E. J. Perreault (2013). The number and choice of muscles impact the results of muscle synergy analyses. *Frontiers in Computational Neuroscience* 7.
- Steele, K. M., M. C. Tresch, and E. J. Perreault (2015). Consequences of biomechanically constrained tasks in the design and interpretation of synergy analyses. *J Neurophysiol* 113(7), 2102–2113.
- Sutherland, D. H. (1964). *Gait disorders in childhood and adolescence*. Williams and Wilkins.
- Takeuchi, N. and S.-I. Izumi (2013). Rehabilitation with poststroke motor recovery: A review with a focus on neural plasticity. *Stroke Research and Treatment* 2013.
- Tilson, J. K., K. J. Sullivan, S. Y. Cen, D. K. Rose, C. H. Koradia, S. P. Azen, P. W. Duncan, and L. E. A. P. S. L. I. Team (2010). Meaningful gait speed improvement during the first 60 days poststroke: minimal clinically important difference. *Phys Ther* 90(2), 196–208.
- Ting, L. H., H. J. Chiel, R. D. Trumbower, J. L. Allen, J. L. McKay, M. E. Hackney, and T. M. Kesar (2015). Neuromechanical principles underlying movement modularity and their implications for rehabilitation. *Neuron* 86(1), 38–54.
- Ting, L. H. and J. M. Macpherson (2005). A limited set of muscle synergies for force control during a postural task. *Journal of Neurophysiology* 93(1), 609–613.
- Ting, L. H. and J. L. McKay (2007). Neuromechanics of muscle synergies for posture and movement. *Current Opinion in Neurobiology* 17(6), 622–628.
- Torres-Oviedo, G., J. M. Macpherson, and L. H. Ting (2006). Muscle synergy organization is robust across a variety of postural perturbations. *J Neurophysiol* 96(3), 1530–1546.
- Torres-Oviedo, G. and L. Ting (2007). Muscle synergies characterizing human postural responses. *J Neurophysiol* 98, 2144–2156.
- Tortora, G. J. and Bryan (2006). *Principles of anatomy and physiology* (11th ed. ed.). Wiley & Sons,.

- Tresch, M. C., V. C. Cheung, and A. d'Avella (2006). Matrix factorization algorithms for the identification of muscle synergies: evaluation on simulated and experimental data sets. *J Neurophysiol* 95(4), 2199–2212.
- Tresch, M. C. and A. Jarc (2009). The case for and against muscle synergies. *Current Opinion in Neurobiology* 19, 601–607.
- Valero-Cuevas, F. J., M. Venkadesan, and E. Todorov (2009). Structured variability of muscle activations supports the minimal intervention principle of motor control. *Journal of Neurophysiology* 102, 59–68.
- van Asseldonk, E. H. F., J. F. Veneman, R. Ekkelenkamp, J. H. Buurke, F. C. T. van der Helm, and H. van der Kooij (2008). The Effects on Kinematics and Muscle Activity of Walking in a Robotic Gait Trainer During Zero-Force Control. *IEEE Trans. Neural Syst. Rehabil. Eng.* 16(4), 360–370.
- van der Salm, A., A. V. Nene, D. J. Maxwell, P. H. Veltink, H. J. Hermens, and M. J. IJzerman (2005). Gait impairments in a group of patients with incomplete spinal cord injury and their relevance regarding therapeutic approaches using functional electrical stimulation. *Artif Organs* 29(1), 8–14.
- van Hedel, H. J., M. Wirz, and A. Curt (2005). Improving walking assessment in subjects with an incomplete spinal cord injury: responsiveness. *Spinal Cord* 44(6), 352–356.
- van Middendorp, J. J., H. Allison, K. Cowan, and S. C. I. P. S. Partnership (2014). Top ten research priorities for spinal cord injury. *Lancet Neurol* 13(2), 1167.
- van Middendorp, J. J., M. H. Pouw, K. C. Hayes, R. Williams, H. S. Chhabra, C. Putz, R. P. Veth, A. C. Geurts, S. Aito, J. Kriz, W. McKinley, F. W. van Asbeck, A. Curt, M. G. Fehlings, H. Van de Meent, A. J. Hosman, and E.-S. S. G. Collaborators (2010). Diagnostic criteria of traumatic central cord syndrome. part 2: a questionnaire survey among spine specialists. *Spinal Cord* 48(9), 657–663.
- Verma, R., K. Arya, P. Sharma, and R. Garg (2012). Understanding gait control in post-stroke: implications for management. *Journal of Bodywork & Movement Therapies* 16(1), 14–21.
- Wakeling, J. M. and T. Horn (2009). Neuromechanics of muscle synergies during cycling. *Journal of Neurophysiology* 101.
- Wall, J. C., C. Bell, S. Campbell, and J. Davis (2000). The timed get-up-and-go test revisited: measurement of the component tasks. *J Rehabil Res Dev* 37(1), 109–113.

- Wang, P., K. H. Low, A. H. McGregor, and A. Tow (2013). Detection of abnormal muscle activations during walking following spinal cord injury (sci). *Res Dev Disabil* 34(4), 1226–1235.
- Weiss, E. J. and M. Flanders (2004). Muscular and postural synergies of the human hand. *J Neurophysiol* 92(1), 523–535.
- Wirz, M. (2013). *Ambulatory rehabilitation in patients with spinal cord injury : a clinical perspective*. Ph. D. thesis, Maastricht, Netherlands.
- Wren, T. A. L., G. E. Gorton, S. O. Öunpuu, and C. A. Tucker (2009). Efficacy of clinical gait analysis: A systematic review. *J Pediatr Orthop* 29(6), 558–563.
- Wright, J. and T. Theologis (2015). Is 3-d gait analysis essential? by professor james wright: Introduction by mr. tim theologis. *Gait Posture* 42(3), 227–229.
- Yakovenko, S., N. Krouchev, and T. Drew (2011). Sequential activation of motor cortical neurons contributes to intralimb coordination during reaching in the cat by modulating muscle synergies. *Journal of Neurophysiology* 105, 388–409.
- Yang, J. and M. Gorassini (2006). Spinal and brain control of human walking: implications for retraining of walking. *Neuroscientist* 12(5), 379–89.
- Yang, R., L. Guo, P. Wang, L. Huang, Y. Tang, W. Wang, K. Chen, J. Ye, C. Lu, Y. Wu, and H. Shen (2014). Epidemiology of spinal cord injuries and risk factors for complete injuries in guangdong, china: A retrospective study. *PLoS One* 9(1).
- Zajac, F. E., R. R. Neptune, and S. A. Kautz (2002). Biomechanics and muscle coordination of human walking. part i: introduction to concepts, power transfer, dynamics and simulations. *Gait & Posture* 16, 215–232.
- Zehr, E. P., J. E. Balter, D. P. Ferris, S. R. Hundza, P. M. Loadman, and R. H. Stoloff (2007). Neural regulation of rhythmic arm and leg movement is conserved across human locomotor tasks. *J Physiol* 582(Pt 1), 209–227.

Appendix A

Muscular system

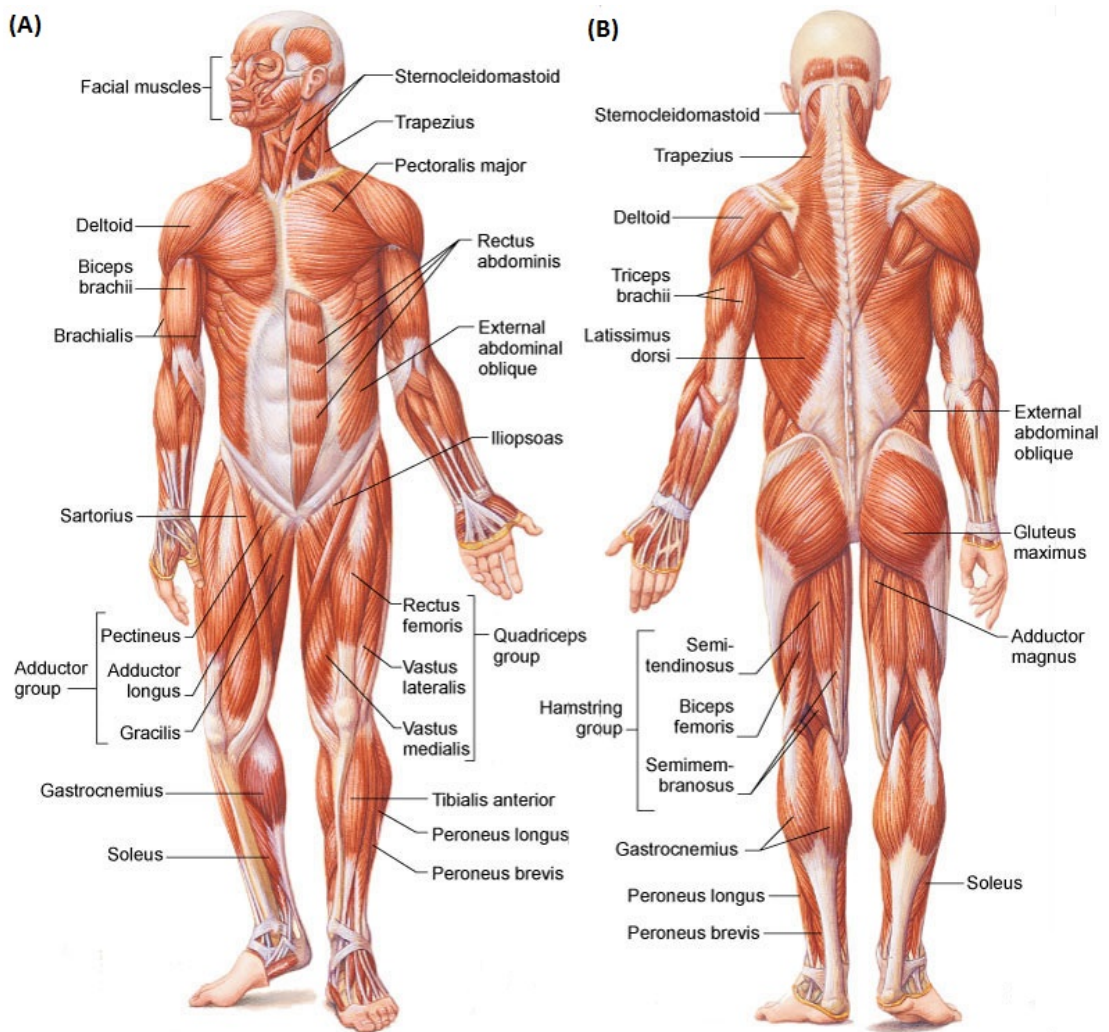




FIGURE A.1: Muscular system. (A) Anterior and (B) Posterior view. (Page, 2016)

Appendix B

ASIA Scale



INTERNATIONAL STANDARDS FOR NEUROLOGICAL CLASSIFICATION OF SPINAL CORD INJURY (ISNCSCI)



Patient Name _____ Date/Time of Exam _____

Examiner Name _____ Signature _____

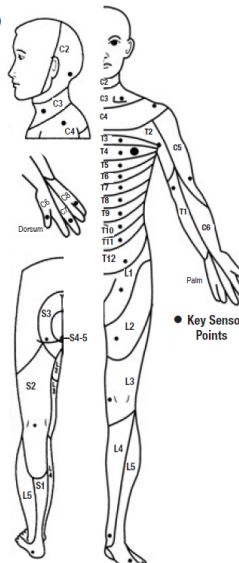
RIGHT

	MOTOR KEY MUSCLES		SENSORY KEY SENSORY POINTS	
	Light Touch (LTR)	Pin Prick (PPR)	Light Touch (LTL)	Pin Prick (PPL)
C2				
C3				
C4				
C5	Elbow flexors			
C6	Wrist extensors			
C7	Elbow extensors			
C8	Finger flexors			
T1	Finger abductors (little finger)			
T2				
T3				
T4				
T5				
T6				
T7				
T8				
T9				
T10				
T11				
T12				
L1				
L2	Hip flexors			
L3	Knee extensors			
L4	Ankle dorsiflexors			
L5	Long toe extensors			
S1	Ankle plantar flexors			
S2				
S3				
S4-5				

(VAC) Voluntary Anal Contraction (Yes/No)

RIGHT TOTALS (MAXIMUM) (50) (56) (56)

MOTOR SUBSCORES
 UER + UEL = UEMS TOTAL (MAX 25) (25)
 LER + LEL = LEMS TOTAL (MAX 25) (25)



● Key Sensory Points

LEFT

	MOTOR KEY MUSCLES		SENSORY KEY SENSORY POINTS	
	Light Touch (LTR)	Pin Prick (PPR)	Light Touch (LTL)	Pin Prick (PPL)
C2				
C3				
C4				
C5	Elbow flexors			
C6	Wrist extensors			
C7	Elbow extensors			
C8	Finger flexors			
T1	Finger abductors (little finger)			
T2				
T3				
T4				
T5				
T6				
T7				
T8				
T9				
T10				
T11				
T12				
L1				
L2	Hip flexors			
L3	Knee extensors			
L4	Ankle dorsiflexors			
L5	Long toe extensors			
S1	Ankle plantar flexors			
S2				
S3				
S4-5				

(DAP) Deep Anal Pressure (Yes/No)

LEFT TOTALS (MAXIMUM) (50) (56) (56)

MOTOR SUBSCORES
 LTR + LTL = LT TOTAL (MAX 56) (56)
 PPR + PPL = PP TOTAL (MAX 56) (56)

NEUROLOGICAL LEVELS (Steps 1-5 for classification as on reverse)

1. SENSORY	R	L	3. NEUROLOGICAL LEVEL OF INJURY (NLI)		4. COMPLETE OR INCOMPLETE? (Incomplete = Any sensory or motor function in S4-5)		5. ASIA IMPAIRMENT SCALE (AIS)		(In complete injuries only) ZONE OF PARTIAL PRESERVATION (Most caudal level with any innervation)		SENSORY	R	L
2. MOTOR	<input type="checkbox"/>	<input type="checkbox"/>	<input type="checkbox"/>	<input type="checkbox"/>	<input type="checkbox"/>	<input type="checkbox"/>	<input type="checkbox"/>	<input type="checkbox"/>	<input type="checkbox"/>	<input type="checkbox"/>	<input type="checkbox"/>	<input type="checkbox"/>	<input type="checkbox"/>

This form may be copied freely but should not be altered without permission from the American Spinal Injury Association. REV 11/15

FIGURE B.1: Neurological classification of spinal cord injury proposed by the American Spinal Injury Association (ASIA).

Appendix **C**

SynergiesLAB

Supporting Online Material:

<https://www.dropbox.com/sh/88qiu6n3mjbv9c9/AAA8v8BjZ4EDX5PhZ2RSwM9ma?dl=0#>

Appendix **D**

MATLAB code to implement NNMF

```

function [W,H] = Lee_NNMF(X,K,maxiter,speak, W)
%
% NMF using euclidean distance update equations:
% Lee, D..D., and Seung, H.S., (2001), 'Algorithms for Non-negative
Matrix
Factorization', Adv. Neural Info. Proc. Syst. 13, 556-562.
%
% INPUT:
% X (N,M) : N (dimensionallity) x M (samples) non negative input matrix
% K       : Number of components
% maxiter : Maximum number of iterations to run
% speak  : prints iteration count and changes in connectivity matrix
%           elements unless speak is 0
%
% OUTPUT:
% W       : N x K matrix
% H       : K x M matrix
%
% Kasper Winther Joergensen
% Informatics and Mathematical Modelling
% Technical University of Denmark
% kwj@imm.dtu.dk
% 2006/11/16

%%%%%%%%%%%%%%%%%%%%%%%%%%%%%%%%%%%%%%%%%%%%%%%%%%%%%%%%%%%%%%%%%%%%%%%%
% User adjustable parameters
%%%%%%%%%%%%%%%%%%%%%%%%%%%%%%%%%%%%%%%%%%%%%%%%%%%%%%%%%%%%%%%%%%%%%%%%

print_iter = 50; % iterations between print on screen and convergence
test

%%%%%%%%%%%%%%%%%%%%%%%%%%%%%%%%%%%%%%%%%%%%%%%%%%%%%%%%%%%%%%%%%%%%%%%%
% test for negative values in X
%%%%%%%%%%%%%%%%%%%%%%%%%%%%%%%%%%%%%%%%%%%%%%%%%%%%%%%%%%%%%%%%%%%%%%%%

if min(min(X)) < 0
    error('Input matrix elements can not be negative');
    return
end

%%%%%%%%%%%%%%%%%%%%%%%%%%%%%%%%%%%%%%%%%%%%%%%%%%%%%%%%%%%%%%%%%%%%%%%%
% initialize random W and H
%%%%%%%%%%%%%%%%%%%%%%%%%%%%%%%%%%%%%%%%%%%%%%%%%%%%%%%%%%%%%%%%%%%%%%%%

[n,m]=size(X);
if nargin<5
    W=rand(n,K);
end
H=rand(K,m);

% use W*H to test for convergence
Xr_old=W*H;

for iter=1:maxiter
    % Euclidean multiplicative method

```



```
H = H.*(W'*X)./((W'*W)*H+eps);
if nargin<5
    W = W.*(H*X')'./(W*(H*H')+eps);
end

% print to screen
if (rem(iter,print_iter)==0) & speak,
    Xr = W*H;
    diff = sum(sum(abs(Xr_old-Xr)));
    Xr_old = Xr;
    eucl_dist = norm((X-Xr),'fro');
    errorx = mean(mean(abs(X-W*H)))/mean(mean(X));
    if errorx < 10^(-5)
        break
    end
end
end
```


Appendix **E**

Informed Consents from the Ethical
Committees

E.1 Study 2

E.2 Study 3

E.3 Study 4

HOJA DE CONSENTIMIENTO INFORMADO PARA EL PACIENTE EN EL PROYECTO:**Coherencia y sinergia muscular durante el movimiento de pedaleo como medidas de recuperación motriz.**

De acuerdo con la *LEY 14/2007, de 3 de julio, de Investigación biomédica*.

Yo, D/Dña, como participante en el estudio (o D./Dña, como su representante), en pleno uso de mis facultades, libre y voluntariamente:

EXPONGO que he sido debidamente **INFORMADO/A** por D....., en entrevista personal realizada el día dede, de que entro a formar parte de un estudio clínico sobre la evaluación de nuevas mediciones de la recuperación motriz durante la fase subaguda de la lesión medular incompleta.

Con este estudio se pretende identificar nuevas medidas diagnósticas sobre la evolución y recuperación de la lesión medular incompleta, para ello los pacientes realizarán unas pruebas de pedaleo con una bicicleta motorizada, del mismo tipo que se usa en el Hospital Nacional de Paraplégicos durante la fase de rehabilitación, por lo que los pacientes estarán familiarizados con ella, utilizando únicamente electrodos de superficie que registrarán la actividad muscular durante el movimiento de pedaleo a distintas velocidades. Además se realizará un registro de medidas clínicas (fuerza y marcha) y de espasticidad (movilizaciones y cuestionarios) por parte del personal clínico del grupo de Función Sensitivomotora. El protocolo de experimentación no conlleva ningún riesgo para los pacientes y los posibles beneficios personales se relacionan a la recuperación motora de un día de entrenamiento adicional.

Afirmo que he recibido explicaciones tanto de forma verbal como escrita, sobre la naturaleza y propósitos del procedimiento, beneficios, riesgos, alternativas y medios con que cuenta el Hospital de Paraplégicos para su realización, habiendo tenido ocasión de aclarar dudas que me han surgido (si desea más información puede contactar con el siguiente teléfono 925247700 extensión 47112 o bien por correo electrónico a jgsoriano@sescam.jccm.es

MANIFIESTO: que he entendido y estoy satisfecho de todas las explicaciones y aclaraciones recibidas sobre el proceso citado.

Y OTORGO MI CONSENTIMIENTO para que me sea realizado este estudio por parte del Grupo de Función Sensitivo-Motora del Hospital Nacional de Paraplégicos y el Instituto de Automática Industrial (IAI) del CSIC.

Entiendo que este consentimiento puede ser revocado por mí en cualquier momento, Entiendo que este consentimiento puede ser revocado por mí en cualquier momento, antes y durante la realización del procedimiento. Sin necesidad de dar explicaciones

Y, para que así conste, firmo el presente documento. Toledo, a de de 20.....

CONSENTIMIENTO ORAL ANTE TESTIGO

Coherencia y sinergia muscular durante el movimiento de pedaleo como medidas de recuperación motriz.

Yo,, declaro bajo mi responsabilidad que:

..... (nombre del participante en el ensayo)

- ha recibido la hoja de información sobre el estudio
- ha podido hacer preguntas sobre el estudio
- ha recibido información y aclarado las dudas con el Dr.(nombre del investigador)
- comprende que su participación es voluntaria
- comprende que puede retirarse del estudio:
 - cuando quiera
 - sin tener que ofrecer explicaciones
 - sin que esto repercuta en sus cuidados médicos futuros
- y presta libremente su conformidad para participar en el estudio

.....
Fecha

.....
Firma del testigo

HOJA DE INFORMACIÓN

HOJA DE INFORMACIÓN DEL ESTUDIO DEL ANÁLISIS BIOMECÁNICO DE LA MARCHA EN PACIENTES CON LESIÓN MEDULAR PARA EL DESARROLLO DE DISPOSITIVOS HÍBRIDOS NEUROPROTÉSICOS Y NEUROROBÓTICOS PARA COMPENSACIÓN FUNCIONAL Y REHABILITACIÓN DE TRASTORNOS DEL MOVIMIENTO.

Se le informa que se pretende realizar un ESTUDIO DEL ANÁLISIS BIOMECÁNICO DE LA MARCHA EN PACIENTES CON LESIÓN MEDULAR PARA EL DESARROLLO DE DISPOSITIVOS HÍBRIDOS NEUROPROTÉSICOS Y NEUROROBÓTICOS PARA COMPENSACIÓN FUNCIONAL Y REHABILITACIÓN DE TRASTORNOS DEL MOVIMIENTO del que se detalla a continuación toda la información de interés.

El objetivo principal de este estudio es estudiar la marcha en pacientes con lesión medular incompleta para ayudar en el desarrollo de neurorobots y neuroprótesis. Estos neurorobots y neuroprótesis van a ser diseñados para restaurar la función motora en pacientes con lesión medular a través de la compensación funcional.

Para ello, se procederá a un análisis biomecánico que constará de un estudio cinemática, cinético y electromiográfico. El cinemática se llevará a cabo con un equipo de análisis del movimiento en 3D que está compuesto por 2 escáneres Coda-Motion que registran la posición de unos marcadores situados en los miembros inferiores. El cinético se realizará en dos plataformas de fuerza ocultas en el pasillo de marcha de manera que no condicione los apoyos. Y el electromiográfico (actividad muscular) se realiza mediante un equipo de electromiografía de superficie, Noraxon, con electrodos pegados en la piel. En cada ensayo, se debe caminar a velocidad libre por un pasillo de 10 metros de longitud, al menos 5 veces. Siendo analizado posteriormente para la extracción de datos de interés para el estudio.

Los riesgos derivados del estudio se reducen a la posibilidad de caída durante el registro de la marcha. Para lo cual se establece con anterioridad las medidas de seguridad oportunas para evitarlo.

La participación del usuario es voluntaria, pudiendo abandonar en cualquier momento sin tener que dar explicaciones y que ello repercuta en posteriores cuidados médicos. Sólo es necesario una única visita para llevar a cabo el estudio. Se realizarán capturas de vídeo al paciente con una cámara, con el fin de completar de manera visual la información aportada por los demás equipos.

Los datos de este estudio serán manejados única y exclusivamente por el personal de la Unidad de Biomecánica manteniendo la confidencialidad en todo momento.

El médico rehabilitador responsable de la Unidad de Biomecánica y Ayudas Técnicas, Ángel Gil Agudo, o en su caso, el personal encargado del estudio, estarán disponible durante todo el proceso del ensayo para aclarar o contestar a cualquier duda que pueda surgir durante los ensayos. En caso de urgencia se podrá contactar con nosotros a través del teléfono del Hospital Nacional de Paraplégicos de Toledo en la extensión telefónica de la Unidad de Biomecánica y Ayudas Técnicas (763).

El usuario se beneficiará de la información objetiva obtenida de los distintos parámetros recogidos de la marcha, quedando definida por completo sus características.

HYPER_CSD2009-00067

Deliverable 1.2.1. B (RT1)

MODELO CONSENTIMIENTO INFORMADO

Para satisfacción de los Derechos del Paciente, como instrumento favorecedor del correcto uso de los Procedimientos Diagnósticos y Terapéuticos, y en cumplimiento de la Ley General de Sanidad.

Yo, D/Dña....., como paciente
(o D./Dña....., como su
representante), en pleno uso de mis facultades, libre y voluntariamente,

EXPONGO:

Que he sido debidamente INFORMADO/A por el
D./Dña....., en entrevista personal realizada el día
....., de que se va a realizar un estudio biomecánico con el equipo de análisis
cinemático Coda-motion, el equipo de análisis fisiológico NORAXON, y el equipo de análisis
cinético Kistler, a fin de evaluar la marcha.

Que he recibido explicaciones, sobre la naturaleza y propósitos del procedimiento,
beneficios, riesgos, alternativas y medios con que cuenta el Hospital para su realización,
habiendo tenido ocasión de aclarar las dudas que me han surgido.

He entendido que este estudio está prohibido en personas que tienen marcapasos y
declaro no encontrarme en esta condición.

MANIFIESTO:

Que he entendido y estoy satisfecho de todas las explicaciones y aclaraciones recibidas
sobre el proceso médico citado

Y OTORGO MI CONSENTIMIENTO para que me sea realizado este estudio.

Entiendo que este consentimiento puede ser revocado por mí en cualquier momento
antes o durante la realización del procedimiento.

Y, para que así conste, firmo el presente documento

Toledo, a _____, de _____ de _____

Firma del paciente y Nº D.N.I

Firma del informante

(O su representante legal en caso en caso de incapacidad)

HYPER, CSD2009-00067

Deliverable 1.2.1. B (RT1)

MODELO CONSENTIMIENTO INFORMADO ORAL ANTE TESTIGO

Para satisfacción de los Derechos del Paciente, como instrumento favorecedor del correcto uso de los Procedimientos Diagnósticos y Terapéuticos, y en cumplimiento de la Ley General de Sanidad.

Yo, D/Dña....., como testigo del paciente
....., en pleno uso de mis facultades, libre y voluntariamente,

EXPONGO:

Que el paciente ha sido debidamente **INFORMADO/A** por el D./Dña....., en entrevista personal realizada el día, de que se va a realizar un estudio biomecánico con el equipo de análisis cinemático Coda-motion, el equipo de análisis fisiológico NORAXON, y el equipo de análisis cinético Kistler, a fin de evaluar la marcha.

Que ha recibido explicaciones, sobre la naturaleza y propósitos del procedimiento, beneficios, riesgos, alternativas y medios con que cuenta el Hospital para su realización, habiendo tenido ocasión de aclarar las dudas que han surgido.

El paciente ha entendido que este estudio está prohibido en personas que tienen marcapasos y declara no encontrarme en esta condición.

MANIFIESTO:

Que el paciente ha entendido y está satisfecho de todas las explicaciones y aclaraciones recibidas sobre el proceso médico citado

Y OTORGO MI FIRMA COMO TESTIGO para que sea realizado este estudio.

Y, para que así conste, firmo el presente documento

Toledo, a _____, de _____ de _____

Firma del testigo y N° D.N.I

Firma del informante

CONSENTIMIENTO INFORMADO

APELLIDOS:

NOMBRE:

Le proponemos participar en una línea de investigación del Laboratorio de Análisis del Movimiento, Biomecánica, Ergonomía y Control Motor (LAMBECOM) de la Universidad Rey Juan Carlos. El objetivo que persigue la línea de investigación consiste en aumentar el conocimiento sobre la evaluación y el tratamiento rehabilitador mediante diferentes tecnologías en sujetos con ictus. La presente línea de investigación se enmarca dentro del proyecto de ámbito nacional HYPER correspondiente a la convocatoria CONSOLIDER-Ingenio 2010.

1. ¿Qué es y qué persigue este estudio?

El objetivo de este estudio es verificar la hipótesis de que la composición de las sinergias cambia en el tiempo después de que surge el ictus. La confirmación de la hipótesis apoyará el análisis de sinergias como una medida de la recuperación motora, para ser utilizado en la práctica clínica.

2. ¿Cómo se realizará el estudio y lugar de realización?

La actuación prevista se desempeñará en el Laboratorio de Análisis del Movimiento, Biomecánica, Ergonomía y Control Motor (LAMBECOM) ubicado en la Facultad de Ciencias de la Salud de la Universidad Rey Juan Carlos (<http://www.redlabu-rjrc.es/content/laboratorio-de-an%C3%A1lisis-del-movimiento-biomec%C3%A1nica-ergonom%C3%ADa-y-control-motor>), perteneciente a la RED-LAB: red de Laboratorios oficial de la I+D+i de la Comunidad de Madrid (<http://www.madrimasd.org/laboratorios/>).

Está previsto que el paciente pueda realizar el protocolo de estudio en una sola sesión. Si fuera necesario alguna otra visita se solicitará previamente su consentimiento. No existen riesgos para la salud de los participantes puesto que se les someterá a pruebas en las que se les exigirá únicamente caminar. Sin embargo, puede resultar algo incómodo la colocación en el sujeto de los diferentes marcadores y accesorios necesarios para el

registro. Los sujetos participantes que así lo soliciten recibirán un informe detallado de su valoración, que podrá serle de utilidad para una mejor orientación terapéutica.

3. Beneficios y riesgos

Respecto a los beneficios para los pacientes, la obtención de información objetiva y cuantitativa sobre sus alteraciones funcionales puede mejorar el éxito del tratamiento rehabilitador y la participación socio-laboral de cada individuo.

4. Confidencialidad de los datos e imágenes

El tratamiento de sus datos se hará de acuerdo con la Ley Orgánica 15/1999, de 13 de diciembre, de protección de datos de carácter personal, y demás legislación aplicable.

El investigador principal, su equipo y cualquier persona que intervenga en el proyecto están obligados legalmente a guardar el secreto y confidencialidad sobre cuantas informaciones y/o datos puedan obtenerse del sujeto por su participación en el proyecto. Los datos personales serán incorporados y tratados en el fichero del LAMBECOM, inscrito en el Registro de Ficheros de Datos Personales de la Agencia de Protección de Datos de la Comunidad de Madrid (www.madrid.org/apdcm) y no serán cedidos a terceros.

El órgano responsable del fichero es el VICERRECTORADO DE INVESTIGACIÓN, de la Universidad Rey Juan Carlos, y la dirección donde el interesado podrá ejercer los derechos de acceso, rectificación, cancelación y oposición ante el mismo es C/ Tulipán s/n Móstoles Madrid, todo lo cual se informa en cumplimiento del artículo 5 de la Ley Orgánica 15/1999, de 13 de diciembre, de Protección de Datos de Carácter Personal.

También se le ha informado que la participación o no en la investigación no afectará a ningún tipo de servicio o cobertura sanitaria o social con la que esté vinculado o pueda estarlo en un futuro.

Con las garantías legales oportunas, los resultados del estudio podrán ser comunicados a la comunidad científica a través de congresos y publicaciones, garantizando que en todo el proceso de difusión, se omitirá su identidad y cualquier dato personal que pueda facilitar que se le identifique.

Los resultados de la investigación le serán proporcionados si los solicita al investigador D. Francisco Molina Rueda, quien atenderá cualquier tipo de duda o pregunta que tenga que realizarle en relación al estudio. Su centro de trabajo está ubicado en el Despacho 1069, teléfono 914888913.

La Universidad Rey Juan Carlos y el equipo de investigación que lidera el referido proyecto están exentos de cualquier responsabilidad que se derive de la investigación que no se haya manifestado en el presente escrito, sea cual fuere el momento y lugar en donde se realizara.

Declara que ha recibido suficiente información sobre el estudio y que ha tenido oportunidad de efectuar preguntas sobre el mismo y, en su caso, ha recibido respuestas satisfactorias del investigador/investigadores responsables. Ha comprendido la información recibida y la decisión que toma es libre y voluntaria pudiendo en cualquier momento revocar por escrito este consentimiento sin expresar la causa y sin que suponga perjuicio alguno en la asistencia sanitaria suya. Declara que se le entrega una copia de este documento.

En Madrid, a _____ de _____ de 20__.

Firma y nombre del Investigador (DNI).

Firma y nombre del participante (DNI).